

FEASIBILITY OF WAVEFORM
CAPNOGRAPHY AS A NON-INVASIVE
MONITORING TOOL DURING
CARDIOPULMONARY
RESUSCITATION

BY

MIKEL LETURIONDO SOTA

SUPERVISORS:

SOFÍA RUIZ DE GAUNA GUTIÉRREZ

JOSÉ JULIO GUTIÉRREZ RUIZ

PHD THESIS

eman ta zabal zazu



Universidad
del País Vasco

Euskal Herriko
Unibertsitatea

DEPARTMENT OF COMMUNICATIONS ENGINEERING

Bilbao, January 2021

*Dedicated to my parents,
brother and sister,
for always being there.*

*To Leire, for her tireless
way of being, which makes
everything even more fun.*

ABSTRACT

Sudden cardiac arrest (SCA) is one of the leading causes of death in the industrialized world and it includes the sudden cessation of circulation and consciousness, confirmed by the absence of pulse and breathing. Cardiopulmonary resuscitation (CPR) is one of the key interventions for patient survival after SCA, a life-saving procedure that combines chest compressions and ventilations to maintain a minimal oxygenated blood flow.

To deliver oxygen, an adequate blood flow must be generated, by effective CPR, during the majority of the cardiac arrest time. Although monitoring the quality of CPR performed by rescuers during cardiac arrest has been a huge step forward in resuscitation science, in 2013, a consensus statement from the American Heart Association prioritized a new type of CPR quality monitoring focused on the physiological response of the patient instead of how the rescuer is doing.

To that end, current resuscitation guidelines emphasize the use of waveform capnography during CPR for patient monitoring. Among several advantages such as ensure correct tube placement, one of its most important roles is to monitor ventilation rate, helping to avoid potentially harmful over-ventilation. In addition, waveform capnography would enable monitoring CPR quality, early detection of ROSC and determining patient prognosis. However, several studies have reported the appearance of fast oscillations superimposed on the capnogram, hereinafter CC-artifact, which may hinder a feasible use of waveform capnography during CPR.

In addition to the possible lack of reliability, several factors need to be taken into account when interpreting ETCO_2 measurements. Chest compressions and ventilation have opposing effects on ETCO_2 levels. Chest compressions increase CO_2 concentration, delivering CO_2 from the tissues to the lungs, whilst ventilations remove CO_2 from the lungs, decreasing ETCO_2 . Thus, ventilation rate acts as a significant confounding factor.

This thesis analyzes the feasibility of waveform capnography as non-invasive monitoring tool of the physiological response of the patient to resuscitation efforts. A set of four intermediate goals was defined. First, we analyzed the incidence and morphology of the CC-artifact and assessed its negative influence in the detection of ventilations and in ventilation rate and ETCO_2 measurement. Second, several artifact suppression techniques were used to improve ventilation detection and to enhance capnography waveform. Third, we applied a novel strategy to model the impact of ventilations and ventilation rate on the exhaled CO_2 measured in out-of-hospital cardiac arrest capnograms, which could allow to measure the change in ETCO_2 attributable to chest compressions by removing the influence of concurrent ventilations. Finally, we studied if the assessment of the ETCO_2 trends during chest compressions pauses could allow to detect return of spontaneous circulation, a metric that could be useful as an adjunct to other decision tools.

CONTENTS

1	INTRODUCTION	1
1.1	Sudden cardiac arrest. The chain of survival	3
1.2	Cardiopulmonary resuscitation	6
1.3	CPR Quality: A change in the paradigm	8
1.4	Capnography during CPR	12
1.5	Motivation	16
2	BACKGROUND	19
2.1	Uses of Capnography in resuscitation	20
2.2	Capnogram waveform during CPR: The phenomenon of chest compression artifact	26
2.3	Factors complicating the clinical interpretation of ETCO ₂ .	30
3	OBJECTIVES	33
4	MATERIALS AND METHODS	37
4.1	OHCA Databases	37
4.2	Annotation and methodology	41
5	RESULTS AND DISCUSSION	49
6	CONCLUSIONS	57
	BIBLIOGRAPHY	63
A	PUBLICATIONS	81

LIST OF FIGURES

Figure 1.1	The electrical system of the heart and an ECG segment of a sinus rhythm heartbeat	2
Figure 1.2	The chain of survival and its four independent links.	4
Figure 1.3	Heartstart OnSite HS1 (Philips) AED and Heartstart MRx (Philips) monitor/defibrillator equipped with the defibrillation pads and the CPR aid pad for chest compression feedback. . . .	5
Figure 1.4	Airway management devices. Bag-valve-mask, endotracheal tube and supraglottic airway	7
Figure 1.5	Evolution of capnometry in out-of-hospital emergency settings. Qualitative capnometer, semi-quantitative capnometer, quantitative capnometer and waveform capnography	13
Figure 1.6	Brief schemes of different sampling methods used with quantitative capnometry devices, mainstream and sidestream.	14
Figure 1.7	The normal capnogram. Capnography waveform representing the variation of CO ₂ concentration during the respiratory cycle	15
Figure 1.8	Global capnography device market share by application in 2018.	16
Figure 2.1	Capnogram segment acquired during cardiac arrest. High-quality ventilations are provided to the patient at a consistent rate of 11 ventilations per minute	22
Figure 2.2	Capnogram segment acquired during ongoing chest compressions. ET _{CO} ₂ decreases over time with a constant ventilation rate	23

Figure 2.3	Capnogram segment showing a sudden increase in ETCO_2 as a result of the return of spontaneous circulation	25
Figure 2.4	Waveform capnography signal segment during ongoing chest compressions.	27
Figure 2.5	Waveform capnography and tidal volume signals recorded during resuscitation, showing manual and passive ventilations generated by chest compressions	28
Figure 2.6	Mainstream capnography during manual and mechanical CPR performed to the same patient .	31
Figure 2.7	ETCO_2 plotted as a function of the ventilation minute-volume delivered during CPR	32
Figure 4.1	Example segment extracted from an OHCA episode from the TVF&R database.	40
Figure 4.2	OHCA waveform capnography classification chart.	42
Figure 5.1	Example of filtering performance	52
Figure 5.2	Example of envelope filtering performance	52

LIST OF ABBREVIATIONS

AED	Automated External Defibrillator
AHA	American Heart Association
ALS	Advanced life support
AV	Atrioventricular
BLS	Basic life support
BVM	Bag-valve-mask
CO₂	Carbon dioxide
cpm	Compression per minute
CPP	Coronary perfusion pressure
CPR	Cardiopulmonary Resuscitation
E-O	Emergentziak Osakidetza
ECG	Electrocardiogram
EMS	Emergency medical services
epCO₂	Ensemble plateau carbon dioxide
ERC	European Resuscitation Council
ETCO₂	End-tidal carbon dioxide

ETT	Endotracheal tube
ILCOR	International Liaison Committee on Resuscitation
JCR	Journal Citation Reports
NSR	Normal sinus rhythm
OHCA	Out-of-hospital cardiac arrest
PCO₂	Partial pressure of carbon dioxide
PEA	Pulseless electrical activity
PPV	Positive predictive value
PR	Perfusing rhythm
ROC	Resuscitation Outcomes Consortium
ROSC	Return of spontaneous circulation
SA	Sinoatrial
SCA	Sudden cardiac arrest
Se	Sensitivity
SGA	Supraglottic airway
Sp	Specificity
SpO₂	Oxygen saturation
TTI	Transthoracic impedance
TVF&R	Tualatin Valley Fire & Rescue
vpm	Ventilations per minute

1 | INTRODUCTION

The human heart is a complex muscular organ that rhythmically pumps blood through the blood vessels to provide an uninterrupted blood flow throughout the body. It is divided into four different chambers: two atria and two ventricles, the receiving and the discharging chambers, respectively. The right atrium and ventricle, both together, pump blood low in oxygen to the lungs where it receives oxygen and gives off carbon dioxide. Meanwhile, oxygenated blood coming from the lungs is pumped to the circulatory system by their left counterparts.

To ensure that the blood is pumped efficiently, the heart must contract and relax in a precisely synchronous way. In a healthy heart, the normal rhythmical heartbeat is established by a group of cardiac cells, known as the sinoatrial (SA) node. There, an electrical impulse that travels through an elaborate conduction system (Figure 1.1, left) is generated. This electrical activity, recorded using skin electrodes placed on the patient, is known as the electrocardiogram (ECG. Figure 1.1, right), and its analysis provides useful information about the cardiac function.

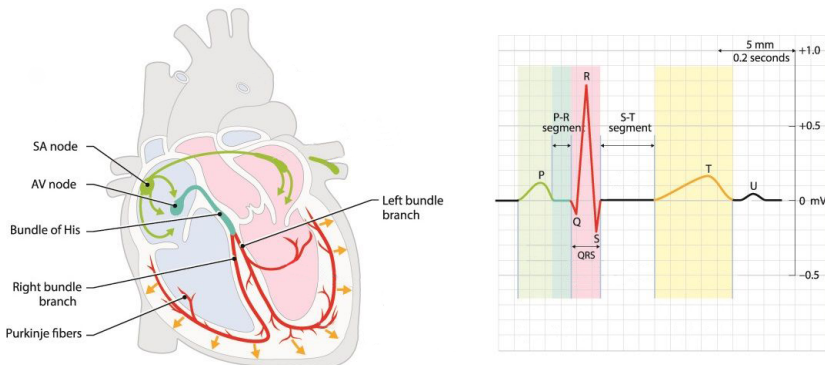


Figure 1.1. The electrical system of the heart (left) and an ECG segment of a sinus rhythm heartbeat (right). Adapted from biologydictionary.net

The sequence of events in which the heart contracts and relaxes with every heartbeat is known as the cardiac cycle. The SA node, acting as the natural pacemaker, initiates an electric impulse that propagates through the atrial muscle contracting the atria, which pump blood from the atria to the ventricles (**P-wave**). To allow them to completely fill with blood, the atrioventricular (AV) node collects and delays the electric impulse (**P-R segment**). Then, it travels through the bundle of His, after which it is divided into the right and left bundle branches, and further into a highly conductive network called the Purkinje fibers. The impulse is rapidly propagated through these conducting fibers producing a unified contraction of the ventricles (**QRS complex**), pumping blood to the lungs or the circulatory system. To conclude the cardiac cycle, ventricles return to their relaxed state (**T-wave**) after a refractory period (**S-T segment**).

This sequence is continuously repeated producing an uninterrupted blood flow and constitutes the normal functioning of the heart – normal sinus rhythm or NSR-. Any rhythm different to the NSR in which the cardiac cycle is too fast (tachycardia), too slow (bradycardia) or irregular is known as an arrhythmia. Although most types of arrhythmias are harmless, some may lead to severe complications such as heart failure, stroke or even cardiac arrest. Life-threatening arrhythmias impede efficient blood pumping and compromise proper lung and brain functioning, which leads to a critical situation that requires immediate intervention. All the efforts carried out to revert this situation and restore spontaneous circulation are endorsed by the science of resuscitation.

1.1 SUDDEN CARDIAC ARREST. THE CHAIN OF SURVIVAL

Cardiac disease has been declared as one of the leading causes of death of the industrialized world, comprising a 30% of the global mortality. It is estimated that sudden cardiac arrest (SCA) is responsible for half of all cardiac disease deaths.^{87,71} SCA is a life-threatening event defined as the sudden cessation of circulation, breathing and consciousness resulting from the failure of the heart to pump effectively.¹⁶³ It usually results from an electrical disturbance in the heart that suddenly disrupts the mechanical activity of the heart, stopping blood flow to vital organs.⁹⁵

The precise incidence of SCA is uncertain, reported annual deaths vary between 150 000 and 535 000 depending on the inclusion criteria used in each study.^{25,162} It is widely accepted an estimate of 275 000 victims per year in Europe,⁸ and around 300 000 in the United States.⁷⁶ Most SCAs, around 80%, occur in an out-of-hospital setting,^{24,162} and at least two thirds of them in patients without previous underlying heart disease.⁹² In addition, only a 60% of the out-of-hospital cardiac arrests (OHCA) are treated by the emergency medical services (EMS),¹⁶² establishing SCA as one of the leading public health problems in the world.

Reported outcomes vary depending on the geographic region, in general, survival rate is dramatically low, around 10%, although it increases to 20% for some cardiac arrest etiologies.^{8,117} Availability of EMS personnel and quality of the protocols are pivotal for a higher survival ratio. For this reason, the probability of a successful resuscitation widely varies between rural areas and certain cities, ranging from less than 2% to more than 20%, respectively.^{13,40}

In an effort to optimize cardiac arrest treatment guidelines with recommendations from organizations such as the European Resuscitation Council (ERC), the American Heart Association (AHA) and resuscitation councils from other parts of the world are published in 5-year cycles. To allow a better cooperation between those regional resuscitation councils, in 1992 the International Liaison Committee on Resuscitation (ILCOR) was formed. Since then, international science and knowledge has been identified and reviewed by committee members in order to achieve a consensus on the science of resuscitation.

The Chain of Survival

The ILCOR promotes the metaphor of the chain of survival (Figure 1.2), a slogan first introduced in the 1980s and developed by the AHA in the 1992 resuscitation guidelines.²⁹ It refers to the series of actions that, properly executed, connects the victim of OHCA with survival. The four independent links are early access, early cardiopulmonary resuscitation (CPR), early defibrillation, and early advanced care.

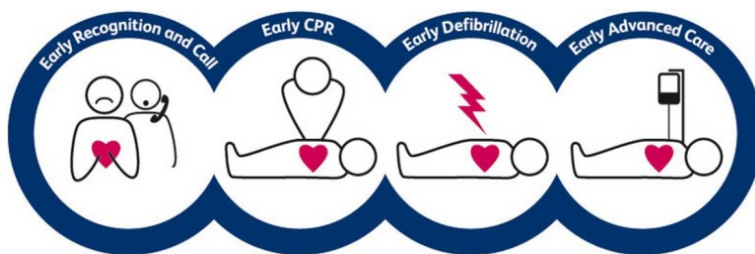


Figure 1.2. The chain of survival and its four independent links. Extracted from learncpronline.net

- *Early access:* The first link involves the early recognition of the symptoms and rapid activation of the EMS services, either by a witness or by the person suffering from cardiac arrest.
- *Early CPR:* The second link refers to the first medical aid provided by laypeople before EMS personnel arrives. It consists of chest compression and ventilation cycles delivered to the patient to maintain an artificial oxygenated blood flow to vital tissues. Immediate CPR has shown to improve neurological outcome and increase survival rates.^{61,153,160}
- *Early defibrillation:* Defibrillation comprises the administration of an electrical shock to the cardiac muscle in order to terminate ventricular arrhythmias –i.e. shockable rhythms– and restore spontaneous circulation.⁷² In out-of-hospital settings, it is normally provided by automated external defibrillators (AED. Figure 1.3, left). AEDs are easy-to-use portable devices that analyze the victim’s ECG and determine whether an electrical shock is needed or not.

Both *early CPR* and *early defibrillation* are considered basic life support (BLS) medical care and it is usually performed by trained personnel, such as emergency medical technicians or qualified bystanders.

- *Early advanced care*: The last link refers to the treatment provided by qualified health care personnel, named as advanced life support (ALS). On site SCA treatment by ALS personnel not only includes CPR and defibrillation, but also intubation, drug administration and advanced monitoring (Figure 1.3, right).¹⁴² The aim of these interventions is to preserve a minimal brain and lung function, which has shown to improve patient outcomes.^{99,142}



Figure 1.3. Heartstart OnSite HS1 (Philips) AED (left) and Heartstart MRx (Philips) monitor/defibrillator equipped with the defibrillation pads and the CPR aid pad for chest compression feedback (right).

From these interventions, early CPR and early defibrillation are key for a successful outcome of the patient. If bystander CPR is provided within the first five minutes, probability of successful resuscitation declines an average of 4% per minute.¹⁵³ Whereas, if no CPR is provided, it decreases a 7-10% for every minute that defibrillation is delayed.^{77,155} Thus, early CPR scenario increases survival between 2 to 3 times compared to a scenario without early CPR, in which outcome is almost fatal.⁶³

1.2 CARDIOPULMONARY RESUSCITATION

CPR is a life-saving procedure that combines external chest compressions and ventilations in an effort to maintain a minimal oxygenated blood flow.¹⁰⁶ Its main purpose is to delay tissue death and preserve some degree of cerebral perfusion, necessary to prevent brain death, until advanced procedures are performed to restore spontaneous blood circulation in victims suffering from cardiac arrest.

The mechanism by which external chest compressions generate blood flow is still uncertain. Several hypothesis have been proposed, in all of them the CPR technique generates a pressure gradient between the arterial and venous vascular beds, oxygenating the blood and maintaining a cardiac output to keep vital organs alive.⁵⁵ In absence of CPR the brain may sustain irreversible damage after blood flow has been stopped for about seven minutes.¹⁵³ Therefore, it is only effective when performed within the first seven minutes of blood flow stoppage.¹⁵⁵

Even if the maneuver is started on time, CPR by itself is unlikely to restart the heart's pumping function in the majority of cardiac arrest victims. Administration of an electrical shock – defibrillation – is needed in order to restore a perfusing heart rhythm. Although the physiological process is not fully understood, the procured shock depolarizes a critical mass of the myocardium, subduing the arrhythmia. Subsequently, the body's natural pacemaker is able to re-establish the coordinated electrical activity of the heart.⁸⁹

Resuscitation guidelines for BLS and ALS

Resuscitation guidelines describe how CPR and defibrillation should be performed in both BLS and ALS settings. BLS comprises the wide variety of non-invasive life-saving procedures that could be performed to revert the life-threatening situation. BLS guidelines indicate that in presence of an adult cardiac arrest, all rescuers should perform CPR despite being trained or not.^{26,109} First responders should provide chest compressions pressing down the center of the chest. Trained bystanders should also perform mouth-to-mouth rescue breaths watching for the chest to rise. CPR should be continuously performed until an AED

is available, alternating cycles of 30 chest compressions with two ventilations. Then, the AED should be attached to the patient and, if needed, a defibrillation should be procured after rhythm analysis. This process remains uninterrupted in two minute cycles, with intermediate pauses for rhythm assessment, until professional help arrives and takes over or the victim starts to move and breathe normally.

ALS guidelines indicate the procedures and interventions that would require physicians themselves or physician's orders to be delivered. ALS personnel, skilled in laryngoscopy and intubation, should attempt advanced airway placement while minimizing the interruption of chest compressions.¹³⁸ Maintaining airway integrity while providing proper oxygenation to the brain is critical for a successful outcome. To that end, a wide range of devices and techniques are available for ALS personnel (Figure 1.4). Once the airway is placed, continuous chest compressions and ventilations should be provided, pausing every 2 min for rhythm assessment.

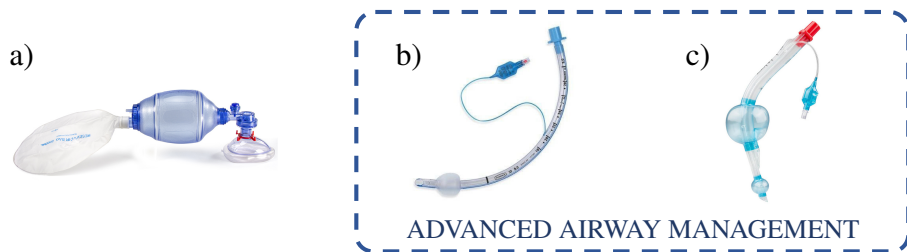


Figure 1.4. Airway management devices. a) Bag-valve-mask (BVM).
b) Endotracheal tube (ETT). c) Supraglottic airway (SGA).

In ALS settings – hospitals or ALS ambulances – sophisticated devices named monitor-defibrillators (Figure 1.3, right) are generally used by professional healthcare providers. These devices are able to monitor several biological signals such as the ECG, transthoracic impedance (TTI), capnography (carbon dioxide (CO₂) concentration), or pulse oximetry (oxygen saturation). They can also measure CPR efforts through CPR aid pads. In addition, this ALS equipment is able to deliver external cardiac pacing and procure manual defibrillation. They are generally used in manual mode, but most of them can also function like AEDs. In manual mode, clinicians decide if an electrical shock is required, using the analyzed rhythm and their medical knowledge, every 2 min.

1.3 CPR QUALITY: A CHANGE IN THE PARADIGM

Oxygen delivery to vital tissues and organs is the main goal of CPR during resuscitation. Thus, an adequate and sustained blood flow must be generated, by effective CPR, during the majority of the cardiac arrest time.⁸⁶ Several animal studies have shown that return of spontaneous circulation (ROSC) is highly dependent on adequate myocardial blood flow and oxygen delivery during CPR.^{56,88,116} Coronary perfusion pressure (CPP) is the primary myocardial blood flow determinant during CPR.^{107,127} Thus, maximizing CPP should be the main physiological goal. However, CPP is not easily measurable in the out-of-hospital setting. Therefore, rescuers should focus on CPR performance metrics with enough clinical evidence that support its improvement in patient hemodynamics or survival ratio.

Over time, five metrics of high-performance CPR have been identified because of their contribution to blood flow and outcome.⁸⁶ Understanding the importance of these metrics and their relationships is essential for providers to improve survival to hospital discharge.

- *Minimize interruptions:* CPR providers should minimize chest compression interruptions to maintain adequate tissue oxygenation and therefore maximizing the chest compression fraction metric.^{14,150} Chest compression fraction is the proportion of time that chest compression are performed during the total cardiac arrest time, from cardiac arrest until first return of sustained circulation. Expert consensus and data on OHCA indicate that lower chest compression fraction values correlate with decreased ROSC and lower survival ratio.^{23,152}
- *Chest compression rate:* Guidelines for CPR have recommended a chest compression rate above 100 compressions per minute (cpm) since lower chest compression rates have shown a significant drop-off in ROSC and outcome. However, there is clinical evidence supporting that excessive rates may reduce coronary blood flow⁴ and worsen the percentage of compression that achieve the depth target.^{90,141}

- *Chest compression depth:* Several studies suggested that a target of ≥ 50 mm may improve defibrillation success and ROSC.^{12,36,74} In addition, a recent study concluded that a consistent depth of < 40 mm was associated with a decrease in ROSC and survival rates.¹⁴¹ Thus, for every adult patient, a single minimum compression depth of ≥ 50 mm is recommended. However, clinical evidence suggests that, despite recommendations, rescuers often do not compress the chest deeply enough. This could be associated with factors such as compression rate, patient chest size or environmental features.
- *Full chest recoil:* Incomplete chest release occurs when the rescuer leans over the patient's chest and does not allow the chest to fully expand on completion of the decompression phase.^{10,161} It is known to decrease the blood flow throughout the heart and can decrease venous return.¹⁶⁴ Human studies have shown that most healthcare providers often lean between consecutive chest compression, not allowing a full chest recoil.^{43,97} Therefore, leaning should be minimized.
- *Ventilation rate:* Providing oxygen to the blood without impeding perfusion is the main goal of assisted ventilation during CPR.⁹³ Guideline recommendations for ventilation rate depend on whether an advanced airway is placed (8 to 10 ventilations per minute (vpm)) or not (series of 30:2). However, excessive ventilation, either by rate or tidal volume, is common in resuscitation.^{3,11,104} Several animal studies reported mixed results regarding the possible harm produced by high ventilation rates,^{11,104,45} but there is no evidence that ventilating a patient at a higher rate is beneficial.

In 2010, the ILCOR and other resuscitation councils updated their resuscitation guidelines emphasizing the importance of high quality CPR – proper depth and rate without excessive ventilations.^{30,94} Currently, optimal CPR technique for every adult patient comprises:

- Providing chest compressions at a rate above 100 cpm, without exceeding 120 cpm.
- Achieving a depth between 5 and 6 cm.
- Allowing a full chest release between compressions.
- Minimizing interruptions of chest compressions.
- *BLS*: Series of 30:2 compression-ventilation approach.
ALS: Continuous ventilations with simultaneous chest compressions, if intubated, at a rate around 10 vpm.

Several studies reported that adequate rate, depth, chest recoil and minimal interruptions improved the quality and effectiveness of CPR.^{10,36,38,65} However, other studies have shown that providing too fast chest compressions is very common, which in turn leads to shallow compressions and frequent pauses between chest compressions due to fatigue.^{42,90} In addition, excessive ventilation rates, as high as 30 vpm, have been shown to be frequent during resuscitation.¹¹ To alleviate this problem, and based in reviewed studies reporting an improvement in CPR quality, 2010 resuscitation guidelines encouraged the use of chest compression feedback devices such as CPR aid pads during resuscitation to be compliant with recommended rate and depth.³⁰ Yet avoiding hyperventilation with the use of mechanical ventilators, was the only advice regarding such high ventilation rates.

Today, a large gap exists between current knowledge of CPR quality and its optimal implementation. Monitoring the quality of CPR performed by rescuers during cardiac arrest has been a huge step forward in resuscitation science and clinical practice. However, resuscitation efforts should be tailored to each patient. In 2013, a consensus statement from the AHA prioritized a new type of CPR quality monitoring focused on physiological metrics (how the patient is doing), instead of the conventional CPR performance (how the rescuers are doing) metrics.⁸⁶

Monitoring the patient's physiological response to resuscitation efforts requires invasive hemodynamic data (e.g. CPP) or non-invasive surrogate markers of blood flow such as pulse or cerebral oximetry, ultrasound or capnography.

There is abundant clinical evidence to support that survival from cardiac arrest is highly dependent on adequate myocardial oxygen and blood flow delivery during CPR, which is directly related with CPP.^{55,88,107,125} Experts recommend that this physiological target should be the primary end point. However, measurement of CPP is not a straightforward practice in OHCA since it involves invasive procedures such as placing arterial and central venous catheters.

Surrogate markers are based on physiological metrics associated with blood flow and can be measured non-invasively. Oximetry measures regional oxygen saturation (SpO₂) using near-infrared spectroscopy sensors placed in the skin (finger, earlobe or forehead). Ultrasound imaging can be used to identify low cardiac output states. Finally, capnography enables CO₂ concentration measurement of the exhaled air. CO₂ concentrations during CPR are primarily dependent on pulmonary blood flow and therefore indirectly reflect cardiac output.^{103,158} Low CO₂ concentrations during adult CPR reflects poor cardiac output and strongly predicts unsuccessful resuscitation.^{19,78,124} Experts recommend that, when available, exhaled CO₂ concentration should be the primary physiological metric when no arterial or venous catheter is present at the time of cardiac arrest.

Current resuscitation guidelines (2015) include a new section on monitoring during ALS treatment. There is an increased emphasis on the use of waveform capnography during CPR for ventilation rate guidance and patient monitoring. Ideally, CPR should be guided based on the patient's response since recommended CPR technique may not be optimal for all individuals.¹⁴³ Hence, the use of capnography during resuscitation establishes a new milestone in CPR quality monitoring. It could allow a change from an homogeneous CPR technique for every adult in cardiac arrest to a more personalized cardiac treatment based on the hemodynamic response of the patient during resuscitation.

1.4 CAPNOGRAPHY DURING CPR

Capnography has become an essential component of standard anesthesia monitoring since CO₂ measuring and recording was first introduced in 1943.⁶⁹ Capnography represents a continuous non-invasive measurement of the partial pressure of carbon dioxide (PCO₂) in the exhaled air. CO₂ is produced in perfused tissues, diffused from the cells into the blood and transported by the venous return to the lungs where it is removed by ventilation.¹²⁸ The CO₂ concentration at the end of the exhalation is known as end-tidal CO₂ (ETCO₂), and its major determinants include CO₂ production, cardiac output, pulmonary blood flow and alveolar ventilation.¹⁵¹

The primary goal of anesthesiologists during anesthesia is to prevent deprivation of adequate oxygen supply – hypoxia –. Improvements with capnography in this field currently allow a rapid and reliable detection of life-threatening conditions and to avoid potentially irreversible brain damage. Because of these improvements and benefits for the patient, the use of capnography has spread from the operating room into emergency medicine environment. In fact, it is increasingly being used by EMS personnel in the out-of-hospital environment to aid their assessment and treatment of patients. Therefore, it could be a potential surrogate marker of perfusion during cardiac arrest.

Evolution of CO₂ feedback systems

Several methods have been used over the years to determine the presence and concentration of CO₂ in the field. The simplest form of CO₂ detection available is qualitative capnometry (Figure 1.5a). The technology behind these devices is based on a paper filter that changes in color in presence of CO₂, from purple to yellow. It is fast, convenient, and useful to verify correct tracheal intubation on scene, yet it may falsely indicate correct tracheal placement in certain emergency situations in which CO₂ may be present in the esophagus.¹¹³ In addition, its inability to accurately detect breath-to-breath changes hinders its use for ventilation guidance.

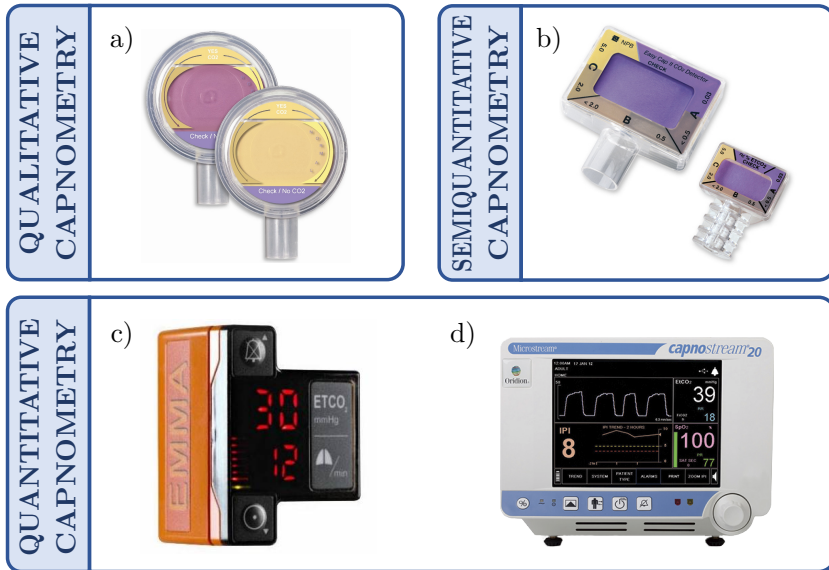


Figure 1.5. Evolution of capnometry in out-of-hospital emergency settings. a) Qualitative capnometer, b) Semiquantitative capnometer, c) Quantitative capnometer and d) Waveform capnography. Courtesy of Ambu, Medtronic and Masimo.

Later, semiquantitative capnometers that provide a rough estimation of the ETCO_2 concentration were developed (Figure 1.5b). The device consists of a clear dome overlying a piece of litmus paper that changes in color as a result of chemical reactions in the presence of CO_2 .⁷⁵ These devices report the ETCO_2 value in a series of stacked colors rather than providing a numerical value. A typical device would have the ability to provide one of the following three readings: purple – exhaled $\text{CO}_2 \leq 0.5$ mmHg; beige – exhaled CO_2 of 0.5-2 mmHg; yellow – exhaled $\text{CO}_2 > 2$ mmHg.^{30,138,157}

Semiquantitative devices are low cost, easy to use, and generally provide reliable confirmation of tube placement. Studies have reported that all erroneous – esophageal – intubations are correctly identified by the color on the device remaining in purple. However, some correctly placed tubes did not result in a color change, prompting paramedics to remove a tracheally placed tube.^{83,124} Furthermore, these devices are limited by their inability to provide reliable information in very low perfusion

states such as prolonged cardiac arrests, and field care providers may not find this system as useful as other methods for ventilation guidance.

More recently, quantitative capnometry, which involves infrared absorption spectroscopy analysis of expired gases, has led to the most accurate method to measure capnometry values (Figure 1.5c).¹²⁴ This technology provides a numerical end-tidal value of CO₂ concentration along with the ventilation rate, which allows an optimal control of ventilation. In a similar way, continuous waveform capnography represents an advance in CO₂ monitoring that offers continuous measurements and improved reliability (Figure 1.5d). It is already available in many EMS systems and, in some regions, it is considered a mandatory device for ALS systems.

Available gas sampling methods

Two different methods of gas sampling are used by quantitative capnometry devices. The sensor unit may be placed in different locations, depending on the method of sampling of exhaled gases, mainstream or sidestream. These two techniques are illustrated in Figure 1.6. The main difference between them is that in the former the sensor is directly placed in the main flow of exhaled gases,⁷⁵ while in the latter little samples of the main flow are aspirated with a capillary sampling tube in which the sensor is located.^{75,124}

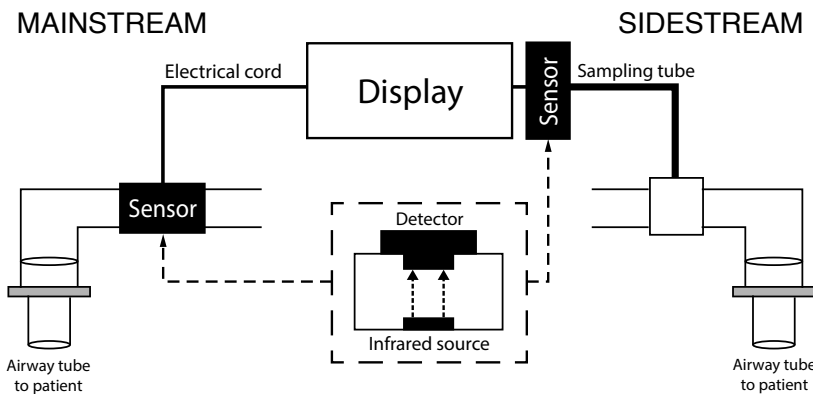


Figure 1.6. Brief schemes of different sampling methods used with quantitative capnometry devices, mainstream and sidestream.

One of the advantages, as opposed to qualitative and semiquantitative devices, is the threshold detection for exhaled CO_2 , which is significantly lower for quantitative capnometry.¹⁰⁰ Additionally, the CO_2 tracing – normal capnogram – produced from a properly placed tracheal tube is characteristic and recognizable. The reliability of waveform capnography during out-of-hospital treatment of cardiac arrest has been verified in both animal and human studies.^{41,131} If the proper waveform is present it confirms correct tube placement, even if the ETCO_2 value is below 10 mmHg.

Morphology of a normal capnogram

The evolution and morphology of CO_2 concentration in the respiratory cycle of a normal capnogram is depicted in [Figure 1.7](#). Over the years, there has been a considerable confusion in naming the various segments of a capnogram. For instance, a wide variety of nomenclatures has been used to describe each segment of the capnogram cycle, such as ABCDE and phases I to IV.¹⁵ Bhavani-Shankar et al.¹⁶ described the terminology shown in [Figure 1.7](#) representing various segments and phases of a capnogram based on logic, convention and tradition.

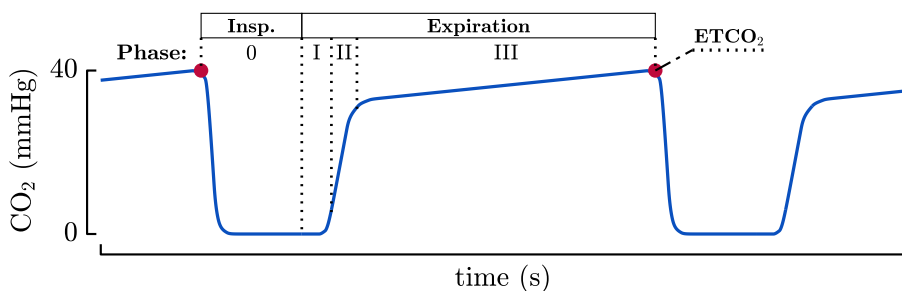


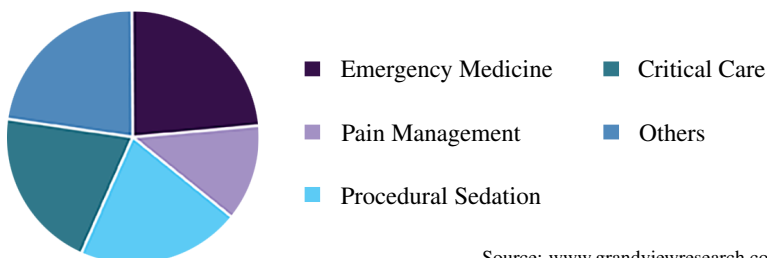
Figure 1.7. The normal capnogram. Capnography waveform representing the variation of CO_2 concentration during the respiratory cycle. Segments and phases follow the nomenclature proposed by Bhavani-Shankar K et. al.¹⁶

The initial rapid decrease of CO₂ concentration named as phase 0 represents the inspiration segment, where the lungs are filled with CO₂-free respiratory gases until a zero level is reached, defining the baseline of the capnogram. The following phases represent the expiration segment: during phase I, the CO₂-free gas in the anatomical dead space (between the alveoli and measurement device) is exhaled; in phase II a mixture of gases from the anatomical dead space and the alveoli quickly rises the level of CO₂ concentration; finally in phase III, CO₂ rich gases coming from the alveoli slowly rise the CO₂ concentration until a peak level is reached, corresponding to the ETCO₂ value.⁵⁰

1.5 MOTIVATION

Respiratory assessment is of crucial importance since gas exchange is a primordial function of the lungs and the conductive airways. Moreover, the ability to safely and effectively manage the airway is among the most fundamental and challenging aspects of out-of-hospital emergency medical treatment.

For over five decades, capnography has been used as a ventilation monitoring tool inside the operating rooms. Measurement of exhaled CO₂ is an established standard of care, and its main development has been as a monitoring tool used by anesthesiologists and intensive care personnel.⁶ However, it is increasingly being employed in the out-of-hospital setting. In fact, in 2018, emergency medicine, either in-hospital or out-of-hospital, became the main area of application (Figure 1.8).



Source: www.grandviewresearch.com

Figure 1.8. Global capnography device market share by application in 2018.

Capnography enables continuous real-time ETCO₂ to be monitored in the field. Besides prevention of unrecognized esophageal intubation,¹³⁶ there is currently no evidence that the use of waveform capnography during CPR results in improved patient outcome. However, new potential uses of waveform capnography are emphasized in current resuscitation guidelines,^{79,138} including monitoring of ventilation rate⁷ and quality of chest compressions,^{33,114} early detection of ROSC^{119,121} and determining patient prognosis.^{112,149,156} Nevertheless, since capnometers were not designed for such a tough environment, are these devices reliable enough during resuscitation efforts? This thesis work expects to shed light to this question and some of the potential uses of waveform capnography during CPR.

2 | BACKGROUND

The use of capnographs during resuscitation was initially proposed by the ILCOR in 2010, and since 2015 it is becoming a standard of care in advanced high-quality CPR.^{73,86,105} In patients with cardiac arrest, CPR temporarily restores cardiac output. Several studies have shown that adequate perfusion to vital organs is key during cardiac arrest.^{96,107,126} However, direct organ blood flow measurement during OHCA is not clinically feasible. Capnography represents a non-invasive measurement of the effectiveness of CPR in terms of generated blood flow.

Among the several advantages of waveform capnography emphasized in current resuscitation guidelines such as ensure correct tube placement, one of its most important roles is to monitor ventilation rate, helping to avoid over-ventilation. Given that ventilations cause downstrokes and upstrokes in waveform capnography, monitoring the capnogram allows tracking respiratory cycles. In addition, waveform capnography would enable monitoring quality of chest compressions during CPR, early detection of ROSC and determining patient prognosis.^{79,128,138}

2.1 USES OF CAPNOGRAPHY IN RESUSCITATION

Ensuring tracheal tube placement

Performing a rapid and successful tracheal intubation during resuscitation from cardiac arrest is of vital importance. However, given the difficulties and complexity of securing the airway in the field, it is not unexpected that unrecognized esophageal intubation may occur.^{59,136}

Detection of CO₂ in exhaled air, along with visualizing tracheal tube placement through the vocal cords are the most specific methods for confirming tracheal tube placement.^{79,80,138} While not ideal, correct tracheal tube placement can be qualitatively confirmed using a qualitative capnometry device.⁴⁴ Upon correct placement, a color change from purple to yellow will prompt. Whereas tube placement should be verified to rule out esophageal intubation in the absence of color change. Unfortunately, this devices showed low sensitivity and specificity, limiting its utility in the out-of-hospital setting, and should be avoided if waveform capnography is available.

With waveform capnography, obtaining the normal capnogram waveform (Figure 1.7) accurately confirms endotracheal tube placement. Whereas a flattened capnogram is more indicative of an esophageal intubation. Several studies containing a total of 440 OHCA patients who underwent out-of-hospital airway management showed that waveform capnography had a 100% specificity and a varying sensitivity between 57% to 100%.^{52,144,147,148} All esophageal intubations were properly detected. However, CO₂ concentration was not measurable in 52 properly positioned airways.¹⁴⁷

In summary, the presence of a detectable waveform capnography accurately confirms endotracheal tube placement, while its absence does not completely rule out a successful intubation.¹²⁸ Nevertheless, in case of an unrecognized esophageal intubation, removing the airway seems to be the reasonable strategy, since it is potentially fatal.

Monitoring ventilation rate

Satisfactory levels of oxygen are only available during the first minutes of cardiac arrest. However, as the resuscitation progresses, ventilation becomes more important as oxygen is exhausted and CO₂ levels begin to rise.^{20,102,137} Thus, proper ventilation management in low blood flow states like cardiac arrest turns a delicate balance between ensuring adequate oxygenation and removal of CO₂.

Current ALS resuscitation guidelines support the use of bag-valve-mask and advanced airways to assist with oxygenation and ventilation during OHCA. Before placement of any advanced airway, interrupted ventilation cycles of 2 ventilations every 30 compressions is the recommended ventilation strategy. Whereas after advanced airway placement, guidelines recommend asynchronous ventilation with continuous chest compression at a rate of 10 vpm.

Despite guidelines recommendations, excessive ventilation rates are common in resuscitation. A majority of EMS personnel ventilate at significant high rates during CPR, which may have clinical importance.^{84,104,110} In a clinical observational study, Aufderheide et al. reported ventilation rates of 30 vpm or more as a norm.⁹ Subsequent clinical studies have also confirmed the tendency to ventilate with such high rates.^{84,104} In addition, a porcine model revealed that animals ventilated at 30 versus 12 vpm showed increased intrathoracic pressures and decreased survival rates.¹¹ However, another animal study by Gazmuri et al.⁴⁵ reported no adverse hemodynamic effects during CPR after increasing ventilation rate and tidal volume over recommended values, although they observed a decrease in ETCO₂ values.

Although the association between hyperventilation and cardiac arrest outcome needs to be better elucidated, current guidelines recommend using waveform capnography feedback, as shown in [Figure 2.1](#), to monitor ventilation rate in order to provide high-quality ventilations and prevent over-ventilation. Automated measurement of ventilation rate and algorithms to detect over-ventilation using capnography were first explored by Edelson et al.³⁷ in 2010 as an alternative to

algorithms based on the detection of slow fluctuations in the TTI signal.^{5,49,120} Authors stated that visual inspection of the capnogram allows tracking respiratory cycles, since the onset of each ventilation causes a downstroke in the waveform capnography.



Figure 2.1. Capnogram segment acquired during cardiac arrest. High-quality ventilations are provided to the patient at a consistent rate of 11 ventilations per minute. Feedback is shown in the right side of the figure. Adapted from the Australian Resuscitation Council ALS guidelines.

Monitoring quality of chest compressions

In patients with cardiac arrest, chest compressions temporarily restore cardiac output. Both experimental and clinical studies have reported that survival from cardiac arrest depends on provision of adequate blood flow to vital organs.^{96,107,126} However, direct organ blood flow measurements is not feasible in out-of-hospital settings.

Studies, both animal^{33,66} and human^{17,114,135}, have shown an excellent correlation between ETCO₂ and cardiac output during states of low flow and during CPR, if chest compression rate and ventilation rate are relatively constant.^{17,44} Therefore, interpretation of ETCO₂ in the field must always take into account that constant controlled chest compressions and ventilations may be difficult or impossible, as this could affect the correlation between ETCO₂ and cardiac output.^{68,135}

Several researchers have suggested that the close correlation between cardiac output and ETCO₂ might be used to monitor the effectiveness of CPR in real time.^{17,44,54} However, to date, few studies have supported whether this can be used to guide care or improve outcome. Hamrick et al.⁵⁷ stated that ETCO₂ values are associated with compression depth and ventilation rate and that a greater depth will increase ETCO₂. Later,

in a multicenter observational study including both in-hospital and out-of-hospital cardiac arrests, Sheak et al.¹³⁴ showed that for every 10 mm increase in depth, ETCO₂ increased by 1.4 mmHg. However, in a larger prospective study conducted by Murphy et al.⁹¹ the same 10 mm increase was associated with a 4.0% increase in ETCO₂. In addition, a 10 cpm increase in chest compression rate and a 10 vpm increase in ventilation rate was associated with a 1.7% increase and a 17.4% decrease in ETCO₂, respectively.

In summary, waveform capnography could perform as a non-invasive measurement of the effectiveness of CPR in terms of generated blood flow. Although the first use of capnography during CPR appears to have come in 1978,⁷⁰ resuscitation guidelines did not specify any method or strategy to assess the effectiveness of chest compressions until recently. In 2013, a consensus document from the AHA recommended capnography as the primary physiological metric during CPR and suggested a CPR performance target of ETCO₂ > 20 mmHg, while values of ETCO₂ < 10-15 mmHg are considered suboptimal.⁸⁶ On the contrary, ERC guidelines on ALS suggest the use of waveform capnography to assess quality of CPR but do not provide a specific ETCO₂ target during resuscitation.¹³⁸ In any case, if ETCO₂ is low or diminishes over time as depicted in [Figure 2.2](#), either chest compression technique should be improved or a different EMS provider should perform chest compressions.



Figure 2.2. Capnogram segment acquired during ongoing chest compressions. ETCO₂ decreases over time with a constant ventilation rate. Chest compression technique or rescuer should be changed. Adapted from the Australian Resuscitation Council ALS guidelines.

Identifying ROSC during CPR

Survival chances of a victim of cardiac arrest highly depend on provision of oxygenated blood flow. Hence, providing an uninterrupted high quality CPR treatment to the patient is critical. In fact, several studies have reported that shorter duration of chest compression interruption – larger chest compression fraction – is associated with greater likelihood of ROSC,¹³³ survival to hospital discharge²² and improved outcomes.¹⁵² Whereas any kind of CPR interruption is potentially detrimental.

Current ALS resuscitation guidelines indicate that to avoid unnecessary CPR interruptions, pulse check in search of ROSC should only be made in two circumstances. When the ECG shows a pulsatile rhythm during rhythm assessment, or when the victim shows spontaneous breathing or movements.^{79,138} Thus, to avoid useless and potentially harmful CPR interruptions, an objective and continuous measurement of ROSC would be preferable.

Carbon dioxide concentration is strongly connected with cardiac output and blood flow through venous return. A return of a perfusing rhythm will increase cardiac output, which will in turn allow for accumulated peripheral CO₂ to reach the lungs, subsequently causing a rapid rise in ETCO₂.^{111,137} Thus, an abrupt increase in the CO₂ concentration could be an early indicator of ROSC and predict resuscitation success.^{35,18,82,132,134} It is important to note that, when evaluating for ROSC, the absolute ETCO₂ values are less important than the change between pre-ROSC to post-ROSC values.

In a pilot study from Pokorna et al.¹¹¹ ROSC was associated with a sudden and sustained increase of ETCO₂ \geq 10 mmHg. With this in mind, and due to the lack of relevant evidence to support a specific target, the latest resuscitation guidelines suggested using an increase in ETCO₂ to detect ROSC during CPR, without providing an exact value. Later, in a paper published by Lui et al.⁸² the diagnostic accuracy of an ETCO₂ sustained (3 min) increase greater than 10 mmHg was evaluated to predict ROSC. The authors included a total of 178 adult patients with non-traumatic OHCA, from which 34% of them had ROSC. Results showed that the post-ROSC median ETCO₂ value was 9 mmHg higher

that the median pre-ROSC value, a very similar value to the 10 mmHg difference reported by Pokorna et al.

Reported sensitivity for predicting ROSC of the 10 mmHg threshold was 33% with an specificity of 97%. However, despite the low sensitivity value, results of the study were promising. Reported specificity value was higher than the value reported by Pokorna et al., and when using a tool to take a potentially harmful decision like stopping CPR, a high specificity is extremely important in order to limit inadvertent interruptions.

In conclusion, providers should look for a jump of at least 10 mmHg on capnometry (Figure 2.3). However, an abrupt rise in ETCO₂ is a non-sensitive marker for ROSC, meaning that the lack of an abrupt rise of ETCO₂ does not necessarily mean absence of ROSC.¹²⁹



Figure 2.3. Capnogram segment showing a sudden increase in ETCO₂ as a result of the return of spontaneous circulation. Adapted from the Australian Resuscitation Council ALS guidelines.

Prognosis during CPR

Since ETCO₂ indirectly reflects organ perfusion during CPR, it may not only represent a target for resuscitation effectiveness, but it also may help guide clinicians in assessing whether continued resuscitation in cardiac arrest is futile or not.^{112,149,156} Values < 10 mmHg after 20 minutes of ongoing resuscitation have been associated with minimal chances of survival.⁷⁸ This was confirmed in a study by Kolar et al. where none of the patients presenting < 10 mmHg at any time survived. In addition, a target of > 10 mmHg has been used as a criterion for considering extracorporeal life support in patients with refractory cardiac arrest,¹³⁹ although two recent studies did not find any evidence supporting the use of ETCO₂ in this context.^{32,34}

Other prognostic indication of ETCO_2 may be prediction of successful defibrillation. A recent study including 62 OHCA episodes showed that non of the patients presenting ETCO_2 values < 7 mmHg before shock had successful defibrillation. Whereas patients whose ETCO_2 value was > 45 mmHg had a 100% chance of successful defibrillation.¹³⁰ Nevertheless, this preliminary data needs further confirmation from other studies.

Unfortunately, large differences in etiology and influence of cause of cardiac arrest, lack of controlled ventilation during CPR, inconsistent or undefined timings of ETCO_2 measurements, and the need for an advanced airway to reliably measure ETCO_2 limits the confidence in the use of capnometry for prognostication. Additional studies are needed to better identify the optimal measurement of ETCO_2 and timing targets. Thus, resuscitation guidelines do not recommend using ETCO_2 as the only factor in the determination to stop CPR efforts.

To conclude, ETCO_2 presents a decreasing trend in patients in whom resuscitation is unsuccessful, while there is an increase tendency in those who survive, indicating a progressive improvement in tissue perfusion and venous return.^{52,78} Hence, ETCO_2 variations could be more suitable than punctual measurements to predict ROSC and subsequent survival, although evidence on this field is still scarce.¹⁸

2.2 CAPNOGRAM WAVEFORM DURING CPR: THE PHENOMENON OF CHEST COMPRESSION ARTIFACT

To ensure a reliable analysis, either visual or automated, and to enable emphasized advantages during resuscitation, quality of the recorded capnogram waveform is essential. All phases of the capnogram (Figure 1.7) must be clearly identifiable in the capnogram during CPR. However, non-distorted capnograms (Figure 2.4, left), in which all different phases of the respiratory cycle (inspiratory downstroke and baseline, expiratory upstroke and alveolar plateau, where the ETCO_2 is measured) are identifiable cannot always be observed during CPR.

Among others, some artifact sources include issues related with the capnography device (such as CO₂ circuit occlusion or leaking) as well as ongoing resuscitation efforts like provided chest compressions and patient movement during transportation.^{62,145}

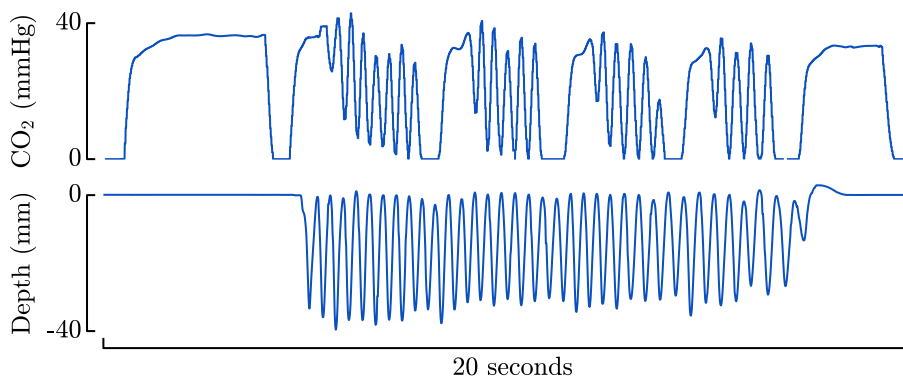


Figure 2.4. Waveform capnography signal segment during ongoing chest compressions.

Several studies have reported the appearance of fast oscillations synchronized with chest compressions (Figure 2.4, right), at different rates and with varying amplitude, superimposed on the capnogram; often completely obscuring the normal tracing.^{31,115,154} Nevertheless, this phenomenon has received little attention in the literature and it was not systematically addressed until 2010 in an abstract of a preliminary study presented at the AHA Resuscitation Science Symposium.⁶⁴ Authors reported the presence of, what they called, chest compression oscillations, in more than 70% of the capnograms in a cohort of 210 OHCA episodes. Since then, only a few studies aimed to explain the origin of the chest compression oscillations have been published.

Origin of induced chest compression oscillations

The mechanism by which external chest compression induce chest compression oscillation on the capnogram is still not clear. There are a few hypothesis that have been proposed. Deakin et al.³¹ suggested that, during compression-only CPR delivered by the LUCAS, external

chest decompression – chest recoil –, which generates a negative intrathoracic pressure, allows air to enter through an open airway, and thus ventilation may occur passively as shown in [Figure 2.5](#).

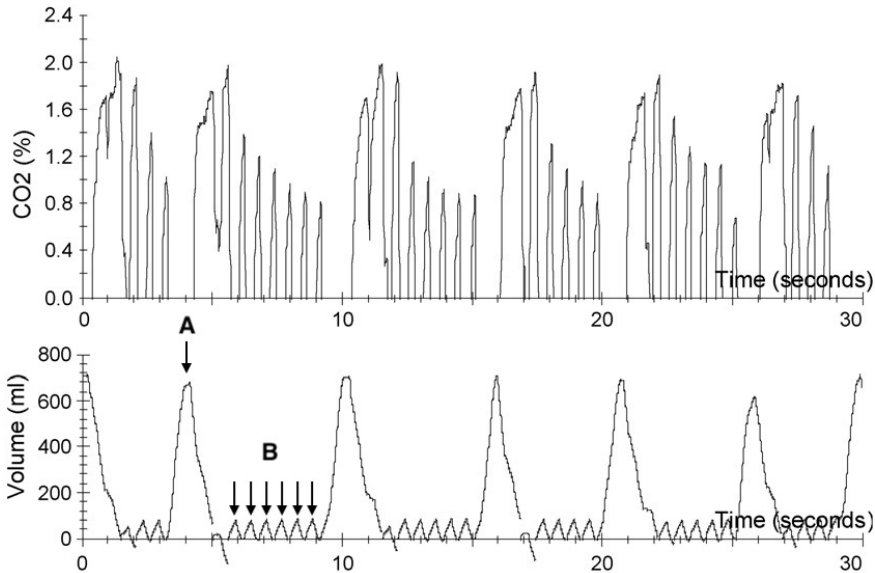


Figure 2.5. Waveform capnography and tidal volume signals recorded during resuscitation, showing manual (A) and passive (B) ventilations generated by chest compressions with volumes around 700 and 60 ml, respectively. Corresponding induced chest compression oscillations are also shown. Extracted from Deakin et al.³¹

In a similar way, Idris et al.⁶⁴ proposed that, during active chest compression and decompression phases, oscillations could be caused by gas moving in and out of the airway and passing in front of the CO₂ sensor.

This phenomenon of *passive ventilations* has been scarcely reported in the literature. Deakin et al.³⁰ found that the median tidal volume of these passive ventilation was 41.5 ml, ranging between 33.0 and 62.1 ml. In a subsequent study, Vanwulpen et al.¹⁵⁴ quantified the inspiratory volumes generated by manual chest compressions in the out-of-hospital setting. Their results were in line with the study by Deakin et al., although they found a wider range of inspiratory volumes, between 4 and 62 ml. In a recent human study of patients with prolonged CPR,

McDannold et al.⁸⁵ reported that passively generated median tidal volume was 7.5 ml. They did observe tidal volumes above 40 ml but most (80%) measured volumes were below 20 ml. Authors concluded that generated tidal volumes were far less than average anatomical dead space, impeding effective alveolar ventilation.

Although these volumes are considerably less than the typical anatomical dead space of an adult patient (≈ 150 ml), they seem to be enough to induce a distortion on the capnogram, hereinafter CC-artifact, as it can be seen in the top panel of [Figure 2.5](#). However, little is known about the potential factors influencing the appearance of the CC-artifact. Indeed, Idris et al.⁶⁴ reported that oscillations appeared in 70% of the episodes, not in all of them. This suggests that factors like airway type, rescuer's chest compression technique, capnography technology or even patient condition could have a role in CC-artifact generation.

In a recent study published by Cordioli et al.²⁸, authors describe a phenomenon associated with lung volume reduction called *intrathoracic airway closure*, which impedes chest compressions to generate passive ventilations and, overall, limits effective alveolar ventilation. This phenomenon represents the physiological lack of communication between the intrathoracic compartment and the airway opening.⁵¹ The presence of airway closure during CPR impedes the transmission of generated inspiratory flow despite the significant negative pressure produced by chest decompressions.²¹ Hence, no passive tidal volumes can be produced and the appearance of CC-artifact is virtually null. Nevertheless, despite the huge clinical relevance of their findings, additional studies on the topic are required in order to assess the relative contribution of airway closure in the generation of CC-artifact.¹¹⁸

In summary, provided chest compressions generate tidal volumes, that, despite being way smaller than anatomical dead space, they are able to induce CC-artifact oscillations in the capnogram. Recent studies have reported that the appearance of the CC-artifact could be limited by intrathoracic airway closure, which hinders expiratory tidal volumes to be transmitted to the airway opening and impedes correct alveolar ventilation.

Possible adverse effects of CC-artifact on ventilation feedback

One of the main hypothesis of this work, never before explored in the literature, was that CC-artifact could negatively affect waveform capnography feedback in three aspects: causing errors in the automated detection of ventilations and consequently in the estimation of ventilation rate, impeding a reliable measurement of ETCO_2 values, and limiting CPR providers' clinical decisions since distorted capnogram are difficult to interpret.

In line with this hypothesis, in a brief letter to the editor, Raimondi et al.¹¹⁵ described a mismatch between capnometry feedback values (ventilation rate and ETCO_2) and the values that could be visually inferred from the capnogram waveform. [Figure 2.6](#) shows two examples of capnogram segments obtained from a waveform capnography device during manual and mechanical CPR in which differences in provided feedback can be observed.

Authors concluded that displayed ventilation rate and ETCO_2 were, respectively, over- and underestimated and continuously changed in the presence of CC-artifact. They suggested looking at the curves instead of the values for proper clinical interpretation. However, there is still room for further research since heavily distorted capnograms could lead to a lack of confidence in the interpretation of the signal.

2.3 FACTORS COMPLICATING THE CLINICAL INTERPRETATION OF ETCO_2

In addition to the possible lack of reliability of capnography in presence of CC-artifact, several factors need to be taken into account when interpreting ETCO_2 measurements during cardiac arrest. First, chest compressions and ventilation have opposing effects on ETCO_2 levels. While chest compressions increase CO_2 concentration proportionally to generated blood flow, delivering CO_2 from the tissues to the lungs, ventilations remove CO_2 from the lungs, decreasing ETCO_2 as ventilation rate or tidal volume increases.²⁷

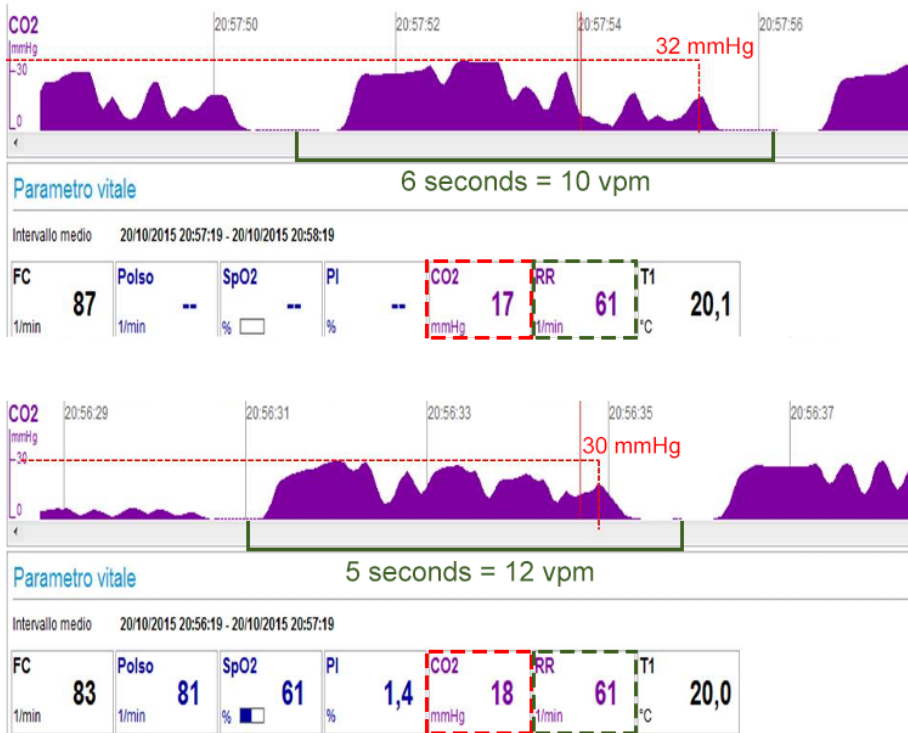


Figure 2.6. Mainstream capnography during manual (top) and mechanical (bottom) CPR performed to the same patient. Extracted from Raimondi et al.¹¹⁵

In an animal model of cardiac arrest Gazmuri et al.⁴⁵ demonstrated that increasing either respiratory rate (from 10 to 33 vpm) or tidal volume (from 6 to 18 ml kg⁻¹) during CPR had similar effects on ETCO₂, which decreased from 43 to 20 mmHg (Figure 2.7). In addition, when both were increased, ETCO₂ decreased to 14 mmHg but in a lower extent, showing that ETCO₂ exponentially decreases when either rate or tidal volume increases.

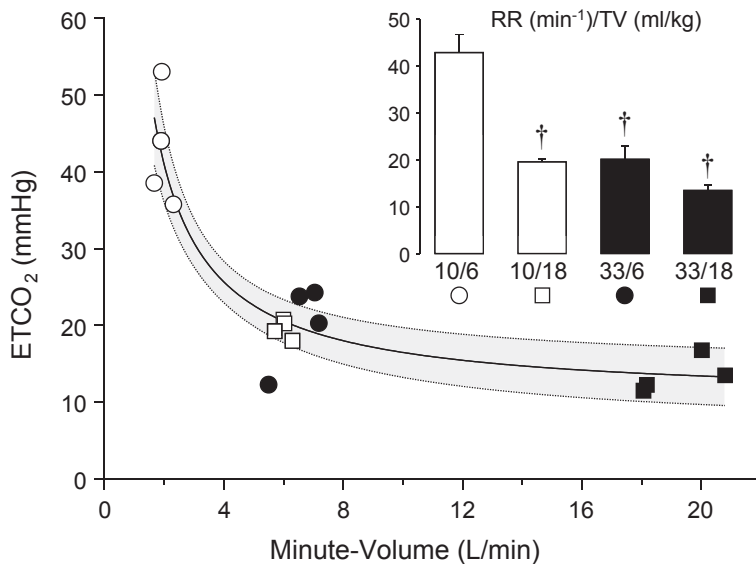


Figure 2.7. ETCO₂ plotted as a function of the ventilation minute-volume delivered during CPR. RR = Respiratory rate; TV = Tidal volume. Adapted from Gazmuri et al.⁴⁵

Second, in patients with an asphyxial cause of arrest, initial ETCO₂ levels may be higher than in cardiac causes. During a respiratory arrest, cardiac output remains stable for a short period of time before cardiac standstill. Meanwhile, the CO₂ produced in the tissues will continue to be delivered to the lungs, increasing CO₂ concentration.^{53,60} This means that, in the absence of respiration, CO₂ will stay in the lungs and, as remaining oxygen is being utilized, more CO₂ will be delivered.

Finally, both ETCO₂ values and its clinical significance may vary during resuscitation depending on the several drugs provided to the patient. Several studies have shown that right after administration of adrenaline an increase in coronary and cerebral perfusion pressure is produced, in parallel with a rapid decrease of ETCO₂ values.^{58,146} Conversely, administration of sodium bicarbonate momentarily raises ETCO₂ values by a mean increase of 6.4 ± 0.5 mmHg.¹⁰¹

3 | OBJECTIVES

Nowadays, waveform capnography is considered a standard of care in advanced CPR. Quality of the recorded capnogram is essential for reliable monitoring of ventilation quality and patient's hemodynamic response. By the time this thesis work started, the phenomenon of high-frequency oscillations superimposed on capnogram waveform during CPR had received little attention in the literature, only a few communications had alerted that accuracy of clinical values derived from waveform capnography in the presence of chest compressions could be called into question.

One of the main hypothesis of this thesis was that the presence of CC-artifact in the capnogram during resuscitation interventions could severely affect ventilation monitoring as well as accurate measurement of ETCO_2 , therefore compromising the reliability of waveform capnography in resuscitation. In addition, at the beginning of this thesis work, capnography was the standard of care to ensure correct airway placement and to prevent over-ventilation. However, there was a large gap of knowledge addressing other potential roles of waveform capnography that were highlighted in the resuscitation guidelines in force.

In this context, the main objective of this thesis work was to **analyze the feasibility of waveform capnography as a reliable non-invasive indicator of CPR quality and ROSC during out-of-hospital cardiac arrest**. In order to accomplish this objective, a set of intermediate goals was defined.

1. *To analyze and quantify the impact of CC-artifact on a capnogram-based monitoring system during CPR.* Although capnographs were initially designed for patient monitoring during in-hospital medical interventions, its use has spread out to out-of-hospital emergency medicine. This could lead to device malfunctioning during resuscitation since capnograph manufacturers may have not taken into account such tough environment. In particular, the following tasks were defined:
 - To address the incidence and morphology of CC-artifact on resuscitation capnograms. (A1, C1, C2, BC1)^a
 - To quantify the influence of CC-artifact on the automated detection of ventilations and therefore on the accuracy of ventilation rate feedback. (A1, C1, C2, BC1)
 - To address the impact of CC-artifact on the reliability of ETCO₂ measurements. (A2, C3)
2. *To design signal processing techniques to remove CC-artifact from the capnogram to improve ventilation rate feedback and to enhance capnogram clinical interpretation.* Under the assumption that CC-artifact would negatively affect capnogram reliability, this work sought to suppress or mitigate its effects. Here two main approaches were studied:
 - To design filtering techniques to suppress the CC-artifact from the capnogram and to evaluate their goodness through the improvement on ventilation detection. (A3, C4, C5, BC1)

^a Related publications. A: Article, C: Conference, BC: Book Chapter

- To develop a novel technique to enhance the capnogram waveform in the presence of CC-artifact in order to improve its clinical usefulness. (A4, C6, C7, BC1)
3. *To characterize the influence of ventilations on ETCO₂ measurement.* Chest compressions and ventilations during CPR have opposing effects on the exhaled carbon dioxide CO₂ concentration, which need to be better characterized. The aim was to obtain a model for explaining the variation of exhaled CO₂ concentration with ventilations. This could allow for explaining the effect of chest compressions on ETCO₂ once the influence of ventilations is compensated. (A5, C8)
 4. *To develop novel strategies to identify ROSC using the capnogram as the reference.* Accurate ROSC detection using waveform capnography during CPR still remains a challenge. Existing methods are based on the detection of a sudden increase in the ETCO₂ level. The aim was to derive a new metric that could allow for accurate detection of ROSC using the ETCO₂ values of consecutive ventilations. (A6)

The accomplishment of these objectives would contribute ultimately to improve the quality of CPR during cardiac arrest. Methods resulting from the first and second objectives could be integrated into commercial capnographs, improving measurement of ventilation rate and ETCO₂. Results from the third objective could help to understand the role of ETCO₂ in monitoring chest compression quality. Finally, results from the fourth objective would provide knowledge about the significance of ETCO₂ as an adjunct to detect ROSC.

4 | MATERIALS AND METHODS

This chapter presents an overview of the materials and methods used in the development of this thesis work. The chapter is organized in two sections. The first one introduces the OHCA databases used as the data source for all the studies. The second section provides an overview of the annotation process and of the methodology followed to address each objective. Study results are presented in [chapter 5](#), while the main conclusions of the thesis are described in [chapter 6](#). Finally, the [Appendix A](#) compiles all the related publications for further information.

4.1 OHCA DATABASES

All studies in this thesis work were retrospective. OHCA episodes were obtained from two prospective collections. The first database was collected by Tualatin Valley Fire & Rescue (TVF&R), an ALS first response EMS agency serving eleven incorporated cities in Oregon (USA). The second database was collected by an ALS agency of Emergentziak-Osakidetza (E-O), located in Artaza (Leioa, Spain), serving eight municipalities.

TVF&R database

Since April 2006, TVF&R has recorded data during resuscitation efforts for cardiac arrest victims. Until December 2017 these agencies have participated in the Resuscitation Outcomes Consortium (ROC) Epidemiological Cardiac Arrest Registry, an effort that has included careful association of clinical data with the technical data obtained during resuscitation. Episodes were recorded using Heartstart MRx (Philips, USA) monitor-defibrillators equipped with real-time CPR feedback technology (Q-CPR) and Microstream™ (Oridion, Israel) sidestream capnography technology. Access to the database was achieved thanks to a collaboration between the GSC^a research group and OHSU.

In the early years, CPR followed the 30:2 compression-ventilation approach. Later, following the High-Quality CPR recommendations made by the AHA in 2012 the approach was changed to manual continuous chest compressions without pauses for ventilation. Ventilations were also manually provided using a bag-valve-mask or an advanced airway. The choices for the latter were ETT or the King LT-D SGA. The data collection for the ROC Epistry was approved by the Oregon Health & Science University (OHSU) Institutional Review Board (IRB00001736).

E-O database

Since June 2018, Emergentziak-Osakidetza has made an effort to consistently develop a new OHCA database including a careful association between clinical and monitor-defibrillator data. Episodes were recorded using Reanibex 500 EMS (Bexen Cardio, Spain) monitor-defibrillators equipped with a proprietary real-time CPR feedback technology known as Push-Pad and Masimo ISA™ CO₂ (Masimo, Sweden) sidestream capnography technology. This data collection was possible thanks to the collaboration between Emergentziak-Osakidetza and the GSC research group.

^a The Signal and Communications Group (GSC by its Spanish acronym) is the research group in which this thesis work has been developed.

For every cardiac arrest episode, alternating series of 30 chest compressions with two ventilations were provided until an ETT airway was placed. Then, continuous chest compressions were manually provided following the ERC guidelines. Ventilations were also manually provided. The data collection for this project was approved by the Ethical Committee of Research with Medicines of the Basque Country^b (PI2018003).

Available signals and clinical information

For each OHCA episode, data were provided anonymous and contained no personal information, but Utstein style sheets with clinical information of the patient such as age, gender, initial rhythm, airway type, ROSC (*yes/no*), disposition and neurological outcome were available for every episode. In addition, defibrillators acquired and stored the following concurrent signals (Figure 4.1):

- *ECG signal*. Obtained from the defibrillation pads, or from limb or precordial leads. Sampling rate of 250 Hz (TVF&R) or 100 Hz (E-O).
- *TTI signal*. Measured by injecting a sinusoidal current through the defibrillation pads. Sampling rate of 200 Hz (TVF&R) or 100 Hz (E-O).
- *Force signal*. Acquired through the pressure sensor in the Q-CPR feedback pad at a sampling rate of 100 Hz. Only available for TVF&R episodes.
- *Acceleration signal*. Obtained by the accelerometer inside the CPR feedback pads. Sampling rate of 100 Hz (TVF&R) or 35 Hz (E-O).
- *Compression depth signal*. Calculated from the acceleration signal using two different algorithms: for TVF&R the algorithm described in Aase and Myklebust² which also needs the force signal; for

^b Comité de Ética de la Investigación con medicamentos de Euskadi (CEIm-E)

E-O the algorithm developed by González-Otero and Ruiz⁴⁸ which only needs the acceleration signal.

- *Capnography signal*. Obtained from a CO₂ detector. Sampling rate of 125 Hz. (TVF&R) or 20 Hz (E-O).

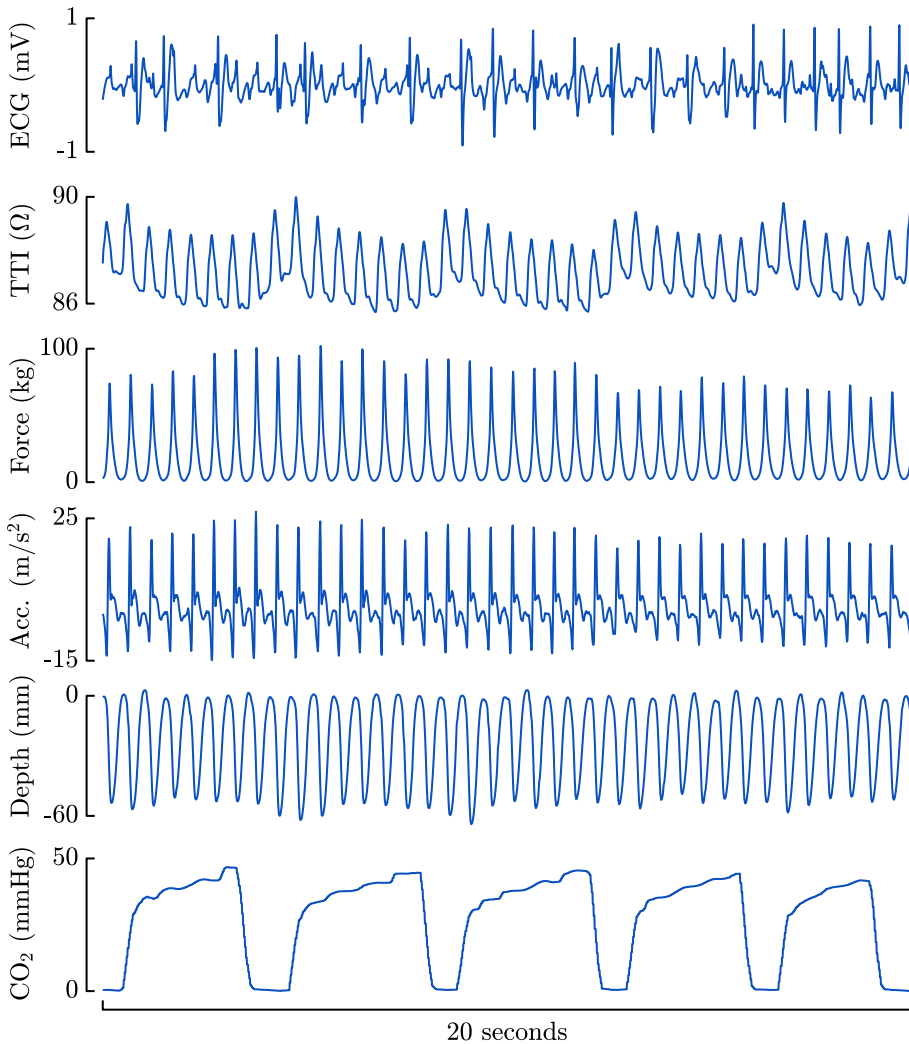


Figure 4.1. Example segment extracted from an OHCA episode from the TVF&R database.

4.2 ANNOTATION AND METHODOLOGY

In general, only episodes with concurrent ECG, compression depth, TTI and capnography signals were included. Signals were reviewed and annotated using custom-made Matlab[®] (Mathworks, USA) programs. Episodes with unreliable raw signals caused by disconnections or excessive noise were discarded. For each episode, capnograms were time-shifted to compensate for the delay introduced by the sidestream technology with respect to the other recorded signals.

Several biomedical engineers with experience in the analysis of OHCA defibrillator signals participated in the annotation process and methodology design of each study. As a normal practice, one third of the cases were jointly reviewed defining needed annotation rules. The rest of the episodes were randomly split into sets and each of them was examined by a single reviewer. At the end of the process, undecided annotations were conjointly solved.

Depending on the particular study, different annotation procedures and methodologies were designed. Next subsections summarize the procedure followed to develop each of the objectives described in [chapter 3](#). For a more detailed explanation, please consult the corresponding journal article in [Appendix A](#).

Objective 1: To analyze and quantify the impact of CC-artifact on a capnogram-based monitoring system during CPR

To address the incidence and morphology of CC-artifact on resuscitation capnograms, episodes were classified into non-distorted and distorted groups regarding the appearance of CC-artifacts on the capnogram. Episodes were grouped as distorted if evident CC-artifact appeared during more than 1 min of the total chest compression time. Otherwise, episodes were grouped in the non-distorted category. Distorted episodes were then grouped into three categories: type I, when the CC-artifact was located in the ventilation plateau; type II, located in the capnogram

baseline; type III, with CC-artifact spanning from the plateau to the baseline. Figure 4.2 summarizes the classification process.

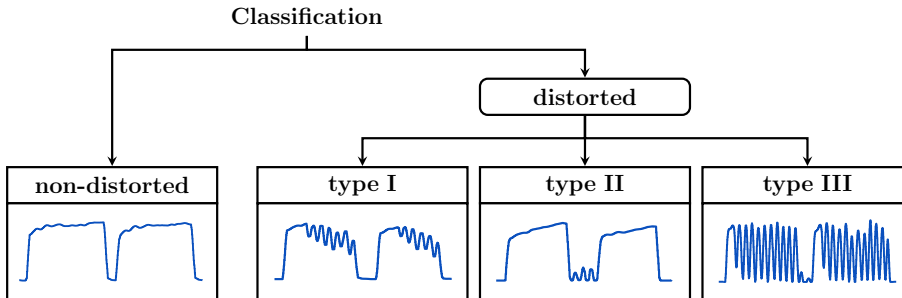


Figure 4.2. OHCA waveform capnography classification chart.

Then, the morphology of the CC-artifact was characterized by the spectral analysis of non-distorted and distorted capnograms. We, computed the power spectral density (PSD) of the capnogram segments, located the frequency components associated with the artifact and compared with the chest compression rate derived from the chest compression depth signal.

To quantify the influence of CC-artifact on the automated detection of ventilations and therefore on the accuracy of ventilation rate, ventilation instances were annotated using the TTI signal (Figure 1 in A1). Ventilations induce slow fluctuations in the TTI signal acquired through defibrillation pads. During inspiration TTI increases due to the increment of the gas volume inside the chest and the longer distance between electrodes which produces a decrease in the conductivity.^{37,81,108} To enhance the slow fluctuations caused by ventilations, the raw TTI signal was low-pass filtered.

The processed signal was visually examined to manually annotate the position of each single ventilation. Ventilations were annotated at the instant corresponding to a rise in the impedance (vertical red lines). The capnogram was used to visually confirm the presence of ventilations. Resulting ventilation annotations were used to evaluate the effectiveness of the proposed filtering techniques and to compute the ventilation rate.

To assess the influence of CC-artifact in the detection of ventilations, a capnogram-based ventilation detection algorithm was used. Figure 2 in [A1](#) shows a detailed scheme of the detector. Basically, the algorithm locates series of consecutive upstrokes (t_{up}) and downstrokes (t_{dw}) in the capnogram by applying a fixed amplitude threshold (Th_{amp}). The durations between those instants, D_{ex} and D_{in} , are the two features used to discriminate true ventilations from the potential candidates, according to a simple decision tree based on thresholds. Similar algorithms to detect ventilations in the capnogram have been previously described in the literature.³⁷

Finally, ventilation detection performance was evaluated in terms of its sensitivity (Se) and positive predictive value (PPV). To assess the influence of the CC-artifact in the estimation of ventilation rate, the ventilation rate value per minute was computed using the ventilations detected by our algorithm and compared to the values obtained annotated ventilations.

To address the impact of CC-artifact on the reliability of ETCO₂ measurements, 1-min length capnogram segments containing series of complete ventilations were extracted (Figure 1 in [A2](#)). Only segments with regularly reported capnometry events were included. Two types of segments were identified: non-distorted capnograms and distorted capnograms of any type. Each individual ventilation was identified as described above and corresponding ETCO₂ values were manually annotated as the maximum CO₂ level in each ventilation cycle.⁵¹

To conclude, differences between the annotated and the capnometer ETCO₂ value per ventilation in the segment were analyzed. Measurement error was defined as the difference between the extracted and the annotated ETCO₂ values. Comparisons between airway types and between capnometers were also assessed.

Objective 2: To design signal processing techniques to remove CC-artifact from the capnogram to improve ventilation rate feedback and to enhance capnogram clinical interpretation

Using the database developed for the previous objective, the next step was to remove the CC-artifact from the capnogram and test if ventilation feedback improved. Moreover, recovered capnogram had to be suitable for clinical interpretation.

To suppress the CC-artifact from the capnogram, three different filtering techniques were used. In addition to the annotations previously made, chest compression instances were annotated at the local minima corresponding to the maximum depth reached for each chest compression. Chest compression rate was calculated from the annotations as the inverse of the distance between consecutive maxima, expressed in compressions per minute.

Filtering techniques have been typically used for the suppression of chest compression artifact present in most of the signals acquired by monitor-defibrillators, especially in the ECG and TTI signals.⁴⁶ Likewise, the objective was to apply some of these techniques to distorted capnograms:

- *Fixed-coefficient filtering.* Observation of the spectral content of the distorted signal sometimes supports the use of a simple filter with fixed coefficients to suppress the undesired frequencies.^{47,49,140} Observation of the PSD (Figure 2 in A3) supports the use of a simple filter to suppress the spectral content of the capnogram above 1 Hz (60 cpm). To that end, we implemented a digital infinite impulse response low-pass Butterworth filter.
- *Adaptive filtering.* Variability of chest compression rate may affect the effectiveness of the fixed-coefficient filter.^{4,86} Adaptive approaches in which the filter configuration is adjusted in time according to the varying characteristics of the artifact could be a suitable solution.^{1,39,67,123} Two adaptive filtering configurations were designed, an open-loop and a closed-loop adaptive filter.¹⁵⁹ Both approaches used the annotated chest compression instances

as a reference to adjust the parameters of the adaptive filter. Details of the adaptive filters are addressed in the supporting materials in [A3](#).

To enhance the capnogram waveform in the presence of CC-artifact in order to improve its clinical usefulness, a novel CC-artifact suppression technique was proposed. Although classic filtering techniques may improve ventilation detection, artifact oscillations cannot always be successfully removed (Figure 1 in [A4](#)). This new approach relies on the hypothesis that the envelope of the capnogram contains the information needed to suppress the CC-artifact and to rebuild a reliable capnogram waveform.

To quantitatively assess the goodness of the proposed techniques, the previously designed ventilation detection algorithm was used before and after applying the suppression techniques. For each episode, we also computed the number of ventilations provided every minute (ventilation rate) and compared ventilation rate measurements computed from the estimated ventilations before and after filtering with those computed from the annotated ventilations.

Objective 3: To characterize the influence of ventilations on ETCO₂ measurement

Many factors influence ETCO₂ during CPR, and ventilation rate is a significant confounding factor. The hypothesis was that that the effect of ventilations on ETCO₂ could be modeled separately from other confounders. First, modeling the impact of ventilation on the capnogram would facilitate a better assessment of the relationship between chest compression quality and waveform capnography. Second, it would allow accounting for the confounding factor of ventilation rate in studies analyzing the correlation between ETCO₂ values and ROSC or patient outcome.

The aim of this study was to model the decrease in exhaled CO₂ concentration with ventilations. For that purpose, capnogram segments during chest compression pauses (no flow time), and with no perfusing rhythm (no circulation) were selected (Figure 1 in [A5](#)). Absence of chest

compression was verified using compression depth and TTI signals. Ventilation instances were identified following the procedure described in the first objective. Absence of pulse-generating rhythm was verified by inspecting the ECG. Pulseless electrical activity and perfusing rhythm were distinguished by additional checking of the circulatory component of the TTI signal.¹²²

When analyzing the capnogram segments, the duration of each ventilation cycle was different within each segment. This phenomenon affects the ETCO_2 value since the plateau phase usually presents a low ascendant slope. In order to compare analogous points, decreasing CO_2 values at a fixed delay from the beginning of the expiratory upstroke were annotated. This novel metric, named ensemble plateau CO_2 or epCO_2 , was defined to represent the end-tidal values obtained if all ventilations had the same exhalation time (Figure 2 in A5).

The decay in epCO_2 , as illustrated in Figure 3 in A5, suggested an exponential decay model. Thus, the trend in epCO_2 variation was modeled through a Matlab[®] curve fitting tool using an exponential decay function. The decay factor between consecutive ventilations D was computed and goodness of fit of the model was evaluated using the coefficient of determination R^2 , which provides a measure of the epCO_2 variation that is explained by the model. Differences in the decay factor D with respect to the airway, ETT or SGA, was also analyzed.

Objective 4: To develop novel strategies to identify ROSC using the capnogram as the reference

The working hypothesis for this objective was that the variation of ETCO_2 between consecutive ventilations during chest compression pauses would allow for a reliable ROSC detection. The analysis of the ETCO_2 trend could help to confirm ROSC if an organized rhythm is observed. A decay in the ETCO_2 values would indicate the absence of pulse (i.e. no ROSC). Whereas a constant or increasing ETCO_2 trend would indicate the presence of pulse and therefore ROSC.

Segments of capnography signal during chest compression pauses were identified (Figure 1 in A6). In this case, only segments shorter than 20s, with at least three ventilations, and with $ETCO_2$ values equal or greater than 10mmHg were included in the analysis. The selected segments were then grouped into ROSC and non-ROSC groups. The clinical ROSC annotations, made by ALS providers, and the presence of an organized rhythm in the ECG were reviewed in order to classify the segments. In case of doubt between an organized pulseless electrical activity (PEA) or a pulsatile rhythm (PR), TTI signal was examined to locate a possible circulation component.¹²² A single ROSC segment was selected per patient. Conversely, several non-ROSC segments per patient were included.

Once a segment met the inclusion criteria, several values were annotated such as segment duration, number of ventilations per segment and the $ETCO_2$ value per ventilation (ET_n), obtained as the maximum CO_2 concentration reached in the capnogram plateau. Segments were then characterized by: the mean ventilation rate, the $ETCO_2$ value for the first ventilation (ET_0), percentage $ETCO_2$ variation between consecutive ventilations (ET_n) and the mean percentage variation (ΔET_{avg}).

Discrimination between ROSC and non-ROSC groups was conducted using the ΔET_{avg} feature as an indicator of the positive or negative slope of the $ETCO_2$ trend. Based on a simple decision threshold, segments presenting greater ΔET_{avg} were classified as ROSC and values equal to or less than the threshold were classified as non-ROSC. Finally, the predictive ability of the discrimination method was evaluated in terms of its sensitivity (Se) and specificity (Sp).

5 | RESULTS AND DISCUSSION

This chapter summarizes and discusses the results of this thesis work, all of which have been published in indexed JCR journals. The chapter is organized by the objectives defined in [chapter 3](#).

Objective 1: To analyze and quantify the impact of CC-artifact on a capnogram-based monitoring system during CPR

The incidence and nature of the artifact was not previously studied in the literature. To our knowledge, only one prior study examined the impact of chest compressions and reported that 73% (154/210) of the episodes were distorted by oscillations. In our retrospective study (A1) a lower incidence (42%) of distorted capnograms was found with a similar number of OHCA episodes, although this difference could be partly explained by different annotation criteria. Oscillations did not appear in the episodes where BVM was used. However, it appeared in both advanced airway types, although the incidence was higher for SGA. In addition, the conducted spectral analysis quantitatively confirmed the pure sine wave nature of the artifact, with a frequency matching the chest compression rate.

Waveform capnography is currently a standard monitoring tool used during resuscitation. Unfortunately, our findings demonstrated the negative impact of CC-artifact on the reliability of capnogram guided ventilation monitoring. Detection of ventilations was accurate for non-distorted capnograms, Se and PPV median values were 99.4% and 98.6%, respectively. However, detection performance significantly decreased in the presence of CC-artifact to Se and PPV values well below 80% and errors in ventilation rate measurement were as high as 50%.

Once demonstrated that the presence of CC-artifact diminishes the accuracy of automated capnogram-based ventilation detectors, we also wanted to analyze if this could also have a negative impact on ET CO_2 measurement. When obscured by CC-artifact, the capnogram tracing becomes difficult to interpret; clinicians might then rely on capnometry values reported on the monitor screen. However, the reliability of these numbers has also been questioned.

In another retrospective study (A2), we quantified the influence of the CC-artifact in the automated ET CO_2 measurements performed by capnometers from TVF&R and E-O. After extensive analysis of the extracted capnogram segments, we demonstrated that the presence of CC-artifact also affects reported ET CO_2 values. For capnogram segments without CC-artifact, the obtained measurement error was negligible. However, errors increased in the presence of CC-artifact to 1.3 mmHg, but, more importantly, we found errors exceeding 10 mmHg in 9% of the distorted ventilations (15 mmHg in 5%). Moreover, we found errors as high as 20 mmHg in some capnogram segments. No significant differences were found between capnometers ($p = 0.41$) nor airway types ($p = 0.28$).

In conclusion, CC-artifact provokes continuous and significant errors in the algorithm designed to detect ventilations and, therefore, to estimate a single ET CO_2 value per ventilation. If ventilation rate and ET CO_2 values were displayed on the monitor-defibrillator screen, clinicians would see them changing rapidly, and ventilation monitoring as well as clinical decision rules could be seriously compromised.

Objective 2: To design signal processing techniques to remove CC-artifact from the capnogram to improve ventilation rate feedback and to enhance capnogram clinical interpretation

From a clinical perspective, the presence of CC-artifact has several important drawbacks: firstly, it impedes a reliable automated detection of ventilations, causing inaccuracies in the measurement of ventilation rate. Moreover, a distorted capnogram tracing becomes difficult to interpret by clinicians; and finally, measurement of reliable ETCO_2 values becomes impossible. Hence, CC-artifact may jeopardize most potential uses of waveform capnography during resuscitation. In this context, we hypothesized that recommended uses of waveform capnography would improve if the oscillations induced by chest compressions could be successfully removed from the capnogram.

The initial approach, reported in [A3](#), focused on the improvement of automated detection of ventilations using three different filtering techniques, a fixed coefficient and two adaptive filters (open-loop and closed-loop); to pre-process the raw capnogram before the ventilation detector is used. All the proposed filters performed similarly, reporting improved results for the distorted episodes, with Se and PPV values well above 97% and 96%, respectively. This also caused an improvement in the measurement of ventilation rate with a median error decreasing from values as high as 50% to values below 3.6%.

Despite the improvement achieved in ventilation detection, the filtered capnogram is still difficult to interpret by clinicians. The capnogram waveform achieved after filtering approximates the mean peak-to-peak amplitude of the oscillations, as shown in [Figure 5.1](#). The resulting capnogram waveform hinders the reliable analysis of ETCO_2 values and trends, a very useful clinical information during OHCA.

In a subsequent study ([A4](#)) we proposed a CC-artifact suppression technique aimed to preserve the real tracing of the waveform capnography. The development of the method relied on the hypothesis that the envelope of the capnogram could be a reliable tracing for clinical interpretation. An example of the method performance is illustrated in [Figure 5.2](#). For a detailed explanation of the method please consider reading the supplementary materials available in the attached [A4](#) article.

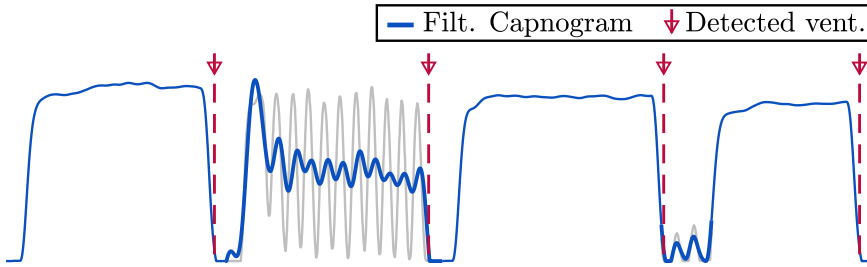


Figure 5.1. Example of filtering performance. Original capnogram with non-distorted and distorted capnogram cycles depicted in gray. Filtered capnogram (in blue) superimposed to the original capnogram. Detected ventilations are depicted with vertical dashed red lines.

The resulting corrected waveform is useful to improve the automated assessment of ventilations, real-time estimation of ventilation rate, and, more importantly, it allows a reliable measurement of ETCO_2 values. Performance results were comparable and even better than the ones obtained using classic filtering approaches. In most cases, the envelope of the distorted capnogram resembled the CO_2 tracing observed in the preceding and following non-distorted respiratory cycles. Therefore, this method could enhance capnometer algorithms to account for the chest compression artifact effect.

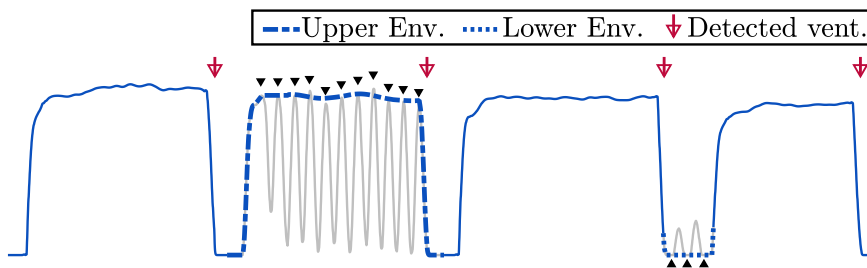


Figure 5.2. Example of envelope filtering performance. A distorted capnogram interval is depicted by the gray line. The blue line illustrates the waveform capnography envelope extraction process. Upper envelope (dashed blue line) is extracted through the detection of each local maxima (downward arrowheads), and lower envelope (dotted blue line) is extracted through the detection of each local minima (upward arrowheads). Detected ventilations are depicted with vertical red arrows.

Objective 3: To characterize the influence of ventilations on ETCO₂ measurement

During CPR, ETCO₂ values mainly depend on the blood flow generated by chest compressions, on ventilation rate and tidal volume, and on the metabolic activity of the patient tissues. Several studies have tried to model the influence of chest compression quality or to early detect ROSC relying on the direct comparison of measured ETCO₂ values. However, some animal studies have suggested that ventilation rate significantly influences ETCO₂ levels, which may act as an important confounding factor in the mentioned studies.

In this context, we separately modeled the effect of ventilation on the capnogram by analyzing CO₂ concentration variations during chest compression pauses (published in A5). When all the segments were included, the median decay factor was 10.0% (7.8–12.9) with R² equal to 0.98 (0.95–0.99). The model fitted the annotated data very well as proven by the obtained high median R² value. The moderate dispersion of the estimated decay factor could be related with differences in patient anatomic dead space and in the ventilation volumes provided with each breath. Nevertheless, a decay factor of 10% per ventilation may be useful as a reference level.

One of the potential clinical applications of this study is to facilitate the analysis of the relationship between ETCO₂ and CPR quality. Two recent studies have investigated this relationship.^{134,91} Sheak et al. reported that for every 10 mm increase in depth, ETCO₂ rose 1.4 mmHg; that for every 10 vpm increase in ventilation rate, ETCO₂ dropped 3.0 mmHg; and that compression rate was not a predictor of ETCO₂ variation. Murphy et al. concluded that a 10 mm increase in depth was associated with a 4.0% increase in ETCO₂; a 10 vpm increase in ventilation rate with a 17.4% decrease in ETCO₂; and a 10 cpm increase in chest compression rate with a 1.7% increase in ETCO₂.

Direct comparison between both studies is challenging because Sheak et al. reported absolute differences (mmHg) while Murphy et al. reported relative differences (%). The conclusions of both studies significantly diverge from what would be expected during resuscitation episodes. In addition, the main factor compromising the applicability of their models

is that the nature of dependence between ETCO_2 variations and the source of that variation may not be linear or logarithmic for all the studied variables. According to the novel approach modeled in this study, the change in ETCO_2 in a given interval which is attributable to chest compressions could be estimated by removing the influence of concurrent ventilation, which we can now model. However, further analysis of resuscitation episodes is required in order to confirm the validity of the model during ongoing chest compressions.

Objective 4: To develop novel strategies to identify ROSC using the capnogram as the reference

Advanced CPR techniques require minimizing interruptions in chest compressions, and pauses for pulse assessment should be kept as short as possible to optimize blood perfusion. In this context, a reliable and automated detection of ROSC based on the signals acquired by monitor-defibrillator would be of high benefit. It could prevent prolonged detrimental interruptions in patients in PEA and avoid unnecessary chest compression and drug administration to patients with a PR.

The initial ETCO_2 value measured within the chest compression pause is influenced by several factors such as the quality of chest compressions and ventilations. Therefore, absolute values are not a reliable indicator of ROSC. Our method did not rely on absolute measurements, but on the ETCO_2 variation. This work (A6) demonstrated that the decay or increment of the ETCO_2 levels during chest compression pauses allows for a reliable automated classification between non-ROSC and ROSC segments.

This method yielded a sensitivity and specificity for predicting the presence of ROSC of 95.4% and 94.9%, respectively. Nevertheless, pauses no longer than 20 s were included and ALS guidelines recommend not interrupting chest compressions for more than 10 s.¹³⁸ To test the algorithm with pauses closer to the recommendations, we applied the method to the first three and two ventilations of the included segments. In case of three ventilations, the performance was similar to the global results, although the median duration of the segments was 11 s. In case

of two ventilations, the median duration was 7.7 s and the performance slightly decreased to Se and Sp values of 90.0% and 81.3%, respectively.

In conclusion, during chest compression pauses for rhythm assessment by the ALS, the ECG can be directly analyzed to establish whether the electrical activity of the heart is organized or not. Organized rhythms can be PEA (non-ROSC) or PR (ROSC). Our method would allow to determine whether there is ROSC or not by the assessment of the evolution of ETCO_2 values. ROSC is more likely if the level of ETCO_2 is maintained or increased, whereas if the level clearly decreases non-ROSC should be suspected. Figure 3 in [A6](#) illustrates this idea.

6 | CONCLUSIONS

This chapter highlights the main findings and contributions of the thesis work and provides a detailed list of the articles published in indexed journals (A1-A6), the abstracts or proceedings presented at indexed international conferences (C1-C8) and book chapters (BC1).

Main contributions of the thesis work

The main objective of this thesis work was to analyze the feasibility and reliability of waveform capnography as a non-invasive indicator of CPR quality and ROSC during OHCA resuscitation. Its main contributions are those presented as intermediate goals in [chapter 3](#), and can be summarized in the following points:

- The important role of waveform capnography in ventilation monitoring is compromised by the high-incidence of CC-artifact. It affects ventilation detection, and, consequently, ventilation rate feedback and increases ETCO₂ measurement errors. This finding suggests that filtering techniques or adapted capnometer algorithms should be implemented to reliably perform during CPR, avoiding the detection of false ventilations when CC-artifact appears in the capnogram.

- Several filtering alternatives for suppressing the CC-artifact have been designed and ventilation detection improved after CC-artifact was removed from distorted capnograms. Moreover, the envelope algorithm enhanced the capnogram tracing, potentially favoring its interpretation during CPR. Nevertheless, further research in clinical settings is required to understand the feasibility and utility of these methods.
- We obtained a model to explain the decrease on exhaled CO₂ concentration with each ventilation during chest compression pauses. Our results provide a novel framework to explain the effect of chest compressions on ETCO₂, compensating for ventilation rate as a confounder. However, further work is required to confirm the validity of the model during ongoing chest compressions.
- ETCO₂ trend during chest compression pauses is a valuable metric to detect ROSC during resuscitation. A decreasing trend suggests a non-ROSC state, whereas constant or positive trends reflect ROSC. The proposed metric could help to confirm the presence or absence of pulse during pauses for rhythm assessment in those ALS agencies that have ETCO₂ monitoring capability.

Financial support

This thesis work received financial support from a predoctoral research grant (PRE-2016-1-0104), from the Basque Government through the project IT1087-16 and a health research program (2019222053), and from the Spanish Ministry of Science, Innovation and Universities through the grant RTI2018-094396-B-I00. The funders had no role in any study design, data collection and analysis, decision to publish, or preparation of the manuscript.

Indexed journals

A1 *"Influence of chest compression artefact on capnogram-based ventilation detection during out-of-hospital cardiopulmonary resuscitation"*

Authors: M. Leturiondo, S. Ruiz de Gauna, J. Ruiz, J.J. Gutiérrez, L.A. Leturiondo, D.M. González-Otero, J.K. Russell, D. Zive, M.R. Daya

Published in: Resuscitation 2018, vol. 124, p. 63-68

Type of publication: Journal paper indexed in JCR

Quality indices: Ranking: 1/26 (Q1). JCR impact factor: 5.863

Research impact: This article was referenced in the Resuscitation Highlights in 2017 published in the Resuscitation journal.⁹⁸ It was also awarded by the Spanish Resuscitation Council (CERCP^a) for being the most referenced article in 2018 written by Spanish authors.

A2 *"Chest compressions induce errors in end-tidal carbon dioxide measurement"*

Authors: M. Leturiondo, S. Ruiz de Gauna, J.J. Gutiérrez, D. Alonso, C. Corcuera, J.F. Urtusagasti, D.M. González-Otero, J.K. Russell, M.R. Daya, J. Ruiz

Published in: Resuscitation 2020, vol. 153, p. 195-201

Type of publication: Journal paper indexed in JCR

Quality indices: Ranking: 2/31 (Q1). JCR impact factor: 4.215

A3 *"Enhancing ventilation detection during cardiopulmonary resuscitation by filtering chest compression artifact from the capnography waveform"*

Authors: J.J. Gutiérrez, M. Leturiondo, S. Ruiz de Gauna, J. Ruiz, L.A. Leturiondo, D.M. González-Otero, D. Zive, J.K. Russell, M.R. Daya

Published in: PLoS One 2018, vol. 13, n. 8, p. e0201565

Type of publication: Journal paper indexed in JCR

Quality indices: Ranking: 15/64 (Q1). JCR impact factor: 2.766

^a Consejo Español de Resuscitación Cardiopulmonar

- A4** "*Enhancement of capnogram waveform in the presence of chest compression artefact during cardiopulmonary resuscitation*"
Authors: S. Ruiz de Gauna, **M. Leturiondo**, J.J. Gutiérrez, J. Ruiz, D.M. González-Otero, J.K. Russell, M.R. Daya
Published in: Resuscitation 2018, vol. 133, p. 53-58
Type of publication: Journal paper indexed in JCR
Quality indices: Ranking: 1/26 (Q1). JCR impact factor: 5.863
- A5** "*Modeling the impact of ventilations on the capnogram in out-of-hospital cardiac arrest*"
Authors: J.J. Gutiérrez, J. Ruiz, S. Ruiz de Gauna, D.M. González-Otero, **M. Leturiondo**, J.K. Russell, C. Corcuera, J.F. Urtusagasti, M.R. Daya
Published in: PLoS One 2020, vol. 15, n. 2, p. e0228395
Type of publication: Journal paper indexed in JCR
Quality indices: Ranking: 27/71 (Q2). JCR impact factor: 2.740
- A6** "*Assessment of the evolution of end-tidal carbon dioxide within chest compression pauses to detect restoration of spontaneous circulation*"
Authors: J.J. Gutiérrez, **M. Leturiondo**, S. Ruiz de Gauna, J. Ruiz, I. Azcarate, D.M. González-Otero, J.F. Urtusagasti, J.K. Russell, M.R. Daya
Published in: PLoS One 2020, *acceptance pending*
Type of publication: Journal paper indexed in JCR
Quality indices: Ranking: 27/71 (Q2). JCR impact factor: 2.740

Indexed international conferences

- C1** "*Reliability of ventilation guidance using capnography during ongoing chest compressions in out-of-hospital cardiopulmonary resuscitation*"
Authors: **M. Leturiondo**, S. Ruiz de Gauna, J. Ruiz, L.A. Leturiondo, J.M. Bastida, M.R. Daya
Published in: Resuscitation 2017, vol. 118, p. e18-e19
Type of publication: Indexed congress in JCR
Quality indices: Ranking: 2/24 (Q1). JCR impact factor: 5.230

- C2** "*A simple algorithm for ventilation detection in the capnography signal during cardiopulmonary resuscitation*"
Authors: M. Leturiondo, J. Ruiz, S. Ruiz de Gauna, D.M. González-Otero, J.M. Bastida, M.R. Daya
Published in: Proceedings of the IEEE Conference Computing in Cardiology 2017, vol. 44, p. 1-4
Type of publication: Indexed congress in SJR
Quality indices: SJR impact factor: 0.336
- C3** "*Chest compression artefact compromises real-time feedback capnometry: quantification of differences in end-tidal measurements by two capnometers*"
Authors: M. Leturiondo, S. Ruiz de Gauna, J.J. Gutiérrez, J. Ruiz, C. Corcuera, J.F. Urtusagasti, J.K. Russell, M.R. Daya
Published in: Resuscitation 2019, vol. 142, p. e32
Type of publication: Indexed congress in JCR
Quality indices: Ranking: 2/29 (Q1). JCR impact factor: 4.572
- C4** "*Open-loop adaptive filtering for suppressing chest compression oscillations in the capnogram during cardiopulmonary resuscitation*"
Authors: M. Leturiondo, J. Ruiz, J.J. Gutiérrez, L.A. Leturiondo, J.K. Russell, M.R. Daya
Published in: Proceedings of the IEEE Conference Computing in Cardiology 2017, vol. 44, p. 1-4
Type of publication: Indexed congress in SJR
Quality indices: SJR impact factor: 0.336
- C5** "*Closed-loop adaptive filtering for suppressing chest compression oscillations in the capnogram during cardiopulmonary resuscitation*"
Authors: M. Leturiondo, J.J. Gutiérrez, S. Ruiz de Gauna, S. Plaza, J.F. Veintemillas, M.R. Daya
Published in: Proceedings of the IEEE Conference Computing in Cardiology 2017, vol. 44, p. 1-4
Type of publication: Indexed congress in SJR
Quality indices: SJR impact factor: 0.336

- C6** "*Suppression of chest compression artefact to enhance reliability of capnography waveform analysis during cardiopulmonary resuscitation.*"
Authors: M. Leturiondo, J.J. Gutiérrez, S. Ruiz de Gauna, J. Ruiz, L.A. Leturiondo, J.K. Russell, M.R. Daya
Published in: Resuscitation 2018, vol. 130, e15-e16
Type of publication: Indexed congress in JCR
Quality indices: Ranking: 1/26 (Q1). JCR impact factor: 5.863
- C7** "*A Method to Suppress Chest Compression Artifact Enhancing Capnography-Based Ventilation Guidance During Cardiopulmonary Resuscitation*"
Authors: M. Leturiondo, J.J. Gutiérrez, S. Ruiz de Gauna, J. Ruiz, L.A. Leturiondo, J.K. Russell, M.R. Daya
Published in: Proceedings of the IEEE Conference Computing in Cardiology 2018, vol. 45 p. 1-4
Type of publication: Indexed congress in SJR
Quality indices: SJR impact factor: 0.191
- C8** "*A model for quantifying the influence of ventilations on end-tidal carbon dioxide variation during out-of-hospital cardiac arrest*"
Authors: J.J. Gutiérrez, S. Ruiz de Gauna, J. Ruiz, M. Leturiondo, J.K. Russell, M.R. Daya
Published in: Resuscitation 2018, vol. 130, p. e34-e35
Type of publication: Indexed congress in JCR
Quality indices: Ranking: 1/26 (Q1). JCR impact factor: 5.863

Book chapters

- BC1** "*Waveform Capnography for Monitoring Ventilation during Cardiopulmonary Resuscitation: The Problem of Chest Compression Artifact*"
Authors: M. Leturiondo, S. Ruiz de Gauna, J.J. Gutiérrez, D.M. González-Otero, J. Ruiz, L.A. Leturiondo, P. Saiz
Published in: Cardiac Diseases and Interventions in 21st Century. IntechOpen, 2019

BIBLIOGRAPHY

- [1] Aase SO, Eftestol T, Husoy J, Sunde K, and Steen PA. CPR artifact removal from human ECG using optimal multichannel filtering. *IEEE Transactions on Biomedical Engineering* 2000;47(11); 1440–1449.
- [2] Aase SO and Myklebust H. Compression depth estimation for CPR quality assessment using DSP on accelerometer signals. *IEEE Transactions on Biomedical Engineering* 2002;49(3); 263–268.
- [3] Abella BS, Alvarado JP, Myklebust H, Edelson DP, et al. Quality of cardiopulmonary resuscitation during in-hospital cardiac arrest. *Jama* 2005;293(3); 305–310.
- [4] Abella BS, Sandbo N, Vassilatos P, Alvarado JP, et al. Chest compression rates during cardiopulmonary resuscitation are suboptimal: a prospective study during in-hospital cardiac arrest. *Circulation* 2005;111(4); 428–434.
- [5] Alonso E, Ruiz J, Aramendi E, González-Otero D, et al. Reliability and accuracy of the thoracic impedance signal for measuring cardiopulmonary resuscitation quality metrics. *Resuscitation* 2015; 88; 28–34.
- [6] American Society of Anesthesiologists. Standards for basic anesthetic monitoring. *ASA* 2015;1; 1–4.
- [7] Aramendi E, Elola A, Alonso E, Irusta U, et al. Feasibility of the capnogram to monitor ventilation rate during cardiopulmonary resuscitation. *Resuscitation* 2017;110; 162–168.
- [8] Atwood C, Eisenberg MS, Herlitz J, and Rea TD. Incidence of EMS-treated out-of-hospital cardiac arrest in Europe. *Resuscitation* 2005; 67(1); 75–80.

- [9] Aufderheide TP and Lurie KG. Death by hyperventilation: a common and life-threatening problem during cardiopulmonary resuscitation. *Critical care medicine* 2004;32(9); S345–S351.
- [10] Aufderheide TP, Pirrallo RG, Yannopoulos D, Klein JP, et al. Incomplete chest wall decompression: a clinical evaluation of CPR performance by EMS personnel and assessment of alternative manual chest compression–decompression techniques. *Resuscitation* 2005;64(3); 353–362.
- [11] Aufderheide TP, Sigurdsson G, Pirrallo RG, Yannopoulos D, et al. Hyperventilation-induced hypotension during cardiopulmonary resuscitation. *Circulation* 2004;109(16); 1960–1965.
- [12] Babbs CF, Kemeny AE, Quan W, and Freeman G. A new paradigm for human resuscitation research using intelligent devices. *Resuscitation* 2008;77(3); 306–315.
- [13] Berdowski J, Berg RA, Tijssen JG, and Koster RW. Global incidences of out-of-hospital cardiac arrest and survival rates: systematic review of 67 prospective studies. *Resuscitation* 2010; 81(11); 1479–1487.
- [14] Berg RA, Hemphill R, Abella BS, Aufderheide TP, et al. Part 5: adult basic life support: 2010 American Heart Association guidelines for cardiopulmonary resuscitation and emergency cardiovascular care. *Circulation* 2010;122(18); S685–S705.
- [15] Bhavani-Shankar K, Kumar A, Moseley H, and Ahyee-Hallsworth R. Terminology and the current limitations of time capnography: a brief review. *Journal of clinical monitoring* 1995;11(3); 175–182.
- [16] Bhavani-Shankar K and Philip JH. Defining segments and phases of a time capnogram. *Anesthesia & Analgesia* 2000;91(4); 973–977.
- [17] Blumenthal SR and Voorhees WD. The relationship between airway carbon dioxide excretion and cardiac output during cardiopulmonary resuscitation. *Resuscitation* 1997;34(3); 263–270.
- [18] Brinkrolf P, Borowski M, Metelmann C, Lukas RP, Pidde-Küllenberg L, and Bohn A. Predicting ROSC in out-of-hospital cardiac arrest using expiratory carbon dioxide concentration: Is

- trend-detection instead of absolute threshold values the key? *Resuscitation* 2018;122; 19–24.
- [19] Cantineau JP, Lambert Y, Merckx P, Reynaud P, et al. End-tidal carbon dioxide during cardiopulmonary resuscitation in humans presenting mostly with asystole: a predictor of outcome. *Critical care medicine* 1996;24(5); 791–796.
- [20] Chandra NC, Gruben KG, Tsitlik JE, Brower R, et al. Observations of ventilation during resuscitation in a canine model. *Circulation* 1994;90(6); 3070–3075.
- [21] Charbonney E, Delisle S, Savary D, Bronchti G, et al. A new physiological model for studying the effect of chest compression and ventilation during cardiopulmonary resuscitation: The Thiel cadaver. *Resuscitation* 2018;125; 135–142.
- [22] Cheskes S, Schmicker RH, Verbeek PR, Salcido DD, et al. The impact of peri-shock pause on survival from out-of-hospital shockable cardiac arrest during the Resuscitation Outcomes Consortium PRIMED trial. *Resuscitation* 2014;85(3); 336–342.
- [23] Christenson J, Andrusiek D, Everson-Stewart S, Kudenchuk P, et al. Resuscitation Outcomes Consortium Investigators: Chest compression fraction determines survival in patients with out-of-hospital ventricular fibrillation. *Circulation* 2009;120(13); 1241–1247.
- [24] Chugh SS, Jui J, Gunson K, Stecker EC, et al. Current burden of sudden cardiac death: multiple source surveillance versus retrospective death certificate-based review in a large US community. *Journal of the American College of Cardiology* 2004;44(6); 1268–1275.
- [25] Cobb LA, Fahrenbruch CE, Olsufka M, and Copass MK. Changing incidence of out-of-hospital ventricular fibrillation, 1980-2000. *Jama* 2002;288(23); 3008–3013.
- [26] Colwell CB and Soriya G. Basic Life Support. In *Encyclopedia of Intensive Care Medicine*. Springer 2012;pages. 285–288.
- [27] Cone D, Cahill J, and Wayne M. Cardiopulmonary resuscitation. In *Capnography*. Cambridge 2011;pages. 185–194.

- [28] Cordioli RL, Grieco DL, Charbonney E, Richard JC, and Savary D. New physiological insights in ventilation during cardiopulmonary resuscitation. *Current opinion in critical care* 2019;25(1); 37–44.
- [29] Cummins RO, Ornato JP, Thies WH, and Pepe PE. Improving survival from sudden cardiac arrest: the "chain of survival" concept. A statement for health professionals from the Advanced Cardiac Life Support Subcommittee and the Emergency Cardiac Care Committee, American Heart Association. *Circulation* 1991; 83(5); 1832–1847.
- [30] Deakin CD, Nolan JP, Soar J, Sunde K, et al. European resuscitation council guidelines for resuscitation 2010 section 4. Adult advanced life support. *Resuscitation* 2010;81(10); 1305.
- [31] Deakin CD, O'Neill JF, and Tabor T. Does compression-only cardiopulmonary resuscitation generate adequate passive ventilation during cardiac arrest? *Resuscitation* 2007;75(1); 53–59.
- [32] Debaty G, Babaz V, Durand M, Gaide-Chevronnay L, et al. Prognostic factors for extracorporeal cardiopulmonary resuscitation recipients following out-of-hospital refractory cardiac arrest. A systematic review and meta-analysis. *Resuscitation* 2017;112; 1–10.
- [33] Ditchey R, Winkler JV, and Rhodes CA. Relative lack of coronary blood flow during closed-chest resuscitation in dogs. *Circulation* 1982;66(2); 297–302.
- [34] D'Arrigo S, Cacciola S, Dennis M, Jung C, et al. Predictors of favourable outcome after in-hospital cardiac arrest treated with extracorporeal cardiopulmonary resuscitation: a systematic review and meta-analysis. *Resuscitation* 2017;121; 62–70.
- [35] Eckstein M, Hatch L, Malleck J, McClung C, and Henderson SO. End-tidal CO₂ as a predictor of survival in out-of-hospital cardiac arrest. *Prehospital and disaster medicine* 2011;26(3); 148–150.
- [36] Edelson DP, Abella BS, Kramer-Johansen J, Wik L, et al. Effects of compression depth and pre-shock pauses predict defibrillation failure during cardiac arrest. *Resuscitation* 2006;71(2); 137–145.
- [37] Edelson DP, Eilevstjønn J, Weidman EK, Retzer E, Hoek TLV, and Abella BS. Capnography and chest-wall impedance algorithms

- for ventilation detection during cardiopulmonary resuscitation. *Resuscitation* 2010;81(3); 317–322.
- [38] Eftestøl T, Sunde K, and Steen PA. Effects of interrupting precordial compressions on the calculated probability of defibrillation success during out-of-hospital cardiac arrest. *Circulation* 2002; 105(19); 2270–2273.
- [39] Eilevstjønn J, Eftestøl T, Aase SO, Myklebust H, Husøy JH, and Steen PA. Feasibility of shock advice analysis during CPR through removal of CPR artefacts from the human ECG. *Resuscitation* 2004; 61(2); 131–141.
- [40] Eisenberg M and White RD. The unacceptable disparity in cardiac arrest survival among American communities. *Annals of emergency medicine* 2009;54(2); 258.
- [41] Falk JL, Rackow EC, and Weil MH. End-tidal carbon dioxide concentration during cardiopulmonary resuscitation. *New England Journal of Medicine* 1988;318(10); 607–611.
- [42] Field RA, Soar J, Davies RP, Akhtar N, and Perkins GD. The impact of chest compression rates on quality of chest compressions—a manikin study. *Resuscitation* 2012;83(3); 360–364.
- [43] Fried DA, Leary M, Smith DA, Sutton RM, et al. The prevalence of chest compression leaning during in-hospital cardiopulmonary resuscitation. *Resuscitation* 2011;82(8); 1019–1024.
- [44] Garnett AR, Ornato JP, Gonzalez ER, and Johnson EB. End-tidal carbon dioxide monitoring during cardiopulmonary resuscitation. *Jama* 1987;257(4); 512–515.
- [45] Gazmuri RJ, Ayoub IM, Radhakrishnan J, Motl J, and Upadhyaya MP. Clinically plausible hyperventilation does not exert adverse hemodynamic effects during CPR but markedly reduces end-tidal PCO₂. *Resuscitation* 2012;83(2); 259–264.
- [46] Gong Y, Chen B, and Li Y. A review of the performance of artifact filtering algorithms for cardiopulmonary resuscitation. *Journal of Healthcare Engineering* 2013;4.

- [47] González-Otero D, Alonso E, Ruiz J, Aramendi E, et al. A simple impedance-based method for ventilation detection during cardiopulmonary resuscitation. In *Computing in Cardiology 2013* 2013, IEEE, pages. 807–810.
- [48] González-Otero DM, Ruiz JM, Ruiz de Gauna S, Gutiérrez JJ, et al. Monitoring chest compression quality during cardiopulmonary resuscitation: Proof-of-concept of a single accelerometer-based feedback algorithm. *PloS one* 2018;13(2); e0192810.
- [49] González-Otero DM, Ruiz de Gauna S, Gutiérrez JJ, Saiz P, and Ruiz JM. Applications of the Transthoracic Impedance Signal during Resuscitation. In *Special Topics in Resuscitation*. IntechOpen 2018;pages. 57–72.
- [50] Gravenstein JS, Jaffe MB, Gravenstein N, and Paulus DA. *Capnography*. Cambridge University Press 2011.
- [51] Grieco DL, J Brochard L, Drouet A, Talias I, et al. Intrathoracic airway closure impacts CO₂ signal and delivered ventilation during cardiopulmonary resuscitation. *American journal of respiratory and critical care medicine* 2019;199(6); 728–737.
- [52] Grmec Š. Comparison of three different methods to confirm tracheal tube placement in emergency intubation. *Intensive care medicine* 2002;28(6); 701–704.
- [53] Grmec Š, Lah K, and Tušek-Bunc K. Difference in end-tidal CO₂ between asphyxia cardiac arrest and ventricular fibrillation/pulseless ventricular tachycardia cardiac arrest in the prehospital setting. *Critical Care* 2003;7(6); R139.
- [54] Gudipati CV, Weil M, Bisera J, Deshmukh HG, and Rackow E. Expired carbon dioxide: a noninvasive monitor of cardiopulmonary resuscitation. *Circulation* 1988;77(1); 234–239.
- [55] Halperin HR. Mechanisms of forward flow during external chest compression. In *Cardiac arrest: the science and practice of resuscitation medicine*. Cambridge University Press 2007;pages. 326–346.

- [56] Halperin HR, Tsitlik JE, Guerci AD, Mellits E, et al. Determinants of blood flow to vital organs during cardiopulmonary resuscitation in dogs. *Circulation* 1986;73(3); 539–550.
- [57] Hamrick JL, Hamrick JT, Lee JK, Lee BH, Koehler RC, and Shaffner DH. Efficacy of chest compressions directed by end-tidal CO₂ feedback in a pediatric resuscitation model of basic life support. *Journal of the American Heart Association* 2014;3(2); e000450.
- [58] Hardig BM, Götberg M, Rundgren M, Götberg M, et al. Physiologic effect of repeated adrenaline (epinephrine) doses during cardiopulmonary resuscitation in the cath lab setting: a randomised porcine study. *Resuscitation* 2016;101; 77–83.
- [59] Hazinski MF and Field JM. 2010 American Heart Association guidelines for cardiopulmonary resuscitation and emergency cardiovascular care science. *Circulation* 2010;122; S639–S946.
- [60] Heradstveit BE, Sunde K, Sunde GA, Wentzel-Larsen T, and Heltne JK. Factors complicating interpretation of capnography during advanced life support in cardiac arrest—a clinical retrospective study in 575 patients. *Resuscitation* 2012;83(7); 813–818.
- [61] Herlitz J, Bång A, Gunnarsson J, Engdahl J, et al. Factors associated with survival to hospital discharge among patients hospitalised alive after out of hospital cardiac arrest: change in outcome over 20 years in the community of Göteborg, Sweden. *Heart* 2003;89(1); 25–30.
- [62] Herry CL, Townsend D, Green GC, Bravi A, and Seely AJE. Segmentation and classification of capnograms: application in respiratory variability analysis. *Physiological measurement* 2014; 35(12); 2343.
- [63] Holmberg M, Holmberg S, and Herlitz J. Effect of bystander cardiopulmonary resuscitation in out-of-hospital cardiac arrest patients in Sweden. *Resuscitation* 2000;47(1); 59–70.
- [64] Idris AH, Daya M, Owens P, O’Neill S, et al. High incidence of chest compression oscillations associated with capnography

during out-of-hospital cardiopulmonary resuscitation. *Circulation* 2010;122; A83.

- [65] Idris AH, Guffey D, Aufderheide TP, Brown S, et al. Relationship between chest compression rates and outcomes from cardiac arrest. *Circulation* 2012;125(24); 3004–3012.
- [66] Idris AH, Staples ED, O'Brien DJ, Melker RJ, et al. End-tidal carbon dioxide during extremely low cardiac output. *Annals of emergency medicine* 1994;23(3); 568–572.
- [67] Irusta U, Ruiz J, de Gauna SR, Eftestøl T, and Kramer-Johansen J. A least mean-square filter for the estimation of the cardiopulmonary resuscitation artifact based on the frequency of the compressions. *IEEE Transactions on Biomedical Engineering* 2009; 56(4); 1052–1062.
- [68] Isserles SA and Breen PH. Can changes in end-tidal PCO₂ measure changes in cardiac output? *Anesthesia and analgesia* 1991;73(6); 808–814.
- [69] Jaffe MB. Infrared measurement of carbon dioxide in the human breath: “breathe-through” devices from Tyndall to the present day. *Anesthesia & Analgesia* 2008;107(3); 890–904.
- [70] Kalenda Z. The capnogram as a guide to the efficacy of cardiac massage. *Resuscitation* 1978;6(4); 259–263.
- [71] Katritsis DG, Gersh BJ, and Camm AJ. A clinical perspective on sudden cardiac death. *Arrhythmia & electrophysiology review* 2016; 5(3); 177.
- [72] Kerber RE, Becker LB, Bourland JD, Cummins RO, et al. Automatic external defibrillators for public access defibrillation: recommendations for specifying and reporting arrhythmia analysis algorithm performance, incorporating new waveforms, and enhancing safety: a statement for health professionals from the American Heart Association Task Force on Automatic External Defibrillation, Subcommittee on AED Safety and Efficacy. *Circulation* 1997;95(6); 1677–1682.

- [73] Kodali BS and Urman RD. Capnography during cardiopulmonary resuscitation: current evidence and future directions. *Journal of emergencies, trauma, and shock* 2014;7(4); 332.
- [74] Kramer-Johansen J, Myklebust H, Wik L, Fellows B, et al. Quality of out-of-hospital cardiopulmonary resuscitation with real time automated feedback: a prospective interventional study. *Resuscitation* 2006;71(3); 283–292.
- [75] Krauss B. Capnography in EMS. A powerful way to objectively monitor ventilatory status. *JEMS: a journal of emergency medical services* 2003;28(1); 28.
- [76] Kronick SL, Kurz MC, Lin S, Edelson DP, et al. Part 4: systems of care and continuous quality improvement: 2015 American Heart Association guidelines update for cardiopulmonary resuscitation and emergency cardiovascular care. *Circulation* 2015;132(18); S397–S413.
- [77] Larsen MP, Eisenberg MS, Cummins RO, and Hallstrom AP. Predicting survival from out-of-hospital cardiac arrest: a graphic model. *Annals of emergency medicine* 1993;22(11); 1652–1658.
- [78] Levine RL, Wayne MA, and Miller CC. End-tidal carbon dioxide and outcome of out-of-hospital cardiac arrest. *New England Journal of Medicine* 1997;337(5); 301–306.
- [79] Link MS, Berkow LC, Kudenchuk PJ, Halperin HR, et al. Part 7: adult advanced cardiovascular life support: 2015 American Heart Association guidelines update for cardiopulmonary resuscitation and emergency cardiovascular care. *Circulation* 2015;132(18); S444–S464.
- [80] Long B, Koyfman A, and Vivirito MA. Capnography in the emergency department: a review of uses, waveforms, and limitations. *The Journal of emergency medicine* 2017;53(6); 829–842.
- [81] Losert H, Risdal M, Sterz F, Nysæther J, et al. Thoracic impedance changes measured via defibrillator pads can monitor ventilation in critically ill patients and during cardiopulmonary resuscitation. *Critical care medicine* 2006;34(9); 2399–2405.

- [82] Lui CT, Poon KM, and Tsui KL. Abrupt rise of end tidal carbon dioxide level was a specific but non-sensitive marker of return of spontaneous circulation in patient with out-of-hospital cardiac arrest. *Resuscitation* 2016;104; 53–58.
- [83] MacLeod BA, Heller MB, Gerard J, Yealy DM, and Menegazzi JJ. Verification of endotracheal tube placement with colorimetric end-tidal CO₂ detection. *Annals of emergency medicine* 1991;20(3); 267–270.
- [84] Maertens VL, De Smedt LE, Lemoyne S, Huybrechts SA, et al. Patients with cardiac arrest are ventilated two times faster than guidelines recommend: an observational prehospital study using tracheal pressure measurement. *Resuscitation* 2013;84(7); 921–926.
- [85] McDannold R, Bobrow BJ, Chikani V, Silver A, Spaite DW, and Vadeboncoeur T. Quantification of ventilation volumes produced by compressions during emergency department cardiopulmonary resuscitation. *The American journal of emergency medicine* 2018;36(9); 1640–1644.
- [86] Meaney PA, Bobrow BJ, Mancini ME, Christenson J, et al. Cardiopulmonary resuscitation quality: improving cardiac resuscitation outcomes both inside and outside the hospital: a consensus statement from the American Heart Association. *Circulation* 2013; 128(4); 417–435.
- [87] Mehra R. Global public health problem of sudden cardiac death. *Journal of electrocardiology* 2007;40(6); S118–S122.
- [88] Michael J, Guerci A, Koehler R, Shi A, et al. Mechanisms by which epinephrine augments cerebral and myocardial perfusion during cardiopulmonary resuscitation in dogs. *Circulation* 1984;69(4); 822–835.
- [89] Mistovich JJ, Karren KJ, Werman HA, and Hafen BQ. Prehospital emergency care. Brady Prentice Hall Health 2004.
- [90] Monsieurs KG, De Regge M, Vansteelandt K, De Smet J, et al. Excessive chest compression rate is associated with insufficient compression depth in prehospital cardiac arrest. *Resuscitation* 2012; 83(11); 1319–1323.

- [91] Murphy RA, Bobrow BJ, Spaite DW, Hu C, McDannold R, and Vadeboncoeur TF. Association between prehospital CPR quality and end-tidal carbon dioxide levels in out-of-hospital cardiac arrest. *Prehospital Emergency Care* 2016;20(3); 369–377.
- [92] Myerburg RJ and Castellanos A. Emerging paradigms of the epidemiology and demographics of sudden cardiac arrest. *Heart Rhythm* 2006;3(2); 235–239.
- [93] Neth MR, Idris A, McMullan J, Benoit JL, and Daya MR. A review of ventilation in adult out-of-hospital cardiac arrest. *Journal of the American College of Emergency Physicians Open* 2020;1(3); 190–201.
- [94] Neumar RW, Otto CW, Link MS, Kronick SL, et al. Part 8: adult advanced cardiovascular life support: 2010 American Heart Association guidelines for cardiopulmonary resuscitation and emergency cardiovascular care. *Circulation* 2010;122(18); S729–S767.
- [95] Nichol G and Baker D. The epidemiology of sudden death. *Cardiac Arrest* 2007;2007; 26–48.
- [96] Niemann JT, Criley JM, Rosborough JP, Niskanen RA, and Alferness C. Predictive indices of successful cardiac resuscitation after prolonged arrest and experimental cardiopulmonary resuscitation. *Annals of emergency medicine* 1985;14(6); 521–528.
- [97] Niles D, Nysaether J, Sutton R, Nishisaki A, et al. Leaning is common during in-hospital pediatric CPR, and decreased with automated corrective feedback. *Resuscitation* 2009;80(5); 553–557.
- [98] Nolan J, Ornato J, Parr M, Perkins G, and Soar J. Resuscitation highlights in 2017. *Resuscitation* 2018;124; A1 – A8.
- [99] Nolan JP, Neumar RW, Adrie C, Aibiki M, et al. Post-cardiac arrest syndrome: epidemiology, pathophysiology, treatment, and prognostication: a scientific statement from the International liaison Committee on Resuscitation; the American Heart Association Emergency cardiovascular Care Committee; the Council on Cardiovascular Surgery and Anesthesia; the Council on cardiopulmonary, Perioperative, and Critical Care; the Council on

- clinical cardiology; the Council on Stroke. *Resuscitation* 2008;79(3); 350–379.
- [100] O'Connor RE and Swor RA. Verification of endotracheal tube placement following intubation. *Prehospital Emergency Care* 1999; 3(3); 248–250.
- [101] Okamoto H, Hoka S, Kawasaki T, Okuyama T, and Takahashi S. Changes in end-tidal carbon dioxide tension following sodium bicarbonate administration: Correlation with cardiac output and haemoglobin concentration. *Acta anaesthesiologica scandinavica* 1995;39(1); 79–84.
- [102] Ornato JP. Cardiopulmonary resuscitation. In *Essential Cardiology*. Springer 2005;pages. 521–530.
- [103] Ornato JP, Garnett AR, and Glauser FL. Relationship between cardiac output and the end-tidal carbon dioxide tension. *Annals of emergency medicine* 1990;19(10); 1104–1106.
- [104] O'Neill JF and Deakin CD. Do we hyperventilate cardiac arrest patients? *Resuscitation* 2007;73(1); 82–85.
- [105] Pantazopoulos C, Xanthos T, Pantazopoulos I, Papalois A, Kouskouni E, and Iacovidou N. A review of carbon dioxide monitoring during adult cardiopulmonary resuscitation. *Heart, Lung and Circulation* 2015;24(11); 1053–1061.
- [106] Paradis NA, Halperin HR, Kern KB, Wenzel V, and Chamberlain DA. *Cardiac arrest: the science and practice of resuscitation medicine*. Cambridge University Press 2007.
- [107] Paradis NA, Martin GB, Rivers EP, Goetting MG, et al. Coronary perfusion pressure and the return of spontaneous circulation in human cardiopulmonary resuscitation. *Jama* 1990;263(8); 1106–1113.
- [108] Pellis T, Bisera J, Tang W, and Weil MH. Expanding automatic external defibrillators to include automated detection of cardiac, respiratory, and cardiorespiratory arrest. *Critical care medicine* 2002; 30(4); S176–S178.

- [109] Perkins GD, Handley AJ, Koster RW, Castrén M, et al. European Resuscitation Council Guidelines for Resuscitation 2015: Section 2. Adult basic life support and automated external defibrillation. *Resuscitation* 2015;95; 81–99.
- [110] Pitts S and Kellermann AL. Hyperventilation during cardiac arrest. *The Lancet* 2004;364(9431); 313–315.
- [111] Pokorná M, Nečas E, Kratochvíl J, Skřípský R, Andrlík M, and Franěk O. A sudden increase in partial pressure end-tidal carbon dioxide (PETCO₂) at the moment of return of spontaneous circulation. *The Journal of emergency medicine* 2010;38(5); 614–621.
- [112] Poon KM, Lui CT, and Tsui KL. Prognostication of out-of-hospital cardiac arrest patients by 3-min end-tidal capnometry level in emergency department. *Resuscitation* 2016;102; 80–84.
- [113] Puntervoll S, Søreide E, Jacewicz W, and Bjelland E. Rapid detection of oesophageal intubation: take care when using colorimetric capnometry. *Acta anaesthesiologica scandinavica* 2002; 46(4); 455–457.
- [114] Qvigstad E, Kramer-Johansen J, Tømte Ø, Skålhegg T, et al. Clinical pilot study of different hand positions during manual chest compressions monitored with capnography. *Resuscitation* 2013;84(9); 1203–1207.
- [115] Raimondi M, Savastano S, Pamploni G, Molinari S, Degani A, and Belliato M. End-tidal carbon dioxide monitoring and load band device for mechanical cardio-pulmonary resuscitation: Never trust the numbers, believe at the curves. *Resuscitation* 2016;103; e9–e10.
- [116] Ralston SH, Voorhees WD, and Babbs CF. Intrapulmonary epinephrine during prolonged cardiopulmonary resuscitation: improved regional blood flow and resuscitation in dogs. *Annals of emergency medicine* 1984;13(2); 79–86.
- [117] Rea TD, Eisenberg MS, Sinibaldi G, and White RD. Incidence of EMS-treated out-of-hospital cardiac arrest in the United States. *Resuscitation* 2004;63(1); 17–24.
- [118] Rezoagli E, Magliocca A, Ristagno G, and Bellani G. CO₂ Oscillation during Cardiopulmonary Resuscitation: The Role of

Respiratory System Compliance. *American Journal of Respiratory and Critical Care Medicine* 2019;199(10); 1290–1291.

- [119] Risdal M, Aase SO, Kramer-Johansen J, and Eftesol T. Automatic identification of return of spontaneous circulation during cardiopulmonary resuscitation. *IEEE Transactions on Biomedical Engineering* 2007;55(1); 60–68.
- [120] Risdal M, Aase SO, Stavland M, and Eftestol T. Impedance-based ventilation detection during cardiopulmonary resuscitation. *IEEE transactions on biomedical engineering* 2007;54(12); 2237–2245.
- [121] Rognås L, Hansen TM, Kirkegaard H, and Tønnesen E. Predicting the lack of ROSC during pre-hospital CPR: Should an end-tidal CO₂ of 1.3 kPa be used as a cut-off value? *Resuscitation* 2014;85(3); 332–335.
- [122] Ruiz JM, Ruiz de Gauna S, González-Otero DM, Saiz P, et al. Circulation assessment by automated external defibrillators during cardiopulmonary resuscitation. *Resuscitation* 2018;128; 158–163.
- [123] Ruiz de Gauna S, Irusta U, Ruiz J, Ayala U, Aramendi E, and Eftestøl T. Rhythm analysis during cardiopulmonary resuscitation: past, present, and future. *BioMed research international* 2014;2014.
- [124] Sanders AB. Capnometry in emergency medicine. *Annals of emergency medicine* 1989;18(12); 1287–1290.
- [125] Sanders AB, Atlas M, Ewy GA, Kern KB, and Bragg S. Expired PCO₂ as an index of coronary perfusion pressure. *The American journal of emergency medicine* 1985;3(2); 147–149.
- [126] Sanders AB, Ewy GA, and Taft TV. Prognostic and therapeutic importance of the aortic diastolic pressure in resuscitation from cardiac arrest. *Critical care medicine* 1984;12(10); 871–873.
- [127] Sanders AB, Ogle M, and Ewy GA. Coronary perfusion pressure during cardiopulmonary resuscitation. *The American journal of emergency medicine* 1985;3(1); 11–14.
- [128] Sandroni C, De Santis P, and D'Arrigo S. Capnography during cardiac arrest. *Resuscitation* 2018;132; 73–77.

- [129] Sandroni C and Ristagno G. End-tidal CO₂ to detect recovery of spontaneous circulation during cardiopulmonary resuscitation: We are not ready yet. *Resuscitation* 2016;104; A5–A6.
- [130] Savastano S, Baldi E, Raimondi M, Palo A, et al. End-tidal carbon dioxide and defibrillation success in out-of-hospital cardiac arrest. *Resuscitation* 2017;121; 71–75.
- [131] Sayah AJ, Peacock WF, and Overton DT. End-tidal CO₂ measurement in the detection of esophageal intubation during cardiac arrest. *Annals of emergency medicine* 1990;19(8); 857–860.
- [132] Sehra R, Underwood K, and Checchia P. End tidal CO₂ is a quantitative measure of cardiac arrest. *Pacing and clinical electrophysiology* 2003;26(1p2); 515–517.
- [133] Sell RE, Sarno R, Lawrence B, Castillo EM, et al. Minimizing pre- and post-defibrillation pauses increases the likelihood of return of spontaneous circulation (ROSC). *Resuscitation* 2010;81(7); 822–825.
- [134] Sheak KR, Wiebe DJ, Leary M, Babaeizadeh S, et al. Quantitative relationship between end-tidal carbon dioxide and CPR quality during both in-hospital and out-of-hospital cardiac arrest. *Resuscitation* 2015;89; 149–154.
- [135] Shibutani K, Muraoka M, Shirasaki S, Kubal K, Sanchala VT, and Gupte P. Do changes in end-tidal PCO₂ quantitatively reflect changes in cardiac output? *Anesthesia and analgesia* 1994;79(5); 829–833.
- [136] Silvestri S, Ralls GA, Krauss B, Thundiyil J, et al. The effectiveness of out-of-hospital use of continuous end-tidal carbon dioxide monitoring on the rate of unrecognized misplaced intubation within a regional emergency medical services system. *Annals of emergency medicine* 2005;45(5); 497–503.
- [137] Skrifvars M, Olasveengen T, and Ristagno G. Oxygen and carbon dioxide targets during and after resuscitation of cardiac arrest patients 2019.
- [138] Soar J, Nolan JP, Böttiger BW, Perkins GD, et al. European resuscitation council guidelines for resuscitation 2015: section 3. Adult advanced life support. *Resuscitation* 2015;95; 100–147.

- [139] Société française d'anesthésie et de réanimation et al. Guidelines for indications for the use of extracorporeal life support in refractory cardiac arrest. French Ministry of Health. In *Annales francaises d'anesthesie et de reanimation*, vol. 28 2009, page 182.
- [140] Stecher FS, Olsen JA, Stickney RE, and Wik L. Transthoracic impedance used to evaluate performance of cardiopulmonary resuscitation during out of hospital cardiac arrest. *Resuscitation* 2008;79(3); 432–437.
- [141] Stiell IG, Brown SP, Christenson J, Cheskes S, et al. What is the role of chest compression depth during out-of-hospital cardiac arrest resuscitation? *Critical care medicine* 2012;40(4); 1192.
- [142] Sunde K, Pytte M, Jacobsen D, Mangschau A, et al. Implementation of a standardised treatment protocol for post resuscitation care after out-of-hospital cardiac arrest. *Resuscitation* 2007;73(1); 29–39.
- [143] Sutton RM, Friess SH, Maltese MR, Naim MY, et al. Hemodynamic-directed cardiopulmonary resuscitation during in-hospital cardiac arrest. *Resuscitation* 2014;85(8); 983–986.
- [144] Takeda T, Tanigawa K, Tanaka H, Hayashi Y, Goto E, and Tanaka K. The assessment of three methods to verify tracheal tube placement in the emergency setting. *Resuscitation* 2003;56(2); 153–157.
- [145] Takla G, Petre JH, Doyle DJ, Horibe M, and Gopakumaran B. The problem of artifacts in patient monitor data during surgery: a clinical and methodological review. *Anesthesia & Analgesia* 2006; 103(5); 1196–1204.
- [146] Tang W, Weil MH, Gazmuri RJ, Sun S, Duggal C, and Bisera J. Pulmonary ventilation/perfusion defects induced by epinephrine during cardiopulmonary resuscitation. *Circulation* 1991;84(5); 2101–2107.
- [147] Tanigawa K, Takeda T, Goto E, and Tanaka K. Accuracy and reliability of the self-inflating bulb to verify tracheal intubation in out-of-hospital cardiac arrest patients. *Anesthesiology: The Journal of the American Society of Anesthesiologists* 2000;93(6); 1432–1436.

- [148] Tanigawa K, Takeda T, Goto E, and Tanaka K. The efficacy of esophageal detector devices in verifying tracheal tube placement: a randomized cross-over study of out-of-hospital cardiac arrest patients. *Anesthesia & Analgesia* 2001;92(2); 375–378.
- [149] Touma O and Davies M. The prognostic value of end tidal carbon dioxide during cardiac arrest: a systematic review. *Resuscitation* 2013;84(11); 1470–1479.
- [150] Travers AH, Rea TD, Bobrow BJ, Edelson DP, et al. Part 4: CPR overview: 2010 American Heart Association guidelines for cardiopulmonary resuscitation and emergency cardiovascular care. *Circulation* 2010;122(18); S676–S684.
- [151] Trilló G, von Planta M, and Kette F. ETCO₂ monitoring during low flow states: clinical aims and limits. *Resuscitation* 1994;27(1); 1–8.
- [152] Vaillancourt C, Everson-Stewart S, Christenson J, Andrusiek D, et al. The impact of increased chest compression fraction on return of spontaneous circulation for out-of-hospital cardiac arrest patients not in ventricular fibrillation. *Resuscitation* 2011;82(12); 1501–1507.
- [153] Valenzuela TD, Roe DJ, Cretin S, Spaite DW, and Larsen MP. Estimating effectiveness of cardiac arrest interventions: a logistic regression survival model. *Circulation* 1997;96(10); 3308–3313.
- [154] Vanwulpen M, Wolfskeil M, Duchatelet C, Monsieurs K, and Idrissi SH. Quantifying inspiratory volumes generated by manual chest compressions during resuscitation in the prehospital setting. *Resuscitation* 2017;118; e18.
- [155] Waalewijn RA, de Vos R, Tijssen JG, and Koster RW. Survival models for out-of-hospital cardiopulmonary resuscitation from the perspectives of the bystander, the first responder, and the paramedic. *Resuscitation* 2001;51(2); 113–122.
- [156] Wang AY, Huang CH, Chang WT, Tsai MS, Wang CH, and Chen WJ. Initial end-tidal CO₂ partial pressure predicts outcomes of in-hospital cardiac arrest. *The American journal of emergency medicine* 2016;34(12); 2367–2371.

- [157] Wayne MA, Slovis CM, and Pirrallo RG. Management of difficult airways in the field. *Prehospital Emergency Care* 1999;3(4); 290–296.
- [158] Weil MH, Bisera J, Trevino RP, and Rackow EC. Cardiac output and end-tidal carbon dioxide. *Critical care medicine* 1985;13(11); 907–909.
- [159] Widrow B and Stearns SD. Adaptive Signal Processing. *Englewood Cliffs, NJ, Prentice-Hall* 1985;1; 1–491.
- [160] Wissenberg M, Lippert FK, Folke F, Weeke P, et al. Association of national initiatives to improve cardiac arrest management with rates of bystander intervention and patient survival after out-of-hospital cardiac arrest. *Jama* 2013;310(13); 1377–1384.
- [161] Yannopoulos D, McKnite S, Aufderheide TP, Sigurdsson G, et al. Effects of incomplete chest wall decompression during cardiopulmonary resuscitation on coronary and cerebral perfusion pressures in a porcine model of cardiac arrest. *Resuscitation* 2005; 64(3); 363–372.
- [162] Zheng ZJ, Croft JB, Giles WH, and Mensah GA. Sudden cardiac death in the United States, 1989 to 1998. *Circulation* 2001;104(18); 2158–2163.
- [163] Zipes DP and Wellens HJ. Sudden cardiac death. In Professor Hein JJ Wellens. Springer 2000;pages. 621–645.
- [164] Zuercher M, Hilwig RW, Ranger-Moore J, Nysaether J, et al. Leaning during chest compressions impairs cardiac output and left ventricular myocardial blood flow in piglet cardiac arrest. *Critical care medicine* 2010;38(4); 1141.

A | PUBLICATIONS

OBJECTIVE 1: TO ANALYZE AND QUANTIFY THE IMPACT OF CC-ARTIFACT ON A CAPNOGRAM-BASED MONITORING SYSTEM DURING CPR

Indexed journals

A1 *"Influence of chest compression artefact on capnogram-based ventilation detection during out-of-hospital cardiopulmonary resuscitation"*

Authors: M. Leturiondo, S. Ruiz de Gauna, J. Ruiz, J.J. Gutiérrez, L.A. Leturiondo, D.M. González-Otero, J.K. Russell, D. Zive, M.R. Daya

Published in: Resuscitation 2018, vol. 124, p. 63-68

Type of publication: Journal paper indexed in JCR

Quality indices: Ranking: 1/26 (Q1). JCR impact factor: 5.863

A2 *"Chest compressions induce errors in end-tidal carbon dioxide measurement"*

Authors: M. Leturiondo, S. Ruiz de Gauna, J.J. Gutiérrez, D. Alonso, C. Corcuera, J.F. Urtusagasti, D.M. González-Otero, J.K. Russell, M.R. Daya, J. Ruiz

Published in: Resuscitation 2020, vol. 153, p. 195-201

Type of publication: Journal paper indexed in JCR

Quality indices: Ranking: 2/31 (Q1). JCR impact factor: 4.215

Indexed international conferences

- C1** *"Reliability of ventilation guidance using capnography during ongoing chest compressions in out-of-hospital cardiopulmonary resuscitation"*
Authors: M. Leturiondo, S. Ruiz de Gauna, J. Ruiz, L.A. Leturiondo, J.M. Bastida, M.R. Daya
Published in: Resuscitation 2017, vol. 118, p. e18-e19
Type of publication: Indexed congress in JCR
Quality indices: Ranking: 2/24 (Q1). JCR impact factor: 5.230
- C2** *"A simple algorithm for ventilation detection in the capnography signal during cardiopulmonary resuscitation"*
Authors: M. Leturiondo, J. Ruiz, S. Ruiz de Gauna, D.M. González-Otero, J.M. Bastida, M.R. Daya
Published in: Proceedings of the IEEE Conference Computing in Cardiology 2017, vol. 44, p. 1-4
Type of publication: Indexed congress in SJR
Quality indices: SJR impact factor: 0.336
- C3** *"Chest compression artefact compromises real-time feedback capnometry: quantification of differences in end-tidal measurements by two capnometers"*
Authors: M. Leturiondo, S. Ruiz de Gauna, J.J. Gutiérrez, J. Ruiz, C. Corcuera, J.F. Urtusagasti, J.K. Russell, M.R. Daya
Published in: Resuscitation 2019, vol. 142, p. e32
Type of publication: Indexed congress in JCR
Quality indices: Ranking: 2/29 (Q1). JCR impact factor: 4.572



Clinical paper

Influence of chest compression artefact on capnogram-based ventilation detection during out-of-hospital cardiopulmonary resuscitation[☆]

Mikel Leturiondo^a, Sofía Ruiz de Gauna^{a,*}, Jesus M. Ruiz^a, J. Julio Gutiérrez^a, Luis A. Leturiondo^a, Digna M. González-Otero^a, James K. Russell^b, Dana Zive^b, Mohamud Daya^b

^a Department of Communications Engineering, University of the Basque Country, UPV/EHU, 48013 Bilbao, Spain

^b Department of Emergency Medicine, Oregon Health & Science University, OHSU, 97239-3098 Portland, OR, USA

ARTICLE INFO

Article history:

Received 5 August 2017

Received in revised form 4 December 2017

Accepted 11 December 2017

Keywords:

Cardiopulmonary resuscitation

Advanced life support

Capnography

Ventilation

Chest compression artefact

ABSTRACT

Background: Capnography has been proposed as a method for monitoring the ventilation rate during cardiopulmonary resuscitation (CPR). A high incidence (above 70%) of capnograms distorted by chest compression induced oscillations has been previously reported in out-of-hospital (OOH) CPR. The aim of the study was to better characterize the chest compression artefact and to evaluate its influence on the performance of a capnogram-based ventilation detector during OOH CPR.

Methods: Data from the MRx monitor–defibrillator were extracted from OOH cardiac arrest episodes. For each episode, presence of chest compression artefact was annotated in the capnogram. Concurrent chest compression depth and transthoracic impedance signals were used to identify chest compressions and to annotate ventilations, respectively. We designed a capnogram-based ventilation detection algorithm and tested its performance with clean and distorted episodes.

Results: Data were collected from 232 episodes comprising 52 654 ventilations, with a mean (\pm SD) of 227 (\pm 118) per episode. Overall, 42% of the capnograms were distorted. Presence of chest compression artefact degraded algorithm performance in terms of ventilation detection, estimation of ventilation rate, and the ability to detect hyperventilation.

Conclusion: Capnogram-based ventilation detection during CPR using our algorithm was compromised by the presence of chest compression artefact. In particular, artefact spanning from the plateau to the baseline strongly degraded ventilation detection, and caused a high number of false hyperventilation alarms. Further research is needed to reduce the impact of chest compression artefact on capnographic ventilation monitoring.

© 2017 Elsevier B.V. All rights reserved.

Introduction

Capnography is now considered a standard of care in advanced cardiopulmonary resuscitation (CPR) [1–3]. As emphasized in current resuscitation guidelines, advantages of capnography during CPR include assessment of the correct placement of the endotracheal tube [4], monitoring quality of chest compressions [5,6], early

identification of restoration of spontaneous circulation (ROSC) [7], and determination of patient prognosis [3,8,9].

Another important role of capnography during CPR is ventilation rate monitoring to prevent inadvertent hyperventilation [8]. Guidelines recommend ventilating the lungs at approximately 10 breaths per minute. However, excessive ventilation rates are common in resuscitation. In a clinical observational study, Aufherheide et al. reported ventilation rates of 30 breaths per minute or more as a norm [10]. Subsequent clinical studies have also confirmed the tendency to ventilate with such high rates [11,12]. One animal study revealed that similar excessive ventilation rates increased intrathoracic pressures and decreased coronary perfusion pressures and survival rates [13]. Another animal study by Gazmuri et al. reported no adverse hemodynamic effects during CPR after

[☆] A Spanish translated version of the summary of this article appears as Appendix in the final online version at <https://doi.org/10.1016/j.resuscitation.2017.12.013>.

* Corresponding author.

E-mail address: sofia.ruizdegauna@ehu.es (S. Ruiz de Gauna).

increasing ventilation rate and tidal volume over the recommended values, although they observed a decrease in end-tidal CO₂ values [14].

Current guidelines recommend using capnography during CPR to monitor ventilation rate and avoid hyperventilation. Visual inspection of the capnogram allows tracking respiratory cycles, since the onset of each ventilation causes a downstroke in the capnography waveform. Automated measurement of ventilation rate and algorithms for hyperventilation detection using capnography were first explored by Edelson et al. in 2010 [15], as an alternative to customary algorithms based on the transthoracic impedance recorded through defibrillation pads [16].

Quality of the recorded capnogram is essential for a reliable analysis, either visual or automated. However, a clean capnogram, in which the different phases of the respiratory cycle are identifiable (inspiratory downstroke, inspiratory baseline, expiratory upstroke, and alveolar plateau, where end-tidal CO₂ value is measured) cannot always be observed during CPR. Sources of artefact include issues related to the capnography device (occlusion in the CO₂ circuit, leaking) as well as the ongoing resuscitation efforts [1,17,18]. In this study, we focused on analysing the artefact induced on the capnogram by chest compressions during CPR. This artefact appears in the form of fast oscillations at different rates and with varying amplitude superimposed on the capnogram. This phenomenon has received little attention in the literature to date. An abstract presented at the 2010 American Heart Association Resuscitation Science Symposium reported chest compression artefact presence in greater than 70% of capnograms in a sample of 210 out-of-hospital (OOH) cardiac arrest episodes [19]. To our knowledge there are no published studies that systematically analyse the morphology of this artefact. We hypothesized that chest compression artefact may impede a reliable analysis of the capnogram, compromising its application for ventilation rate monitoring.

The purpose of this study was three-fold. First, we identified capnograms distorted by chest compression artefact in a large dataset of OOH cardiac arrest episodes in order to confirm the high incidence of this artefact during CPR. Second, we characterized the morphology of chest compression artefact. Third, we assessed the impact of chest compression artefact on the reliability of automated capnogram-based guidance of ventilation rate.

Materials and methods

Data collection

Data were extracted from a database of 691 OOH episodes collected between 2011 and 2016 by Tualatin Valley Fire & Rescue (TVF&R), an advanced life support first response Emergency Medical Services (EMS) agency serving eleven incorporated cities (about 1015 km²) in Oregon, USA. Episodes were collected as part of the Resuscitation Outcomes Consortium (ROC) Epidemiological Cardiac Arrest Registry. The data collection for the ROC Epistry was approved by the Oregon Health & Science University (OHSU) Institutional Review Board (ID: IRB00001736). No patient private data was required for this study.

Episodes were recorded with Heartstart MRx monitor-defibrillators (Philips, USA), equipped with real-time CPR feedback technology (Q-CPR). Capnography was acquired using sidestream technology (Microstream, Orion Systems Ltd., Israel). Ventilation was provided with a bag-valve-mask or an advanced airway. The choices for the latter were the endotracheal tube or the King LT-D (supraglottic). Defibrillator signals used in the study were the capnogram, the compression depth (CD) signal measured by the Q-CPR chest pad, and the transthoracic impedance (TI) signal acquired from defibrillation pads.

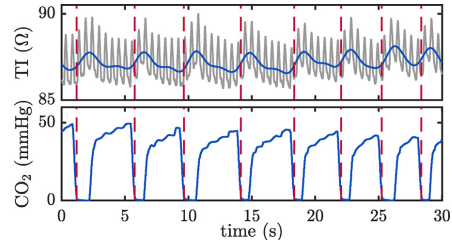


Fig. 1. Example of ventilations annotated using the low frequency component of the TI signal (top panel, blue line). This signal was obtained after low pass filtering the raw TI signal (top panel, grey line). Each ventilation was identified at the instant corresponding to a rise in each TI fluctuation (vertical dashed red lines). The capnogram (bottom panel) is depicted with the annotations to visually confirm ventilations at the instants where CO₂ concentration rapidly decays to zero.

Episodes with at least 20 min of continuous and simultaneous signals, and with a minimum of 500 chest compressions were included in the study, which yielded a total of 301 episodes.

Data annotation

Signals were reviewed and annotated using a custom-made Matlab (Mathworks, USA) program. Intervals with unreliable raw TI signal or capnogram caused by disconnections or excessive noise were discarded. For each episode, capnograms were time-shifted to compensate for the delay with respect to CD and TI signals.

Three biomedical engineers with experience in the analysis of OOH defibrillator signals participated in the annotation process. They reviewed one third of the cases jointly, and defined the annotation rules for identifying capnograms distorted by chest compression artefact, and for annotating ventilations using the TI signal. The rest of episodes were randomly split in three parts, each of them examined by a single reviewer. At the end of this process, the three experts joined again to solve by consensus undecided annotations.

Experts annotated intervals in which capnograms were distorted by chest compression artefact, with the support of the CD signal. Episodes were classified as distorted if evident chest compression artefact appeared during more than 1 min of the chest compression time. In addition, they annotated the location of the artefact with respect to the respiratory phase (e.g. appearing mainly on the expiratory phase or on the inspiratory phase).

Ventilations were manually annotated using the low frequency component of the TI signal. A low-pass filter was applied to the raw TI signal to suppress fast oscillations caused by chest compressions and enhance slow fluctuations caused by ventilations. Fig. 1 (top panel) shows the raw TI signal in grey with the low frequency TI component superimposed in blue. Each ventilation was annotated at the instant corresponding to a rise in each TI fluctuation (marked with a vertical dashed red line in Fig. 1). The capnogram is depicted in the bottom panel to visually confirm the presence of ventilations. The resulting annotations were used as our gold standard to test the performance of the automated capnogram-based ventilation detection algorithm.

Automated capnogram-based ventilation detection algorithm

The algorithm used in this study processes the capnogram, and was designed following a finite-state-machine model. Fig. 2 shows the flow chart of the algorithm (top) and the definition of the main parameters of the algorithm (bottom). Basically, the algorithm searches for an abrupt upstroke in the capnogram, $r_{i_{up}}$,

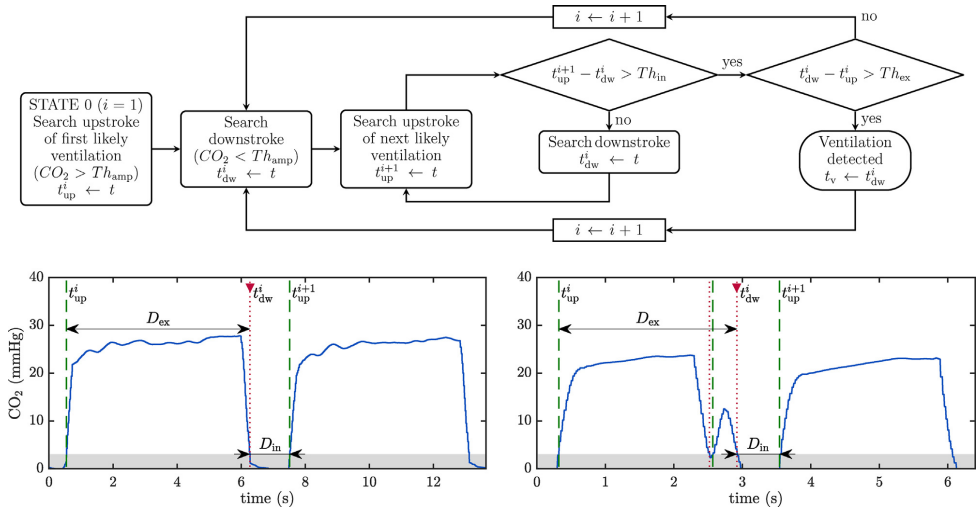


Fig. 2. Flow chart of the ventilation detector (top). Main parameters of the algorithm (bottom). Capnogram ascents and descents crossing the shadowed area (amplitude threshold) are depicted with dashed/dotted lines. Downward arrow marks the position of the detected ventilation.

which is detected when the amplitude of the capnogram exceeds a fixed threshold, Th_{amp} (mmHg). Then, the algorithm searches for an abrupt downstroke, t_{dw}^i , detected when the capnogram goes below the same threshold, Th_{amp} . To detect a ventilation, the duration of the interval $D_{ex} = t_{dw}^i - t_{up}^i$ and the duration of the interval $D_{in} = t_{up}^{i+1} - t_{dw}^i$ must exceed thresholds Th_{ex} and Th_{in} , respectively. If both conditions are satisfied, the ventilation is annotated at the instant when the inspiratory downstroke occurs, t_{dw}^i .

To account for observed double ventilation effects (Fig. 2, bottom right), the algorithm discards any ventilation for which the interval D_{in} is below Th_{in} , and searches for the next downstroke and upstroke until D_{in} exceeds Th_{in} .

Data analysis

Ventilation detector performance was evaluated in terms of its sensitivity (Se) and positive predictive value (PPV). Se was defined as the proportion of annotated ventilations detected by the algorithm. PPV was the proportion of detections that were indeed annotated ventilations. We allowed a tolerance of $\pm 0.5s$ between the detection and the annotation instant. The algorithm was trained with a subset of clean (non-distorted) episodes applying the criterion of maximum Se while assuring a PPV $> 98\%$.

In order to assess the influence of the artefact in the estimation of ventilation rate, we computed, for each episode, ventilation rate value per minute, updated every 10 s. These ventilation rate measurements were computed using the gold standard (annotated ventilations) and using the ventilations detected by our algorithm.

We also computed hyperventilation alarms from the ventilation rate per minute measurements. Results were obtained for hyperventilation thresholds set at 10, 15, and 20 min^{-1} . Then, we tested the ability of our algorithm to correctly detect hyperventilation. In this case, Se was defined as the proportion of annotated hyperventilation alarms that were given by the algorithm, and PPV as the proportion of hyperventilation alarms given that were indeed annotated.

Data were reported as mean (\pm SD) if they passed Lilliefors normality test, and as median (IQR) otherwise. Distribution of Se and

PPV per record, and distributions of the percent error in the estimation of ventilation rate were depicted with boxplots.

Finally, the morphology of the artefact was characterized by the spectral analysis of clean and distorted capnograms. We computed the power spectral density (PSD) of the capnogram and located the frequency components associated with the artefact. We used the chest compression rate derived from the CD signal as reference.

Results

From the original dataset of 301 episodes, 69 were discarded (23%) due to unreliable capnogram or TI signals. Reasons for elimination were: permanent signal disconnection or saturation, capnogram below 5 mmHg along the entire episode or without variations associated to respiratory cycles, and failure to observe ventilation waves in the filtered TI signal. Thirty-two episodes out of 69 were discarded due to unreliable capnogram, 20 to unreliable TI signal, and 17 due to unreliability of both signals. Overall, unreliable capnograms were found in 16.3% of the episodes included in the study. The remaining 232 episodes had a mean duration of 31 (± 9.5) min, with a mean of 2301 (± 1230) annotated chest compressions per episode.

Ninety-eight episodes (42%) were annotated as distorted. We classified the artefact into three types: observed primarily in the expiratory plateau of the capnogram (type I), in the baseline (type II), and spanning from the plateau to the baseline (type III). Fig. 3A shows examples of capnogram intervals observed during chest compressions.

We conducted a spectral analysis to characterize the waveform nature of the chest compression artefact. This is illustrated in Fig. 3B, which depicts an interval of corrupted capnogram (top), the concurrent CD signal (middle) and the PSD of the capnogram. A primary peak is clearly observed at 1.94 Hz, with no peaks at frequencies multiple of this fundamental frequency, i.e. no harmonic components. This value corresponds to the fundamental frequency of the artefact, f_{art} , and matches the average compression rate in that interval ($f_{art} \cdot 60 = 116$ compressions per minute). This proves

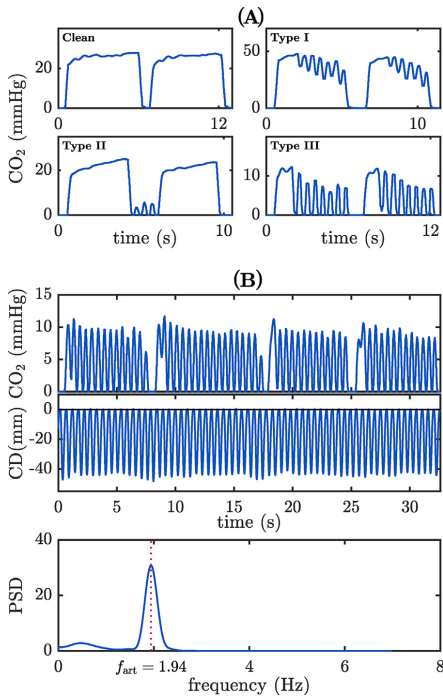


Fig. 3. (A) Examples of chest compression artefact observed in OOH capnograms during chest compressions: clean capnogram; Type I artefact, located in the plateau; Type II, located in the baseline; Type III, spanning from the plateau to the baseline. (B) Spectral characterization of chest compression artefact in a distorted capnogram (top), CD signal, with average chest compression rate of 116 compressions per minute (middle), PSD of the distorted capnogram (bottom): the observed single peak corresponds to the fundamental frequency of the artefact, i.e. a sine wave superimposed to the lower frequency capnogram waveform.

that the artefact is mainly sinusoidal and that it is directly caused by chest compressions during CPR.

Table 1 shows the incidence of each artefact type in relation to the airway system used in each case. Type I artefact was annotated in 48% of the distorted episodes, type II in 21%, and type III in 31% of the episodes. Artefact did not appear in the episodes where bag-valve-mask was used. However, all types of artefact appeared in every advanced airway type, although the incidence was higher for supraglottic cases. Incidence of type III artefact (plateau to baseline) was more prevalent in endotracheal intubation, and incidence of type I (plateau) was more prevalent in supraglottic.

A total number of 52 654 ventilations were annotated, with a mean of 227 (± 118) ventilations per episode. Clean episodes comprised 30 814 ventilations, and distorted episodes 21 840 ventilations (Type I: 10 119, Type II: 5228, and Type III: 6493).

The ventilation detection algorithm was trained with a subset of 30 clean episodes. Optimal values for algorithm parameters Th_{ex} and Th_{in} were achieved for a Se/PPV of 99.8/99.0%. Fig. 4A shows the performance results of the ventilation detector algorithm using the test subset. Boxplots depict the distribution of the Se and PPV calculated per episode. For the whole test subset, median (IQR) Se was 99.4 (97.8–100)%, and PPV was 98.6 (96.4–99.5)%. For the distorted test subset, Se was 97.4 (90.3–99.3)%, and PPV was 95.6 (85.9–98.3)%. For type III episodes, Se decreased to 85.2

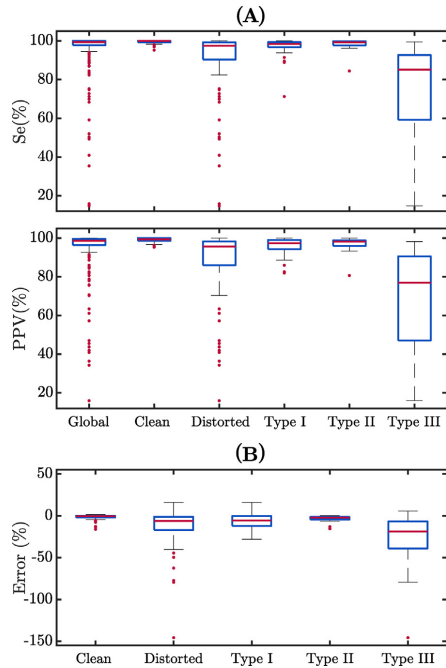


Fig. 4. (A) Performance of the ventilation detector algorithm. (B) Distribution of the error in the estimation of ventilation rate. Results are provided globally and for the different subgroups. The boxes show the median and IQR and the whisker shows the last datum within the ± 1.5 IQR. Outliers are represented by dots.

(59.2–92.7)%, and PPV to 76.9 (47.0–90.5)%. Fig. 4B shows the distribution of the percent error in the estimation of the ventilation rate. For the clean episodes, median error was -0.6 (-1.9 to 0.0)%. For the distorted test subset, error was -6.1 (-16.9 to 1.2)%. For type III episodes, error was -18.8 (-39.1 to 6.7)%.

Table 2 shows the algorithm performance in the detection of hyperventilation alarms. Hyperventilation was accurately detected regardless of the hyperventilation threshold in the clean episodes. Performance decreased in the distorted group, particularly with respect to PPV. Detection of hyperventilation was particularly compromised in the presence of type III artefact.

Discussion

Monitoring ventilation rate is one of the recommended uses of capnography waveform during CPR. However, the presence of high-frequency oscillations in the capnogram during chest compressions may compromise the interpretation of the signal.

Our findings demonstrated the impact of this artefact on the reliability of capnogram guided ventilation monitoring. Detection of ventilations was accurate for clean episodes (Se and PPV were above 95% for all episodes), but algorithm performance significantly decreased when artefact was present. For some of the cases Se and PPV were well below 80%, and errors in the measurement of ventilation rate were as high as 50%. This means that, with such a degree of distortion, reliable ventilation rate guidance would not be feasible for those patients. These poor results were mainly attributable to type III artefact, annotated in 31% of the distorted episodes (13% of all episodes). Oscillations disturbing the capnogram from the

Table 1
Distribution of episodes according to artefact classification and type of ventilation.

Episodes	Ventilation type					Total
	BVM	ETT	SGA	NA		
Total	7	149	73	3		232
Clean	7	90	35	2		134
Distorted	0	59 (39.6%) ^a	38 (52.1%) ^a	1		98 (42.2%) ^a
Type I	0	19 (32.2%) ^b	28 (73.7%) ^b	0		47 (47.9%) ^b
Type II	0	15 (25.4%) ^b	6 (15.8%) ^b	0		21 (21.4%) ^b
Type III	0	25 (42.4%) ^b	4 (10.5%) ^b	1		30 (30.7%) ^b

BVM: bag-valve-mask; ETT: endotracheal tube; SGA: supraglottic airway.

NA: not available.

^a Referred to the total number of episodes in the category (column).

^b Referred to the total number of distorted episodes in the category (column).

Table 2

Algorithm performance (Se and PPV) in the detection of hyperventilation alarms; *n* (total) is the number of ventilation rate per minute measurements annotated in the test subset, and *n* is the number of annotated ventilation rate per minute measurements above the hyperventilation threshold.

Group	<i>n</i> (total)	Alarms (>10 min ⁻¹)			Alarms (>15 min ⁻¹)			Alarms (>20 min ⁻¹)		
		<i>n</i>	Se (%)	PPV (%)	<i>n</i>	Se (%)	PPV (%)	<i>n</i>	Se (%)	PPV (%)
Total	31 760	17 901	99.1	92.6	8966	98.1	87.2	3567	95.1	86.8
Clean	17 413	10 511	99.7	98.0	5710	99.5	96.8	2502	97.7	95.1
Distorted	14 347	7390	98.2	85.8	3256	95.7	73.9	1065	88.8	70.9
Type I	7167	3398	98.9	90.8	1275	95.9	79.5	431	88.4	82.5
Type II	2826	1837	99.8	96.6	1120	99.2	92.1	355	97.2	86.0
Type III	4354	2155	95.5	72.1	861	90.9	53.2	279	78.9	46.6

plateau to the baseline impeded the reliable detection of CO₂ concentration changes associated to a true ventilation.

Ventilation rates above the recommended 10 breaths per minute were common in our database, with a 56.4% of annotated hyperventilation alerts. Regardless the established hyperventilation threshold, sensitivity for alarm detection was high for clean and also for distorted cases in general. However, the presence of artefact caused an increase in the number of false hyperventilation alarms, and this was especially noticeable for type III cases. This shows the tendency of the algorithm to overestimate ventilation rate, as the presence of artefact caused many false ventilation detections.

The incidence and nature of the artefact has not been studied in the literature. To our knowledge, only one prior study has examined the impact of chest compression artefact on the capnogram during OOH CPR [19]. In this study only published as a conference abstract, Idris et al. reported that 73% (154/210) of the episodes were disturbed by oscillations due to chest compressions. In our study, we found a lower incidence (42%) of corrupted capnograms for a similar number of OOH records (232 vs. 210). This difference could be partly explained by different annotation criteria for corrupted episodes. Nevertheless, characterization and analysis of potential effects of such artefact on the interpretation of the capnogram are warranted.

We quantitatively confirmed the pure sine wave nature of the chest compression artefact, with a frequency matching the chest compression rate. This suggests that the artefact is directly caused by chest compressions during CPR. We consider that chest compressions cause incidental ventilations of sufficient volume to alter the CO₂ concentration sensed by the capnography device, distorting the capnogram. Few studies have documented low ventilation volumes incidental to chest compressions [20,21]. These volumes were lower than the anatomical dead space, and therefore generated limited gas exchange. Additionally, in our study artefact appeared when advanced airway was used, and was more predominant for supraglottic (King LT-D). However, the most compromising type III artefact was more pronounced with endotracheal intubation. Differences in the seal position and the cuff size might explain this, but more studies are necessary to interpret these findings.

One of the hypothesis we will explore in further research is that automatic ventilation detection would improve if the artefact could be successfully removed from the capnogram. Designing filtering approaches for this aim will be our next step, exploring different alternatives. We will focus on the preservation of the capnogram waveform after filtering in order to allow the clinical interpretation of the signal.

Our study has several limitations. First, almost a quarter of episodes were discarded due to poor signal quality. Unreliable capnogram represented the 10% of the study dataset. Recordings of unreliable capnograms would limit its use to determine ventilation rate. In addition, our gold standard for ventilation detection was derived from the TI signal, and the annotation of TI fluctuations caused by ventilations is not straightforward during CPR. We had to discard several episodes because of unreliable TI signal (noisy, disconnections) and for those included in the study, filtering was needed to remove the artefact due to chest compressions from the TI signal. Unfortunately, no other reference signal (such as airway pressure or volume) was available to be used as an alternative gold standard. The inability to control for tidal volume was thus a clear limitation of the study. Another limitation is that ventilations corresponding with capnogram amplitudes below the algorithm amplitude threshold (3 mmHg) could not be detected. However, in our data that was rarely observed. Finally, data came from a single EMS system and so results may not be generalizable. Further studies are needed to clarify our findings with other EMS agencies and monitor-defibrillators.

Conclusions

The important role of capnography waveform in ventilation rate monitoring and hyperventilation prevention during CPR is compromised by the high-incidence of chest compression artefact. Among the different locations in which it may present, artefact spanning from the plateau to the baseline strongly affected ventilation detection, and caused a high number of false hyperventilation alarms. Further research could explore filtering techniques to suppress

M. Leturiondo et al. / Resuscitation 124 (2018) 63–68

chest compression artefact in order to improve ventilation monitoring for corrupted capnograms.

Conflict of interest

The authors declare no conflicts of interest.

Acknowledgements

This work received financial support from the Basque Government (Basque Country, Spain) through the project IT1087-16 and the predoctoral research grant PRE-2016-1-0104. The authors thank the TVF&R EMS providers for collecting the data used in this study.

References

- [1]. Pantazopoulos C, Xanthos T, Pantazopoulos I, Papalois A, Kouskouni E, Iacovidou N. A review of carbon dioxide monitoring during adult cardiopulmonary resuscitation. *Heart Lung Circ* 2015;24(11):1053–61.
- [2]. Meaney PA, Bobrow BJ, Mancini ME, et al. Cardiopulmonary resuscitation quality: improving cardiac resuscitation outcomes both inside and outside the hospital: a consensus statement from the American Heart Association. *Circulation* 2013;128(4):417–35.
- [3]. Kodali BS, Urman RD, et al. Capnography during cardiopulmonary resuscitation: current evidence and future directions. *J Emerg Trauma Shock* 2014;7(4):332.
- [4]. Silvestri S, Ralls GA, Krauss B, et al. The effectiveness of out-of-hospital use of continuous end-tidal carbon dioxide monitoring on the rate of unrecognized misplaced intubation within a regional emergency medical services system. *Ann Emerg Med* 2005;45(5):497–503.
- [5]. Ditchey RV, Winkler JV, Rhodes CA. Relative lack of coronary blood flow during closed-chest resuscitation in dogs. *Circulation* 1982;66(2):297–302.
- [6]. Qvigstad E, Kramer-Johansen J, Tømte Ø, et al. Clinical pilot study of different hand positions during manual chest compressions monitored with capnography. *Resuscitation* 2013;84(9):1203–7.
- [7]. Pokorná M, Nečas E, Kratochvíl J, Skřípský R, Andrlík M, Franěk O. A sudden increase in partial pressure end-tidal carbon dioxide (PETCO₂) at the moment of return of spontaneous circulation. *J Emerg Med* 2010;38(5):614–21.
- [8]. Soar J, Nolan JP, Böttiger BW, et al. European Resuscitation Council guidelines for resuscitation 2015. Section 3. Adult advanced life support. *Resuscitation* 2015;95:100–47.
- [9]. Touma O, Davies M. The prognostic value of end tidal carbon dioxide during cardiac arrest: a systematic review. *Resuscitation* 2013;84(11):1470–9.
- [10]. Aufderheide TP, Lurie KG. Death by hyperventilation: a common and life-threatening problem during cardiopulmonary resuscitation. *Crit Care Med* 2004;32(9):S345–51.
- [11]. O'Neill JF, Deakin CD. Do we hyperventilate cardiac arrest patients? *Resuscitation* 2007;73(1):82–5.
- [12]. Maertens VL, De Smedt LE, Lemoine S, et al. Patients with cardiac arrest are ventilated two times faster than guidelines recommend: an observational prehospital study using tracheal pressure measurement. *Resuscitation* 2013;84(7):921–6.
- [13]. Aufderheide TP, Sigurdsson G, Pirralo RG, et al. Hyperventilation-induced hypotension during cardiopulmonary resuscitation. *Circulation* 2004;109(16):1960–5.
- [14]. Gazmuri RJ, Ayoub IM, Radhakrishnan J, Motl J, Upadhyaya MP. Clinically plausible hyperventilation does not exert adverse hemodynamic effects during CPR but markedly reduces end-tidal PCO₂. *Resuscitation* 2012;83(2):259–64.
- [15]. Edelson DP, Eilevstjønn J, Weidman EK, Retzer E, Hoek TLV, Abella BS. Capnography and chest-wall impedance algorithms for ventilation detection during cardiopulmonary resuscitation. *Resuscitation* 2010;81(3):317–22.
- [16]. Alonso E, Ruiz J, Aramendi E, et al. Reliability and accuracy of the thoracic impedance signal for measuring cardiopulmonary resuscitation quality metrics. *Resuscitation* 2015;88:28–34.
- [17]. Takla G, Petre JH, Doyle DJ, Horibe M, Gopakumaran B. The problem of artifacts in patient monitor data during surgery: a clinical and methodological review. *Anesthes Analg* 2006;103(5):1196–204.
- [18]. Herry CL, Townsend D, Green GC, Bravi A, Seely AJE. Segmentation and classification of capnograms: application in respiratory variability analysis. *Physiol Meas* 2014;35(12):2343.
- [19]. Idris AH, Daya M, Owens P, et al. High incidence of chest compression oscillations associated with capnography during out-of-hospital cardiopulmonary resuscitation. *Circulation* 2010;122:A83.
- [20]. Idris AH, Banner MJ, Wenzel V, Fuerst RS, Becker LB, Melker RJ. Ventilation caused by external chest compression is unable to sustain effective gas exchange during CPR: a comparison with mechanical ventilation. *Resuscitation* 1994;28(2):143–50.
- [21]. Vanwulpen M, Wolfskeil M, Duchatelet C, Monsieurs K, Idrissi SH. Quantifying inspiratory volumes generated by manual chest compressions during resuscitation in the prehospital setting. *Resuscitation* 2017;118:e18.



ELSEVIER

Available online at www.sciencedirect.com

Resuscitation

journal homepage: www.elsevier.com/locate/resuscitation

Clinical paper

Chest compressions induce errors in end-tidal carbon dioxide measurement



Mikel Leturiondo^{a,*}, Sofía Ruiz de Gauna^a, José Julio Gutiérrez^a, Daniel Alonso^b, Carlos Corcuera^b, Juan Francisco Urtusagasti^b, Digna María González-Otero^{a,c}, James Knox Russell^d, Mohamud Ramzan Daya^d, Jesus María Ruiz^a

^a University of the Basque Country, UPV/EHU, Bilbao, Bizkaia, Spain

^b Emergentziak-Osakidetza, Basque Country Health System, Basque Country, Spain

^c BEXEN Cardio, Ermua, Bizkaia, Spain

^d Oregon Health & Science University, OHSU, Portland, OR, USA

Abstract

Background: Real-time measurement of end-tidal carbon dioxide (ETCO₂) is used as a non-invasive estimate of cardiac output and perfusion during cardiopulmonary resuscitation (CPR). However, capnograms are often distorted by chest compressions (CCs) and this may affect ETCO₂ measurement. The aim of the study was to quantify the effect of CC-artefact on the accuracy of ETCO₂ measurements obtained during out-of-hospital manual CPR.

Methods: We retrospectively analysed monitor-defibrillator recordings collected by two advanced life support agencies during out-of-hospital cardiac arrest. These two agencies, represented as A and B used different side-stream capnometers and monitor-defibrillators. One-minute capnogram segments were reviewed. Each ventilation within each segment was identified using the transthoracic impedance signal and the capnogram. ETCO₂ values per ventilation were manually annotated and compared to the corresponding capnometry values stored in the monitor-defibrillator. Ventilations were classified as distorted or non-distorted by CC-artefact.

Results: A total of 407 1-min capnogram segments from 65 patients were analysed. Overall, 4095 ventilations were annotated, 2170 (32.4% distorted) and 1925 (31.8% distorted) for agency A and B, respectively. Median (IQR) unsigned error in ETCO₂ measurement increased from 1.5 (0.6–3.1)% for non-distorted to 5.5 (1.8–14.1)% for distorted ventilations; from 0.7 (0.3–1.2)% to 3.7 (1.0–9.9)% in agency A and from 2.3 (1.2–3.9)% to 8.3 (3.9–19.5)% in agency B ($p < 0.001$). Errors were higher than 10 mmHg in 9% and higher than 15 mmHg in 5% of the distorted ventilations.

Conclusion: CC-artefact causes ETCO₂ measurement errors in the two studied devices. This suggests that capnometer algorithms may need to be adapted to reliably perform in the presence of CC-artefact during CPR.

Keywords: Cardiopulmonary resuscitation, Advanced life support, Capnometry, Waveform capnography, End-tidal CO₂, Chest compressions, Ventilations

Introduction

Capnometry includes the measurement of the end-tidal carbon dioxide (ETCO₂) value in the exhaled air during the breathing cycle, described as the partial pressure of carbon dioxide (PCO₂) at the end

of expiration.¹ Since 2010, advanced life support (ALS) resuscitation guidelines^{2,3} have recommended the adoption of capnometry and continuous waveform capnography as a noteworthy non-invasive monitoring tool during cardiopulmonary resuscitation (CPR) that reflects ventilation and perfusion of the patient.¹ The value of waveform capnography for monitoring the effectiveness of CPR

* Corresponding author.

E-mail address: mikel.leturiondo@ehu.eus (M. Leturiondo).

<https://doi.org/10.1016/j.resuscitation.2020.05.029>

Received 10 January 2020; Received in revised form 17 April 2020; Accepted 9 May 2020

0300-9572/© 2020 Elsevier B.V. All rights reserved.

during out-of-hospital cardiac arrest (OHCA) was then further emphasized in an expert consensus statement.⁴

Waveform capnography (the capnogram) has currently several important roles during cardiac arrest.⁵ It can be used to assess the correct placement of the airway tube⁶ and for ventilation rate monitoring.^{7–9} Furthermore, monitoring of ET CO_2 may allow for the assessment of the quality of CPR,^{10,11} early detection of ROSC^{10,12,13} and prediction of survival from cardiac arrest.^{14–16} Accuracy of measured ET CO_2 values is essential for the validity and reliability of clinical decision rules that might be used during the resuscitation attempt. For a reliable automated ET CO_2 measurement during CPR, all phases of the respiratory cycle must be identifiable in the capnogram. However, oscillations induced in OHCA capnograms at the same rate of chest compressions (CC) are frequent¹⁷ and these can obscure capnogram measurements during chest compressions.^{18,19} In a letter to the editor, Raimondi et al. described the differences observed between the capnometry numbers and the values that could be inferred by the observation of the CO_2 waveform.²⁰ They concluded that the displayed ET CO_2 value was underestimated and changed continuously in the presence of chest compressions, and suggested looking at the curves for interpretation. However, CO_2 waveform distortion caused by chest compressions could lead to a lack of confidence in the interpretation of the signal.

This phenomenon was previously assessed in an observational study aimed at characterizing the CC-artefact in OHCA capnograms.¹⁹ This study quantified the negative effect of the CC-artefact on the automated detection of ventilations. Chest compression fluctuations in the capnogram caused false ventilation detections. We observed that these oscillations also made detection of the ends of expirations very difficult. Thus, we hypothesized that the accuracy and reliability of the measured ET CO_2 obtained in the presence of CC-artefact could be inaccurate, which is in line with the observations made by Raimondi et al.²⁰

The aim of the study was to quantify the impact of CC-artefact on ET CO_2 measurement provided by two different CO_2 detectors during manual CPR. For that purpose, we collected OHCA recordings from two ALS agencies, each one using a different brand of CO_2 detector and monitor-defibrillator. We manually annotated the ET CO_2 values using the capnogram waveforms and compared them with the capnometry values obtained directly from the recordings.

Methods

Data collection

Episodes included in the study were obtained from two OHCA databases. Several episodes were extracted from a large database of OHCA episodes collected by Tualatin Valley Fire & Rescue (TVF&R), an ALS first response emergency medical services (EMS) agency serving eleven incorporated cities in Oregon, USA. Other episodes were extracted from a database collected by the ALS of Emergentziak-Osakidetza, the EMS system of the Basque Country (Spain). Data collections were approved by the Oregon Health & Science University (OHSU) Institutional Review Board (IRB00001736) and by the Ethical Committee of Research with Medicines of the Basque Country (PI2018003), respectively. Each agency used different side-stream capnography technology and monitor-defibrillators: Heartstart MRx (Philips, USA) equipped with Microstream™ (Oridion, Israel) capnography technology and Reanibex 500 EMS (Bexen Cardio, Spain)

equipped with Masimo ISA™ CO_2 (Masimo, Sweden) capnometer, respectively. Endotracheal tube (ETT) or supraglottic King LT-D™ devices were used to secure the airway. After the airway was secured, continuous CCs and ventilations were provided manually.

Episodes contained no personal information. Only recordings containing concurrent capnogram, compression depth (CD) and transthoracic impedance (TI) signals were included in the study. Signal recordings were exported to a common format using Matlab (Mathworks, USA). Additionally, capnometry values and their corresponding timestamps were extracted from the monitor-defibrillator recordings.

Segment selection and data annotation

Episodes were examined and annotated by ML and reviewed by JG and SRG, all with experience in analysing monitor-defibrillator signals. A custom-made program was used to concurrently visualize the three signals and the capnometry events extracted from each recording. Intervals with signal disconnections or noise were discarded. Within each episode, capnogram segments containing series of complete ventilations of approximately 1-min length were extracted. A 1-min interval was used in order to have a sufficient number of ventilations for averaging our annotations, and to accommodate any undisclosed differences in the proprietary algorithms used to record the ET CO_2 values to which we compared our annotations. Only segments with regularly reported capnometry events were included. The CD signal was used as the reference to determine when CCs were provided. Two types of segments were identified: distorted segments, when evident CC-artefact appeared in the whole interval; and non-distorted segments, with no ventilation distorted by CC-artefact in its entire duration.

Compressions and ventilations induce fluctuations in the TI signal.^{21,22} TI increases during inspiration due to the rise in the gas volume of the chest, therefore ventilations induce slow fluctuations in the TI signal around patient's impedance baseline. In order to enhance slow fluctuations caused by ventilations, a low-pass filter was applied to the raw TI signal to suppress fast oscillations caused by chest compressions. Each individual ventilation was identified using both the filtered TI signal and the original capnogram. Fig. 1 shows an example of non-distorted segment (a) and an example of distorted segment (b), showing the TI signal (top panel) and the capnogram. In the top panel, the low frequency TI component allowing tracking of ventilations is depicted in blue superimposed to the raw TI signal in grey. As shown in the bottom panel, ventilations were annotated at the instant corresponding to the peak in the TI confirmed by a zero level in the capnogram (green dashed vertical lines). Each ventilation was classified as distorted or non-distorted by CC-artefact using the criteria applied in a previous work.¹⁹ Finally, ET CO_2 level was manually annotated as the maximum CO_2 level in each ventilation cycle (red dots).²³

Data analysis

Differences between the annotated and the capnometer ET CO_2 value per each ventilation in the segment were analysed. Measurement error was defined as the difference between the extracted and the annotated ET CO_2 values. Data were reported as median (IQR) since no distribution passed the Lilliefors normality test. Comparison between groups was assessed using the Wilcoxon rank sum test. p -values <0.05 were considered significant.

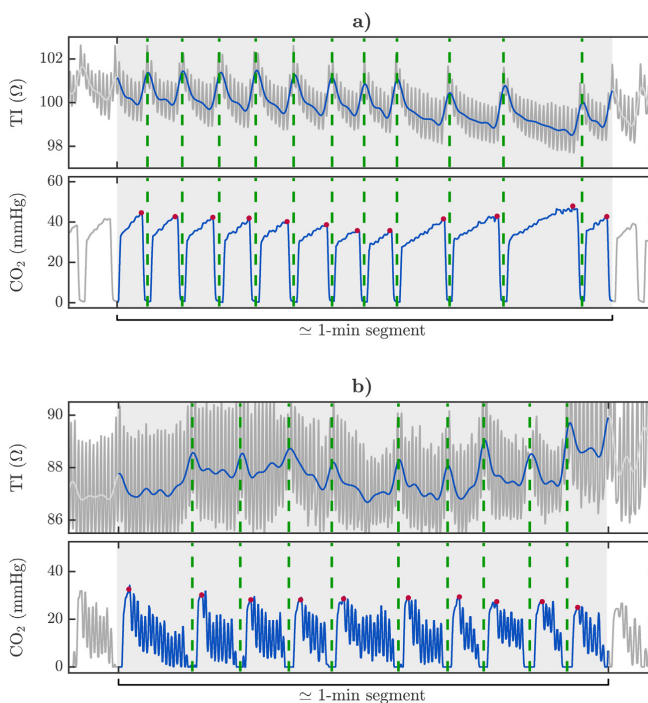


Fig. 1 – Example of identification of non-distorted (a) and distorted (b) 1-min capnogram segments. Top panel: The raw TI signal is depicted in grey, showing CC activity (fast oscillations) and ventilation activity (slow oscillations). The low-pass filtered TI signal (only ventilation activity) is depicted in blue. Bottom panel: capnogram signal where each ventilation is marked with a green vertical dashed line. Manually annotated ETCO₂ values are depicted with red dots. (For interpretation of the references to color in this figure legend, the reader is referred to the web version of this article.)

Table 1 – Summary of the characteristics of the dataset. Statistics are reported as median (IQR). N/A stands for Not Available.

	Agency A	Agency B	Global
Episodes	47	18	65
1-min segments	237	170	407
Distorted	104 (43.8%)	50 (29.4%)	154 (37.8%)
Duration (s) per segment	60.2 (57.5–63.9)	60.8 (58.6–63.4)	60.6 (58.1–63.6)
Num. ventilations	2170	1925	4095
Distorted	703 (32.4%)	612 (31.8%)	1315 (32.1%)
Vent. per segment	8 (6–12)	11 (10–13)	10 (7–12)
Vent. rate per segment (vpm)	8.2 (6.1–12.1)	10.9 (9.6–12.3)	9.9 (7.4–12.2)
Mean ETCO ₂ per segment (mmHg)	40.6 (26.5–51.1)	16.9 (13.2–22.4)	25.7 (16.5–44.6)
Airway type			
ETT	104	170	274
King LT-D™	113	–	113
N/A	20	–	20

Results

Henceforth, results from each data subset (agency) are identified as from agency A and agency B. Thus, we avoid tracking of the capnometer and monitor-defibrillator type associated to each subset.

Data characteristics

Episodes from agency A were collected from 2016 through 2017 and episodes from agency B were collected from 2018 to 2019. All available episodes from agency B by the time we initiated our study were analysed ($n=26$). Since the dataset from agency A was much larger, we arbitrarily selected twice the former number. Five episodes from agency A and 8 from agency B were discarded since they did not contain all concurrent signals and/or capnometry values. The included episodes had a median (IQR) duration of 19 (13–27) min, corresponding to a total capnogram duration of 1303 min (A: 947 min, B: 355 min).

Table 1 summarises the characteristics of the database. A total of 407 1-min segments from 65 episodes comprising 4095 ventilations, with a median (IQR) of 10 (7–12) ventilations per segment, were included in the study. Overall, 37.8% of the segments were distorted by CC-artefact, corresponding to 32.1% distorted ventilations. Segments from agency A had a total of 2170 ventilations (32.4% distorted), whereas segments from agency B had 1925 ventilations (31.8% distorted). Median (IQR) ventilation rate was 9.9 (7.4–12.2) ventilations per minute (vpm). Despite ventilation rates were higher for agency B ($p < 0.001$), both were close to the guidelines recommendation of 10 vpm after placement of an advanced airway.^{24,25} Mean $ETCO_2$ per segment was higher for agency A ($p < 0.001$), with a median (IQR) of 40.6 (26.5–51.1) mmHg, than for agency B, with a median (IQR) of 16.9 (13.2–22.4). Airway type was ETT in 67.3% of these segments and supraglottic King LT-D™ in 27.8% (not used by agency B). Airway type was unknown for 4.9% of the segments.

Analysis of $ETCO_2$ errors

Fig. 2 shows the distributions of the unsigned error for non-distorted and distorted ventilations, in percentage (top panel) and in mmHg (middle panel), for each agency and for all analysed ventilations. Median unsigned error in $ETCO_2$ measurement for all non-distorted ventilations was 1.5 (0.6–3.1)%; it was 0.7 (0.3–1.2)% for agency A and 2.3 (1.2–3.9)% for agency B. In pressure units, median unsigned error was 0.4 (0.2–0.6) mmHg; 0.3 (0.1–0.5) mmHg for agency A and 0.4 (0.2–0.7) mmHg for agency B; no statistical differences were found between agencies ($p=0.41$). However, errors significantly increased for distorted ventilations ($p < 0.001$). Global median error was 5.5 (1.8–14.1)%; 3.7 (1.0–9.9)% for agency A and 8.3 (3.9–19.5)% for agency B. In pressure units, median unsigned error was 1.3 (0.5–3.6) mmHg, 1.2 (0.4–4.1) mmHg for agency A and 1.2 (0.6–2.9) mmHg for agency B ($p < 0.001$). Globally, the error was higher than 10 mmHg in 9% of the distorted ventilations and higher than 15 mmHg in 5% of the distorted ventilations. Bottom panel in Fig. 2 shows the error with respect to the annotated $ETCO_2$ range. As expected, error in mmHg increased with the rise of $ETCO_2$.

Fig. 3 shows one scatter plot per agency depicting the measurement error in mmHg as a function of the annotated $ETCO_2$ value per ventilation. Errors for non-distorted and distorted ventilations are depicted with red dots and blue circles, respectively. Error

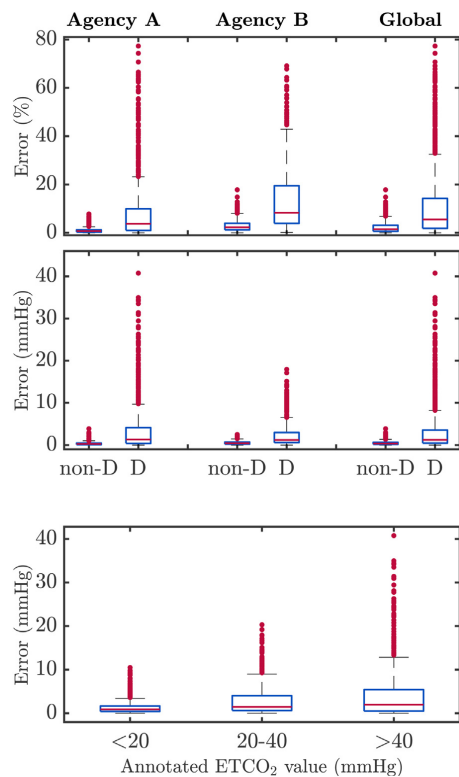


Fig. 2 – Distribution of the unsigned error in $ETCO_2$ measurement in percentage (top panel) and in mmHg (middle panel), for each agency (dataset) and globally. Error was computed as the difference between the annotated and the reported capnometry value per ventilation. non-D: non-distorted segments. D: distorted segments. Bottom panel: distribution of the unsigned error in mmHg clustered by annotated $ETCO_2$ range. The boxes show the median and IQR and the whisker shows the last datum within the ± 1.5 IQR.

dispersion increased substantially in the presence of CC-artefact, with values close to or even exceeding 20 mmHg.

Finally, we found no significant differences in the $ETCO_2$ measurement error with respect to the airway type, ETT or supraglottic King LT-D™ ($p=0.28$).

Case examples

Fig. 4 (a) shows an example of a clean capnogram with $ETCO_2$ values reported correctly by the monitor-defibrillator. Panels (b) and (c) in Fig. 4 illustrate how the measurement errors increase in the presence of CC-artefact. Annotated $ETCO_2$ values are depicted with green dots and values extracted from the monitor-defibrillator with red triangles. Green vertical dashed lines separate ventilation cycles. Middle panel shows several false detections due to CC-artefact within the ventilation. Oscillations in the capnogram seem to be confounded

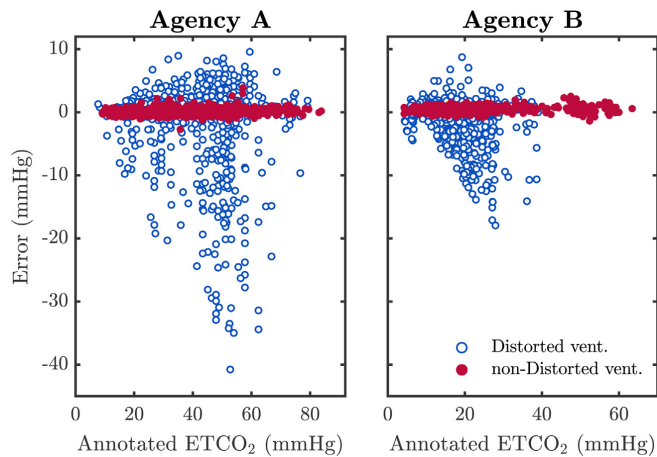


Fig. 3 – ETCO₂ measurement error (difference between the extracted and the annotated values) as a function of the annotated value per ventilation. Errors for non-distorted and distorted ventilations are depicted with red dots and blue circles, respectively. (For interpretation of the references to color in this figure legend, the reader is referred to the web version of this article.)

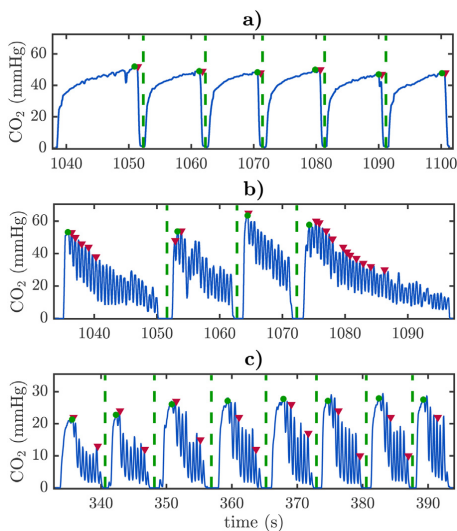


Fig. 4 – Examples of the negative effect of CC-artefact in the ETCO₂ measurement. (a) Example of correctly reported ETCO₂ values. (b) Example of several false ETCO₂ values within each ventilation (red triangles) caused by CC-artefact. (c) Measurement alternation between 20 mmHg (true) and 10 mmHg (false) within each ventilation. (For interpretation of the references to color in this figure legend, the reader is referred to the web version of this article.)

with fast ventilations. Fig. 4(c) depicts a typical occurrence where ETCO₂ values quickly alternate between 20 mmHg (true value) and 10 mmHg (artefact-originated). These rapid changes could confound clinicians during capnometry assessment.

Discussion

The clinical use of real-time waveform capnography during CPR^{24,25} could be seriously compromised since CO₂ waveform is often distorted by chest compressions.^{17,19} Observational human studies have reported that ventilation volumes incidental to chest compressions are smaller than the anatomical dead space^{18,26–28} suggesting little change in the alveolar PCO₂. However, such low volumes are sufficient to produce oscillatory patterns in the capnogram that compromise capnometry accuracy.²⁰ It has been demonstrated that the presence of CC-artefact diminishes the accuracy of automated capnogram-based ventilation detectors.¹⁹ This may have a negative impact on the guidance of ventilation rate during CPR. More importantly, the capnogram tracing becomes difficult to interpret when obscured by CC-artefact; clinicians might then rely on the capnometry numbers displayed on the monitor screen. However, the reliability of these numbers has been also questioned.²⁰

In this retrospective observational study, we quantified the influence of CC-artefact in the automated measurement of ETCO₂ during OHCA. After extensive analysis of the extracted capnograms, an overall 37.8% of 1-min segments were distorted by CC-artefact. We demonstrated that the presence of CC-artefact also affects the ETCO₂ measurements reported by different monitor-defibrillators and capnometers from different manufacturers. For capnograms without

CC-artefact, the obtained unsigned error was 0.4 (0.2–0.6) mmHg. However, these errors increased in the presence of the CC-artefact to 1.3 (0.5–3.6) mmHg. More importantly, we found errors exceeding 10 mmHg in 9% of the distorted ventilations and exceeding 15 mmHg in 5% of the distorted ventilations. In some 1-min intervals, we found errors as high as 20 mmHg. Finally, since we found no error differences between the use of ETT or supraglottic King LT-D™ to secure the airway, the airway type does not appear to be an influencing factor.

Fast oscillations provoke continuous and significant errors in the algorithm designed to estimate a single ETCO₂ value per ventilation. CC-artefact provokes many false ventilation detections with a corresponding erroneous ETCO₂ value. This is illustrated in the examples shown in Fig. 4, panels b and c. If ETCO₂ values were displayed on the monitor screen, clinicians would see the numbers changing rapidly, and ETCO₂ monitoring as well as clinical decision rules could be seriously compromised.²⁰ The scatter plot depicted in Fig. 3 suggests that CC-artefact induces errors in both directions although negative errors (ETCO₂ underestimation) are more profound. ETCO₂ values lower than real ones might lead to earlier termination of resuscitation whereas positive errors might lead to prolonged resuscitation efforts and possibly hospital transport for OHCA. Finally, segments from agency A presented larger errors than those from agency B. This could be in part explained by the higher ETCO₂ values per ventilation in the subset of agency A. This is illustrated in Fig. 3 where larger errors were associated with annotated values greater than 40 mmHg.

Our main conclusion is that the decrease in ETCO₂ measurement accuracy is related to the characteristics of the proprietary algorithms inside CO₂ devices. Commercial capnometers perform well during resuscitation when there is no artefact induced by chest compressions in the capnogram. In this case, ventilations are accurately detected and reported ETCO₂ values are reliable. However, we hypothesize that detection algorithms have not been designed to distinguish between actual ventilations and pseudo-ventilations caused by chest compressions.

Although statistical differences were found in ventilation rate and ETCO₂ values between agencies, we found no statistical differences in measurement errors during normal operating (i.e. during absence of CC-artefact). However, errors were slightly higher for agency B in the presence of CC-artefact. In this case, differences between agencies could be related with how each proprietary algorithm reports ETCO₂ values during CC-artefact. One algorithm seemed to provide an average ETCO₂ value from the previous ventilations instead of the instantaneous ETCO₂ value. Averaging could reduce the impact of CC-artefact in the ETCO₂ measurement.

We propose two main approaches to address the problem of erroneous computation of ETCO₂ in the presence of CC-artefact. One approach could be to enhance current capnometer detection algorithms in order to avoid confounding fast oscillations caused by CC-artefact with true ventilations. Another approach could be to preprocess the capnogram to remove the oscillations, e.g. with an envelope-based technique.²⁹ Since the incidence of CC-artefact is significant and there is still lack of knowledge about how to avoid the artefact, we suggest that commercial capnometers and monitor-defibrillator devices should be adapted to improve the accuracy and reliability of ETCO₂ measurements during resuscitation.

Limitations

This study has several limitations. We found considerably fewer eligible capnogram segments per episode from agency A than from agency B. Due to the strict inclusion criteria, we could only use 25% of the total time in recordings from agency A and 50% in the recordings from agency B. Segments were required to have either not distortion at all in the whole minute or being severely distorted most of the time. In addition, many segments from agency A did not have the corresponding capnometry values stored in the monitor-defibrillator, so they were not included in the analysis. In addition, we did not have information about the details of the measurement capnometer algorithm or the frequency of data storage in the monitor-defibrillator, since those are proprietary to the device manufacturer. Our conclusions are derived from the available capnometry events from two representative monitor-defibrillator devices, but additional research with other manufacturers would contribute to the generalizability of these results.

Conclusion

Currently, ETCO₂ measurement is the only widespread non-invasive clinical tool for estimating blood flow and organ perfusion during resuscitation. However, the presence of CC-artefact increased ETCO₂ measurement errors in the analysed CO₂ detector devices. This finding suggests that capnometer algorithms need to be adapted to reliably perform during CPR, avoiding false ventilation detections when CC-artefact oscillations appear in the capnogram.

Authors' contributions

Mikel Leturiondo: Conceptualization; Data curation; Software; Methodology; Validation; Roles/Writing – original draft; Writing – review & editing.

Sofía Ruiz de Gauna: Conceptualization; Funding acquisition; Methodology; Project administration; Resources; Supervision; Writing – original draft; Writing – review & editing.

José Julio Gutiérrez: Data curation; Formal analysis; Investigation; Software; Validation; Writing – review & editing.

Daniel Alonso: Resources; Writing – review & editing; Project administration.

Carlos Corcuera: Resources; Data curation; Writing – review & editing.

Juan Francisco Urtusagasti: Data curation; Writing – review & editing.

Digna María González-Otero: Data curation; Software; Writing – review & editing.

James Knox Russell: Resources; Data curation; Writing – review & editing.

Mohamud Ramzan Daya: Resources; Writing – review & editing; Supervision.

Jesus María Ruiz: Conceptualization; Funding acquisition; Methodology; Formal analysis; Writing – original draft.

Conflict of interest

The authors declare no conflicts of interest.

Source of funding

Authors Mikel Leturiondo, Sofía Ruiz de Gauna, José Julio Gutiérrez and Jesus María Ruiz received financial support from the Basque Government through the grants IT1087-16 (for research groups) and 201922053 (for health research), and Mikel Leturiondo through the predoctoral grant PRE-2019-2-0251.

Authors Mikel Leturiondo, Sofía Ruiz de Gauna, José Julio Gutiérrez and Jesus María Ruiz received financial support from the Spanish Ministry of Economy, Industry and Competitiveness through the grant RTI2018-094396-B-I00 and Digna María González-Otero from the program Torres Quevedo PTQ-16-08201.

Authors Daniel Alonso, Carlos Corcuera, Juan Francisco Urtusagasti, James Knox Russell and Mohamud Ramzan Daya received no funding for this work.

The funders had no role in study design, data collection and analysis, decision to publish, or preparation of the manuscript.

Acknowledgements

The authors thank the TVF&R and Emergentziak-Osakidetza EMS providers for collecting the data used in this study.

REFERENCES

- Gravenstein JS, Jaffe MB, Gravenstein N, Paulus DA. *Capnography*. Cambridge University Press; 2011.
- Deakin CD, Nolan JP, Soar J, et al. European resuscitation council guidelines for resuscitation 2010 section 4. Adult advanced life support. *Resuscitation* 2010;81:1305.
- Neumar RW, Otto CW, Link MS, et al. Part 8: adult advanced cardiovascular life support: 2010 American Heart Association guidelines for cardiopulmonary resuscitation and emergency cardiovascular care. *Circulation* 2010;122:S729–67.
- Meaney PA, Bobrow BJ, Mancini ME, et al. Cardiopulmonary resuscitation quality: improving cardiac resuscitation outcomes both inside and outside the hospital: a consensus statement from the American Heart Association. *Circulation* 2013;128:417–35.
- Sandroni C, De Santis P, D'Arrigo S. Capnography during cardiac arrest. *Resuscitation* 2018;132:73–7.
- Silvestri S, Ralls GA, Krauss B, et al. The effectiveness of out-of-hospital use of continuous end-tidal carbon dioxide monitoring on the rate of unrecognized misplaced intubation within a regional emergency medical services system. *Ann Emerg Med* 2005;45:497–503.
- Edelson DP, Eilevstjonn J, Weidman EK, Retzer E, Hoek TLV, Abella BS. Capnography and chest-wall impedance algorithms for ventilation detection during cardiopulmonary resuscitation. *Resuscitation* 2010;81:317–22.
- Aramendi E, Elola A, Alonso E, et al. Feasibility of the capnogram to monitor ventilation rate during cardiopulmonary resuscitation. *Resuscitation* 2017;110:162–8.
- O'Neill JF, Deakin CD. Do we hyperventilate cardiac arrest patients? *Resuscitation* 2007;73:82–5.
- Pantazopoulos C, Xanthos T, Pantazopoulos I, Papalois A, Kouskouni E, Iacovidou N. A review of carbon dioxide monitoring during adult cardiopulmonary resuscitation. *Heart Lung Circ* 2015;24:1053–61.
- Murphy RA, Bobrow BJ, Spaite DW, Hu C, McDannold R, Vadeboncoeur TF. Association between prehospital CPR quality and end-tidal carbon dioxide levels in out-of-hospital cardiac arrest. *Prehosp Emerg Care* 2016;20:369–77.
- Pokorná M, Nečas E, Kratochvíl J, Skřípský R, Andrlík M, Franěk O. A sudden increase in partial pressure end-tidal carbon dioxide (PETCO₂) at the moment of return of spontaneous circulation. *J Emerg Med* 2010;38:614–21.
- Lui CT, Poon KM, Tsui KL. Abrupt rise of end tidal carbon dioxide level was a specific but non-sensitive marker of return of spontaneous circulation in patient with out-of-hospital cardiac arrest. *Resuscitation* 2016;104:53–8.
- Touma O, Davies M. The prognostic value of end tidal carbon dioxide during cardiac arrest: a systematic review. *Resuscitation* 2013;84:1470–9.
- Rognås L, Hansen TM, Kirkegaard H, Tønnesen E. Predicting the lack of ROSC during pre-hospital CPR: should an end-tidal CO₂ of 1.3 kPa be used as a cut-off value? *Resuscitation* 2014;85:332–5.
- Poon KM, Lui CT, Tsui KL. Prognostication of out-of-hospital cardiac arrest patients by 3-min end-tidal capnometry level in emergency department. *Resuscitation* 2016;102:80–4.
- Idris AH, Daya M, Owens P, et al. High incidence of chest compression oscillations associated with capnography during out-of-hospital cardiopulmonary resuscitation. *Circulation* 2010;122:A83.
- Deakin CD, O'Neill JF, Tabor T. Does compression-only cardiopulmonary resuscitation generate adequate passive ventilation during cardiac arrest? *Resuscitation* 2007;75:53–9.
- Leturiondo M, Ruiz de Gauna S, Ruiz JM, et al. Influence of chest compression artefact on capnogram-based ventilation detection during out-of-hospital cardiopulmonary resuscitation. *Resuscitation* 2018;124:63–8.
- Raimondi M, Savastano S, Pamploni G, Molinari S, Degani A, Belliato M. End-tidal carbon dioxide monitoring and load band device for mechanical cardio-pulmonary resuscitation: never trust the numbers, believe at the curves. *Resuscitation* 2016;103:e9–e10.
- Stecher FS, Olsen JA, Stickney RE, Wik L. Transthoracic impedance used to evaluate performance of cardiopulmonary resuscitation during out of hospital cardiac arrest. *Resuscitation* 2008;79:432–7.
- Losert H, Risdal M, Sterz F, et al. Thoracic impedance changes measured via defibrillator pads can monitor ventilation in critically ill patients and during cardiopulmonary resuscitation. *Crit Care Med* 2006;34:2399–405.
- Grieco DL, Brochard J, Drouet LA, et al. Intrathoracic airway closure impacts CO₂ signal and delivered ventilation during cardiopulmonary resuscitation. *Am J Respir Crit Care Med* 2019;199:728–37.
- Soar J, Nolan JP, Böttiger BW, et al. European resuscitation council guidelines for resuscitation 2015: section 3. Adult advanced life support. *Resuscitation* 2015;95:100–47.
- Link MS, Berkow LC, Kudenchuk PJ, et al. Part 7: Adult advanced cardiovascular life support. *Circulation* 2015;132:S444–64.
- Vanwulpen M, Wolfskeil M, Duchatelet C, Monsieurs K, Idrissi SH. Quantifying inspiratory volumes generated by manual chest compressions during resuscitation in the prehospital setting. *Resuscitation* 2017;118:e18.
- McDannold R, Bobrow BJ, Chikani V, Silver A, Spaite DW, Vadeboncoeur T. Quantification of ventilation volumes produced by compressions during emergency department cardiopulmonary resuscitation. *Am J Emerg Med* 2018;36:1640–4.
- Cordioli RL, Grieco DL, Charbonney E, Richard JC, Savary D. New physiological insights in ventilation during cardiopulmonary resuscitation. *Curr Opin Crit Care* 2019;25:37–44.
- Ruiz de Gauna S, Leturiondo M, Gutiérrez JJ, et al. Enhancement of capnogram waveform in the presence of chest compression artefact during cardiopulmonary resuscitation. *Resuscitation* 2018;133:53–8.

AS040

Quantifying inspiratory volumes generated by manual chest compressions during resuscitation in the prehospital setting

Maxim Vanwulpen^{1,*}, Martha Wolfskeil¹,
Christophe Duchatelet², Koenraad Monsieurs³,
Saïd Hachimi Idrissi²

¹ Faculty of Medicine and Health Sciences, Ghent University, Ghent, Belgium

² Department of Emergency Medicine, Ghent University Hospital, Ghent, Belgium

³ Department of Emergency Medicine, Antwerp University Hospital and University of Antwerp, Antwerp, Belgium

Purpose of the study: Chest compressions have been shown to provide limited passive ventilation during adult out-of-hospital cardiac arrest (OHCA) [1]. In the only available study, data was gathered after arrival of the patient in the emergency department. In the prehospital setting, patients have greater chest and lung compliances [2]. Currently available respiratory monitors are not suitable for prehospital use [3]. Our aim was to develop a device enabling quantification of inspiratory volumes generated by manual chest compressions during prehospital cardiopulmonary resuscitation.

Materials and methods: A medical-grade airflow sensor (SFM3200-AW, Sensirion AG, Switzerland) was linked to a battery-powered microcomputer. This device was used by a prehospital medical team during resuscitation of adult patients with OHCA, at the discretion of the attending physician. Immediately after endotracheal intubation, the airflow sensor was placed between the endotracheal tube and the mechanical ventilator (Oxylog 3000, Dräger AG, Germany). Manual chest compressions were performed. The chest compressions registered in the initial period following endotracheal intubation, during which mechanical ventilations were not yet being performed, were analysed.

Results: The device was used in six adults (3 male) with OHCA, aged 45–84. Return of spontaneous circulation was achieved in three patients. Chest compressions and mechanical ventilations were identifiable in the airflow data. We analysed 75 compressions without mechanical ventilations. The median number of compressions analysed per patient was 10 (range 8–21). The median compression rate was 123/min (range 115–150/min). The median inspiratory volume generated by manual chest compressions was 15 ml (range 4–62 ml).

Conclusion: Using a novel device, we could quantify inspiratory volumes in patients with OHCA. In the small number of patients included in this feasibility study, chest compressions performed in the prehospital setting generated limited inspiratory volumes. These volumes were not higher than the anatomical dead space, and therefore generated limited gas exchange [1,3,4].

References

- [1]. Resuscitation 2007;75:35–9.
[2]. Resuscitation 2015;92:A2–3.
[3]. Resuscitation 2017;110:162–8.
[4]. J Appl Physiol 1959;14:174–6.

<http://dx.doi.org/10.1016/j.resuscitation.2017.08.054>

AS041

Reliability of ventilation guidance using capnography during ongoing chest compressions in out-of-hospital cardiopulmonary resuscitation

Mikel Leturiondo^{1,*}, Sofía Ruiz de Gauna¹,
Jesus Ruiz¹, Jose Julio Gutiérrez¹,
Luis Alberto Leturiondo¹, Jose María Bastida²,
Mohamad Daya³

¹ University of the Basque Country (UPV/EHU), Bilbao, Bizkaia, Spain

² Basque Country Emergency Medical System (Osakidetza), Basque Country, Spain

³ Oregon Health & Science University (OHSU), Portland, OR, USA

Introduction: Resuscitation guidelines emphasize the importance of capnography for monitoring ventilation during cardiopulmonary resuscitation (CPR). A high incidence (above 70%) of chest compression (CC) induced oscillations in the capnogram has been reported. CC oscillations are of high frequency and overlap the capnogram (Fig. 1b–d). Thus, we hypothesized that they could affect the reliability of capnogram-based ventilation guidance.

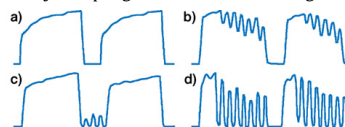


Fig. 1. Examples of OOH capnograms.

Purpose of the study: To evaluate the influence of CC oscillations in the performance of a capnogram-based ventilation detector during out-of-hospital (OOH) CPR.

Materials and methods: Data were extracted from 209 OOH records from a cardiac arrest registry maintained by TVF&R Emergency Medical System (OR, USA). For each record, we analysed the continuous capnogram and the transthoracic impedance signal, which was used to annotate ventilations. Records with presence of CC oscillations in the capnogram corresponding to at least 50% of the total duration of CC intervals were classified as corrupted. Three different types of CC oscillations were identified: observed primarily in the plateau phase of the capnogram (type I, Fig. 1b), in the baseline (type II, Fig. 1c), and from the plateau to the baseline (type III, Fig. 1d). We evaluated the sensitivity (Se) and the positive predictive value (PPV) of an algorithm for ventilation detection based solely on the continuous analysis of the capnogram.

Results: 47467 ventilations were annotated. Detector results are reported in Table 1.

Table 1

Ventilation detector performance.

Record type	n	Se (%)	PPV (%)
Non-corrupted	132	99.5	99.2
Corrupted	77	90.6	90.7
Type I	29	97.4	97.3
Type II	20	98.9	98.1
Type III	28	75.7	76.6

Conclusions: Detector's performance degraded in the presence of chest compressions. Development of signal processing techniques to suppress CC oscillations in the capnogram could be useful to improve automated ventilation detection, limiting the need for interruptions in compressions.

<http://dx.doi.org/10.1016/j.resuscitation.2017.08.055>

A Simple Algorithm for Ventilation Detection in the Capnography Signal During Cardiopulmonary Resuscitation

Mikel Leturiondo¹, Jesús Ruiz¹, Sofía Ruiz de Gauna¹, Digna M González-Otero¹, José M Bastida², Mohamud Daya³

¹University of the Basque Country (UPV/EHU), Bilbao, Spain

²Emergentziak Osakidetza (Basque Health Service), Basque Country, Spain

³Oregon Health & Science University (OHSU), Portland OR, USA

Abstract

During cardiopulmonary resuscitation, excessive ventilation rates reduce the chance of survival. We have developed a simple method to automatically detect ventilations based on the analysis of the capnography signal recorded with monitor-defibrillators. We used 60 out-of-hospital cardiac arrest episodes that contained both clean and chest compressions (CC) corrupted capnograms. The detection algorithm first identified ventilation candidates in the capnography signal. Then, it characterized every candidate by features related to inspiration and expiration durations, and finally a decision system based on static thresholds was applied in order to determine whether each candidate corresponded to a true ventilation. Sensitivity (Se) and positive predictive value (PPV) for the clean set (3905 ventilations) were 99.8% and 99.1%, respectively. With the corrupted set (6778 ventilations) Se and PPV decreased to 85.3% and 85.6%, respectively. For the whole test set (10683 ventilations) Se and PPV were 90.6% and 90.6%, respectively. Detector's performance clearly degraded when applied to corrupted episodes, this demonstrates the need for techniques to suppress CC artefact to improve ventilation detection.

1. Introduction

Cardiac arrest is the sudden cessation of the heart's effective pumping function. Medical treatment of cardiac arrest involves early cardiopulmonary resuscitation (CPR) and early defibrillation. During CPR, ventilations and chest compressions (CC) provide oxygen to the lungs and help oxygenated blood circulate to the vital organs. High-quality CPR is an important factor for the successful resuscitation of cardiac arrest patients. Current resuscitation guidelines recommend providing continuous CC and ventilations with a ventilation rate around 10 per minute for intubated patients in cardiac arrest [1].

Nevertheless, hyperventilation is often reported for in-hospital and out-of-hospital cardiac arrest (OHCA) interventions [2,3]. Previous animal studies revealed that excessive ventilation rates resulted in decreased coronary perfusion pressures and poor outcomes [4].

Continuous guidance of satisfactory ventilation rate is usually achieved from the analysis of the capnography signal. Figure 1 depicts two capnograms in which two ventilation cycles can be observed. Capnography signal fluctuates during ventilation because of changes in the CO₂ partial pressure. The partial pressure increases during expiration (exhaled air contains more CO₂) and decreases during inspiration. However, the presence of high-frequency oscillations induced by CC in the capnogram is frequent during resuscitation [5]. An example of a capnogram corrupted by CC artefact is shown in Figure 1B. Fast oscillations caused by the rhythmic compression of the chest overlap the capnogram waveform, highly distorting the signal. The presence of CC artefact may affect the reliability of capnogram-based ventilation detection [6].

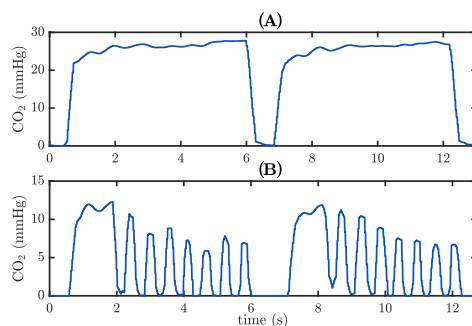


Figure 1. OHCA capnography signal segments. A) Clean waveform; B) Capnogram corrupted by oscillations induced by CC.

In this study, we present a simple method for automated detection of ventilations during CPR, based on the analysis of the capnography signal acquired by monitor-defibrillators during OHCA interventions.

2. Materials and methods

2.1. Database description and annotation

The dataset used in this study was a subset (60 episodes) of a large database collected between 2011 and 2016 maintained by Tualatin Valley Fire & Rescue (TVF&R), an advanced life support first response Emergency Medical Services (EMS) agency (Oregon, USA). Episodes were recorded using Heartstart MRx monitor-defibrillators (Philips USA) equipped with a real-time CPR feedback system (QCPR, Laerdal Medical, Norway). For each episode, we extracted three concurrent signals: the transthoracic impedance (TI) signal, acquired from the defibrillation pads; the compression depth (CD) signal obtained from the QCPR system; the capnogram, acquired using sidestream technology (Microstream, Oridion Systems Ltd., Israel).

Signals were reviewed and annotated using a custom-developed Matlab program. Capnograms were time-shifted to compensate delay with respect to CD and TI signals. Three biomedical engineers independently classified the capnograms as clean or corrupted using the CD signal. A capnogram was classified as corrupted if evident CC artefact appeared during more than 1 min of the CC time. Experts also annotated the position of each ventilation using the TI signal as the reference. TI signal was low-pass filtered (2nd-order Butterworth, cut-off frequency of 0.6 Hz) to remove oscillations caused by CC. Thus, slow oscillations caused by ventilations could be more clearly observed in the filtered TI. Figure 2 shows an example of the annotation process. Ventilations were annotated in the position corresponding to a raise in the TI, associated to the inspiration onset (Figure 2, vertical lines). Filtered TI (top panel) appears overlapped to the raw TI (where both oscillations caused by CC and by ventilations are observed).

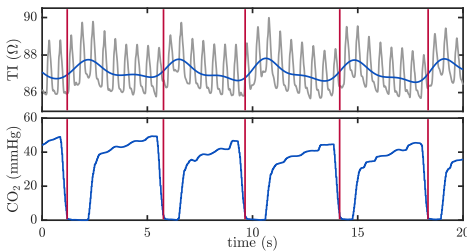


Figure 2. Example of ventilation annotation.

The resulting annotations were used as the gold standard to test the reliability of the automated capnogram-based ventilation detection algorithm. Clean episodes (30) were randomly and equally split into a training and a test set. Corrupted episodes were added to the test set.

2.2. Capnogram-based ventilation detection

Ventilations produce identifiable variations in the capnogram. A capnogram cycle is composed of a short inspiration time (starting with a CO₂ rapid fall to zero) and a longer expiration time (slow raising expired CO₂ followed by a plateau). The basis of the ventilation detection algorithm is the identification of the changes between inspiration and expiration phases.

The flowchart of the algorithm is presented in Figure 3, and can be described in three main steps:

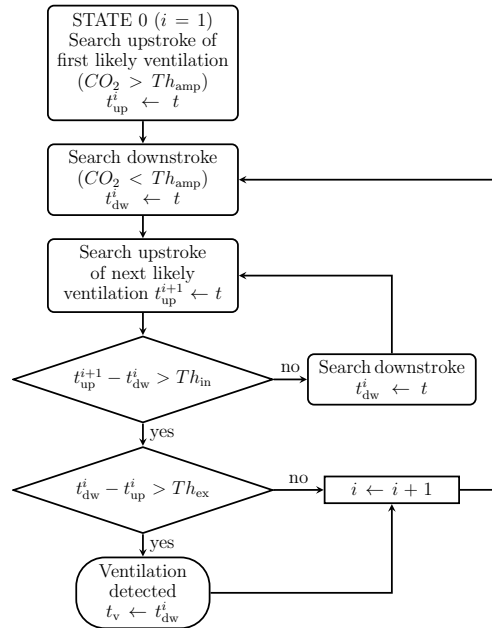


Figure 3. Flowchart of the ventilation detection algorithm.

- **Candidate identification:** the algorithm searches for abrupt upstrokes, t_{up}^i , and downstrokes, t_{dw}^i , as potential onsets of the expiratory and inspiratory phases, detected when the amplitude of the capnogram exceeds or goes below a fixed threshold, Th_{amp} .
- **Feature extraction:** every candidate is characterized by two features extracted from the capnogram signal:

- D_{ex} : Duration of the expiratory phase of a ventilation, $D_{ex} = t_{dw}^i - t_{up}^i$
- D_{in} : Duration of the inspiratory phase of the next ventilation, $D_{in} = t_{up}^{i+1} - t_{dw}^i$
- **Candidate classification:** each candidate is classified as true ventilation if the computed parameters are above certain thresholds. We applied static thresholds for the expiratory phase duration (Th_{ex}) and the inspiratory phase duration (Th_{in}).

Figure 4 provides a graphical example of the features computed by the algorithm. To take account for observed “double inhalation” effects (Figure 4B), the algorithm discards any candidate for which the inspiratory phase D_{in} is below Th_{in} , and searches for the next downstroke and upstroke until D_{in} exceeds Th_{in} .

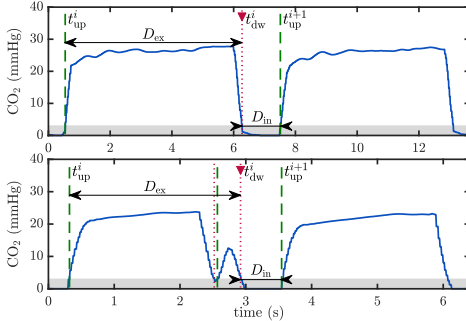


Figure 4. Graphical definition of the detector parameters.

2.3. Performance evaluation

We evaluated the algorithm in terms of its sensitivity (Se) and its positive predictive value (PPV). Se was defined as the percentage of annotated ventilations that were correctly detected. PPV was defined as the percentage of detected ventilations that were correct. The maximum admissible tolerance for the position of the detection and the annotation was 500ms.

We optimized the algorithm parameters with the clean training set to maximize Se while maintaining PPV above 98%. 95% confidence intervals (95%CI) were computed for both metrics.

3. Results

The amplitude threshold Th_{amp} for candidate identification was fixed to 3 mmHg . Algorithm optimization was achieved for $Th_{in} = 0.11\text{ s}$ and $Th_{ex} = 0.8\text{ s}$. For the training set (4614 annotated ventilations), Se and PPV were 99.7% (95%CI, 99.5-99.9)

and 99.0% (98.7-99.3), respectively.

Table 1 summarizes Se and PPV results. For the whole test set, comprising 10683 ventilations, global Se and PPV were 90.6% and 90.6%, respectively. For the clean set (3905 ventilations) Se and PPV were 99.8% and 99.1%, respectively. However, with the corrupted set (6778) Se and PPV decreased to 85.3% and 85.6%, respectively.

Table 1. Algorithm performance with the test set. n: number of annotated ventilations.

	n	Se (95% CI)	PPV (95% CI)
Whole set	10683	90.6 (90.0-91.1)	90.6 (90.0-91.1)
Clean	3905	99.8 (99.7-99.9)	99.1 (98.7-99.3)
Corrupted	6778	85.3 (84.4-86.1)	85.6 (84.8-86.4)

Figure 5 shows some examples of algorithm’s performance. For each example, the capnogram with the detected ventilations is depicted in the top panel and the TI signal with the annotated ventilations is depicted in the bottom panel.

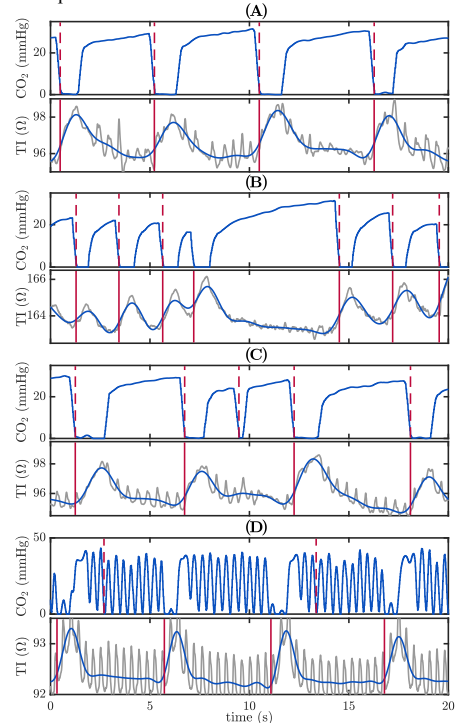


Figure 5. Graphical examples of the algorithm’s performance. (A) Good performance; (B) Ventilation misdetection; (C) False positive; (D) Very poor performance caused by CC artefact.

4. Discussion

Monitoring ventilation rate is one of the recommended uses of the capnogram during CPR, according to current resuscitation guidelines for advanced life support. However, the presence of high-frequency oscillations in the capnogram during CC may compromise the interpretation of the signal. Although a high incidence of this CC artefact has been reported in OHCA episodes [5], the influence of this artefact on the reliability of capnogram-based ventilation detection has not been previously studied.

Our algorithm was simple and presented a very good performance with clean capnograms, not affected by CC artefact. One example of good performance was shown in Figure 5A. A few cases of misdetections (Figure 5B) or false positives (Figure 5C) had not a great impact on performance.

However, Se and PPV significantly degraded when the algorithm was applied to the corrupted capnograms. CC artefact often appeared overlapping the capnogram from the plateau to the baseline and in the inspiration phase, making detection unreliable (Figure 5D).

Other studies proposing alternatives for ventilation detection either with the TI signal or the capnogram have also mentioned the signal limitations due to the presence of CC artefact [6]. Our study has been the first to quantitatively characterize and measure the impact of CC artefact on OHCA capnograms. Our subsequent hypothesis is that automatic ventilation detection would improve if the artefact could be successfully removed from the capnogram. Designing filtering approaches for this aim will be our next step, exploring different alternatives.

Our study has several limitations. First, the annotation of TI fluctuations was not straightforward during CPR. Some intervals were discarded because of unreliable TI signal (noise, disconnections) and filtering was needed to remove the CC artefact. The capnogram was sometimes used to confirm the presence of ventilations. No other reference signal was available to be used as an alternative gold standard. Second, ventilations delivered to patients with capnogram below the algorithm amplitude threshold (3 mmHg) cannot be detected. However, in our data this was rarely observed. Finally, data came from a single EMS system and so results may not be generalizable. We need to characterize this further with other EMS systems and monitor-defibrillators.

5. Conclusions

The important role of capnography waveform in ventilation rate monitoring during CPR is compromised by CC artefact superimposed on the capnogram. Further research should explore filtering techniques to suppress CC artefact in order to improve ventilation monitoring for corrupted capnograms.

Acknowledgements

This work received financial support from the Basque Government (Basque Country, Spain) through the project IT1087-16 and the predoctoral research grant PRE-2016-1-0104. The authors thank the TVF&R EMS providers for collecting the data used in this study.

References

- [1] Soar J, Nolan JP, Böttiger BW, et al. European Resuscitation Council guidelines for resuscitation 2015. Section 3. Adult advanced life support. *Resuscitation* 2015;95:100-147.
- [2] O'Neill JF, Deakin CD. Do we hyperventilate cardiac arrest patients? *Resuscitation* 2007;73(1):82-85.
- [3] Maertens VL, De Smedt LE, Lemoine S, et al. Patients with cardiac arrest are ventilated two times faster than guidelines recommend: an observational prehospital study using tracheal pressure measurement. *Resuscitation* 2013; 84(7):921-926.
- [4] Aufderheide TP, Sigurdsson G, Pirralo RG, et al. Hyperventilation-induced hypotension during cardiopulmonary resuscitation. *Circulation* 2004; 109(16):1960-1965.
- [5] Idris AH, Daya M, Owens P, et al. High incidence of chest compression oscillations associated with capnography during out-of-hospital cardiopulmonary resuscitation. *Circulation* 2010;122:A83.
- [6] Edelson DP, Eilevstjønn J, Weidman EK, Retzer E, Hoek TLV, Abella BS. Capnography and chest-wall impedance algorithms for ventilation detection during cardiopulmonary resuscitation. *Resuscitation* 2010;243 81(3):317-322.

Address for correspondence.

Mikel Leturiondo Sota
mikel.leturiondo@ehu.eus
 School of Engineering
 Alameda Urquijo s/n, 48013-Bilbao (Spain)

AP009

Defibrillation success in out-of-hospital cardiac arrest: Point in time of ventricular fibrillation recurrence after successful shock during early phase of cardiopulmonary resuscitation

Martin Christian Sassen^{1,*}, Dana Maresa Spies¹, Jonathan Kiekenap¹, Susanne Betz¹, Clemens Kill²

¹ Center of Emergency Medicine, Philipps-University, Marburg, Germany

² Center of Emergency Medicine, University Hospital Essen, Essen, Germany

Purpose of the study: In case of an out-of-hospital cardiac arrest (OHCA) due to ventricular fibrillation (VF) guidelines recommend early defibrillation followed by chest-compressions for two minutes before analyzing shock success. If rhythm analysis reveals VF again, it is obscure whether VF persisted or re-occurred within the two-minutes-cycle of chest-compressions after successful defibrillation. We investigated the point in time of VF-recurrence.

Materials and Methods: Between February 2014 and March 2018 we examined retrospectively 185 consecutive shocks of all patients presenting with initial VF at arrival of ALS-ambulance in OHCA (Marburg-Biedenkopf-County, 252.000 inhabitants). Three independent investigators analyzed ECG-recordings of the defibrillator Corpuls.³ We enclosed ECG-data from CPR-beginning until 2 min after the third shock. Using filters from 2–10 Hz we reduced chest-compression-artifacts. Successful shock was defined as VF-termination within 5s after a shock. A relapse was defined as VF-recurrence in the interval 5s after a shock and the following shock.

Results: We enclosed 185 shocks of 82 patients. 74.1% ($n = 137$) of the shocks were successful, recurrence-rate of VF was 88.3% ($n = 121$). The median of point in time of VF-recurrence was 33s (16s/106s) after shock. 47.1% ($n = 57$) of VF-recurrence occurred ≤ 30 s after shock, 12.4% ($n = 15$) of VF-recurrence occurred 31–60s after shock, 13.7% ($n = 16$) of VF-recurrence occurred 61–90s after shock, 27.3% ($n = 33$) of VF-recurrence occurred >90 s after shock.

Conclusions: Although VF was terminated by rectilinear-waveform-defibrillation in 74%, VF recurred within two minutes of chest-compressions in 88%. Thus, VF reappears frequently and early. It is unclear to which extend chest-compressions influence VF-relapse. Further studies need to re-evaluate the best shock-compression-analysis-algorithm and the regime of antiarrhythmic therapy in the early phase of CPR in OHCA with initial VF.

References

- 1 Resuscitation. 2005 Aug;66(2):149–57.
- 2 Circ Arrhythm Electrophysiol. 2010 Feb;3(1):72–8.
- 3 Resuscitation. 2011 Jun;82(6):685–9.
- 4 Circulation. 2018 Dec 4;138(23):e740–e749.

<https://doi.org/10.1016/j.resuscitation.2019.06.079>

AP010

Chest compression artefact compromises real-time feedback capnometry: quantification of differences in end-tidal measurements by two capnometers

Mikel Leturiondo^{1,*}, Sofia Ruiz de Gauna¹, Jose Julio Gutiérrez¹, Jesus Ruiz¹, Carlos Corcuera², Juan Francisco Ustusagasti², James K. Russell³, Mohamud R. Daya³

¹ University of the Basque Country (UPV/EHU), Bilbao, Spain

² The Basque Country Emergency Medical Services System, Artaza, Spain

³ Oregon Health & Science University, OHSU, Portland, OR, USA

Purpose of the study: Real-time capnometry is a valuable monitoring tool during cardiopulmonary resuscitation (CPR). However, waveform capnography is often distorted by chest compressions (CC)¹ and CC artefact might compromise the end-tidal CO₂ (ETCO₂) measurements provided by capnometers.² We quantified the differences in ETCO₂ measurements by two CO₂ detector devices caused by CC artifact during manual CPR.

Materials and methods: We retrospectively analysed out-of-hospital cardiac arrest monitor-defibrillator recordings from two different agencies ($n = 30$ from agency A and $n = 14$ from agency B). Each agency used a different side-stream capnography technology and monitor-defibrillators. Capnograms were reviewed in 3-min segment and each segment was classified as distorted or non-distorted by CC artefact. Ventilations were identified using both the transthoracic impedance signal and the capnogram. ETCO₂ level was manually annotated as the maximum CO₂ level in each ventilation, and compared to values extracted from the monitor-defibrillators.

Results: Eighty capnogram segments were analysed, containing a total of 2,087 ventilations with a 43.5% of them distorted by CC artefact. Segments from agency A had a total of 1,125 ventilations (50.5% distorted), whereas those from agency B had 962 ventilations (35.1% distorted). Globally, ETCO₂ median (IQR) unsigned error in percentage for non-distorted and distorted intervals was 3.2 (2.1–4.6)% and 9.4 (6.9–12.9)%, respectively. In device A the median unsigned error was 2.1 (1.3–3.1)% and 8.4 (6.4–10.4)%, while in device B the median error was 3.9 (3.3–6.0)% and 13.9 (10.6–15.8)%, respectively.

Conclusion: Presence of CC artefact increased ETCO₂ measurement errors in the assessed CO₂ detector devices. CC artefact suppression techniques are needed to enhance waveform capnography, allowing reliable and clinically useful ETCO₂ analysis during CPR.

References

- 1 Leturiondo M, et al. Resuscitation 2018;124:63–8.
- 2 Raimondi M, et al. Resuscitation 2016;103:e9–10.

<https://doi.org/10.1016/j.resuscitation.2019.06.080>

OBJECTIVE 2: TO DESIGN SIGNAL PROCESSING
TECHNIQUES TO REMOVE CC-ARTIFACT FROM THE
CAPNOGRAM TO IMPROVE VENTILATION RATE
FEEDBACK AND TO ENHANCE CAPNOGRAM CLINICAL
INTERPRETATION

Indexed journals

A3 *"Enhancing ventilation detection during cardiopulmonary resuscitation by filtering chest compression artifact from the capnography waveform"*

Authors: J.J. Gutiérrez, **M. Leturiondo**, S. Ruiz de Gauna, J. Ruiz, L.A. Leturiondo, D.M. González-Otero, D. Zive, J.K. Russell, M.R. Daya

Published in: PLoS One 2018, vol. 13, n. 8, p. e0201565

Type of publication: Journal paper indexed in JCR

Quality indices: Ranking: 15/64 (Q1). JCR impact factor: 2.766

A4 *"Enhancement of capnogram waveform in the presence of chest compression artefact during cardiopulmonary resuscitation"*

Authors: S. Ruiz de Gauna, **M. Leturiondo**, J.J. Gutiérrez, J. Ruiz, D.M. González-Otero, J.K. Russell, M.R. Daya

Published in: Resuscitation 2018, vol. 133, p. 53-58

Type of publication: Journal paper indexed in JCR

Quality indices: Ranking: 1/26 (Q1). JCR impact factor: 5.863

Indexed international conferences

- C4** *"Open-loop adaptive filtering for suppressing chest compression oscillations in the capnogram during cardiopulmonary resuscitation"*
Authors: M. Leturiondo, J. Ruiz, J.J. Gutiérrez, L.A. Leturiondo, J.K. Russell, M.R. Daya
Published in: Proceedings of the IEEE Conference Computing in Cardiology 2017, vol. 44, p. 1-4
Type of publication: Indexed congress in SJR
Quality indices: SJR impact factor: 0.336
- C5** *"Closed-loop adaptive filtering for suppressing chest compression oscillations in the capnogram during cardiopulmonary resuscitation"*
Authors: M. Leturiondo, J.J. Gutiérrez, S. Ruiz de Gauna, S. Plaza, J.F. Veintemillas, M.R. Daya
Published in: Proceedings of the IEEE Conference Computing in Cardiology 2017, vol. 44, p. 1-4
Type of publication: Indexed congress in SJR
Quality indices: SJR impact factor: 0.336
- C6** *"Suppression of chest compression artefact to enhance reliability of capnography waveform analysis during cardiopulmonary resuscitation."*
Authors: M. Leturiondo, J.J. Gutiérrez, S. Ruiz de Gauna, J. Ruiz, L.A. Leturiondo, J.K. Russell, M.R. Daya
Published in: Resuscitation 2018, vol. 130, e15-e16
Type of publication: Indexed congress in JCR
Quality indices: Ranking: 1/26 (Q1). JCR impact factor: 5.863
- C7** *"A Method to Suppress Chest Compression Artifact Enhancing Capnography-Based Ventilation Guidance During Cardiopulmonary Resuscitation"*
Authors: M. Leturiondo, J.J. Gutiérrez, S. Ruiz de Gauna, J. Ruiz, L.A. Leturiondo, J.K. Russell, M.R. Daya
Published in: Proceedings of the IEEE Conference Computing in Cardiology 2018, vol. 45 p. 1-4
Type of publication: Indexed congress in SJR
Quality indices: SJR impact factor: 0.191

RESEARCH ARTICLE

Enhancing ventilation detection during cardiopulmonary resuscitation by filtering chest compression artifact from the capnography waveform

Jose Julio Gutiérrez¹*, Mikel Leturiondo¹*, Sofía Ruiz de Gauna¹, Jesus María Ruiz¹, Luis Alberto Leturiondo¹, Digna María González-Otero¹, Dana Zive², James Knox Russell², Mohamud Daya²

1 Department of Communications Engineering, University of the Basque Country (UPV/EHU), Bilbao, Bizkaia, Spain, **2** Department of Emergency Medicine, Oregon Health & Science University (OHSU), Portland, Oregon, United States of America

* mikel.leturiondo@ehu.eus



OPEN ACCESS

Citation: Gutiérrez JJ, Leturiondo M, Ruiz de Gauna S, Ruiz JM, Leturiondo LA, González-Otero DM, et al. (2018) Enhancing ventilation detection during cardiopulmonary resuscitation by filtering chest compression artifact from the capnography waveform. *PLoS ONE* 13(8): e0201565. <https://doi.org/10.1371/journal.pone.0201565>

Editor: Chiara Lazzeri, Azienda Ospedaliero Universitaria Careggi, ITALY

Received: March 23, 2018

Accepted: July 17, 2018

Published: August 2, 2018

Copyright: © 2018 Gutiérrez et al. This is an open access article distributed under the terms of the [Creative Commons Attribution License](https://creativecommons.org/licenses/by/4.0/), which permits unrestricted use, distribution, and reproduction in any medium, provided the original author and source are credited.

Data Availability Statement: All relevant data are within the paper and its Supporting Information file.

Funding: Gobierno Vasco (Eusko Jauriaritza), Actividades de Grupos de Investigación 2016 (Research Groups Activities), http://www.hezkuntza.ejgv.euskadi.eus/r43-5552/es/contenidos/informacion/dib4/es_2035/gsvuv_c.html, Grant Number: IT1087-16, and Gobierno Vasco (Eusko Jauriaritza), Carrera investigadora.

Abstract

Background

During cardiopulmonary resuscitation (CPR), there is a high incidence of capnograms distorted by chest compression artifact. This phenomenon adversely affects the reliability of automated ventilation detection based on the analysis of the capnography waveform. This study explored the feasibility of several filtering techniques for suppressing the artifact to improve the accuracy of ventilation detection.

Materials and methods

We gathered a database of 232 out-of-hospital cardiac arrest defibrillator recordings containing concurrent capnograms, compression depth and transthoracic impedance signals. Capnograms were classified as non-distorted or distorted by chest compression artifact. All chest compression and ventilation instances were also annotated. Three filtering techniques were explored: a fixed-coefficient (FC) filter, an open-loop (OL) adaptive filter, and a closed-loop (CL) adaptive filter. The improvement in ventilation detection was assessed by comparing the performance of a capnogram-based ventilation detection algorithm with original and filtered capnograms.

Results

Sensitivity and positive predictive value of the ventilation algorithm improved from 91.9%/89.5% to 97.7%/96.5% (FC filter), 97.6%/96.7% (OL), and 97.0%/97.1% (CL) for the distorted capnograms (42% of the whole set). The highest improvement was obtained for the artifact named type III, for which performance improved from 77.8%/74.5% to values above 95.5%/94.5%. In addition, errors in the measurement of ventilation rate decreased and accuracy in the detection of over-ventilation increased with filtered capnograms.

Programa Predoctoral 2016 (PhD Program), <http://www.euskadi.eus/informacion/ayudas-al-personal-investigador-programa-predocctoral/web01-a3predoc/es/>, Grant Number: PRE-2017-2-0201. The funders had no role in study design, data collection and analysis, decision to publish, or preparation of the manuscript.

Competing interests: The authors have declared that no competing interests exist.

Conclusions

Capnogram-based ventilation detection during CPR was enhanced after suppressing the artifact caused by chest compressions. All filtering approaches performed similarly, so the simplicity of fixed-coefficient filters would take advantage for a practical implementation.

Introduction

Sudden cardiac arrest is defined as the sudden and often unexpected cessation of the effective contraction of the heart, confirmed by the absence of signs of circulation and breathing [1]. The key techniques during resuscitation of cardiac arrest include airway, breathing and circulation support by means of cardiopulmonary resuscitation (CPR) and defibrillation. In out-of-hospital (OOH) settings, advanced life support (ALS) includes manual defibrillation, advanced airway management, and drug administration during CPR [2, 3].

Capnography is increasingly used by ALS Emergency Medical Services (EMS) systems during the treatment of OOH cardiac arrest [4, 5]. Capnography allows the assessment of the partial pressure of carbon dioxide (CO_2) in the respiratory gases. The concentration of CO_2 at the end of the exhalation (ET CO_2) is considered a surrogate measurement of the pulmonary circulation generated during resuscitation efforts [6]. Customarily, monitoring the capnogram is widely used for guiding ventilation. Excessive ventilation rate has been shown to be frequent and detrimental to the patient during CPR [7–9]. Other uses of capnography in EMS include assessment of the correct positioning of the endotracheal tube [10], monitoring the effectiveness of CPR, identification of restoration of spontaneous circulation [11], and determination of patient prognosis [2, 5, 12].

Quality of the recorded capnogram is essential for a reliable analysis, either visual or automated. However, several authors have reported the appearance of oscillations synchronized with chest compressions distorting capnograms recorded during OOH cardiac arrests [13–17]. Idris et al. specifically reported a high incidence of 70% of distorted OOH capnograms [13]. This phenomenon was not systematically assessed until a recent observational study, in which researchers retrospectively analyzed more than 200 capnograms collected during OOH cardiac arrests [17]. The episodes were classified into distorted (42%) or undistorted (58%), restricting the number of distorted capnograms to those with at least 1 min of distorted ventilations. Three types of artifact were defined according to the location of the oscillations in the respiratory cycle. Finally, the authors reported the negative influence of chest compression artifact in automated detection of ventilations, compromising the reliability of capnogram-based ventilation guidance during CPR.

In this context, we hypothesized that suppressing chest compression artifact from the capnogram was possible using adequate filtering techniques. Filtering would improve the capnogram signal quality and consequently the reliability of automated ventilation detection even in the presence of chest compression oscillations.

The purpose of this study was to explore different filtering techniques to eliminate chest compression artifact from the capnogram. Fixed-coefficient filtering as well as classical adaptive schemas were examined. To assess the filter performance we compared the accuracy of a capnogram-based algorithm for automated detection of ventilations before and after filtering OOH capnograms. We also evaluated the improvement in the measurement of ventilation rate and in the detection of over-ventilation after artifact suppression.

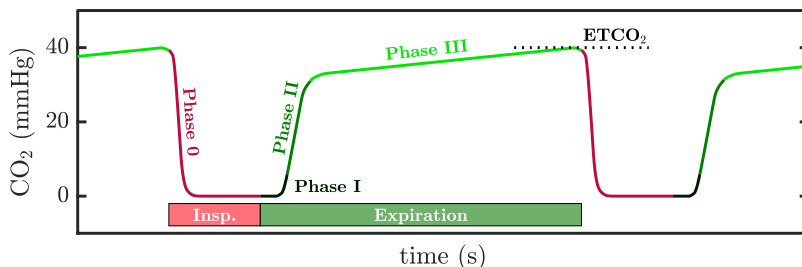


Fig 1. A normal capnogram. The waveform represents the varying CO₂ levels during the respiratory cycle. Typical segments and phases are named according to [18].

<https://doi.org/10.1371/journal.pone.0201565.g001>

Chest compression artifact in the capnogram during CPR

Fig 1 shows the morphology of a normal capnogram, representing the evolution of CO₂ concentration in the airway with time. Typical intervals and phases are named according to the terminology used by Bhavani-Shankar et al. [18]. During inspiration or phase 0, the airway is filled with CO₂-free gases, resulting in a rapid decrease of CO₂ concentration to a zero level that defines the baseline of the capnogram. Expiration comprises three intervals: phase I represents the CO₂-free gas in anatomical dead space, between the patient's alveoli and the measurement device; phase II represents the mixture of gases from the anatomical dead space and the alveoli; phase III defines the alveolar plateau, representing the rising of the CO₂ concentration produced by CO₂ rich gases coming from the alveoli. The alveolar plateau ends up at a peak level corresponding to the end-tidal CO₂ concentration (ETCO₂) [6].

The studies presented in references [14, 15] reported that during CPR, chest compressions generate a fluctuation of little gas volumes that are detected by the capnography sensor, producing oscillations in the capnogram waveform. This artifact has been recently examined in more detail by our research team in a retrospective observational study [17]. We worked with a set of undistorted (clean) and distorted capnograms from patients in OOH cardiac arrest and observed that the artifact appeared as oscillations of varying amplitudes and locations in the capnogram. In that study, we identified three types of artifact, depending on the location of the oscillations: type I, if oscillations appeared in the alveolar plateau; type II, in the baseline; and type III, the most confounding artifact, if the artifact spanned from the plateau to the baseline. No induced oscillations were found in the slopes of phases 0 and II.

Fig 2A shows examples of distorted capnograms corresponding to the three observed types of artifact (upper panel). The compression depth (CD) signal depicted below each capnogram shows that the artifact is synchronous with the CD waveform. Fig 2B shows the normalized power spectral density (PSD) estimated for both the capnogram (in solid blue line) and the CD signal (in dotted red line). The PSD of the capnogram presents a low frequency band associated to the ventilation rate (close to 10 per minute in the three examples), and a single peak corresponding to the artifact oscillation frequency. This frequency is exactly the fundamental frequency of the CD signal (f_{cc}), that is, the chest compression rate. Hence, the artifact presents a sinusoidal characteristic with a fundamental frequency equal to the frequency of the chest compressions.

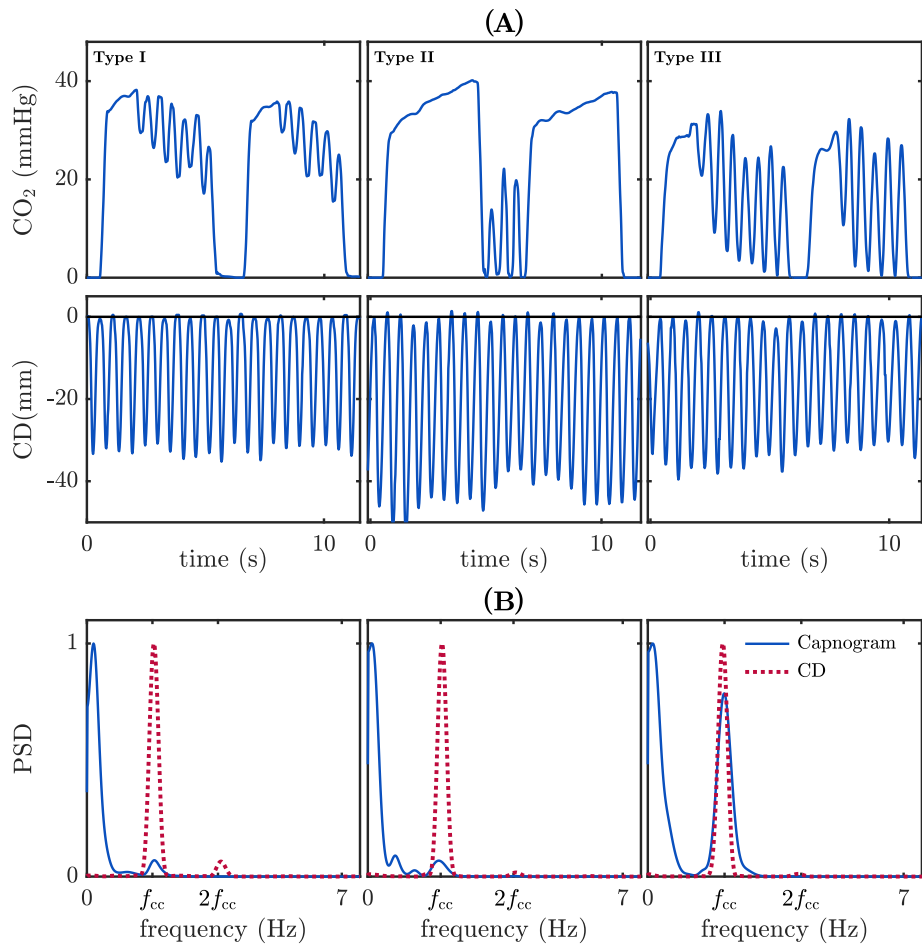


Fig 2. The three different types of observed artifact. (A) Type I, located in the plateau of the capnogram; type II, in the baseline, and type III, spanning from the plateau to the baseline. Each capnogram is depicted with the corresponding CD signal. (B) Power spectral density (PSD) of each capnogram (in solid blue line) and CD signal (in dotted red line). Capnograms present a significant peak at the fundamental frequency of the artifact, f_{cc} , with highest amplitudes in type III samples.

<https://doi.org/10.1371/journal.pone.0201565.g002>

Materials and methods

Data collection and annotation

For this study, data were extracted from OOH cardiac arrest episodes from the Resuscitation Outcomes Consortium (ROC) Epidemiological Cardiac Arrest Registry approved by the Oregon Health & Science University (OHSU) Institutional Review Board (IRB00001736). No

patient private data was required for this study. All episodes were recorded using Heartstart MRx monitor-defibrillators (Philips, USA), equipped with real-time CPR feedback technology (Q-CPR) and capnography monitoring using sidestream technology (Microstream, Oridion Systems Ltd, Israel). As the database for this study was the same used in reference [17], we provide here a brief description of the materials. Readers are encouraged to consult the original reference for additional details.

We gathered 232 episodes with the concurrent capnogram, compression depth (CD) signal computed by the Q-CPR technology, and transthoracic impedance (TI) signal acquired from defibrillation pads. Experts participating in the review process manually and visually examined each capnogram and the concurrent CD signal. The CD signal was used as the reference to determine whether chest compressions were provided or not. Episodes were classified as distorted if evident chest compression artifact appeared during more than 1 min of the total chest compression time. Otherwise, episodes were grouped in the clean category. Distorted episodes were then categorized into the artifact categories type I, type II, or type III.

Ventilations were annotated using the TI signal. Ventilations induce slow fluctuations in the TI signal acquired by defibrillators. TI increases during inspiration due to the increment of the gas volume of the chest and to the longer distance between the electrodes, that produces a decrement in the conductivity [19–21]. The raw TI signal was low-pass filtered to enhance the slow fluctuations caused by ventilations. Experts visually examined the processed TI signal to manually annotate the position of each single ventilation. Fig 3 shows an example of the ventilation annotation. The top panel depicts the raw TI signal in gray with the enhanced low frequency component in blue. Ventilations were annotated at the instant corresponding to a rise in the impedance (vertical red lines). To visually confirm the presence of ventilations the capnogram is depicted in the middle panel. Resulting ventilation annotations were used as the gold standard to evaluate the effectiveness of the proposed filtering techniques. Chest compression instances were annotated at the local minima (Fig 3, bottom panel red dots) corresponding to the maximum depth reached for each chest compression.

Methods

Algorithm for ventilation detection. To assess filtering performance we applied a capnogram-based ventilation detection algorithm before and after artifact suppression [17]. A simplified scheme of the detector is shown in Fig 4. Basically, the algorithm locates series of consecutive upstrokes (t_{up}) and downstrokes (t_{dw}) in the capnogram applying an amplitude threshold (Th_{amp}). Durations between those instants, D_{ex} and D_{in} , are the two features used to classify potential candidates as true ventilations, according to a simple decision tree based on thresholds Th_{ex} and Th_{in} , respectively. Other similar detection algorithms have been previously described in the literature [21].

In the next sections the filtering techniques used for the suppression of the chest compression artifact are presented. We studied three different alternatives: a simple fixed-coefficient filter and two more computationally intensive adaptive filtering techniques.

Fixed coefficient (FC) filtering. Observation of the PSD in Fig 2B supports the use of a simple filter with fixed coefficients to suppress the spectral content of the capnogram above 1 Hz (60 cpm). To that end, we implemented a digital infinite impulse response low-pass Butterworth filter.

Adaptive filtering. Variability of chest compression rate may affect the efficacy of the FC filter [8, 9, 22, 23]. Adaptive techniques in which the filter parameters are adjusted in time according to the varying characteristics of the artifact could be a suitable solution. In the

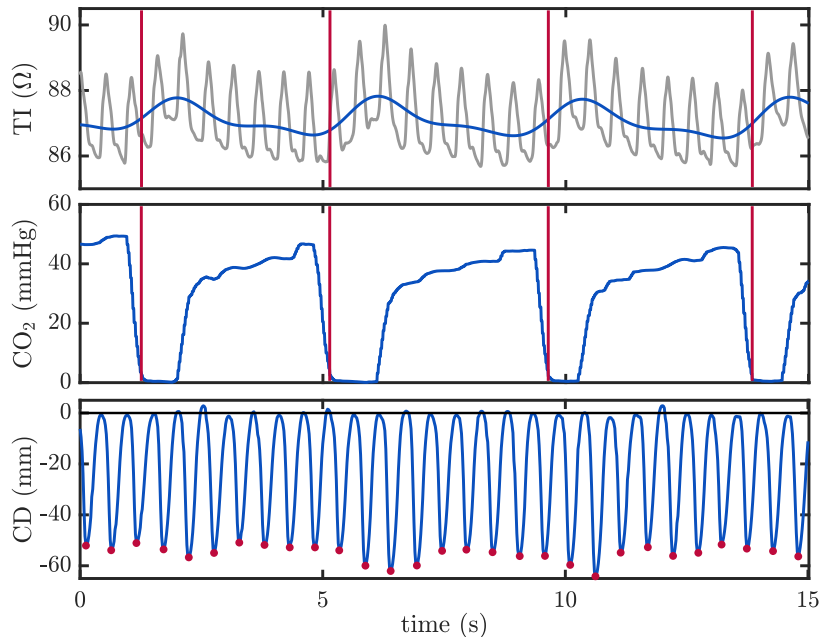


Fig 3. Annotation of ventilations and chest compressions. Ventilations were annotated using the low frequency component of the TI signal (upper panel, in blue), obtained by low-pass filtering the raw TI signal (in gray). Each ventilation was annotated at the rise of a TI fluctuation (red vertical lines). In the capnogram (middle panel), these annotations corresponded to CO₂ concentration's rapid decay to zero. Chest compression instances were annotated in the CD signal (lower panel), and are depicted with red dots corresponding to the instants where the maximum compression depth was achieved.

<https://doi.org/10.1371/journal.pone.0201565.g003>

literature, adaptive filtering has been extensively used for the suppression of the artifact induced by chest compressions in the electrocardiogram recorded by defibrillators during CPR [24–28].

In this study, we designed two different adaptive filtering configurations, an open-loop and a closed-loop adaptive filter [29]. Details of the adaptive filters are addressed in the supporting information [S1 Appendix](#).

[Fig 5](#) illustrates the performance of the filters. The three filtering techniques were applied to the same capnogram (top panel), and the resulting filtered waveforms are depicted in the lower panels (blue line) superimposed on the original capnogram (gray line). Ventilations detected before and after filtering are marked with vertical red dotted lines. Ventilations with chest compression artifact (the four consecutive ventilations in the center of the tracing) were not detected in the original capnogram, but they were successfully identified after artifact cancellation.

Data analysis and performance evaluation

Ventilation annotations in the database constituted the gold-standard used to evaluate the performance of the automated ventilation detection algorithm applied to the original and to the

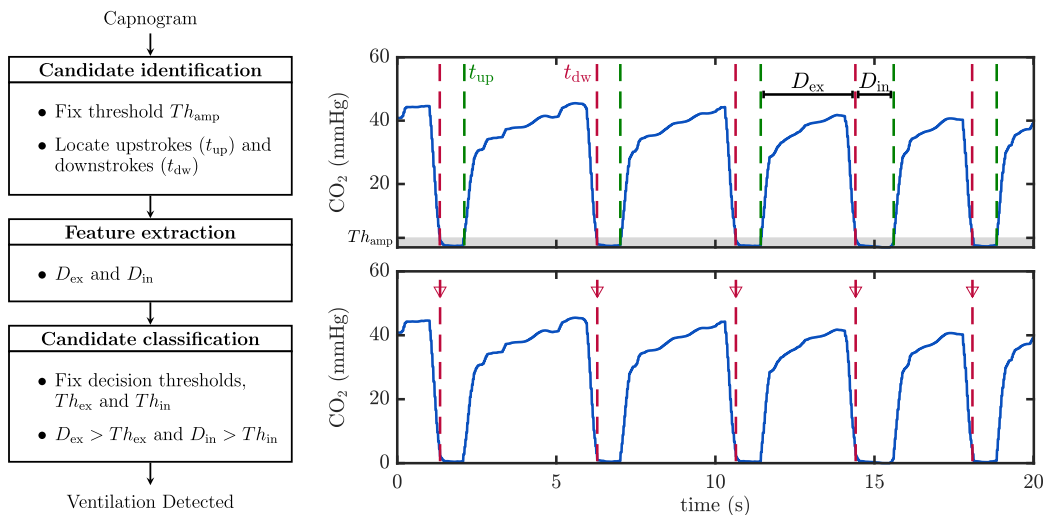


Fig 4. Scheme of the ventilation detector. The algorithm locates upstrokes (t_{up}) and downstrokes (t_{dw}) in the capnogram signal (right) applying a fixed amplitude threshold Th_{amp} . It extracts the duration of the intervals D_{ex} and D_{in} . Finally, fixed duration thresholds Th_{ex} and Th_{in} are used to discriminate true ventilation from the potential candidates. Detected ventilations are depicted with vertical red dotted lines in the bottom panel.

<https://doi.org/10.1371/journal.pone.0201565.g004>

filtered capnograms. The reliability of the proposed filtering techniques was assessed by comparing the sensitivity (Se) and positive predictive value (PPV) of the ventilation detector before and after filtering. Se was defined as the proportion of annotated ventilations that were correctly detected by the algorithm and PPV was the proportion of detected ventilations that were true ventilations.

Filter parameters were optimized for all filtering strategies with a training subset of 15 clean and 15 distorted capnograms. Optimization criteria was maximum Se for a minimum PPV of 95%. Filter performance was reported for the remaining 202 episodes comprising the test subset.

For each episode in the whole set, we computed the number of ventilations provided every minute (ventilation rate), using a 1 minute sliding window with an overlap factor of 1/6, i.e. the ventilation rate value was updated every 10 s. We compared the ventilation rate measurements computed from the estimated ventilations before and after filtering with those computed from the gold-standard ventilations.

We also tested the accuracy in the detection of over-ventilation, defined as a ventilation rate greater than 10 per minute. This value was selected according to the general recommendation in current resuscitation guidelines [2, 3]. For that purpose, Se was defined as the proportion of annotated over-ventilation intervals that were detected by the algorithm, and PPV as the proportion of true over-ventilation instances among all the over-ventilation alarms provided by the algorithm.

Results

Table 1 shows a summary of the episodes included in the study. Mean (\pm standard deviation) duration of the episodes was 31 (\pm 10) min. Airway types were endotracheal tube (ETT) in

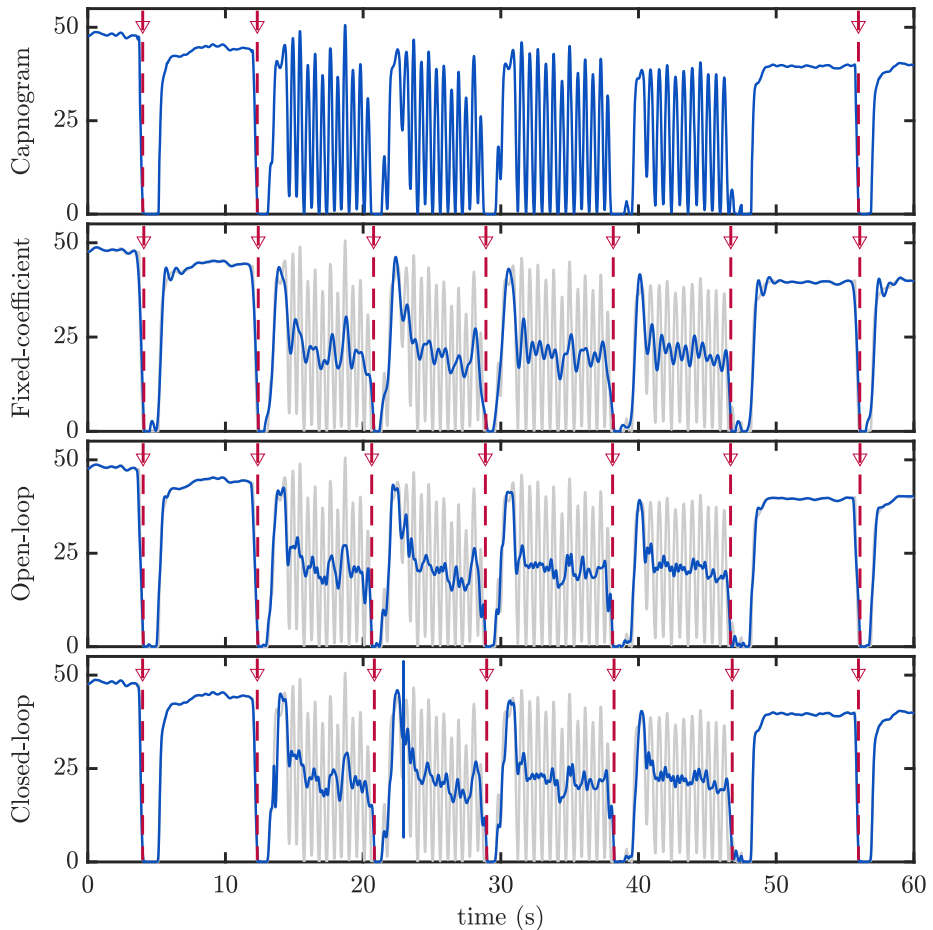


Fig 5. Examples of filtering performance. Original capnogram with clean and distorted respiration cycles (top panel). Detected ventilations are depicted with vertical lines. Distorted ventilations could not be detected by the algorithm. Lower panels show the filtered capnogram (in blue) superimposed to the original capnogram (in gray), for the three filtering alternatives. Detected ventilations are depicted with vertical red dashed lines. In this example, all ventilations were correctly detected after filtering.

<https://doi.org/10.1371/journal.pone.0201565.g005>

64.2%, supraglottic airway (SGA) in 31.7%, and bag-valve-mask (BVM) in 0.03% of the episodes. Distorted episodes comprised 42.2% of the whole set. Type I artifact was annotated in 48%, type II in 21% and type III in 31% of the distorted episodes. A total of 52654 ventilations were annotated, with a mean of 224 (± 115) ventilations per episode. A total of 532597 chest compressions were annotated, with a mean of 2296 (± 1230) per episode. Mean chest compression rate was 114.0 (± 14.4) compressions per minute.

Table 1. Characteristics of the episodes included in the study. Values are expressed as mean (\pm standard deviation).

Group	Episodes	Ventilation type				Duration (min)	Ventilations	Compressions
		BVM	ETT	SGA	NA			
Total	232	7	149	73	3	31 (\pm 10)	224 (\pm 115)	2296 (\pm 1230)
Clean	134	7	90	35	2	30 (\pm 8)	227 (\pm 124)	1994 (\pm 1247)
Distorted	98	0	59	38	1	32 (\pm 12)	221 (\pm 102)	2708 (\pm 1084)
Type I	47	0	19	28	0	31 (\pm 7)	212 (\pm 105)	2893 (\pm 1089)
Type II	21	0	15	6	0	29 (\pm 6)	249 (\pm 108)	2507 (\pm 1079)
Type III	30	0	25	4	1	34 (\pm 18)	214 (\pm 92)	2558 (\pm 1068)

BVM: bag-valve-mask; ETT: endotracheal tube; SGA: supraglottic airway; NA: not available

<https://doi.org/10.1371/journal.pone.0201565.t001>

Ventilation detection performance

Table 2 shows the performance of the ventilation detection algorithm for the test set before and after filtering. For the whole test set, Se/PPV improved from 96.4%/95.0% before filtering to values above 98.2%/97.7%. The results for the clean subset stayed stable before and after filtering. In the distorted subset, Se/PPV improved from 91.9%/89.5% before filtering to values above 97.0%/96.5%. The improvement was much higher for type III records, for which Se/PPV improved from 77.6%/73.5% to values above 95.5%/94.5%.

The box plots in Fig 6A show the distribution of Se and PPV per episode for each type of artifact, before and after filtering with the three proposed techniques. Box plots graphically show median (central line in the box) and interquartile values (edges of the box), maximum and minimum values (extreme values of the whiskers), and outliers (red dots). In general, Se and PPV improved after filtering. Furthermore, the high dispersion among type III episodes was drastically reduced after artifact cancellation with all three filtering approaches.

Ventilation rate estimation

Fig 6B shows the distributions of the unsigned error in percentage per episode between the estimated ventilation rate and the gold-standard value. Again, errors for type III subgroup decreased notably after filtering, as well as errors for type I subgroup, although to a much lesser extent.

Detection of over-ventilation

Table 3 shows the influence of filtering in the detection of over-ventilation (ventilation rate above 10 min⁻¹). From the annotations of the whole dataset, there was a 56.4% (17 901/31 760) of 1-minute intervals with over-ventilation. Globally, the algorithm yielded a Se/PPV of

Table 2. Performance of the ventilation detection algorithm before and after filtering for each type of artifact.

Group	Episodes	Before		Fixed-coefficient		Open-loop		Closed-loop	
		Se(%)	PPV(%)	Se(%)	PPV(%)	Se(%)	PPV(%)	Se(%)	PPV(%)
Total	202	96.4	95.0	98.4	97.7	98.5	97.9	98.2	98.3
Clean	119	99.6	99.0	99.0	98.5	99.2	98.7	99.1	99.2
Distorted	83	91.9	89.5	97.7	96.5	97.6	96.7	97.0	97.1
Type I	42	97.6	96.2	98.3	97.2	98.3	97.1	98.0	97.6
Type II	16	98.5	97.2	98.2	97.7	98.1	98.0	96.5	98.1
Type III	25	77.6	73.5	96.3	94.5	96.0	95.1	95.5	95.5

<https://doi.org/10.1371/journal.pone.0201565.t002>

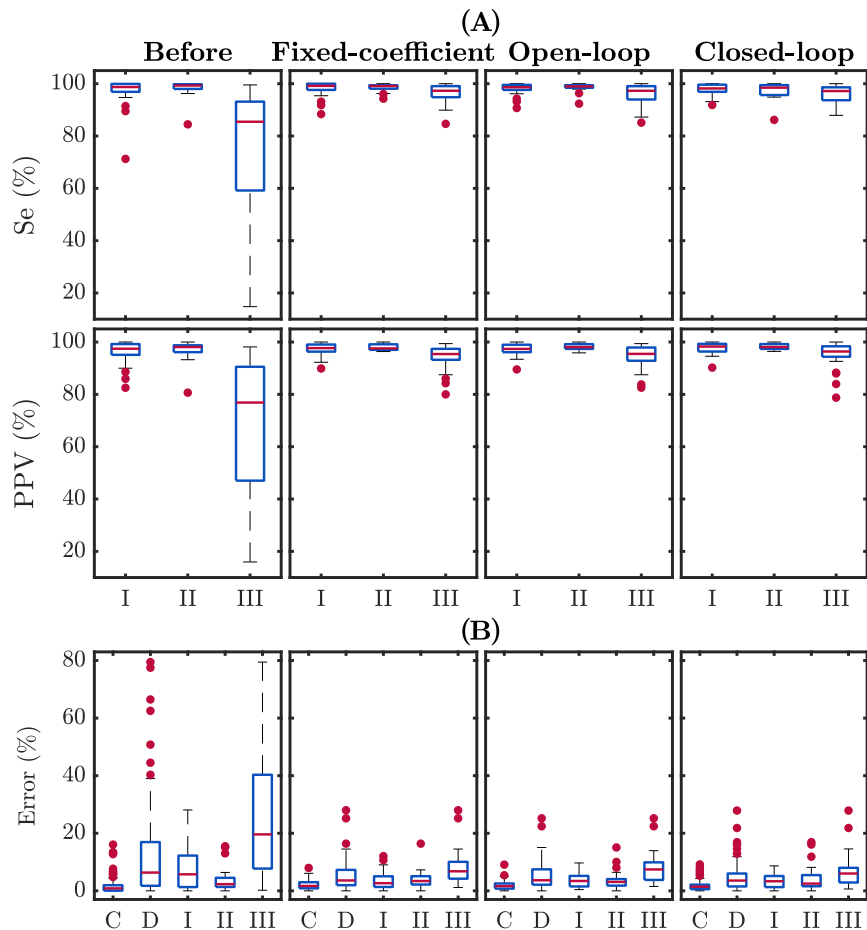


Fig 6. (A) Distributions of Se/PPV values per episode in each artifact category, before and after filtering. (B) Distribution of the unsigned error in percentage in the estimation of ventilation rate. Results are provided for all categories: C: clean, D: distorted, I: type I artifact, II: type II, III: type III.

<https://doi.org/10.1371/journal.pone.0201565.g006>

99.1%/92.6% before and above 97.9%/97.2% after filtering. For the distorted subset, Se/PPV was 98.2%/85.8% before and above 96.3%/95.2% after filtering. Improvement was higher for type III episode, with Se/PPV of 95.5%/72.1% before and above 94.8%/91.1% after filtering.

Discussion

In 2010, Idris et al. observed “chest compression oscillations” in more than 70% OOH capnograms [13]. In a recent study, we reported 42% of distorted capnography tracings during CPR

Table 3. Detection of over-ventilation (ventilation rate > 10 min⁻¹).

Group	Gold Standard		Before		Fixed-coefficient		Open-loop		Closed-loop	
	n _v	n _{hv}	Se(%)	PPV(%)	Se(%)	PPV(%)	Se(%)	PPV (%)	Se(%)	PPV(%)
Total	31 760	17 901	99.1	92.6	98.6	97.3	98.4	97.2	97.9	98.0
Clean	17 413	10 511	99.7	98.0	99.1	98.3	99.0	98.4	98.9	98.9
Distorted	14 347	7 390	98.2	85.8	97.9	95.6	97.4	95.2	96.3	96.6
Type I	7 167	3 398	98.9	90.8	98.9	96.8	98.4	96.4	98.0	97.0
Type II	2 826	1 837	99.8	96.6	97.6	98.2	97.2	97.8	95.2	98.3
Type III	4 354	2 155	95.5	72.1	96.5	91.5	95.9	91.1	94.8	94.2

n_v is the number of annotated ventilation rate values in the gold standard (whole set), and n_{hv} is the number of annotated over-ventilation intervals.

<https://doi.org/10.1371/journal.pone.0201565.t003>

[17]. Among the distorted episodes, artifact appearing in the capnogram plateau (type I) was the most prevalent (48%), followed by artifact spanning from the plateau to the baseline (type III) in 31%, and artifact appearing in the capnogram baseline (type II) in 21% of the episodes.

The nature of the artifact is a sinusoid at the frequency of the chest compressions, with varying amplitude. Our findings are in line with the few studies to date which have reported low ventilation volumes incidental to chest compressions [13, 14]. These volumes, although lower than the anatomical dead space, are sufficient to alter the measurement of the capnogram device.

From a clinical perspective, the presence of chest compression artifact has three important drawbacks: first, it impedes the automated detection of ventilations, causing inaccuracies in the measurement of ventilation rate and false over-ventilation alarms. Moreover, the distorted capnogram tracing is difficult to interpret by clinicians. Measurement of reliable ETCO₂ values becomes impossible, compromising the analysis of ETCO₂ trends. In conclusion, chest compression artifact may jeopardize most potential uses of capnography during resuscitation, including CPR quality assessment, detection of restoration of spontaneous circulation and prognosis assessment.

The present study focused on the improvement of automated ventilation detection using filtering techniques to pre-process the raw capnogram before the application of the detector algorithm. All the proposed filter schemes performed similarly, reporting favourable Se and PPV values well above 97% and 96%, respectively, for the distorted episodes. This caused an improvement in the measurement of ventilation rate with errors in median below 3.6%, and over-ventilation detection, with Se and PPV values above 96% and 95%, respectively, for the distorted episodes.

The highest improvement was obtained in type III episodes, the most challenging distortion, with Se/PPV in ventilation detection improving from 78%/74% to values higher than 94%. The detector was designed to detect inspiration and expiration downstrokes in a normal capnogram. In the presence of type I artifact the capnogram remains well-above the baseline, i.e. oscillations do not cause false detections of inspiration onsets. Similarly, in the presence of type II artifact, the value of the distorted CO₂ is not high enough to detect the expiration upstroke. On the contrary, type III artifact spanning from the plateau to the baseline strongly decreases the ventilation detection. Consequently, the positive impact of filtering is much better observable in type III episodes. In addition, the few studies addressing the artifact phenomenon showed graphical examples of type III capnograms, highlighting the importance of this confounding effect [13, 15].

The adaptive filters should present a better performance than the fixed coefficient filter since compression rates tend to vary during CPR. However, none of the approaches showed a

distinctive superiority in terms of performance. The main reason is that, in our recordings, chest compression rate is generally ten times greater than ventilation rate. In this scenario the fixed coefficient filter shows a good performance. The adaptive approaches would be more efficient in case of an excess of ventilation rate with low compression rates. Hence, selection of the filtering algorithm could be analyzed in terms of complexity and computational burden. In this case, adaptive filtering is at a disadvantage compared to the simplicity of a fixed-coefficient filter. Consequently, it seems adequate to apply a filter with fixed coefficients to suppress the chest compression artifact from the capnogram. Nevertheless, the implementation of the three filtering approaches would operate the capnogram signal in real time, being transparent to the user.

The capnogram waveform achieved after filtering approximates the mean peak-to-peak amplitude of the artifact, as illustrated in Fig 5 in the Methods section). After filtering, the capnogram is still difficult to interpret by clinicians. The filtered capnogram waveform hinders the reliable analysis of ETCO₂ trends, a very useful clinical information during CPR. In the figure, reliable ETCO₂ values could only be measured in the undistorted tracing before and after the distorted interval. In practice, capnogram filtering would be an intermediate stage in the ventilation detection algorithm if implemented in the monitor-defibrillator but the resulting waveform would not be displayed on the screen, the raw capnogram would appear instead. The development of other techniques aimed at removing the artifact (to improve ventilation tracking) and at the same time preserving the capnogram tracing would favor clinical interpretation.

Conclusion

We assessed three filtering alternatives for suppressing the artifact caused by chest compressions on OOH capnograms and analyzed their performance in terms of the improvement of the automated detection of ventilations during CPR. All approaches yielded good results, so simplicity and low computational burden could determine the best alternative to be implemented.

Supporting information

S1 Appendix. Description of the adaptive filters.
(PDF)

S1 File. Results of the ventilation detection algorithm before and after capnogram filtering. For all episodes in the database, the file contains all ventilations annotated in the gold standard (named with an ordinal number) and ventilation instances detected by the algorithm before and after filtering. Label FP means False Positive detection. Label FN means False Negative detection.
(XLSX)

Author Contributions

Conceptualization: Jose Julio Gutiérrez, Sofía Ruiz de Gauna, Jesus María Ruiz, Luis Alberto Leturiondo.

Data curation: Jose Julio Gutiérrez, Mikel Leturiondo, Sofía Ruiz de Gauna, Jesus María Ruiz.

Formal analysis: Jose Julio Gutiérrez, Mikel Leturiondo, Sofía Ruiz de Gauna.

Funding acquisition: Jose Julio Gutiérrez, Sofía Ruiz de Gauna, Jesus María Ruiz, Luis Alberto Leturiondo.

Investigation: Jose Julio Gutiérrez, Mikel Leturiondo, Jesus María Ruiz.

Methodology: Jose Julio Gutiérrez, Sofía Ruiz de Gauna, Jesus María Ruiz.

Project administration: Sofía Ruiz de Gauna, Jesus María Ruiz, Luis Alberto Leturiondo.

Resources: Dana Zive, James Knox Russell, Mohamud Daya.

Software: Mikel Leturiondo, Digna María González-Otero.

Supervision: Jose Julio Gutiérrez, Sofía Ruiz de Gauna, Jesus María Ruiz, Luis Alberto Leturiondo.

Validation: Jose Julio Gutiérrez, Mikel Leturiondo, Sofía Ruiz de Gauna, Digna María González-Otero.

Visualization: Mikel Leturiondo, Jesus María Ruiz.

Writing – original draft: Jose Julio Gutiérrez, Mikel Leturiondo, Sofía Ruiz de Gauna, Jesus María Ruiz.

Writing – review & editing: Jose Julio Gutiérrez, Mikel Leturiondo, Sofía Ruiz de Gauna, Jesus María Ruiz, Luis Alberto Leturiondo, Digna María González-Otero, Dana Zive, James Knox Russell, Mohamud Daya.

References

- Nichol G, Baker D. The epidemiology of sudden death. In: Paradir NA, Halperin HR, Kern KB, Wenzel V, Chamberlain D, editors. *Cardiac Arrest: Science and Practice of Resuscitation Medicine*. Cambridge: Cambridge University Press; 2007. p. 26–50.
- Soar J, Nolan JP, Böttiger BW, Perkins GD, Lott C, Carli P, et al. European Resuscitation Council guidelines for resuscitation 2015. Section 3. Adult advanced life support. *Resuscitation*. 2015; 95:100–147. <https://doi.org/10.1016/j.resuscitation.2015.07.016> PMID: 26477701
- Link MS, Berkow LC, Kudenchuk PJ, Halperin HR, Hess EP, Moitra VK, et al. 2015 American Heart Association Guidelines Update for Cardiopulmonary Resuscitation and Emergency Cardiovascular Care. Part 7: adult advanced cardiovascular life support. *Circulation*. 2015; 132(18 suppl 2):S444–S464.
- Pantazopoulos C, Xanthos T, Pantazopoulos I, Papalios A, Kouskouni E, Iacovidou N. A review of carbon dioxide monitoring during adult cardiopulmonary resuscitation. *Heart Lung Circ*. 2015; 24(11):1053–1061. <https://doi.org/10.1016/j.hlc.2015.05.013> PMID: 26150002
- Kodali BS, Urman RD, et al. Capnography during cardiopulmonary resuscitation: current evidence and future directions. *J Emerg Trauma Shock*. 2014; 7(4):332. <https://doi.org/10.4103/0974-2700.142778> PMID: 25400399
- Gravenstein JS, Jaffe MB, Gravenstein N, Paulus DA. *Capnography*. Cambridge University Press; 2011.
- Aufderheide TP, Lurie KG. Death by hyperventilation: a common and life-threatening problem during cardiopulmonary resuscitation. *Crit Care Med*. 2004; 32(9):S345–S351. <https://doi.org/10.1097/01.CCM.0000134335.46859.09> PMID: 15508657
- O'Neill JF, Deakin CD. Do we hyperventilate cardiac arrest patients? *Resuscitation*. 2007; 73(1):82–85. <https://doi.org/10.1016/j.resuscitation.2006.09.012> PMID: 17289248
- Maertens VL, De Smedt LE, Lemoyne S, et al. Patients with cardiac arrest are ventilated two times faster than guidelines recommend: an observational prehospital study using tracheal pressure measurement. *Resuscitation*. 2013; 84(7):921–926. <https://doi.org/10.1016/j.resuscitation.2012.11.015> PMID: 23178868
- Silvestri S, Ralls GA, Krauss B, Thundiyil J, Rothrock SG, Senn A, et al. The effectiveness of out-of-hospital use of continuous end-tidal carbon dioxide monitoring on the rate of unrecognized misplaced intubation within a regional emergency medical services system. *Ann Emerg Med*. 2005; 45(5):497–503. <https://doi.org/10.1016/j.annemergmed.2004.09.014> PMID: 15855946
- Pokorná M, Nečas E, Kratochvíl J, Skřipický R, Andrlík M, Franěk O. A sudden increase in partial pressure end-tidal carbon dioxide (PETCO₂) at the moment of return of spontaneous circulation. *J Emerg Med*. 2010; 38(5):614–621. <https://doi.org/10.1016/j.jemermed.2009.04.064> PMID: 19570645

12. Touma O, Davies M. The prognostic value of end tidal carbon dioxide during cardiac arrest: a systematic review. *Resuscitation*. 2013; 84(11):1470–1479. <https://doi.org/10.1016/j.resuscitation.2013.07.011> PMID: 23871864
13. Idris AH, Daya M, Owens P, O'Neill S, Helfenbein ED, Babaeizadeh S, et al. High incidence of chest compression oscillations associated with capnography during out-of-hospital cardiopulmonary resuscitation. *Circulation*. 2010; 122:A83.
14. Vanwulpen M, Wolfskeil M, Duchatelet C, Monsieurs K, Idrissi SH. Quantifying inspiratory volumes generated by manual chest compressions during resuscitation in the prehospital setting. *Resuscitation*. 2017; 118:e18. <https://doi.org/10.1016/j.resuscitation.2017.08.054>
15. Deakin CD, O'Neill JF, Tabor T. Does compression-only cardiopulmonary resuscitation generate adequate passive ventilation during cardiac arrest? *Resuscitation*. 2007; 75(1):53–59. <https://doi.org/10.1016/j.resuscitation.2007.04.002> PMID: 17507138
16. Aramendi E, Elola A, Alonso E, Irusta U, Daya M, Russell JK, et al. Feasibility of the capnogram to monitor ventilation rate during cardiopulmonary resuscitation. *Resuscitation*. 2017; 110:162–168. <https://doi.org/10.1016/j.resuscitation.2016.08.033> PMID: 27670357
17. Leturiondo M, Ruiz de Gauna S, Ruiz JM, Gutiérrez JJ, Leturiondo LA, González-Otero DM, et al. Influence of chest compression artefact on capnogram-based ventilation detection during out-of-hospital cardiopulmonary resuscitation. *Resuscitation*. 2017; 124:63–68. <https://doi.org/10.1016/j.resuscitation.2017.12.013> PMID: 29246741
18. Bhavani-Shankar K, Kumar AY, Moseley HSL, Ahjee-Hallsworth R. Terminology and the current limitations of time capnography: a brief review. *Journal of clinical monitoring*. 1995; 11(3):175–182. <https://doi.org/10.1007/BF01617719> PMID: 7623057
19. Pellis T, Bisera J, Tang W, Weil MH. Expanding automatic external defibrillators to include automated detection of cardiac, respiratory, and cardiorespiratory arrest. *Critical Care Medicine*. 2002; 30(4):S176–S178. <https://doi.org/10.1097/00003246-200204001-00012> PMID: 11953646
20. Losert H, Risdal M, Sterz F, Nysaether J, Köhler K, Eftestøl T, et al. Thoracic impedance changes measured via defibrillator pads can monitor ventilation in critically ill patients and during cardiopulmonary resuscitation. *Critical Care Medicine*. 2006; 34(9):2399–2405. <https://doi.org/10.1097/01.CCM.0000235666.40378.60> PMID: 16850000
21. Edelson DP, Eilevstjønn J, Weidman EK, Retzer E, Hoek TLV, Abella BS. Capnography and chest-wall impedance algorithms for ventilation detection during cardiopulmonary resuscitation. *Resuscitation*. 2010; 81(3):317–322. <https://doi.org/10.1016/j.resuscitation.2009.11.003> PMID: 20036047
22. Abella BS, Sandbo N, Vassilatos P, Alvarado JP, O'hearn N, Wigder HN, Becker LB. Chest compression rates during cardiopulmonary resuscitation are suboptimal: a prospective study during in-hospital cardiac arrest. *Circulation*. 2005; 111(4):428–434. <https://doi.org/10.1161/01.CIR.0000153811.84257.59> PMID: 15687130
23. Meaney PA, Bobrow BJ, Mancini ME, Christenson J, De Caen AR, Bhanji F, Aufderheide TP. Cardiopulmonary resuscitation quality: improving cardiac resuscitation outcomes both inside and outside the hospital: a consensus statement from the American Heart Association. *Circulation*. 2013; 128(4):417–435. <https://doi.org/10.1161/CIR.0b013e31829d8654> PMID: 23801105
24. Aase SO, Eftestøl T, Husoy J, Sunde K, Steen PA. CPR artifact removal from human ECG using optimal multichannel filtering. *IEEE Trans Biomed Eng*. 2000; 47(11):1440–1449. <https://doi.org/10.1109/10.880095> PMID: 11077737
25. Eilevstjønn J, Eftestøl T, Aase SO, Myklebust H, Husøy JH, Steen PA. Feasibility of shock advice analysis during CPR through removal of CPR artefacts from the human ECG. *Resuscitation*. 2004; 61(2):131–141. <https://doi.org/10.1016/j.resuscitation.2003.12.019> PMID: 15135189
26. Irusta U, Ruiz J, de Gauna SR, Eftestøl T, Kramer-Johansen J. A least mean-square filter for the estimation of the cardiopulmonary resuscitation artifact based on the frequency of the compressions. *IEEE Trans Biomed Eng*. 2009; 56(4):1052–1062. <https://doi.org/10.1109/TBME.2008.2010329> PMID: 19150778
27. Gong Y, Chen B, Li Y. A review of the performance of artifact filtering algorithms for cardiopulmonary resuscitation. *J Healthc Eng*. 2013; 4(2):185–202. <https://doi.org/10.1260/2040-2295.4.2.185> PMID: 23778011
28. Ruiz de Gauna S, Irusta U, Ruiz J, Ayala U, Aramendi E, Eftestøl T. Rhythm analysis during cardiopulmonary resuscitation: past, present, and future. *Biomed Res Int*. 2014; 2014. <https://doi.org/10.1155/2014/386010>
29. Widrow B, Stearns SD. *Adaptive signal processing*. Englewood Cliffs, NJ, Prentice-Hall, Inc. 1985; 1:491.

S1 Appendix: Adaptive filtering

Variability of chest compression and ventilation rates during cardiopulmonary resuscitation (CPR) may affect the efficacy of the fixed-coefficient filter [1–4]. Adaptive techniques in which the filter parameters are adjusted in time according to the varying characteristics of the artifact could be a suitable solution. In the literature, adaptive filtering has been extensively used for the suppression of the artifact induced by chest compressions in the electrocardiogram recorded by defibrillators during CPR [5–9].

For the capnogram artifact issue, we designed two different adaptive filtering configurations, an open-loop and a closed-loop adaptive filter [10].

Open-loop (OL) adaptive filter:

The OL adaptation is illustrated in Figure 1A. This technique is based on the adaptive adjustment of the filter to the information extracted from the compression depth (CD) signal, used as a reference in this case.

The filter was a stop-band Butterworth filter whose central frequency is adaptively adjusted according to the chest compression rate. We estimated the average chest compression rate in 2-s intervals, using the annotated compression instances in the CD signal. Thus, the coefficients of the filter were updated every 2 s [10].

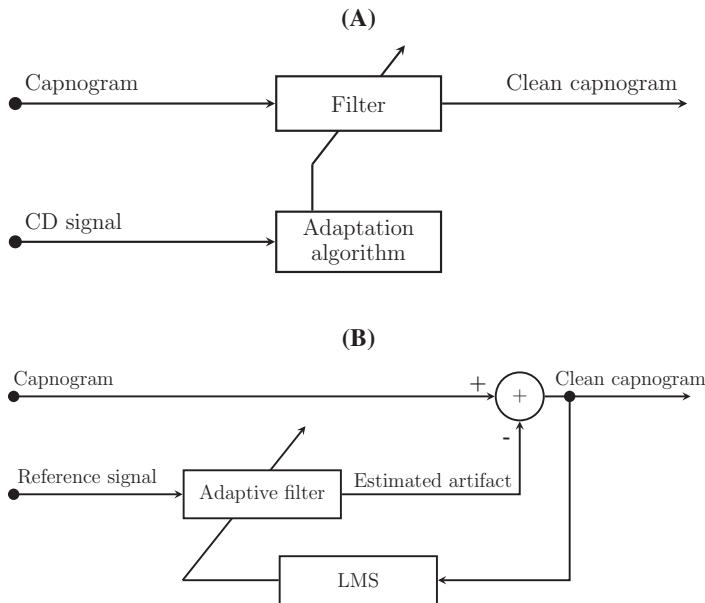


Figure 1: **(A) Open-loop adaptive filter.** The adaptation algorithm uses the capnogram and the CD signal to adjust the filter coefficients every 2-s. **(B) Closed-loop adaptive filter.** Configuration for adaptive cancellation of the chest compression artifact.

Closed-loop (CL) adaptive filter:

Figure 1B shows the scheme of the CL adaptive filter applied to canceling sinusoidal interference [10]. This system requires an additional reference input signal. In our approach, this reference signal is modeled as a pure cosine wave of time-varying amplitude and phase, with a fundamental frequency matching the chest compression rate. The chest compression instants detected in the CD signal were used to estimate the instantaneous chest compression rate, which may vary between compressions.

In this configuration, the artifact is adaptively estimated and subtracted from the input capnogram to obtain a clean capnogram. The filter coefficients are updated sample by sample by applying the Least-Mean-Square algorithm (LMS). The resulting system is equivalent to a notch filter at the frequency of chest compressions, capable of adaptively tracking the exact frequency of the artifact [10].

References

1. Abella BS, Sandbo N, Vassilatos P, Alvarado JP, O’hearn N, Wigder HN, Becker LB. Chest compression rates during cardiopulmonary resuscitation are suboptimal: a prospective study during in-hospital cardiac arrest. *Circulation*. 2005;111(4):428–434.
2. Meaney PA, Bobrow BJ, Mancini ME, Christenson J, De Caen AR, Bhanji F, Aufderheide TP. Cardiopulmonary resuscitation quality: improving cardiac resuscitation outcomes both inside and outside the hospital: a consensus statement from the American Heart Association. *Circulation*. 2013;128(4):417–435.
3. O’Neill JF, Deakin CD. Do we hyperventilate cardiac arrest patients? *Resuscitation*. 2007;73(1):82–85.
4. Maertens VL, De Smedt LE, Lemoyne S, et al. Patients with cardiac arrest are ventilated two times faster than guidelines recommend: an observational prehospital study using tracheal pressure measurement. *Resuscitation*. 2013;84(7):921–926.
5. Aase SO, Eftestøl T, Husoy J, Sunde K, Steen PA. CPR artifact removal from human ECG using optimal multichannel filtering. *IEEE Trans Biomed Eng*. 2000;47(11):1440–1449.
6. Eilevstjønn J, Eftestøl T, Aase SO, Myklebust H, Husøy JH, Steen PA. Feasibility of shock advice analysis during CPR through removal of CPR artefacts from the human ECG. *Resuscitation*. 2004;61(2):131–141.
7. Irusta U, Ruiz J, de Gauna SR, Eftestøl T, Kramer-Johansen J. A least mean-square filter for the estimation of the cardiopulmonary resuscitation artifact based on the frequency of the compressions. *IEEE Trans Biomed Eng*. 2009;56(4):1052–1062.
8. Gong Y, Chen B, Li Y. A review of the performance of artifact filtering algorithms for cardiopulmonary resuscitation. *J Healthc Eng*. 2013;4(2):185–202.
9. Ruiz de Gauna S, Irusta U, Ruiz J, Ayala U, Aramendi E, Eftestøl T. Rhythm analysis during cardiopulmonary resuscitation: past, present, and future. *Biomed Res Int*. 2014;2014.
10. Widrow B, Stearns SD. *Adaptive signal processing*. Englewood Cliffs, NJ, Prentice-Hall, Inc. 1985;1:491.



Clinical paper

Enhancement of capnogram waveform in the presence of chest compression artefact during cardiopulmonary resuscitation



Sofía Ruiz de Gauna^{a,*}, Mikel Leturiondo^a, J. Julio Gutiérrez^a, Jesus M. Ruiz^a,
Digna M. González-Otero^a, James K. Russell^b, Mohamud Daya^b

^a Department of Communications Engineering, University of the Basque Country, UPV/EHU, 48013 Bilbao, Spain

^b Department of Emergency Medicine, Oregon Health & Science University, OHSU, 97239-3098 Portland, OR, USA

ARTICLE INFO

Keywords:

Cardiopulmonary resuscitation
Advanced life support
Waveform capnography
Ventilation
Chest compressions
Chest compression artefact

ABSTRACT

Background: Current resuscitation guidelines emphasize the use of waveform capnography to help guide rescuers during cardiopulmonary resuscitation (CPR). However, chest compressions often cause oscillations in the capnogram, impeding its reliable interpretation, either visual or automated. The aim of the study was to design an algorithm to enhance waveform capnography by suppressing the chest compression artefact.

Methods: Monitor-defibrillator recordings from 202 patients in out-of-hospital cardiac arrest were analysed. Capnograms were classified according to the morphology of the artefact. Ventilations were annotated using the transthoracic impedance signal acquired through defibrillation pads. The suppression algorithm is designed to operate in real-time, locating distorted intervals and restoring the envelope of the capnogram. We evaluated the improvement in automated ventilation detection, estimation of ventilation rate, and detection of excessive ventilation rates (over-ventilation) using the capnograms before and after artefact suppression.

Results: A total of 44 267 ventilations were annotated. After artefact suppression, sensitivity (Se) and positive predictive value (PPV) of the ventilation detector increased from 91.9/89.5% to 98.0/97.3% in the distorted episodes (83/202). Improvement was most noticeable for high-amplitude artefact, for which Se/PPV raised from 77.6/73.5% to 97.1/96.1%. Estimation of ventilation rate and detection of over-ventilation also upgraded. The suppression algorithm had minimal impact in non-distorted data.

Conclusion: Ventilation detection based on waveform capnography improved after chest compression artefact suppression. Moreover, the algorithm enhances the capnogram tracing, potentially improving its clinical interpretation during CPR. Prospective research in clinical settings is needed to understand the feasibility and utility of the method.

Introduction

Treatment of out-of-hospital cardiac arrest (OHCA) by advanced life support (ALS) usually includes advanced airway placement, administration of medications along with high quality cardiopulmonary resuscitation (CPR) [1–3].

Most monitor-defibrillators are equipped with electronic carbon dioxide (CO₂) detectors which allow end-tidal CO₂ (ETCO₂) measurement. ETCO₂ is the partial pressure of carbon dioxide at the end of an exhaled breath, and reflects ventilation and perfusion of the patient [4]. Electronic CO₂ detectors can be of two types: those that report the results in a numeric display (non-waveform detectors), and those that provide waveform graphical display where the respiratory cycle can be directly observed [2,5]. The latter have become more important, since

the last release of international resuscitation guidelines emphasized the use of waveform capnography for ALS guidance and patient monitoring [2,3]. Currently, waveform capnography can be used for assessing the correct placement of the tracheal tube and monitoring ventilation rate. Other potential uses of waveform capnography include monitoring of CPR quality [5–7], early detection of restoration of spontaneous circulation [5,8] and determining patient prognosis during CPR [9,10].

To be clinically interpretable, the different phases of the respiratory cycle must be identifiable in the capnogram during CPR, including the end of expiration where ETCO₂ is measured. However, several studies have reported the appearance of fast oscillations synchronized with chest compressions superimposed on the capnogram [11–13], often completely obscuring the normal tracing. This distortion could negatively affect waveform capnography in three aspects: causing errors in

* Corresponding author.

E-mail address: sofia.ruizdegauna@ehu.es (S. Ruiz de Gauna).

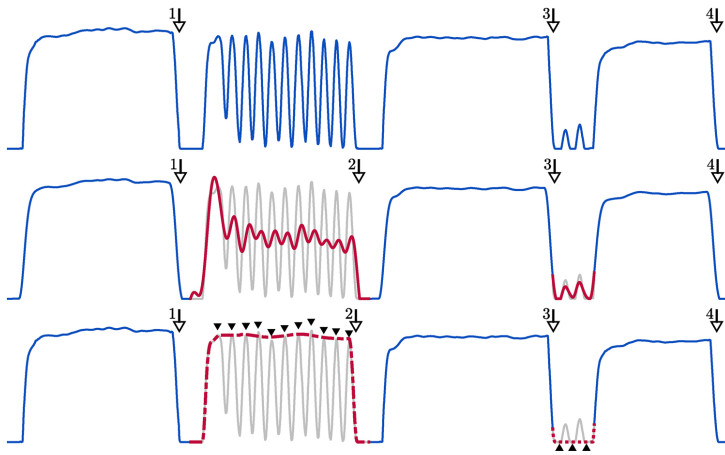


Fig. 1. Alternatives for chest compression artefact suppression. A distorted capnogram is depicted at the top. Each vertical arrow indicates a ventilation. Oscillations of type III impede the correct detection of the second ventilation. The middle panel represents in red the resulting waveform after applying one of the filters proposed in reference [15]. The bottom panel illustrates the extraction of the envelope waveform capnography through the detection of, respectively, the local maxima of the original capnogram in the plateau and the local minima in the baseline.

the automated detection of ventilations and consequently in the estimation of ventilation rate, impeding reliable measurement of ETCO₂ values, and limiting CPR providers since distorted capnograms are difficult to interpret.

In a recent study, we retrospectively analysed monitor-defibrillator recordings from OHCA episodes and reported that 42% of capnograms were distorted by chest compression oscillations [14]. That study also quantified significant errors in the capnogram-based estimation of ventilation rate, attributable to the oscillations interference. In a follow-up study, we proposed a solution to remove chest compression oscillations from the capnogram by filtering, which improved the automated detection of ventilation rate. Unfortunately, filtered capnograms were far from being reliable for clinical interpretation [15].

In this study, we explored an alternative method to suppress chest compression oscillations from the capnography waveforms. The method was designed to improve ventilation detection and more importantly, to provide a capnogram that was reliable for clinical interpretation. For quantitatively assessing the goodness of the method, the accuracy of a capnogram-based algorithm for ventilation detection was tested before and after applying the suppression method. In addition to ventilation detection, we also quantified the improvement in the computation of ventilation rate and in the detection of excessive ventilation rates.

Materials and methods

Data collection and annotation

Data were extracted from a database of OHCA episodes collected between 2011 and 2016 as a part of the Resuscitation Outcomes Consortium (ROC) Epidemiological Cardiac Arrest Registry. The data collection for the ROC Epistry was approved by the Oregon Health & Science University (OHSU) Institutional Review Board (IRB00001736). Patient private data was not available for the study. Episodes were recorded using Heartstart MRx monitor-defibrillators (Philips, USA), equipped with real-time CPR feedback technology (Q-CPR) and waveform capnography using sidestream technology (Microstream, Oridion Systems Ltd, Israel). Ventilation was provided through an endotracheal tube, supraglottic airway (King Laryngeal Tube) or with a bag-valve mask device.

This study analysed the monitor-defibrillator recordings of 202 patients, containing at least 20 min of concurrent capnogram, compression depth (CD) signal, and transthoracic impedance (TI) signal

acquired through the defibrillation pads. We used the annotations from a previous study [14], in which biomedical experts classified the episodes as distorted if chest compression artefact appeared during more than one minute of the chest compression time. Furthermore, experts classified the artefact into three types according to its location: type I (chest compression oscillations appearing in the expiratory plateau of the capnogram), type II (in the baseline), and type III (oscillations spanning from the plateau to the baseline) [14]. Finally, experts annotated each ventilation using the low frequency component of the TI signal, as the impedance of the chest measured through defibrillation pads fluctuates during each ventilation [16–18]. Resulting ventilation annotations were used in the present study as the gold standard to quantify the effectiveness of the suppression method.

Chest compression artefact suppression method

Filtering techniques have been widely proposed in the literature to remove chest compression artefact from the electrocardiogram during CPR [19–23]. Likewise, those techniques can be applied to a distorted capnogram. An example of filtering is shown in Fig. 1. A segment of a distorted capnogram is depicted in the top panel. Each vertical arrow indicates a ventilation. Oscillations of type III impede the correct detection of the second ventilation. The middle panel represents (in red) the resulting capnogram after applying one of the filters proposed by Gutierrez et al. [15]. The filtered capnogram appears highly distorted and, although all ventilations are correctly detected, the waveform is not easily interpretable.

The principle of the method proposed in the present study relies on the hypothesis that the envelope of the capnogram could be a reliable tracing for clinical interpretation. An example of the method's performance is given in the bottom panel of Fig. 1. As the artefact morphology and location is variable [14] the algorithm distinguishes between low and high CO₂ concentration intervals to determine how to extract the envelope of the capnogram. The algorithm, which can operate in real-time, detects the local maxima in the plateau phase and applies a smoothing filter to restore the upper envelope of the capnogram (see the dashed red line depicted in the bottom panel of Fig. 1). Similarly, local minima are detected in the capnogram baseline to extract the lower envelope (see the dotted red line). A detailed explanation of the algorithm is provided in the supplementary materials published online with the electronic version of this article.

Automated ventilation detection algorithm

For the automated detection of ventilations in the waveform capnography, we used an algorithm designed and tested in a previous study [14], quite similar to others used in the literature [24]. The algorithm was computationally simple, and relied on the automated identification of CO₂ concentration downstrokes and upstrokes during inspiration and expiration, respectively, as the basis for detecting ventilations in real-time.

Data analysis

The artefact suppression algorithm was applied to the raw capnogram of each OHCA episode. Sensitivity (Se) and positive predictive value (PPV) of the automated ventilation detection algorithm were computed before and after artefact suppression to be used as figures of merit. Se values were calculated as the proportion of correctly detected ventilations among all ventilations that were annotated. PPV values were the proportion of correctly detected ventilations among all the detections.

We also evaluated the performance of the algorithm in the estimation of ventilation rate as follows: we computed, for each episode, ventilation rate values per minute (the number of ventilations given in the last minute), updated every 10 s. The ventilation rate measurements obtained before and after applying the artefact suppression method to the raw capnograms were compared with the measurements computed from the gold standard by calculating the unsigned percent error in each case.

According to the general recommendation in current resuscitation guidelines, ventilation rates above 10 min⁻¹ during CPR can be considered as excessive [2,3]. The accuracy in the detection of excessive ventilation rates was also tested. For that purpose, an alarm was annotated when a ventilation rate measurement was higher than 10 min⁻¹. In this case, Se was defined as the proportion of annotated alarms that were correctly detected, and PPV as the proportion of detected over-ventilation alarms that were indeed annotated.

Data were reported as mean (± SD) if they passed the Lilliefors test of normality, and as median (IQR) otherwise. Distribution of Se and PPV per episode and distribution of the percent error were depicted with box plots, which graphically show median, IQR values and possible outliers.

Results

Table 1 shows a summary of the characteristics of the episodes, clustered according to the artefact type. From the 202 OHCA episodes that were analysed, 83 (41.1%) were classified as distorted. Among the distorted episodes, type I artefact was primarily annotated in 50.6%, type II in 19.3% and type III in 30.1% of the cases. A total of 44 267 ventilations were annotated, with a mean of 219 (± 115) ventilations per episode. From these, 25 936 (58.6%) corresponded to non-distorted episodes and 18 331 (41.4%) to distorted episodes.

The performance of the automated ventilation algorithm with the raw capnograms and after applying the suppression method is described in Table 2. For the whole set, global Se/PPV improved from 96.4%/95.0% to 98.5%/98.3%. The algorithm had minimal impact in non-distorted episodes, whereas Se/PPV largely increased from 91.9%/89.5% to 98.0%/97.3% for distorted episodes. Performance particularly improved in type III episodes, for which Se/PPV increased from 77.6%/73.5% to 97.1%/96.1%. Fig. 2A depicts through box plots the distribution of Se and PPV per episode given by the ventilation detection algorithm. In general, medians of both figures of merit increased after artefact suppression, but to a greater extent for type III episodes. Dispersion in Se and PPV also reduced for all groups, but this reduction was more noticeable for type III episodes, as Se/PPV IQR reduced from 20.1%/29.2% to 1.6%/3.8%.

Table 1

Characteristics of the episodes included in the study clustered by the type of artefact. Values are expressed as mean (± SD).

Group	Episodes	Ventilation type				Duration (min)	Ventilations
		BVM	ETT	SGA	NA		
Total	202	6	126	68	2	30 (± 10)	219 (± 115)
Non-distorted	119	6	79	33	1	30 (± 8)	218 (± 123)
Distorted	83	0	47	35	1	31 (± 12)	221 (± 102)
Type I	42	0	17	25	0	31 (± 7)	203 (± 96)
Type II	16	0	10	6	0	29 (± 7)	274 (± 110)
Type III	25	0	20	4	1	34 (± 20)	216 (± 99)

BVM: bag-valve-mask; ETT: endotracheal tube; SGA: supraglottic airway (King Laryngeal Tube); NA: information not available.

Fig. 2B illustrates performance regarding the estimation of ventilation rate. Box plots depict the distribution of the unsigned error in percentage between the estimation and the gold-standard ventilation rate value. Error reduced in all cases, but again, the error decreased noticeably in type III subset after artefact suppression: median error reduced from 19.6% to 4.5%, and IQR from 32.6% to 6.3%.

The influence of artefact suppression in the detection of excessive ventilation rates (above the recommended 10 min⁻¹) is illustrated in Table 3. Globally, Se/PPV were 99.3%/93.1% before and 98.9%/97.8% after applying the method. For the distorted subset, Se/PPV was 98.8%/86.7% before and 98.4%/96.3% after, i.e. the increase in PPV implied a reduction in false over-ventilation alarms. Once again, the improvement was significantly higher for type III subgroup, with Se slightly increasing from 97.2% to 98.7%, but PPV increasing from a poor 73.9% to 93.6% after artefact cancellation.

Finally, Fig. 3 visually illustrates the performance of the method. Each example corresponds to one artefact category (A: type I, B: type II, C, D: type III). The raw capnogram is depicted in blue and the resulting waveform in red superimposed to the raw capnogram.

Discussion

The presence of fast oscillations of varying amplitude superimposed on waveform capnography is common during pre-hospital CPR. Two recent studies have characterized the nature of the oscillations appearing on OHCA capnograms during chest compressions, demonstrating that oscillations have a sinusoidal waveform with a fundamental frequency matching the chest compression rate [14,15].

The origin of this phenomenon has been scarcely studied. Deakin et al. found that compression-only CPR induces passive ventilations of limited volumes, with a median tidal volume per compression of 41.5 ml (range 33.0–62.1 ml) [13]. These volumes are considerably less than typical adult dead space, which is on the order of 150 ml. These authors also suggested the possibility of a minor diaphragmatic activity caused by manual chest compressions after the observation of matching oscillations in the aligned volume and CO₂ curves. In a conference

Table 2

Performance of the ventilation detection algorithm before and after artefact suppression. Global sensitivity (Se) and positive predictive value (PPV) are reported for the whole set, and for each artefact category.

Group	Episodes	Before		After	
		Se(%)	PPV(%)	Se(%)	PPV(%)
Total	202	96.4	95.0	98.5	98.3
Non-distorted	119	99.6	99.0	99.0	99.0
Distorted	83	91.9	89.5	98.0	97.3
Type I	42	97.6	96.2	98.4	97.7
Type II	16	98.5	97.2	98.0	97.9
Type III	25	77.6	73.5	97.1	96.1

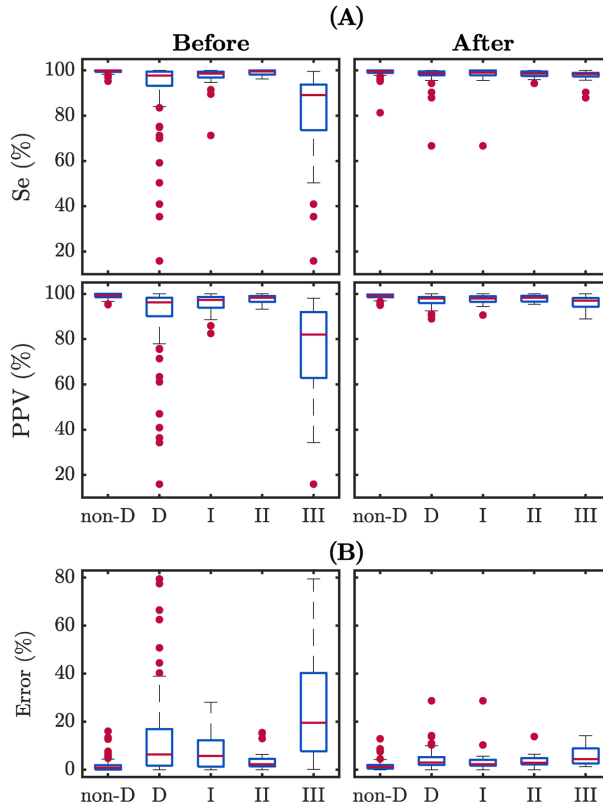


Fig. 2. (A) Distribution of Se and PPV per episode given by the ventilation detection algorithm before and after artefact suppression. (B) Distribution of the unsigned error in percentage per episode in the estimation of ventilation rate. The boxes represent the median and IQR and the whiskers indicate the last value within ± 1.5 IQR. Outliers are represented by dots. Results are provided for all categories: non-D: non-distorted. D: distorted. I: type I artefact. II: type II. III: type III.

Table 3

Detection of excessive ventilation rates during CPR ($> 10 \text{ min}^{-1}$): n_{vr} is the number of annotated ventilation rate values in the gold standard, and n_{ov} is the number of annotated over-ventilation alarms.

Group	Gold standard		Before		After	
	n_{vr}	n_{ov}	Se(%)	PPV(%)	Se(%)	PPV(%)
Total	25 833	15 237	99.3	93.1	98.9	97.8
Non-distorted	14 889	8873	99.7	98.2	99.3	98.9
Distorted	10 944	6364	98.8	86.7	98.4	96.3
Type I	5823	2961	99.1	90.7	98.7	97.2
Type II	2160	1570	99.8	97.8	97.5	97.7
Type III	2961	1833	97.2	73.9	98.7	93.6

abstract, Vanwulpen et al. quantified the inspiratory volumes during manual chest compressions in the pre-hospital setting [12]. Their measurements were in line with the study by Deakin et al., with a median inspiratory volume generated by manual chest compressions of 15 ml (range 4–62 ml).

On the other hand, little is known about potential factors influencing the appearance of the artefact. According to the amplitude variability and the location of the oscillations in the respiratory cycle, type I

(plateau) had an incidence in our data of 20.8%, type II (baseline) of 7.9%, and type III (spanning from plateau to baseline) of 12.4%. In episodes where patients were ventilated with bag-valve-mask no artefact was observed, although the sample was very small. Type III, the most confounding artefact, appeared mostly in episodes with endotracheal intubation. Type I was the most prevalent in the cases where a supraglottic device was used. However, the correlation between the morphology of the artefact and the airway type deserves further investigation. From our experience, we hypothesize that in addition to the airway type, other factors should be explored, such as rescuer's chest compression technique, capnography technology, or even patient condition could have a role in the artefact generation.

Automated ventilation detection is negatively affected by the presence of chest compression artefact on OHCA capnograms. Consequently, real time monitoring of ventilation rate as well as over-ventilation with feedback to rescuers, could become unreliable in these instances. Whether the artefact will appear during chest compressions is unknown. Using the suppression algorithm to continuously process the acquired capnogram could be a reasonable approach to enhance capnography waveform.

Different approaches have been designed to mitigate this problem: sophisticated ventilation detection methods based on the extraction of several features from the capnogram [25], or filtering methods to

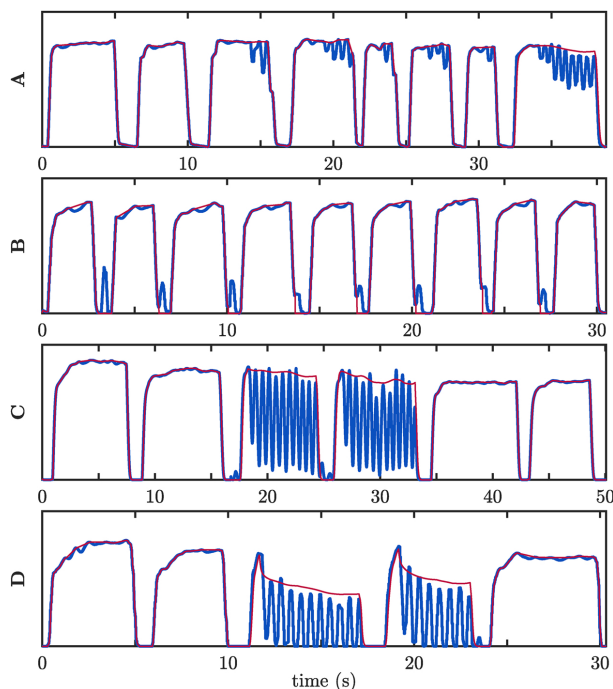


Fig. 3. Examples of method performance. The raw capnogram (in blue) and the resulting waveform (in red) for: A: type I, B: type II, C, D: type III).

remove the oscillations from the capnogram [15]. Classic low pass filtering, with either fixed or adaptive schemas, improved ventilation detection accuracy considerably and was suitable to operate in real time. However, these methods present an important limitation. In the intervals where the artefact appeared, filtered capnogram represents the average of the original CO_2 concentration, as shown in the middle panel of Fig. 1. This averaged waveform does not accurately represent the CO_2 concentration, limiting the application of filtering to a pre-processing stage of the automated ventilation algorithm. In other words, filtered waveform capnography is not suitable for visual analysis so it would not be appropriate to show this signal on the monitor-defibrillator screen.

The presence of oscillations superimposed on capnograms during CPR may impede the correct assessment of clinically relevant information, e.g. visual tracking of ventilation instances or more importantly, analysis of the evolution of ETCO_2 values during the resuscitation attempt. In this study, we proposed an artefact suppression method which tries to preserve the waveform capnography. We demonstrated that the resulting corrected waveform is useful to improve automated assessment of ventilation occurrences, real-time estimation of ventilation rate, and detection of excessive ventilation rates, particularly in the presence of artefact spanning from the plateau to the baseline (type III). Our results were comparable and even slightly better than those obtained using linear filtering [15]. The term “preserve” refers to the extraction of a capnogram useful for clinical interpretation. We visually analysed capnogram segments showing adjacent non-distorted and distorted ventilations (Fig. 3). In the majority of the cases, the envelope of the distorted capnogram resembles the CO_2 tracing observed in the preceding and following undistorted respiratory cycles (Fig. 3, examples A, B, and C). Only in a few cases, the envelope does

not follow the pattern of adjacent non-distorted ventilations, as in the example shown in Fig. 3, panel D.

Limitations of the study

Our study presented some limitations. First, data came from a single monitor-defibrillator model and a single capnograph model, which could limit the generalizability of the results. In addition, we did not have access to patient data associated to the monitor-defibrillation files. On the other hand, lack of knowledge about the origin of the artefact and factors that may cause its appearance could limit the clinical impact of the study.

We have not found any publications analysing how chest compressions artefact affects ETCO_2 measurement performed by capnographs. We were also limited in this regard; our recordings contained the waveform capnography but not the ETCO_2 values measured by the capnograph and their corresponding time line, so we could not statistically quantify the improvement after implementing our method. Clinical utility of envelope extraction from distorted capnograms deserves further investigation and discussion.

Conclusions

Automated ventilation detection, estimation of ventilation rate and detection of excessive ventilation rates based on waveform capnography improved after chest compression artefact suppression. Moreover, the algorithm enhances the capnogram tracing, potentially favouring its interpretation during CPR. Further prospective research in clinical settings is needed to understand the feasibility and utility of the method.

Conflict of interest

The authors declare no conflicts of interest.

Acknowledgements

This work received financial support from the Basque Government (Basque Country, Spain) through the project IT1087-16 and the pre-doctoral research grant PRE-2017-2-0201. The authors thank the TVF&R Emergency Medical Services providers for collecting the data used in this study.

Appendix A. Supplementary data

Supplementary data associated with this article can be found, in the online version, at <https://doi.org/10.1016/j.resuscitation.2018.09.024>.

References

- [1] Nichol G, Baker D. The epidemiology of sudden death. In: Paradir NA, Halperin HR, Kern KB, Wenzel V, Chamberlain D, editors. *Cardiac arrest: science and practice of resuscitation medicine*. Cambridge: Cambridge University Press; 2007. p. 26–50.
- [2] Soar J, Nolan JP, Böttiger BW, et al. European Resuscitation Council guidelines for resuscitation 2015. Section 3. Adult advanced life support. *Resuscitation* 2015;95:100–47.
- [3] Link MS, Berkow LC, Kudenchuk PJ, et al. 2015 American Heart Association Guidelines Update for Cardiopulmonary Resuscitation and Emergency Cardiovascular Care. Part 7: adult advanced cardiovascular life support. *Circulation* 2015;132(18 Suppl 2):S444–64.
- [4] Gravenstein JS, Jaffe MB, Gravenstein N, Paulus DA. *Capnography*. Cambridge University Press; 2011.
- [5] Pantazopoulos C, Xanthos T, Pantazopoulos I, Papalois A, Kouskouni E, Iacovidou N. A review of carbon dioxide monitoring during adult cardiopulmonary resuscitation. *Heart Lung Circ* 2015;24(11):1053–61.
- [6] Qvigstad E, Kramer-Johansen J, Tømte Ø, et al. Clinical pilot study of different hand positions during manual chest compressions monitored with capnography. *Resuscitation* 2013;84(9):1203–7.
- [7] Meaney PA, Bobrow BJ, Mancini ME, et al. Cardiopulmonary resuscitation quality: improving cardiac resuscitation outcomes both inside and outside the hospital: a consensus statement from the American Heart Association. *Circulation* 2013;128(4):417–35.
- [8] Pokorná M, Nečas E, Kratochvíl J, Skřipický R, Andrlík M, Franěk O. A sudden increase in partial pressure end-tidal carbon dioxide (PETCO₂) at the moment of return of spontaneous circulation. *J Emerg Med* 2010;38(5):614–21.
- [9] Touma O, Davies M. The prognostic value of end tidal carbon dioxide during cardiac arrest: a systematic review. *Resuscitation* 2013;84(11):1470–9.
- [10] Kodali BS, Urman RD, et al. Capnography during cardiopulmonary resuscitation: current evidence and future directions. *J Emerg Trauma Shock* 2014;7(4):332–40.
- [11] Idris AH, Daya M, Owens P, et al. High incidence of chest compression oscillations associated with capnography during out-of-hospital cardiopulmonary resuscitation. *Circulation* 2010;122:A83.
- [12] Vanwulpen M, Wolfskeil M, Duchatelet C, Monsieurs K, Idrissi SH. Quantifying inspiratory volumes generated by manual chest compressions during resuscitation in the prehospital setting. *Resuscitation* 2017;118:e18.
- [13] Deakin CD, O'Neill JF, Tabor T. Does compression-only cardiopulmonary resuscitation generate adequate passive ventilation during cardiac arrest? *Resuscitation* 2007;75(1):53–9.
- [14] Leturiondo M, Ruiz de Gauna S, Ruiz JM, et al. Influence of chest compression artefact on capnogram-based ventilation detection during out-of-hospital cardiopulmonary resuscitation. *Resuscitation* 2018;124:63–8.
- [15] Gutierrez JJ, Leturiondo M, Ruiz de Gauna S, et al. Enhancing ventilation detection during cardiopulmonary resuscitation by filtering chest compression artifact from the capnography waveform. *PLOS ONE* 2018;13(8):e0201565.
- [16] Pellis T, Biserà J, Tang W, Weil MH. Expanding automatic external defibrillators to include automated detection of cardiac, respiratory, and cardiorespiratory arrest. *Crit Care Med* 2002;30(4):S176–8.
- [17] Losert H, Risdal M, Sterz F, et al. Thoracic impedance changes measured via defibrillator pads can monitor ventilation in critically ill patients and during cardiopulmonary resuscitation. *Crit Care Med* 2006;34(9):2399–405.
- [18] Risdal M, Aase SO, Stavland M, Eftestøl T. Impedance-based ventilation detection during cardiopulmonary resuscitation. *IEEE Trans Biomed Eng* 2007;54(12):2237–45.
- [19] Aase SO, Eftestøl T, Husoy J, Sunde K, Steen PA. CPR artifact removal from human ECG using optimal multichannel filtering. *IEEE Trans Biomed Eng* 2000;47(11):1440–9.
- [20] Eilevstjønn J, Eftestøl T, Aase SO, Myklebust H, Husøy JH, Steen PA. Feasibility of shock advice analysis during CPR through removal of CPR artefacts from the human ECG. *Resuscitation* 2004;61(2):131–41.
- [21] Irusta U, Ruiz J, Ruiz de Gauna S, Eftestøl T, Kramer-Johansen J. A least mean-square filter for the estimation of the cardiopulmonary resuscitation artifact based on the frequency of the compressions. *IEEE Trans Biomed Eng* 2009;56(4):1052–62.
- [22] Gong Y, Chen B, Li Y. A review of the performance of artifact filtering algorithms for cardiopulmonary resuscitation. *J Healthc Eng* 2013;4(2):185–202.
- [23] Ruiz de Gauna S, Irusta U, Ruiz J, Ayala U, Aramendi E, Eftestøl T. Rhythm analysis during cardiopulmonary resuscitation: past, present, and future. *BioMed Res Int* 2014;2014.
- [24] Edelson DP, Eilevstjønn J, Weidman EK, Retzer E, Hoek TLV, Abella BS. Capnography and chest-wall impedance algorithms for ventilation detection during cardiopulmonary resuscitation. *Resuscitation* 2010;81(3):317–22.
- [25] Aramendi E, Elola A, Alonso E, et al. Feasibility of the capnogram to monitor ventilation rate during cardiopulmonary resuscitation. *Resuscitation* 2017;110:162–8.

Supplementary materials

Chest compression artefact suppression method

The algorithm for chest compression artefact suppression was designed based on the assumption of that the envelope of the capnogram could be a reliable tracing for clinical interpretation. An example of the method's performance is given in [Figure 1](#). A segment of a distorted capnogram is depicted in the top panel. The capnogram obtained after applying the algorithm is represented in the bottom panel.

Due to variability in the morphology of the artefact and its location, the algorithm distinguishes between low and high CO₂ concentration intervals to determine how to extract the envelope of the capnogram. The algorithm operates in real-time with one second buffered delay to process the waveform. During this second, local maxima in the plateau phase are located in the capnogram. Then, a smoothing filter is applied to restore the upper envelope of the capnogram ([Figure 1](#), bottom panel, bold red line). Similarly, local minima are located in the baseline to extract the lower envelope ([Figure 1](#), bottom panel, dotted red line).

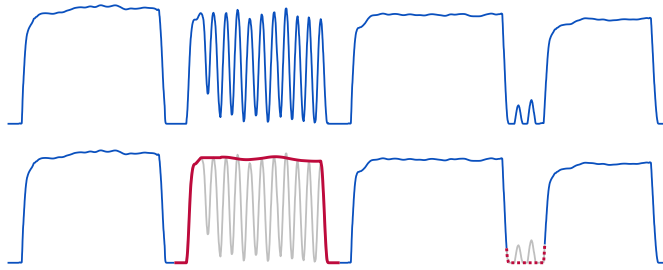


Figure 1: **Graphical example of the suppression of chest compression artefact.** A distorted capnogram is depicted at the top. The bottom panel illustrates how the envelope of the capnogram is extracted by detecting the local maxima of the original capnogram in the plateau and the local minima in the baseline.

Feature computation

The detailed operation of the suppression algorithm is described through [Figure 2](#). The algorithm applies two amplitude thresholds, Th_{lo} and Th_{hi} , to distinguish low and high CO₂ concentration intervals, respectively. In the figure, areas of high CO₂ concentration are shadowed in grey. For each capnogram cycle both thresholds are updated according to a percentage of the last CO₂ value in the high concentration interval (red diamond). The algorithm then computes the duration of each CO₂ concentration interval, D_{lo} and D_{hi} .

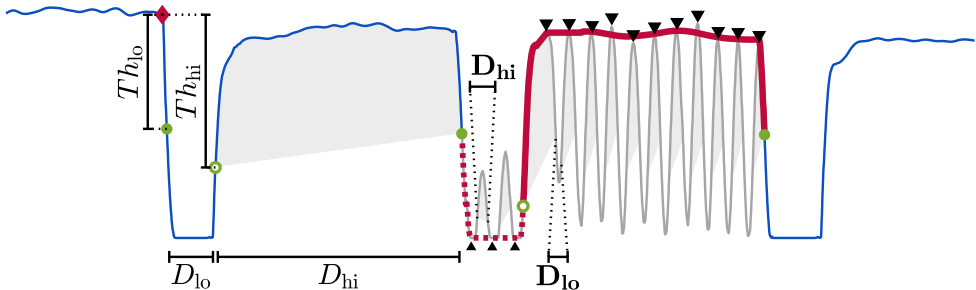


Figure 2: **Example of feature computation.** Th_{lo} and Th_{hi} separate low and high CO₂ concentration intervals. D_{lo} and D_{hi} are the computed durations of low and high (grey areas) CO₂ concentration phases, respectively.

The algorithm operates differently depending on whether a high or a low CO₂ concentration interval is being analysed:

- **During low CO₂ concentration intervals**, the algorithm uses D_{hi} feature to detect the presence of chest compression oscillations. Oscillations are detected when D_{hi} value (see bold \mathbf{D}_{hi} in Figure 2) is less than or equal to an established threshold. In that case, the algorithm extracts the lower envelope (dotted red line) after locating each local minimum (see upward arrowheads).
- **During high CO₂ concentration intervals**, the algorithm works in the same way, but uses D_{lo} to detect the presence of chest compression oscillations. Oscillations are detected if D_{lo} value (see bold \mathbf{D}_{lo} in Figure 2) is less than or equal to an established threshold. In that case, it calculates the upper envelope (bold red line) of the capnogram extracting each local maximum (see downward arrowheads). Additionally, a sliding window average filter is applied to obtain a smooth upper envelope tracing.

Open-loop Adaptive Filtering for Suppressing Chest Compression Oscillations in the Capnogram During Cardiopulmonary Resuscitation

Mikel Leturiondo¹, Jesús Ruiz¹, J.J. Gutiérrez¹, Luis A Leturiondo¹, James K Russell², Mohamud Daya²

¹University of the Basque Country (UPV/EHU), Bilbao, Spain

²Oregon Health & Science University (OHSU), Portland OR, USA

Abstract

Capnography is often used for the guidance on ventilation rate during cardiopulmonary resuscitation (CPR). However, capnogram waveform frequently presents oscillations induced by chest compressions (CC), affecting the reliability of ventilation detection. The aim of the work was to evaluate the performance of an open-loop adaptive filter in the cancellation of CC oscillations in the capnogram during CPR. For that purpose, we analyzed 60 episodes from an out-of-hospital (OOH) cardiac arrest registry maintained by TVF&R agency (USA). In 50% of the episodes the capnogram was corrupted by CC oscillations. The goodness of the filtering scheme was assessed by comparing the sensitivity (Se) and the positive predictive value (PPV) of an automated ventilation detector before and after filtering. A fixed-coefficient low-pass filter was also designed for comparison. The results showed that both filters reported a good performance although the adaptive scheme presented a slightly higher PPV (+1.2 points globally). The simpler fixed-coefficient scheme avoids the reference signal, but requires validation with larger datasets to ensure stability.

1. Introduction

Current resuscitation guidelines recommend high quality chest compressions (CC) and ventilations during cardiopulmonary resuscitation, in order to increase survival from out-of-hospital (OOH) cardiac arrest [1]. However, the optimal application of the CPR procedure is not easy for both laypeople and well-trained rescuers [2]. Consequently, different indicators of CPR quality during the intervention are used for this purpose.

Capnography is a non-invasive indicator of the concentration of carbon dioxide in the respiratory gases. Monitoring capnography during CPR is widely used for monitoring ventilation rate in order to prevent unintentional hyperventilation [3]. A clean capnogram is fundamental for a reliable visual analysis of the patient

response (Fig. 1A). Unfortunately, different artefacts can frequently be observed in the capnogram during CPR. One of them is induced by CC, and appears superimposed on the capnogram as oscillations at the rate of the compressions and with varying amplitude (Fig. 1B,C). The CC artefact complicates the analysis of the capnogram, compromising the accurate detection of ventilations [4].

This work evaluates the performance of an open-loop adaptive filtering strategy for the cancellation of CC oscillations in the capnogram during CPR. For this purpose, we used a large dataset of OOH cardiac arrest episodes and selected those that were corrupted by CC oscillations. We designed an adaptive stop-band filter to suppress the oscillations from the capnogram. We assessed the performance of the filtering scheme by comparing the sensitivity (Se) and the positive predictive value (PPV) of an automated ventilation detector before and after filtering.

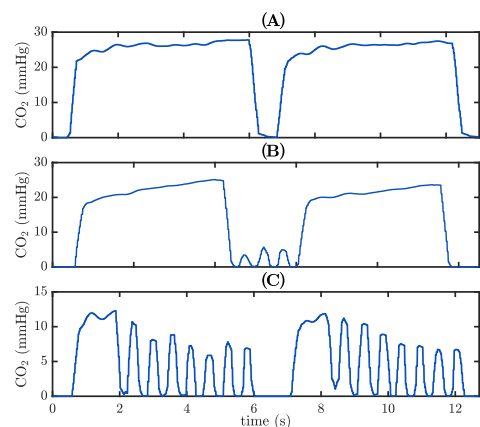


Figure 1. OOH capnograms. A) Clean capnogram B) Corrupted capnogram, with oscillations from CC appearing in the baseline. C) Corrupted capnogram with CC artefact spanning from the plateau to the baseline.

2. Materials and methods

2.1. Database description and annotation

The dataset consisted of a 60 episodes from a large OHCA registry collected between 2011 and 2016 by Tualatin Valley Fire & Rescue (TVF&R), an advanced life support first response Emergency Medical Services (EMS) agency in Oregon (USA). Episodes were recorded using Heartstart MRx monitor-defibrillators (Philips Medical Systems, Andover, MA, USA) equipped with real-time CPR feedback technology (QCPR, Laerdal Medical, Norway). Capnography was acquired using sidestream technology (Microstream, Oridion Systems Ltd, Israel). The signals used in the study were the capnogram, the compression depth (CD) signal from the QCPR system, and the transthoracic impedance (TI) signal acquired from the defibrillation pads.

We annotated a capnogram as corrupted if evident CC oscillations appeared during more than 1 min of CC time. Half of the 60 episodes were corrupted by the CC oscillations. Clean and corrupted capnograms were randomly allocated into a training set (30 episodes, 15 clean + 15 corrupted) and a test set (30 episodes, 15 clean + 15 corrupted).

Ventilations and CC instances were annotated in all the episodes. Figure 2 shows an example of the annotation process. Ventilations were manually annotated using the TI signal which was low-pass filtered in order to suppress CC oscillations (Fig. 2 middle panel, filtered TI depicted in blue, raw TI in grey). Ventilations were annotated in the position associated to the inspiration onset (vertical lines) corresponding to a rise in the TI. CC instances were annotated in every relative maxima of the CD signal (Fig. 2, top panel, red dots) corresponding to the maximum depth reached at each CC.

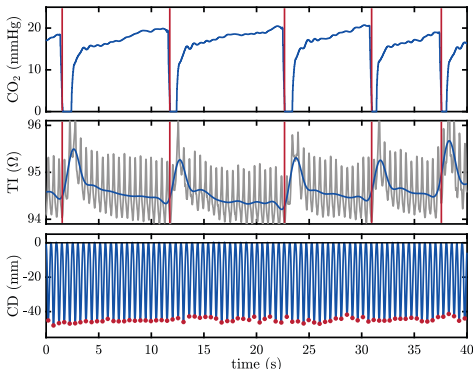


Figure 2. Example of ventilation and CC instance annotation.

2.2. Ventilation detector

The ventilation detection algorithm processes the capnogram and is based on a finite-state-machine model. The capnogram consists of a short inspiration time (low values of CO_2 pressure) and a longer expiration time (high CO_2 values). The aim of the detector to identify the instants corresponding to CO_2 downstrokes and upstrokes.

The algorithm first distinguishes inspiration from expiration identifying potential ventilations. These candidates are characterized by their duration (D_{in} , D_{ex}) and classified as ventilation or non-ventilation, following a decision system based on thresholds (Figure 3). The algorithm is fully described in reference [4].

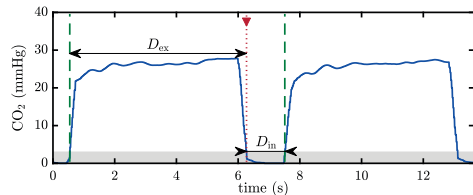


Figure 3. Graphical definition of the detector parameters.

2.2. Filtering strategies

2.2.1 Open-loop adaptive filter

The suppression of the oscillations induced by the CC on the capnogram was based on an open-loop adaptive filter. According to Figure 4, the open-loop adaptive filter is based on the application of the information obtained from a reference input signal to the adjustment of the settings of the filter. In this kind of systems there is no feedback from the output [5].

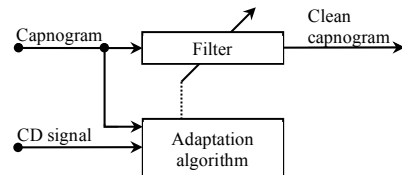


Figure 4. Open-loop adaptive filter diagram.

The open-loop adaptive filtering strategy was designed as a Butterworth band-stop filter, continuously tuned to the average CC rate in 2-s analysis windows. The design parameters were: the order, N_{ol} and the 3dB bandwidth, B_{ol} of the filter, as well as the central frequency of the stop band, f_0 . The frequency f_0 was obtained from the annotations of the CC instances on the CD signal (Figure 5). The parameter f_0 was calculated as the average CC rate

during 2s-intervals. If the 2s-interval contained less than 3 CC, f_0 was the same as the one used in the previous interval.

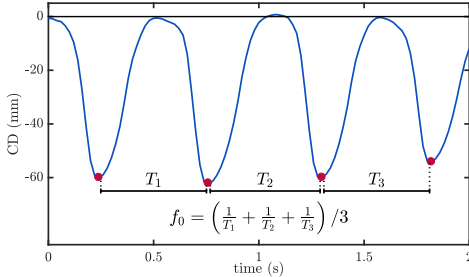


Figure 5. Calculation of parameter f_0 .

The order and the bandwidth of the adaptive filter optimized with the training set, selecting finally $N_{ol} = 2$ and $B_{ol} = 1\text{Hz}$, respectively.

2.2.2 Fixed-coefficient filter

We also used a fixed-coefficient low-pass Butterworth filter for comparison. The design parameters were the order, N_{fc} and the 3dB cut-off frequency of the filter, f_{fc} . After analyzing the spectral characteristics of different capnograms and CD signals, the final values of both parameters were optimized with the training set.

2.3. Performance evaluation

The goodness of the filtering strategy was assessed by comparing the sensitivity (Se) and the positive predictive value (PPV) of the ventilation detector, before and after filtering. Se was defined as the percentage of annotated ventilations that were correctly detected. PPV was defined as the percentage of detected ventilations that were correct. The maximum admissible tolerance for the position of the detection and the annotation was 500ms. We provide separate results for clean and corrupted subsets.

We optimized the adaptive filter parameters (N_{ol} , B_{ol}) and the fixed-coefficient filter parameter (N_{fc} , f_{fc}) with the training set to maximize Se while maintaining PPV above 92%.

3. Results

The order and the bandwidth of the adaptive filter were optimized to $N_{ol} = 2$ and $B_{ol} = 1\text{Hz}$, respectively. Similarly, the order and the bandwidth of the fixed-coefficient filter were $N_{fc} = 8$ and $f_{fc} = 1.5\text{Hz}$.

Table 1 summarizes Se and PPV results for the test set, comprising 7195 ventilations. Globally, Se and PPV before filtering were 93.0% and 92.2%, respectively. In case of

the fixed-coefficient filter, Se and PPV increased to 97.7% and 94.8%, respectively. The increments were similar in case of the open-loop adaptive filter, with a Se of 97.7% and a PPV of 95.3%.

For the clean set (3905 ventilations), the results stayed stable: Se and PPV were close to 99%, before and after filtering, for both filtering strategies. However, for the corrupted subset (3290) Se and PPV were low: 84.8% and 84.0%, respectively, before filtering. After applying the fixed-coefficient filter, Se increased to 95.4% and PPV to 90.3%. Applying the open-loop filter the increment of the values of Se and PPV are similar to those ones obtained with the fixed coefficient filter (95.6/91.5%, respectively),

Table 1. Se and PPV for the test set, before filtering and after fixed-coefficient (FC) and Open-loop (OL) adaptive filtering.

	Before (Se/PPV)	FC (Se/PPV)	OL (Se/PPV)
Whole set	93.0/92.2	97.7/94.8	97.7/95.3
Clean	99.8/99.1	99.6/98.7	99.5/98.7
Corrupted	84.8/84.0	95.4/90.3	95.6/91.5

Figure 6 shows the boxplots of Se and PPV values before and after filtering with both strategies. For both filters, the dispersion of Se and PPV was very low before as well as after filtering, in case of the clean episodes. However, the dispersion of both parameters was quite relevant for corrupted episodes before filtering.

The results demonstrate that filtering the capnogram in case of clean episodes maintains good results of Se and PPV, and improve them in presence of artefact.

4. Conclusions

The current resuscitation guidelines for advanced life support recommend the use of the capnogram during CPR. The presence of high-frequency oscillations in the capnogram during CC may difficult the interpretation of the signal.

The work presents two filtering techniques to suppress the oscillations induced during CC: a simple fixed-coefficients filter and an open-loop adaptive filter.

The results demonstrate that the filtering of the capnogram provides a larger reliability in the automated detection of ventilations. The global results obtained for the complete test set, where clean and corrupted episodes were analyzed, are quite similar for both techniques. The improvement is specifically relevant in the presence of the artefact induced by CC. In this case, the open-loop adaptive strategy provides better results, with a better balance between the sensitivity and the positive predictive value. For the clean subset, the results stay stable before and after filtering.

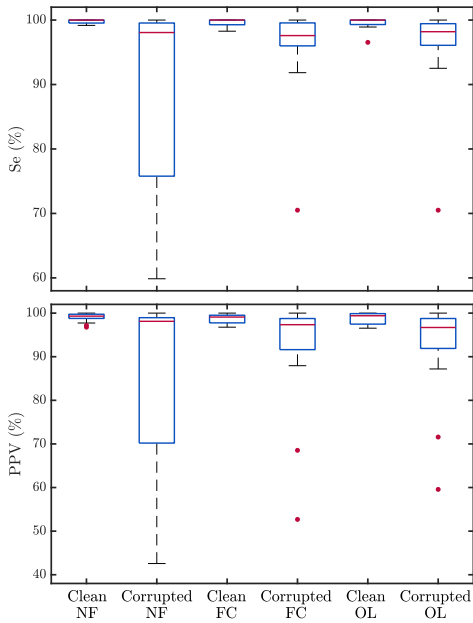


Figure 6. Se and PPV for the test set before filtering (NF, left), after fixed-coefficient filtering (FC, middle) and after closed-loop adaptive filtering (CL, right). Boxes show the median and IQR. Outliers are represented by dots

Acknowledgements

This work received financial support from the Basque Government (Basque Country, Spain) through the project IT1087-16 and the predoctoral research grant PRE-2016-1-0104. The authors thank the TVF&R EMS providers for collecting and maintaining the data used in this study.

References

- [1] Soar J, Nolan JP, Böttiger BW, et al. European Resuscitation Council guidelines for resuscitation 2015. Section 3. Adult advanced life support. *Resuscitation* 2015;95:100-147.
- [2] Wik L, Kramer-Johansen J, Myklebust H, et al. Quality of cardiopulmonary resuscitation during out-of-hospital cardiac arrest. *JAMA* 2005;293:299-304.
- [3] Maertens VL, De Smedt LE, Lemoyne S, et al. Patients with cardiac arrest are ventilated two times faster than guidelines recommend: an observational prehospital study using tracheal pressure measurement. *Resuscitation* 2013; 84(7):921-926.
- [4] Leturiondo M, Ruiz J, Ruiz de Gauna S, González-Otero DM, Bastida JM, Daya M. A simple algorithm for ventilation detection in the capnography signal during cardiopulmonary resuscitation. *Computing in Cardiology* 2017. In press.
- [5] Widrow B, Stearns D. Adaptive signal processing. Prentice Hall. 1985.

Address for correspondence.

Mikel Leturiondo Sota
mikel.leturiondo@ehu.eus
 School of Engineering
 Alameda Urquijo s/n, 48013-Bilbao (Spain)

Closed-loop Adaptive Filtering for Suppressing Chest Compression Oscillations in the Capnogram During Cardiopulmonary Resuscitation

Mikel Leturiondo¹, J.J. Gutierrez¹, Sofia Ruiz de Gauna¹, Sandra Plaza¹, José F Veintemillas², Mohamud Daya³

¹University of the Basque Country (UPV/EHU), Bilbao, Spain

²Emergentziak Osakidetza (Basque Health Service), Basque Country, Spain

³Oregon Health & Science University (OHSU), Portland OR, USA

Abstract

Capnography is widely used by the advanced-life-support during cardiopulmonary resuscitation (CPR). Continuous analysis of the capnogram allows guidance of adequate ventilation rate, currently 10 breaths/min for intubated patients. We used 60 out-of-hospital cardiac arrest episodes containing both clean and CC corrupted capnograms. Chest compressions (CC) induce high-frequency oscillations in the capnography waveform impeding reliable detection of ventilations. Thus, a clean capnogram is essential for a better ventilation detection performance. To clean the capnogram, an adaptive noise cancellation notch filter was designed using a Least Mean Square algorithm to minimize filtering error. A fixed-coefficient low-pass filter was optimized for comparison. For the whole test set, global Se/PPV improved from 93.0/92.2% to 97.6/96.2% after adaptive filtering and to 97.7/94.8% after fixed-coefficient filtering. For the clean subset, Se/PPV maintained stable and for the corrupted subset, Se/PPV improved from 84.8/84.0% to 95.2/92.7% and 95.4/90.3%, respectively. Filtering allowed reliable automated detection of ventilations in the capnogram even in the presence of CC oscillations during CPR. Nevertheless, further evaluation of these techniques in large datasets is warranted.

1. Introduction

Cardiac arrest is one of the main causes of death in developed countries. Patient survival to cardiac arrest is related to several factors. The most important is the early start of cardiopulmonary resuscitation (CPR) which combines chest compressions and ventilations. Hyperventilation is common during CPR for both in-hospital and out-of-hospital cardiac arrests even among highly trained rescuers. Although resuscitation guidelines recommend providing 10 breaths per minute to intubated

patients, some clinical studies have documented ventilation rates over 30 breaths per minute [1], which have been shown to impair hemodynamics and worsen outcomes at cardiac arrest.

The latest resuscitation guidelines recommend the use of capnography waveform to monitor ventilation rate during CPR [2]. A clean capnogram is essential for a reliable analysis of patient response (Figure 1a). However, chest compressions (CC) administered to the patient frequently induce high-frequency oscillations (Figure 1b,c,d) in the capnogram [3] impeding reliable detection of ventilations [4].

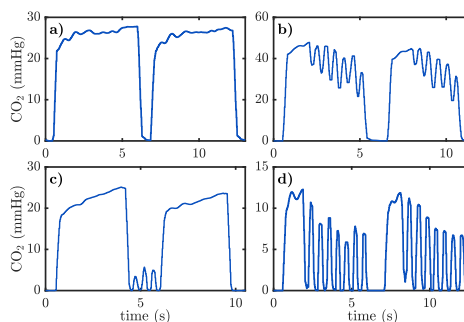


Figure 1. OHCA capnogram segments. a) Clean capnograms; b,c,d) Corrupted capnograms with CC oscillations in the plateau, baseline and form the plateau to the baseline, respectively.

In this context, the present paper describes the observational study performed to assess the performance of an adaptive closed-loop filter for suppressing CC oscillations in the capnogram during CPR. For this aim, we used a previously recorded out-of-hospital cardiac arrest (OHCA) registry.

2. Materials and methods

2.1. Database description and annotation

The dataset analysed in this study was a subset (60 episodes) of a large OHCA registry collected and maintained by Tualatin Valley Fire & Rescue (TVF&R), an advanced life support first response Emergency Medical Services (EMS) agency in Oregon (USA). Episodes were recorded using Heartstart MRx monitor-defibrillators (Philips Medical Systems, Andover, MA, USA), equipped with a real-time CPR feedback system (Q CPR, Laerdal Medical, Norway). Three concurrent signals were extracted: the transthoracic impedance (TI) signal, the compression depth (CD) signal and the capnogram.

For each episode, capnograms were time-shifted to compensate delay with respect CD and TI signals. A capnogram was classified as corrupted if evident CC oscillations appeared during more than 1 min of CC time.

Ventilation and CC instances were also annotated using the TI and the CD signal as the reference, respectively. TI signal was low-pass filtered (2nd-order Butterworth, cut-off frequency of 0.6 Hz) to remove oscillations caused by CC. Thus, slow oscillations caused by ventilations could be better observed in the filtered TI. Figure 2 depicts an example of the annotation process. Ventilations were annotated in the position associated to the inspiration onset (Figure 2, vertical lines) corresponding to a rise in the TI. CC instances were annotated in every relative maxima (Figure 2, red dots) corresponding to the maximum depth reached for each chest compression.

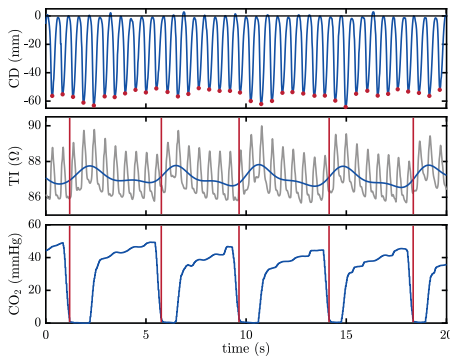


Figure 2. Example of ventilation and CC instance annotation.

Resulting ventilation annotations were our gold-standard to test the reliability of the ventilation detection algorithm. Meanwhile, CC instances were used to control the configuration of the adaptive closed-loop filter. Clean and corrupted capnograms were randomly and equally split into a training and a test set.

2.2. Closed-loop adaptive filtering

Quality of the recorded capnogram is essential for a reliable analysis. However, a clean capnogram, where the different phases of the respiratory cycle are identifiable cannot always be observed during CPR [4,5]. Sometimes ongoing resuscitation efforts induce fast sinusoidal oscillations at different rates and with varying amplitude superimposed on the capnogram. The most common way to suppress this kind of artefact consist of using a *notch* filter. Nevertheless, in this study an adaptive noise cancellation notch filter is proposed, adjusting the filter to the same frequency and phase of the artefact [6]. A *Least Mean Square* (LMS) algorithm has been used. The main objective of this algorithm is to minimize the error sequence power ($e[n]$) produced between the filter response ($y[n]$) and the desired response ($d[n]$).

The LMS filter, shown in Figure 3, is based on estimations, so it achieves an error power $J(\infty)$ higher than the minimum error power (J_{min}) reached by the Wiener solution. In order to control the coefficient correction applied from a previous iteration to the next one, the LMS algorithm uses a parameter called step size (μ). When μ is high, the adjustment is fairly fast, but the difference between the final error power $J(\infty)$ and the minimum value (J_{min}) is higher than with lower μ values.

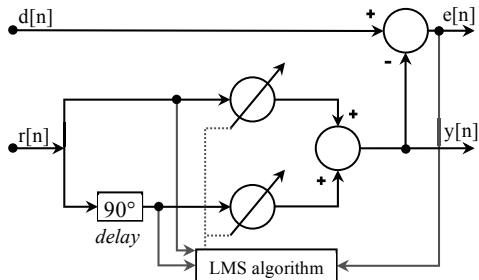


Figure 3. Adaptive noise cancellation LMS filter diagram.

Following the diagram depicted in Figure 3, the main input, $d[n]$, is the capnography signal with induced CC oscillations, while the reference input, $r[n]$, is a pure cosine $C \cdot \cos(\omega_0 n + \theta)$, where $\omega_0 = 2\pi f_0 / f_s$ and f_0 is the instant frequency of the CC. When CC are provided, the cosine amplitude C is '1', and '0' otherwise.

The output of the adaptive filter, $y[n]$ is an estimation of the artefact and the output of the noise cancellation system, $e[n]$, represents the capnography signal without induced CC oscillations. Using $e[n]$ and the reference signals the LMS algorithm adjusts the impulse response of the filter used in the next iteration.

The transference function (1) of this filter demonstrates that the noise cancellation system has the same properties

of a *notch* filter designed to suppress ω_0 . The unique design parameter of this adaptive filter is the 3dB bandwidth (2).

$$H(z) = \frac{z^2 - 2z \cos \omega_0 + 1}{z^2 - 2(1 - \mu C^2)z \cos \omega_0 + 1 - 2\mu C^2} \quad (1)$$

$$BW_{3dB} = 2\mu C^2 \text{ (rad)} = \frac{\mu C^2}{\pi T} \text{ (Hz)} \quad (2)$$

2.3. Performance evaluation

We evaluated the performance of the adaptive filter in terms of its sensitivity (Se) and its positive predictive value (PPV) given by the ventilation detection algorithm and the gold-standard. Se was defined as the percentage of annotated ventilations that were correctly detected. PPV was defined as the percentage of detected ventilations that were correct. The maximum admissible tolerance for the position of the ventilation detection and the gold-standard annotation was 500ms.

We optimized the adaptive filter parameter (BW_{3dB}) with the training set to maximize Se while maintaining PPV above 92%. A fixed-coefficient low-pass filter was designed and optimized (8th-order Butterworth, cut-off frequency of 1.5 Hz) for comparison. The 95% confidence intervals (95%CI) were computed for both metrics.

3. Results

Adaptive closed-loop filter optimization was achieved for $BW_{3dB} = 1 \text{ Hz}$. For the training set (8102 ventilations), the Se and PPV were 98.4% (95%CI, 98.0-98.6) and 96.6% (96.2-97.0), respectively.

Table 1 summarizes Se and PPV results for the LMS filter. Table 2 summarizes Se/PPV before filtering and after applying the fixed-coefficient filter. For the whole test set, global Se/PPV improved from 93.0/92.2% to 97.6/96.2% after adaptive filtering and to 97.7/94.8% after fixed-coefficient filtering. For the clean subset, Se/PPV maintained stable (99.8/99.1% before, 99.8/99.1% and 99.6/98.7% after, respectively). For the corrupted subset, Se/PPV improved from 84.8/84.0% to 95.2/92.7% and 95.4/90.3%, respectively.

Figure 4 shows the boxplots of Se and PPV values before and after filtering. For both fixed-coefficient and adaptive closed-loop the dispersion of Se and PPV was very low before as well as after filtering, in case of clean episodes. However, the dispersion of Se and PPV was quite relevant for corrupted episodes before filtering.

Table 1. Se and PPV for the test set after adaptive filtering. n: number of annotated ventilations.

	n	Se (95% CI)	PPV (95% CI)
Whole set	7195	97.6 (97.3-98.0)	96.2 (95.7-96.6)
Clean	3905	99.8 (99.6-99.9)	99.1 (98.8-99.4)
Corrupted	3290	95.2 (94.4-95.8)	92.7 (91.8-93.6)

Table 2. Se and PPV for the test set before filtering (left) and after fixed-coefficient filtering (right).

	Before		Fixed-coefficient	
	Se(%)	PPV(%)	Se (%)	PPV (%)
Whole set	93.0	92.2	97.7	94.8
Clean	99.8	99.1	99.6	98.7
Corrupted	84.8	84.0	95.4	90.3

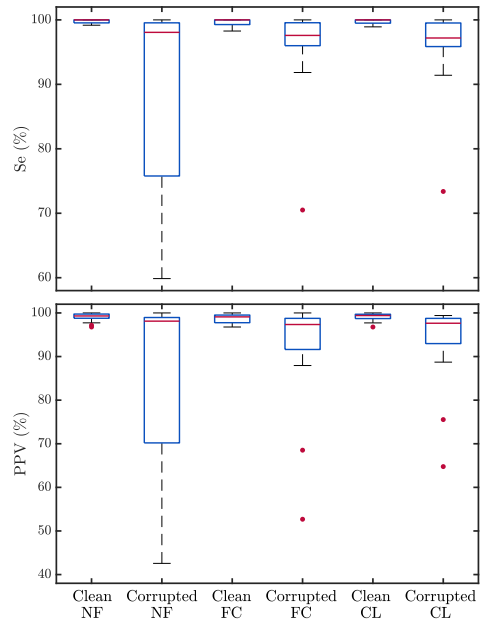


Figure 4. Se and PPV for the test set before filtering (NF, left), after fixed-coefficient filtering (FC, middle) and after closed-loop adaptive filtering (CL, right). Boxes show the median and IQR. Outliers are represented by dots

4. Discussion

According to current resuscitation guidelines for advanced life support, ventilation rate monitoring during CPR is one of the recommended uses of the capnogram. However, the presence of high-frequency oscillations in the capnogram during CC may compromise a reliable detection of ventilations.

Our adaptive noise cancellation filter presented a very good ventilation detection performance. Thus, the results demonstrate that filtering the capnogram in case of clean episodes maintains good results of Se and PPV, and improve them in presence of artefact.

Comparing the results between adaptive and fixed-coefficient filtering, it seems that fixed-coefficient filtering would be enough. Nevertheless, due to CC rate variability, a study with a larger database is needed, while our adaptive filter is CD signal dependent, allowing us to adjust our filter to any kind of CC rate, but this requires using a CPR feedback system providing this signal.

Other studies proposing alternatives for ventilation detection with either the TI signal or the capnogram have also mentioned the signal limitations due to the presence of CC artefact [5]. Although the influence of CC artefact on the reliability of capnogram-based ventilation detection has been demonstrated [4], the suppression of this artefact has not been previously studied.

Our study has been the first to quantitatively characterize and measure the impact of an adaptive CC artefact suppression on OHCA capnograms. Our subsequent hypothesis is that automatic ventilation detection would improve if the capnogram waveform could be successfully restored. Designing new filtering approaches for this aim will be our next step, exploring different alternatives.

Our study has several limitations. First, the annotation of ventilations on the TI was not straightforward during CPR. We discarded some intervals because of unreliable TI signal (noise, disconnections) and filtering was needed to remove the CC artefact. No other reference signal was available as an alternative gold-standard. Finally, data came from a single monitor-defibrillator and so results may not be generalizable. We would need to characterize this further with other monitor-defibrillators.

5. Conclusions

Filtering allowed reliable automated detection of ventilations in the capnogram even in the presence of CC oscillations during CPR. Nevertheless, further evaluation of these techniques in large datasets is warranted given the variability of out-of-hospital CC and ventilation rates.

Acknowledgements

This work received financial support from the Basque Government (Basque Country, Spain) through the project IT1087-16 and the predoctoral research grant PRE-2016-1-0104. The authors thank the TVF&R EMS providers for collecting and maintaining the data used in this study.

References

- [1] Maertens VL, De Smedt LE, Lemoyne S, et al. Patients with cardiac arrest are ventilated two times faster than guidelines recommend: an observational prehospital study using tracheal pressure measurement. *Resuscitation* 2013; 84(7):921-926.
- [2] Soar J, Nolan JP, Böttiger BW, et al. European Resuscitation Council guidelines for resuscitation 2015. Section 3. Adult advanced life support. *Resuscitation* 2015;95:100-147.
- [3] Idris AH, Daya M, Owens P, et al. High incidence of chest compression oscillations associated with capnography during out-of-hospital cardiopulmonary resuscitation. *Circulation* 2010;122:A83.
- [4] Leturiondo M, Ruiz J, Ruiz de Gauna S, González-Otero DM, Bastida JM, Daya M. A simple algorithm for ventilation detection in the capnography signal during cardiopulmonary resuscitation. *Computing in Cardiology* 2017. In press.
- [5] Edelson DP, Eilevstjønn J, Weidman EK, Retzer E, Hoek TLV, Abella BS. Capnography and chest-wall impedance algorithms for ventilation detection during cardiopulmonary resuscitation. *Resuscitation* 2010;243 81(3):317-322.
- [6] Widrow B, Stearns D. Adaptive signal processing. Prentice Hall. 1985.

Address for correspondence.

Mikel Leturiondo Sota
mikel.leturiondo@ehu.eus
 School of Engineering
 Alameda Urquijo s/n, 48013-Bilbao (Spain)

AS023

Incorporating basic life support training into cardiac rehabilitation programs: The CAREBAS project. Analysis of patients' performance

Violeta González Salvado^{1,2}, Cristian Abelairas Gómez^{2,*}, Carmen Neiro Rey¹, Candela Gómez González², Aida Carballo Fazanes², Nuria Álvarez Cebreiro², Cristina Jorge Soto², Antonio Rodríguez Núñez^{3,2}

¹ Cardiology Department, Hospital Clínico Universitario de Santiago de Compostela, Santiago de Compostela, Spain

² Universidade de Santiago de Compostela, Santiago de Compostela, Santiago de Compostela, Spain

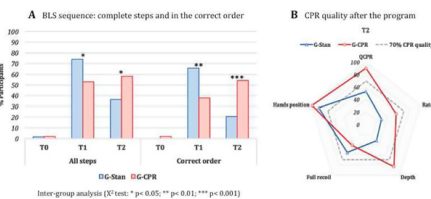
³ Paediatric Emergency and Critical Care Division, Hospital Clínico Universitario de Santiago de Compostela, Santiago de Compostela, Spain

Purpose: To examine the effectiveness of CPR rolling refreshers embedded in a cardiac rehabilitation program at enhancing practical basic life support (BLS) skills and self-efficacy of patients with coronary heart disease.

Methods: 114 patients enrolled on an exercise-based cardiac rehabilitation program were invited to participate. Standard one-time training in BLS (standard group, G-Stan) was compared to CPR hands-on rolling refreshers incorporated into the 2-month exercise program (CPR group, G-CPR). BLS skills and compressions-only CPR quality were assessed at baseline, following brief instruction and after the program on a simulated scenario. Self-efficacy was evaluated using a 10-cm visual analogue scale.

Results: 108 participants (G-Stan:58; G-CPR:50) completed the final evaluation (91.2% male, mean age 53.7 ± 6.4 years) and data from 105 was available for the CPR-quality analysis. BLS sequence performance was equally poor at baseline and improved significantly after instruction. G-CPR showed better retention at 2 months, significantly superior for "checking safety" and "sending for a defibrillator". Low initial CPR quality improved irregularly after instruction in both groups; skill deterioration in G-Stan at 2 months contrasted with further improvement in G-CPR, which achieved superior results regarding % of correct compressions by depth, rate, hands position and global CPR quality, and greater CPR self-efficacy ($p < 0.01$ in all analysis).

Conclusions: Integrating CPR hands-on rolling refreshers into an exercise-based cardiac rehabilitation program is effective at improving patients' BLS skill retention and self-efficacy compared to standard one-time training. Exporting this formula may result in increased numbers of trained citizens, enhanced social awareness and bystander resuscitation.



AS024

Suppression of chest compression artefact to enhance reliability of capnography waveform analysis during cardiopulmonary resuscitation

Mikel Leturiondo^{1,*}, Jose Julio Gutiérrez¹, Sofia Ruiz de Gauna¹, Jesus María Ruiz¹, Luis A. Leturiondo¹, James Knox Russell², Mohamud Daya²

¹ University of the Basque Country, UPV/EHU

² Oregon Health & Science University, OHSU

Introduction: Real-time capnography is an important monitoring tool to guide ventilation rates during cardiopulmonary resuscitation (CPR). However, during CPR capnograms are commonly distorted by chest compressions (CC) [1]. The reliability of automated ventilation detection based on the capnogram decreases in the presence of CC artefact [1].

Purpose of the study: To design a CC artefact suppression technique to improve ventilation detection while preserving CO₂ concentration values produced by ventilations.

Materials and methods: Episodes from an out-of-hospital cardiac arrest (OHCA) registry ($n = 202$) with a mean duration of 30 (± 9.5) min were analysed. Each record comprised concurrent capnogram, compression depth, and transthoracic impedance (TI) signals. The suppression algorithm detects distorted ventilations in the capnography waveform (Fig. 1a). It calculates the upper envelope of the capnogram during the alveolar plateau and extracts the lower envelope during capnogram baseline, obtaining a non-distorted capnogram waveform (Fig. 1b). The algorithm was assessed by comparing the performance of a ventilation detector before and after artefact suppression.

Results: A total of 44,267 ventilations were annotated using the TI signal. Table 1 shows the detector performance for distorted ($n = 83$) and non-distorted episodes. For distorted episodes, sensitivity and positive predictive value (Se/PPV) improved from 91.9/89.5% to 98.0/97.3%. The unsigned error of the estimated ventilation rate for distorted episodes decreased from 6.3% to 3.1%, improving detection of hyperventilation. The algorithm had little effect in non-distorted data.

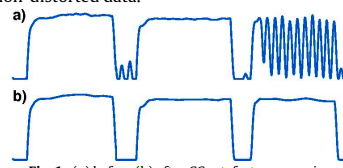


Fig. 1. (a) before (b) after CC artefact suppression.

Table 1

CC artefact suppression method performance.

Record type	n	Before		After	
		Se (%)	PPV (%)	Se (%)	PPV (%)
Non-distorted	119	99.5	99.0	99.0	99.0
Distorted	83	91.9	89.5	98.0	97.3

Conclusions: Ventilation detection during CPR improved after CC artefact suppression. Moreover, the method preserved the capnogram tracing caused by ventilations, enhancing reliability of clinical interpretation of capnography during CPR for OHCA.

Reference

[1] Leturiondo, et al. Resuscitation 2018;124:63–8.

<https://doi.org/10.1016/j.resuscitation.2018.07.337>

A Method to Suppress Chest Compression Artifact Enhancing Capnography-Based Ventilation Guidance During Cardiopulmonary Resuscitation

Mikel Leturiondo¹, JJ Gutiérrez¹, Sofia Ruiz de Gauna¹, Jesus Ruiz¹, Luis A Leturiondo¹, James K Russell², Mohamud Daya²

¹University of the Basque Country (UPV/EHU), Bilbao, Spain

²Oregon Health & Science University (OHSU), Portland OR, USA

Abstract

Capnography-based ventilation rate guidance is valuable and widely used by advanced life support during cardiopulmonary resuscitation (CPR). However, there is a high incidence of induced chest compression (CC) oscillations that decreases the reliability of automated ventilation detection. We used 30 out-of-hospital cardiac arrest episodes containing the capnogram and transthoracic impedance signals. The algorithm detects the presence of distorted ventilations in the capnogram. It calculates the artifact envelope during the alveolar plateau and removes the artifact during capnogram baseline, thus obtaining a non-distorted waveform. The goodness of the method was assessed by comparing the performance of a ventilation detection algorithm before and after artifact suppression. From a total of 6387 annotated ventilations, 34% of them were classified as distorted. Global sensitivity and positive predictive value (Se/PPV, %) improved from 77.9/74.0 to 97.0/95.8. Median value of the unsigned error (%) of the estimated ventilation rate decreased from 19.6 to 4.5 and the accuracy for detection of over-ventilation increased with cleaned capnograms. Capnogram-based ventilation guidance during CPR was enhanced after CC artifact suppression. Our method preserved the tracing of CO₂ concentration caused by ventilations, allowing other clinical uses of the capnography during resuscitation.

1. Introduction

During out-of-hospital cardiac arrest (OHCA) episodes, advanced life support (ALS) treatment usually involves advanced airway placement, high-quality cardiopulmonary resuscitation (CPR) and early defibrillation [1,2].

Guidance on ventilation rate is key during CPR, thus, capnography is widely used by the ALS, but for this purpose, a clinically interpretable waveform where the

different phases of the respiratory cycle must be clearly identifiable. Several studies have reported the appearance of fast oscillations synchronized with provided chest compressions (CCs) superimposed on the capnogram, often completely distorting the normal tracing [3,4].

Filtering approaches have been widely proposed to remove chest compression artifact from the electrocardiogram during CPR [5]. In a recent study, we proposed a few filtering techniques to remove those oscillations from the capnogram [6]. All of them improved the automated detection of ventilations. However, these frequency domain techniques present an important limitation where the artifact appears. Resulting capnogram waveform represents only the average of the original CO₂ concentration. Thus, filtered capnograms are not suitable for clinical analysis.

In this study, we explored an alternative method to suppress chest compression oscillations from the capnography waveform. Our proposal is based on a time domain analysis, and was not only designed to improve ventilation detection, but also to provide a capnogram that resembles the “real” tracing caused by ventilations.

2. Materials and methods

2.1. Database description and annotation

The dataset analyzed in this study was a subset (30 episodes) of highly distorted capnogram waveforms extracted from a large OHCA registry collected by Tualatin Valley Fire & Rescue (TVF&R), an advanced life support (ALS) Emergency Medical Services (EMS) agency, between 2011 and 2016. Episodes were recorded using Heartstart MRx monitor-defibrillators (Philips USA) equipped with real-time CPR feedback (QCPR, Laerdal Medical, Norway) and sidestream capnography (Microstream, Oridion Systems Ltd, Israel) to provide a High-Quality CPR. For each episode, we extracted two

concurrent signals: the transthoracic impedance (TI) signal, acquired from the defibrillation pads and the capnogram, acquired using sidestream technology.

Ventilation annotations from a previous study were used [4]. In that study, episodes with more than 1 min of evident CC artifact were classified as distorted. Distorted episodes were then grouped into type I, type II and type III (highly distorted) artifact categories. Ventilations were annotated using the raw TI signal as reference. TI signal was low-pass filtered to remove oscillations caused by CC. Thus, enhancing slow fluctuations caused by ventilations. All processed TI signals were visually examined to manually annotate the position of each ventilation. Resulting highly distorted episodes and ventilation annotations were used in the present study as our gold standard to prove the reliability of the artifact suppression method. Additionally, in this study we also classified each capnogram cycle (ventilation) as distorted or non-distorted by CC artifact following the pattern shown in Figure 1.

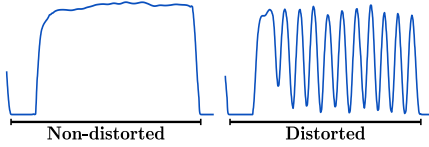


Figure 1. Capnography signal segments.

2.2. Chest compression artifact suppression

Following the hypothesis that the real CO₂ concentration produced by ventilations remains in the envelope of the induced CC artifact, we designed a method that restores the “real” tracing of the capnography waveform. A graphical explanation of the method performance is given in Figure 2, where a segment of a distorted capnogram (blue line) is depicted with the resulting capnogram after applying the method (dotted red line).

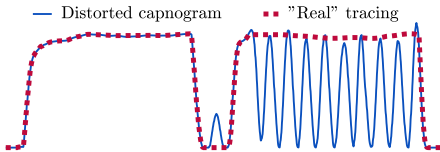


Figure 2. Graphical explanation of the artifact suppression method.

The artifact suppression algorithm operates in real-time, with one second buffered delay, to process, detect and fix the capnography waveform. Due to artifact origin and type variety [4], the suppression method divides its operation into low and high CO₂ concentration intervals. This division helps to determine how to extract the envelope of the capnography waveform.

The functioning of the algorithm can be divided into three main steps:

- **Feature computation:** The algorithm applies two thresholds to distinguish between low CO₂ concentration phase (Figure 3, grey line) and high CO₂ concentration phase (Figure 3, blue line), Th_{lo} and Th_{hi} respectively. This thresholds determine the beginning instances of each interval (t_{lo}^i and t_{hi}^i). For every capnogram fluctuation, both thresholds are updated using the last high CO₂ value (red diamond). Finally, every capnogram fluctuation is characterized by two features:
 - D_{lo} : Low CO₂ interval duration, $D_{lo} = t_{hi}^i - t_{lo}^i$
 - D_{hi} : High CO₂ interval duration, $D_{hi} = t_{lo}^{i+1} - t_{hi}^i$

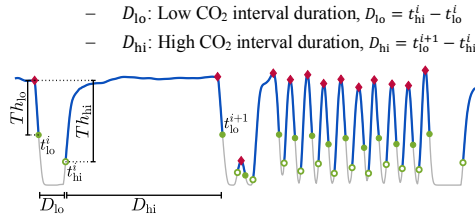


Figure 3. Example of feature computation.

- **Artifact detection and reconstruction:** The operation of the method depends on which interval is analyzing. During a low CO₂ interval, the algorithm analyzes the following CO₂ interval and vice versa, as shown in Figure 4. The algorithm detects the presence of artifact when:
 - During low CO₂ interval (Figure 4, left panel), the following high CO₂ interval duration (D_{hi}) is less than or equal to a high interval duration threshold, Dth_{hi} .
 - During high CO₂ interval (Figure 4, right panel), the following low CO₂ interval duration (D_{lo}) is less than or equal to a low interval duration threshold, Dth_{lo} .

Only in presence of artifact, the algorithm extracts the local minima (upward arrowheads) and local maxima (downward arrowheads) of the oscillations, during low and high intervals respectively. Finally, it connects these points with a linear interpolation obtaining the lower and upper envelopes.

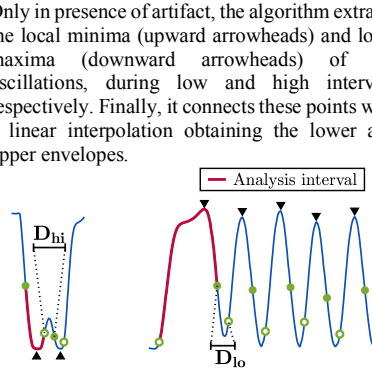


Figure 4. Detection of chest compression oscillations.

- **Envelope smoothing:** Additionally a sliding window average filter (i.e. moving average) is applied only to smooth the upper envelope, as shown in Figure 5.

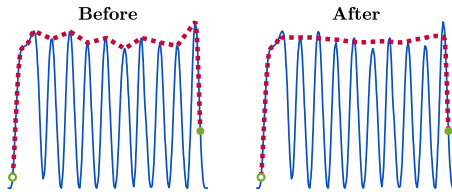


Figure 5. Upper envelope moving average smoothing.

2.3. Performance evaluation

We computed the effectiveness of the artifact suppression method in terms of the sensitivity (Se) and positive predictive value (PPV) of an automated ventilation detection algorithm before and after artifact suppression. Se values were defined as the proportion of correctly detected ventilations among all annotated ventilations. PPV values were defined as the proportion of correctly detected ventilations among all detections.

We also evaluated the performance of the method in the estimation of ventilation rate; we computed, for each episode, the number of ventilations given in the last minute updated every 10s. Ventilation rate measurements obtained before and after applying the artifact suppression method were compared with the measurements computed from the gold standard by calculating the unsigned percent error.

Finally, accuracy in the detection of excessive ventilation rates was also tested. According to the general recommendation in current resuscitation guidelines, ventilation rates above 10min^{-1} during CPR can be considered as excessive [1,2]. In this case, Se was defined as the proportion of annotated alarms that were given by the algorithm, and PPV as the proportion of given alarms that were indeed annotated.

3. Results

From the 30 OHCA episodes that were analyzed, with a mean duration of $34 (\pm 18)$ minutes, a total of 6387 ventilations were annotated, with a mean of $213 (\pm 92)$ ventilations per episode. From these, 4215 (66%) corresponded to non-distorted ventilations and 2172 (34%) to distorted ventilations.

The performance of the automated ventilation detection algorithm was computed before and after applying the suppression method. For the whole set, global Se/PPV improved from 77.9%/74.0% to 97.0%/95.8%. Figure 6A

illustrates the distribution of Se and PPV per episode given by the ventilation detection algorithm. Overall, both medians increased and dispersion in Se and PPV was also reduced. Se/PPV IQR decreased from 20.1%/29.2% to 1.6%/3.8%.

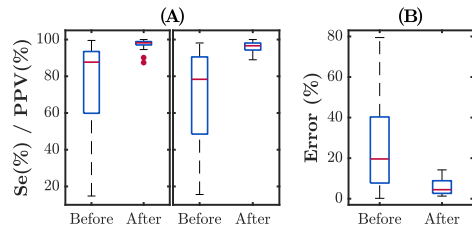


Figure 6. A) Distribution of Se and PPV per episode. B) Distribution of the unsigned error in percentage per episode in the estimation of ventilation rate.

Figure 6B depicts through box plots the distribution of the unsigned error in percentage between the estimation and the gold-standard ventilation rate value. As is the case with Se/PPV, the median error noticeably decreases from 19.6% to 4.5% and the IQR from 32.6% to 6.3%.

The influence of the artifact suppression in the detection of excessive ventilation rates was also computed. Globally, Se/PPV were 95.5%/71.9% before and 98.7%/93.5% after artifact suppression. In this case the improvement was significantly higher for PPV values with a slightly increase in Se. An increase in PPV implied a reduction in false over-ventilation alarms.

Finally, Figure 7 visually illustrates the performance of the method. The raw capnogram is depicted in blue and the resulting artifact suppression waveform in red, superimposed to the raw capnogram.

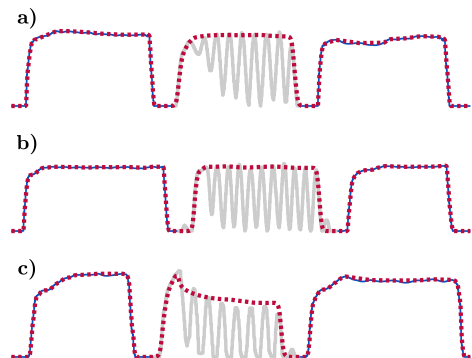


Figure 7. Examples of restored capnograms.

4. Discussion

During OHCA resuscitation episodes a high incidence of induced oscillations has been reported. Induced CC artifact on OHCA capnograms negatively affects the automated detection of ventilations. This means that real time monitoring of ventilation rate could become unreliable in some circumstances. Filtering approaches have been designed to reduce the impact of this problem: classic low pass filtering, with either fixed or adaptive schemas, improved ventilation detection accuracy. However, the resulting capnogram did not accurately represent the “real” tracing caused by ventilations, limiting the application just to improve the automated detection of ventilations.

Visual tracking of ventilation instances and the analysis of the evolution of ETCO₂ values during CPR may be interfered by the presence of induced CC oscillations superimposed on capnograms. In this study, we proposed an artifact suppression method that extracts the envelope of the chest compression oscillations. It has been demonstrated that the resulting artifact suppression output resembles the CO₂ fluctuations caused by ventilations. We also validated the improvement in the automated detection of ventilations, real-time ventilation rate estimation and detection of excessive ventilation rates. Unfortunately, we could not numerically assess the goodness of the resulting capnogram waveform and the error committed. Thus, we visually analyzed capnogram segments showing adjacent distorted and non-distorted ventilations (Figure 5). In most of the cases, the envelope of the distorted capnogram preserves the CO₂ tracing of preceding and following non-distorted ventilations (Figure 5A,B). Only a few of them did not follow the pattern of adjacent non-distorted respiratory cycles (Figure 5C).

5. Conclusions

Capnogram-based ventilation guidance during CPR was enhanced after CC artifact suppression. Our method preserved the tracing of CO₂ concentration caused by ventilations, allowing other clinical uses of capnography during resuscitation.

Acknowledgements

This work received financial support from the Basque Government (Basque Country, Spain) through the project IT1087-16 and the predoctoral research grant PRE-2017-2-0201. The authors thank the TVF&R EMS providers for collecting the data used in this study.

References

- [1] Soar J, Nolan JP, Böttiger BW, et al. European Resuscitation Council guidelines for resuscitation 2015. Section 3. Adult advanced life support. *Resuscitation* 2015;95:100-147.
- [2] Link MS, Berkow LC, Kudenchuk PJ, et al. 2015 American Heart Association Guidelines Update for Cardiopulmonary Resuscitation and Emergency Cardiovascular Care. Part 7: adult advanced cardiovascular life support. *Circulation* 2015;132(18 suppl 2):S444–S464.
- [3] Idris AH, Daya M, Owens P, et al. High incidence of chest compression oscillations associated with capnography during out-of-hospital cardiopulmonary resuscitation. *Circulation* 2010;122:A83.
- [4] Leturiondo M, Ruiz de Gauna S, Ruiz JM, et al. Influence of chest compression artifact on capnogram-based ventilation detection during out-of-hospital cardiopulmonary resuscitation. *Resuscitation* 2018;124:63–68.
- [5] Gong Y, Chen B, Li Y. A review of the performance of artifact filtering algorithms for cardiopulmonary resuscitation. *Journal of Healthcare Engineering* 2013;4(2):185–202.
- [6] Gutierrez JJ, Leturiondo M, Ruiz de Gauna S, et al. Enhancing ventilation detection during cardiopulmonary resuscitation by filtering chest compression artifact from the capnography waveform. *PLOS ONE* 2018; 13(8):e0201565.

Address for correspondence.

Mikel Leturiondo Sota
mikel.leturiondo@ehu.eus
 School of Engineering
 Plaza Torres Quevedo, 1, 48013-Bilbao (Spain)

OBJECTIVE 3: TO CHARACTERIZE THE INFLUENCE OF VENTILATIONS ON ETCO₂ MEASUREMENT

Indexed journals

A5 "Modeling the impact of ventilations on the capnogram in out-of-hospital cardiac arrest"

Authors: J.J. Gutiérrez, J. Ruiz, S. Ruiz de Gauna, D.M. González-Otero, **M. Leturiondo**, J.K. Russell, C. Corcuera, J.F. Urtusagasti, M.R. Daya

Published in: PLoS One 2020, vol. 15, n. 2, p. e0228395

Type of publication: Journal paper indexed in JCR

Quality indices: Ranking: 27/71 (Q2). JCR impact factor: 2.740

Indexed international conferences

C8 "A model for quantifying the influence of ventilations on end-tidal carbon dioxide variation during out-of-hospital cardiac arrest"

Authors: J.J. Gutiérrez, S. Ruiz de Gauna, J. Ruiz, **M. Leturiondo**, J.K. Russell, M.R. Daya

Published in: Resuscitation 2018, vol. 130, p. e34-e35

Type of publication: Indexed congress in JCR

Quality indices: Ranking: 1/26 (Q1). JCR impact factor: 5.863

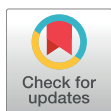
RESEARCH ARTICLE

Modeling the impact of ventilations on the capnogram in out-of-hospital cardiac arrest

Jose Julio Gutiérrez¹, Jesus María Ruiz¹, Sofía Ruiz de Gauna^{1*}, Digna María González-Otero^{1,2}, Mikel Leturiondo¹, James Knox Russell³, Carlos Corcuera⁴, Juan Francisco Urtusagasti⁴, Mohamud Ramzan Daya³

1 Department of Communications Engineering, University of the Basque Country (UPV/EHU), Bilbao, Bizkaia, Spain, **2** Bexen Cardio, Ermua, Bizkaia, Spain, **3** Department of Emergency Medicine, Oregon Health & Science University (OHSU), Portland, Oregon, United States of America, **4** Emergentziak-Osakidetzak, Basque Country Health System, Basque Country, Spain

* sofia.ruizdegauna@ehu.eus



Abstract

Aim

Current resuscitation guidelines recommend waveform capnography as an indirect indicator of perfusion during cardiopulmonary resuscitation (CPR). Chest compressions (CCs) and ventilations during CPR have opposing effects on the exhaled carbon dioxide (CO₂) concentration, which need to be better characterized. The purpose of this study was to model the impact of ventilations in the exhaled CO₂ measured from capnograms collected during out-of-hospital cardiac arrest (OHCA) resuscitation.

Methods

We retrospectively analyzed OHCA monitor-defibrillator files with concurrent capnogram, compression depth, transthoracic impedance and ECG signals. Segments with CC pauses, two or more ventilations, and with no pulse-generating rhythm were selected. Thus, only ventilations should have caused the decrease in CO₂ concentration. The variation in the exhaled CO₂ concentration with each ventilation was modeled with an exponential decay function using non-linear-least-squares curve fitting.

Results

Out of the original 1002 OHCA dataset (one per patient), 377 episodes had the required signals, and 196 segments from 96 patients met the inclusion criteria. Airway type was endotracheal tube in 64.8% of the segments, supraglottic King LT-D™ in 30.1%, and unknown in 5.1%. Median (IQR) decay factor of the exhaled CO₂ concentration was 10.0% (7.8 – 12.9) with $R^2 = 0.98(0.95 - 0.99)$. Differences in decay factor with airway type were not statistically significant ($p = 0.17$). From these results, we propose a model for estimating the contribution of CCs to the end-tidal CO₂ level between consecutive ventilations and for estimating the end-tidal CO₂ variation as a function of ventilation rate.

OPEN ACCESS

Citation: Gutiérrez JJ, Ruiz JM, Ruiz de Gauna S, González-Otero DM, Leturiondo M, Russell JK, et al. (2020) Modeling the impact of ventilations on the capnogram in out-of-hospital cardiac arrest. PLoS ONE 15(2): e0228395. <https://doi.org/10.1371/journal.pone.0228395>

Editor: Tomohiko Ai, Indiana University, UNITED STATES

Received: July 30, 2019

Accepted: January 14, 2020

Published: February 5, 2020

Copyright: © 2020 Gutiérrez et al. This is an open access article distributed under the terms of the [Creative Commons Attribution License](https://creativecommons.org/licenses/by/4.0/), which permits unrestricted use, distribution, and reproduction in any medium, provided the original author and source are credited.

Data Availability Statement: All relevant data are within the paper and its Supporting Information file.

Funding: The Basque Government provided support in the form of a grant for research groups (IT1087-16) for authors Jose Julio Gutierrez, Jesus María Ruiz, Sofía Ruiz de Gauna, and Mikel Leturiondo; and in the form of a predoctoral grant (PRE-2017-2-0201) for author Mikel Leturiondo (<https://www.euskadi.eus>). The Spanish Ministry of Economy, Industry and Competitiveness provided

support in the form of a grant for research projects (RTI2018-094396-B-I00) for authors Jose Julio Gutierrez, Jesus María Ruiz, Sofía Ruiz de Gauna, and Mikel Leturiondo; and in the form of the program Torres Quevedo (PTQ-16-08201) for author Digna María González-Otero (<http://www.ciencia.gob.es/>). Bexen Cardio, a Spanish medical device manufacturer, provided support in the form of a salary for author Digna María González-Otero. None of the above funders had any additional role in study design, data collection and analysis, decision to publish, or preparation of the manuscript. The specific role of each author is articulated in the "author contributions" section. Authors James Knox Russell, Carlos Corcuera, Juan Francisco Urtusagasti, and Mohamad Ramzan Daya received no funding for this work.

Competing interests: Author Digna María González-Otero is employed by Bexen Cardio, a Spanish medical device manufacturer. Bexen Cardio had no additional role in study funding, or study design, data collection and analysis, decision to publish, or preparation of the manuscript. This does not alter our adherence to PLOS ONE policies on sharing data and materials.

Conclusion

We have modeled the decrease in exhaled CO₂ concentration with ventilations during chest compression pauses in CPR. This finding allowed us to hypothesize a mathematical model for explaining the effect of chest compressions on ET_{CO₂} compensating for the influence of ventilation rate during CPR. However, further work is required to confirm the validity of this model during ongoing chest compressions.

Introduction

As emphasized by current resuscitation guidelines, high quality cardiopulmonary resuscitation (CPR) is essential to improving outcomes of cardiac arrest victims [1]. CPR providers should deliver chest compressions of adequate depth (50–60 mm) with a rate of 100–120 compressions per minute (cpm). Observational studies have established that high quality chest compressions are associated with favorable outcomes [2–4]. However, the recommended values may not be optimal for all individuals [5]. Ideally, CPR should be guided based on patient's response, e.g. using a non-invasive haemodynamic indicator [6, 7]. In this way, rescuers could adapt their CPR technique to optimize perfusion.

End-tidal carbon dioxide (ET_{CO₂}) is the partial pressure of carbon dioxide at the end of an exhaled breath. Experimental studies have shown that ET_{CO₂} correlates with cardiac output and coronary perfusion pressure during CPR [8, 9]. Low ET_{CO₂} values during resuscitation reflect the low cardiac output generated by chest compressions [10]. ET_{CO₂} may serve as a non-invasive hemodynamic indicator, albeit with complexities of interpretation. A consensus statement published by the American Heart Association in 2013 recommended using the ET_{CO₂} level as a physiological measure during CPR when an arterial or central venous catheter is not available [11]. Waveform capnography, i.e., continuous measurement of CO₂ concentration with time, enables monitoring of ET_{CO₂} during CPR. Current advanced life support (ALS) resuscitation guidelines [12, 13] emphasize the potential role of waveform capnography in monitoring CPR quality [14, 15], in the early recognition of return of spontaneous circulation (ROSC) during CPR [16, 17], and as a potential indicator of patient outcome [18–20].

During CPR, ET_{CO₂} values depend on the blood flow generated by chest compressions, on ventilation rate and tidal volumes of each breath, and on the metabolic activity of the patient tissues [21, 22]. Chest compressions and ventilations have opposing effects on ET_{CO₂} during CPR: compressions generate blood flow that delivers CO₂ from the tissues to the lungs, with the amount of delivered CO₂ being proportional to the amount of generated blood flow; ventilations, conversely, remove CO₂ from the lungs, and thus ET_{CO₂} decreases as ventilation rate is increased [23].

Recent studies have modeled the influence of chest compression quality (compression depth and rate) and ventilation rate on ET_{CO₂} during CPR using multivariate analysis [14, 15]. Studies on ROSC detection and patient outcome rely on the comparison of measured ET_{CO₂} levels [16–20, 24]. However, animal studies have suggested that ventilation rate significantly influences ET_{CO₂} levels [25]. Consequently, when interpreting ET_{CO₂} during CPR, ventilation rate acts as a significant confounding factor [22].

We hypothesized that the effect of ventilation on the capnogram could be modeled separately by analyzing variations in CO₂ concentration during chest compression pauses. Modeling the impact of ventilation on the capnogram would have two main areas of application.

First, it would facilitate a better assessment of the relationship between chest compression quality and capnography. Second, it would allow accounting for the confounding factor of ventilation rate in studies analyzing the correlation between ET CO_2 and ROSC or patient outcome. In this context, the purpose of this study was to apply a novel strategy to model the impact of ventilations and ventilation rate on the exhaled CO_2 measured in out-of-hospital cardiac arrest capnograms.

Materials and methods

Data collection

The data set used in this study was a subset of a large database of out-of-hospital cardiac arrest (OHCA) episodes collected from 2006 through 2016 by Tualatin Valley Fire & Rescue (TVF&R), an ALS first response emergency medical services (EMS) agency serving nine incorporated cities in Oregon, USA. The database is part of the Resuscitation Outcomes Consortium (ROC) Epidemiological Cardiac Arrest Registry collected by the Portland Regional Clinical Center. The data collection was approved by the Oregon Health & Science University (OHSU) Institutional Review Board (IRB00001736). Data were provided anonymous and contained no personal information.

Episodes were recorded using Heartstart MRx monitor-defibrillators (Philips, USA), equipped with capnography monitoring using sidestream technology (Microstream, Oridion Systems Ltd, Israel) and CPR quality monitors (Q-CPR). TVF&R used endotracheal tube or supraglottic (King LT-D™) devices to secure the airway. Ventilations were provided manually before and after patient intubation. For this study, we only included recordings with concurrent capnogram, compression depth signal, electrocardiogram (ECG) and transthoracic impedance (TI) signals.

Segment selection

Two biomedical experts (JJG and JMR) used a custom-made Matlab (Mathworks, USA) program to visually inspect the four signals extracted from each recording. Within each episode, they selected segments with no chest compressions where two or more complete ventilations were provided, and where the patient presented no spontaneous circulation. It was assumed that during those intervals, the decrease in the exhaled CO_2 concentration was caused only by ventilations. Absence of chest compressions was verified using compression depth and TI signals. Ventilation instances were identified using both the capnogram and the TI signal. Absence of a pulse-generating rhythm was verified by inspecting the ECG. Pulseless electrical activity and perfusing rhythm were distinguished by checking the circulatory component of the TI signal [26]. The beginning of each segment meeting the inclusion criteria was annotated 3 seconds after the interruption of chest compressions, to reject the period where blood pressures change rapidly and blood flow induced by chest compressions decreases to a sustained low flow level [27–29]. Fig 1 shows an example of a selected segment, highlighted in blue. This segment presents five complete ventilations, which can be observed in the capnogram and in the TI signal as slow fluctuations. The flat line in the compression depth signal indicates the absence of chest compressions, confirmed by the cessation of the fast fluctuations caused by chest compressions in the TI signal. Finally, the artifact-free ECG segment reveals ventricular fibrillation.

Data annotation

When analyzing the capnogram in the segments included in this study, we found that the duration of each ventilation cycle was different within each segment (see Fig 1). The duration

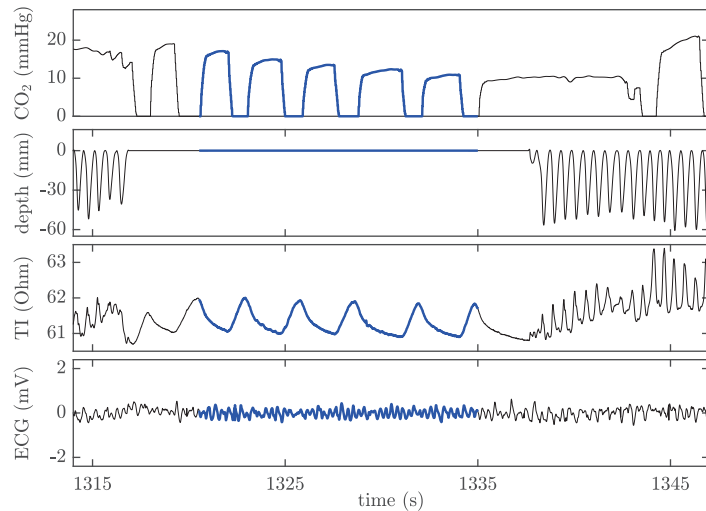


Fig 1. Example of segment selection. Required concurrent signals, with the segment highlighted in blue. From top to bottom: capnogram, compression depth, TI signal, and ECG.

<https://doi.org/10.1371/journal.pone.0228395.g001>

of each ventilation affects the $ETCO_2$ value since the plateau usually presents a low ascendant slope. To compare analogous points of exhaled CO_2 pressure values in the ventilations of each segment, we annotated the CO_2 value at a fixed delay from the beginning of the expiratory upstroke. We took the shortest plateau duration within each segment as the reference delay, and named this new metric *ensemble plateau CO_2* or $epCO_2$. In the absence of spontaneous circulation, CO_2 concentration during pauses in chest compressions decreases with each ventilation. However, this decrease may not be reliably measured since $ETCO_2$ value is highly dependent on the duration of the expiratory plateau. Fig 2 illustrates this idea depicting a short

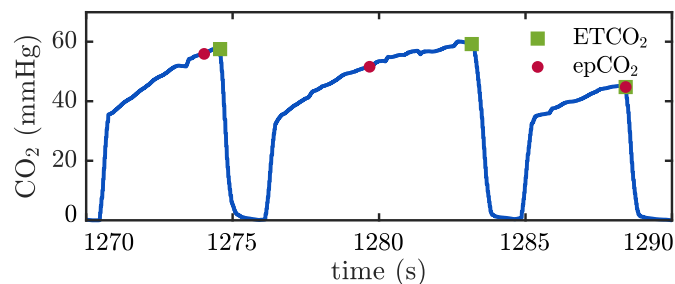


Fig 2. Example illustrating the metric $epCO_2$. Short capnogram interval with three ventilations and the corresponding annotated $ETCO_2$ (green squares) and $epCO_2$ (red dots) values. The novel metric $epCO_2$ was defined to represent the end-tidal values obtained if all ventilations had the same exhalation time. In the example, $epCO_2$ value decays with each ventilation.

<https://doi.org/10.1371/journal.pone.0228395.g002>

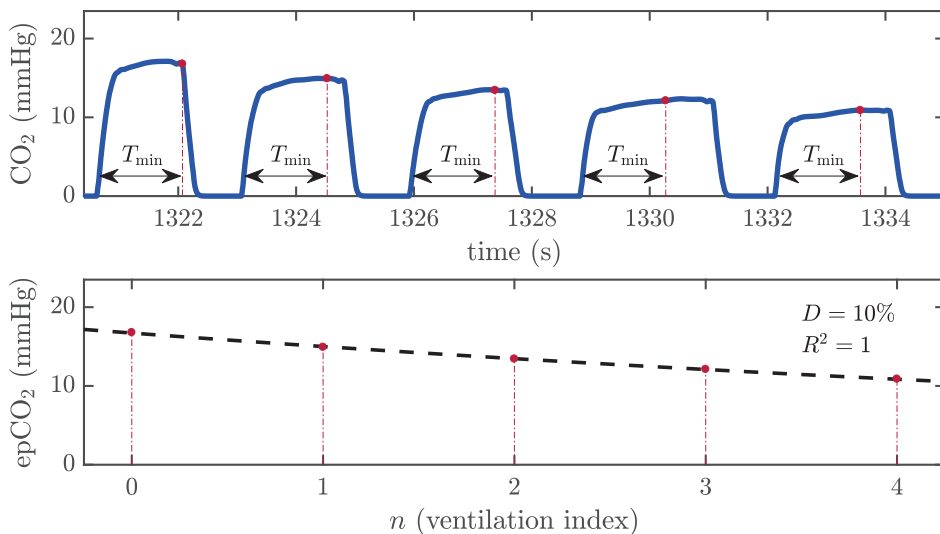


Fig 3. Data annotation and model fitting. Top panel: the annotated epCO₂ values within the segment selected in Fig 1 are marked in the capnogram with red dots. Bottom panel: the epCO₂ values are depicted as a function of the ventilation index, with the curve fitted using Eq (3) (dashed black line), and the decay factor and the coefficient of determination for the analyzed segment.

<https://doi.org/10.1371/journal.pone.0228395.g003>

capnogram interval with three ventilations and the corresponding annotated ETCO₂ values (green squares). The value annotated in the second ventilation is higher than the value annotated in the first ventilation. The novel metric epCO₂ was defined to represent the end-tidal values obtained if all ventilations had the same exhalation time. The values of epCO₂ depicted with red dots in Fig 2, clearly show the expected decay with each ventilation.

Top panel of Fig 3 shows the same capnogram segment from Fig 1 with the annotated epCO₂ values depicted as red dots.

Model fitting

The decay in epCO₂, as illustrated in Fig 3, suggested an exponential decay model. Thus, we modeled the trend in epCO₂ variation using the following expression:

$$ep_n = k \cdot ep_{n-1} \quad \text{for } n = 1, 2, \dots, N-1, \quad (1)$$

where ep_n represents the epCO₂ value corresponding to the ventilation of index n within the segment and N the total number of ventilations in the segment. The decay factor between consecutive ventilations D (%) was computed as:

$$D(\%) = 100 \cdot (1 - k) \quad (2)$$

Factor k was adjusted through a Matlab curve fitting tool using a decay exponential function as follows:

$$ep_n = a \cdot b^n \quad \text{for } n = 0, 1, \dots, N-1 \quad (3)$$

where a is an estimate of the initial epCO₂ value ($n = 0$) in the segment and b provides the adjusted k factor for each segment. We used non-linear least squares as the fitting method.

Fig 3 illustrates the process of curve fitting for one segment. In the example, the fitting process yielded $a = 16.7$ mmHg and $b = 0.90$, indicating that on average epCO₂ declined 10% with each ventilation.

Statistical analysis

Values that did not follow a normal distribution according to the Lilliefors normality test were reported as median (IQR). Goodness of fit of the model was evaluated using the coefficient of determination R^2 , which provides a measure of the epCO₂ variation that is explained by the model.

The distributions of the initial epCO₂ values (annotated at the beginning of the segment), of the decay factor D and of R^2 were represented using boxplots (a graphical depiction of the median, quartiles, and potential outliers). The relationship between D and the initial epCO₂ value was analyzed using linear regression, and the coefficient of determination R^2 was reported.

We also analyzed differences in the decay factor D with respect to the airway management technique (endotracheal or supraglottic). ANOVA analysis of variance was used to perform between groups comparisons since distributions were normal. P-values < 0.05 were considered significant.

Results

The original database comprised 1002 distinct OHCA episodes. In 377 of them (37.6%) the four signals of interest (capnogram, compression depth, TI, and ECG) were concurrently available. After visual inspection, 196 segments from 96 episodes meeting the inclusion criteria were extracted for the study. Airway type was endotracheal tube in 64.8% of these segments and supraglottic in 30.1%. Airway type was unknown for 5.1% of the segments. The median ventilation rate measured in the included segments was 15.1 (10.5–20.9) ventilations per minute (vpm), much higher than the guidelines recommendation of 10 vpm after placement of an advanced airway.

Fig 4 shows an example segment. Eleven ventilations were provided to the patient during the chest compression pause. The model fitting results are depicted in the figure.

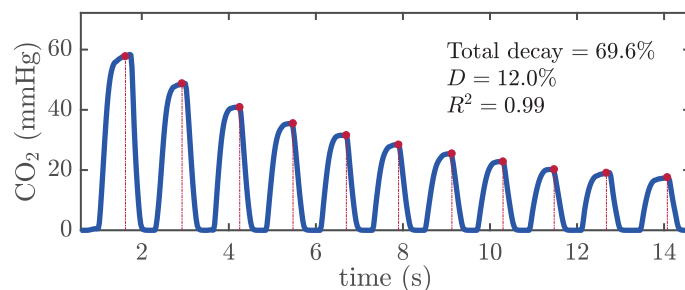


Fig 4. Example of epCO₂ decay with ventilations during a pause in chest compressions.

<https://doi.org/10.1371/journal.pone.0228395.g004>

Table 1. Number of segments (n), decay factor D (%), coefficient of determination R^2 of the model, and initial epCO₂ (ep₀) in mmHg, as a function of the number of ventilations provided per segment (N). Values are reported as median (IQR).

	N = 2	N = 3	N = 4	N = 5	N ≥ 6	Total
Segments (n)	40	58	31	22	45	196
D (%)	12.0 (10.1–15.9)	10.3 (8.6–13.2)	8.9 (7.4–10.2)	9.6 (6.4–12.3)	8.8 (6.1–11.7)	10.0 (7.8–12.9)
R^2	0.99 (0.96–1.00)	0.97 (0.96–0.99)	0.97 (0.94–0.99)	0.99 (0.96–0.99)	0.98 (0.96–0.99)	0.98 (0.95–0.99)
ep ₀ (mmHg)	21.0 (15.1–36.0)	20.7 (11.6–28.5)	21.9 (15.3–30.9)	17.2 (11.5–20.9)	22.7 (10.0–36.0)	20.0 (11.9–31.0)

<https://doi.org/10.1371/journal.pone.0228395.t001>

Table 1 shows the median (IQR) of the decay factor D , of the coefficient R^2 of the model fitted, and of the initial epCO₂ value as a function of the number of ventilations in the segment (N). When all the segments were included, the median decay factor was 10.0% (7.8–12.9) with R^2 equal to 0.98 (0.95–0.99), and the initial epCO₂ value was 20.0 mmHg (11.9–31.0). Fig 5 shows the distributions of these three measures using boxplots.

Decay factor (D) was unrelated to initial epCO₂ ($R^2 = 0.03$).

We did not find significant differences in the decay factor with respect to the airway type, endotracheal or supraglottic ($p = 0.17$).

Application of the findings

We have assessed the decrease in CO₂ concentration caused by ventilations during chest compression pauses. Our results provide a potentially novel framework for the accurate interpretation of ETCO₂ variation when chest compressions are provided. Our approach is based on the two hypotheses described below:

- First hypothesis: Contribution of chest compressions to the ETCO₂ level between two consecutive ventilations.
- Suppose that $ET1$ is the ETCO₂ level after a given ventilation, and that $ET2$ is the ETCO₂ level reached after the following ventilation when chest compressions are ongoing, as in intermittent ventilations after securing the airway.
- In the absence of chest compressions, the ETCO₂ level in the second ventilation would be $k \cdot ET1$, in accordance to our model.

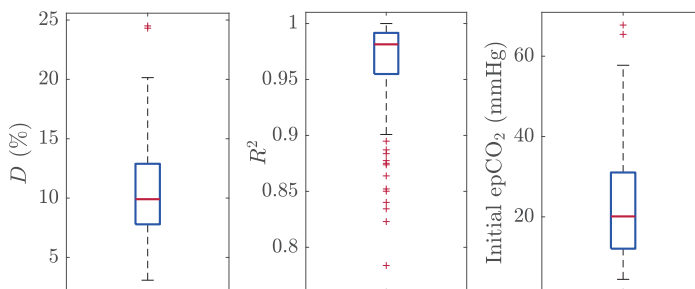


Fig 5. Distribution of the decay factor D , the coefficient R^2 for the model, and the initial epCO₂ value for all the segments included in the study.

<https://doi.org/10.1371/journal.pone.0228395.g005>

- We propose that the contribution of chest compressions to the $ETCO_2$ level between two consecutive ventilations could be estimated as $ET2 - k \cdot ET1$.
- Thus, that contribution per time unit could be expressed as:

$$\frac{ET2 - k \cdot ET1}{t_2 - t_1}, \quad (4)$$

where $t_2 - t_1$ is the duration of the ventilation.

- Second hypothesis: Variation of the $ETCO_2$ level with respect to ventilation rate.
 - Suppose that the $ETCO_2$ level keeps stable at $ET1$ mmHg during 1 minute of chest compressions when ventilation rate is $vr1$ vpm.
 - In the absence of chest compressions, the achieved $ETCO_2$ level after $vr1$ ventilations would be $ET1 \cdot k^{vr1}$ according to our model.
 - We could then estimate the contribution of chest compressions to the $ETCO_2$ level in that 1-min interval as:

$$ET1 - ET1 \cdot k^{vr1} = ET1 \cdot (1 - k^{vr1}) \quad (5)$$

- Now, for a different ventilation rate of $vr2$ vpm, and a stable $ETCO_2$ level of $ET2$, the contribution of chest compressions would be $ET2 \cdot (1 - k^{vr2})$.
- For chest compressions contributing equally to the $ETCO_2$ level, we could write:

$$ET1 \cdot (1 - k^{vr1}) = ET2 \cdot (1 - k^{vr2})$$

$$\frac{ET2}{ET1} = \frac{1 - k^{vr1}}{1 - k^{vr2}} \quad (6)$$

Taking the recommended ventilation rate of 10 vpm as the reference, i.e., $vr1 = 10$ vpm, Eq (6) expresses the $ETCO_2$ level relationship as a function of ventilation rate. Fig 6 shows a graphical depiction of Eq (6) normalized to $vr1 = 10$ vpm, and for $k = 0.9$ (the median value reported in our results). For example, the $ETCO_2$ level at a ventilation rate of 5 vpm would be 1.59 times the level at 10 vpm, chest compression performance being equal. Similarly, the estimated $ETCO_2$ level at 15 vpm would be 0.82 times the $ETCO_2$ at 10 vpm for the same compression performance. Thus, we could convert all $ETCO_2$ measurements to a normalized $ETCO_2$ value, by applying the corresponding correction factor (the inverse of the corresponding value in the vertical axis of Fig 6). Ultimately, we propose using this expression (6) for accurately comparing the $ETCO_2$ level of different CPR intervals by correcting the confounding factor of ventilation rate.

Discussion

We investigated the decrease in the exhaled CO_2 concentration with each ventilation provided to the patient during CPR. Our aim was to isolate the effect of ventilations on CO_2 concentration. This required that we identify pauses in chest compressions to select our analysis segments. Another advantage of this selection is that we had reliable capnogram tracings, since there is no presence of artifact caused by chest compressions compromising the analysis of ventilations [30, 31]. As the EMS agency that collected these episodes achieved very high chest

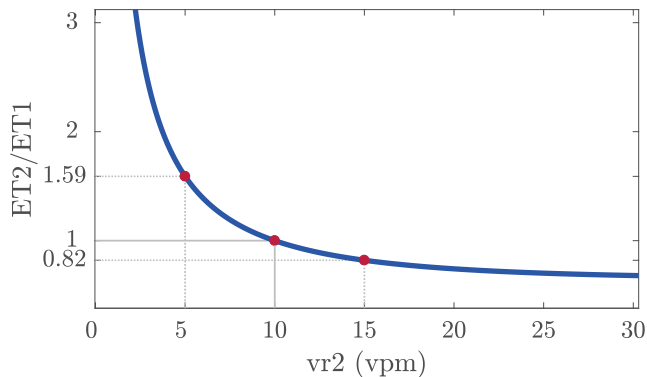


Fig 6. Graphical representation of the mathematical relationship of Eq (6) for a reference ventilation rate of 10 vpm and $k = 0.9$.

<https://doi.org/10.1371/journal.pone.0228395.g006>

compression fractions (minimal pauses), we could only identify 197 segments from the 1002 recordings.

When there is no CO_2 exchange in the lungs, ventilation adds oxygen to highly CO_2 concentrated volumes, so that CO_2 concentration decreases (CO_2 dilutes) in the lungs. The new concentration depends on the functional residual capacity, on the patient anatomic dead space and on the ventilation volume. Since we analyzed consecutive ventilations in each segment, similar volumes were assumed. For this reason, our model fitted the data very well, as proven by the high R^2 obtained (Fig 5, middle panel). However, the estimated decay factor D per segment showed a moderate dispersion (Fig 5, left panel) with a median (IQR) of 10% (7.8–12.9). This dispersion could be attributable to differences in patient functional residual capacity and anatomic dead space, and in the ventilation volumes provided with each breath. Since those parameters are unknown in the field, the median decay factor of 10% per ventilation may be useful as a sensible reference level. For example, in the absence of perfusion replenishing CO_2 , the median decrease after 10 ventilations could be estimated as 65.1% (i.e., $100 \cdot (1 - 0.9^{10})$) of the initial epCO_2 value. Fig 4 shows a segment of our database in which 10 ventilations were administered after the initial epCO_2 value. In this case, the actual decrease in epCO_2 after 10 ventilations was 69.6%, very close to the estimated value (1.59 and 0.82, respectively).

The decay factor D had no correlation with the initial epCO_2 value ($R^2 = 0.03$), i.e., the initial epCO_2 predicted almost none of the variation in the decay factor, favoring the strength of the model. This finding shows that the decay factor is not related to the factors that condition the initial epCO_2 value of each segment, such as the cardiac arrest etiology, the initial rhythm, the airway type, or the chest compression quality (rate, depth, recoil) and the ventilation rate being administered before the analyzed segment. We found a considerable number of segments (13.8%, 27/196) with initial epCO_2 values higher than 40 mmHg (Fig 5, right panel). Most of these segments corresponded to the beginning of the capnogram in the file, when CO_2 concentrations different from zero started to be measured. A possible explanation is that these episodes could correspond to primary respiratory failure leading to cardiac arrest [32], although we were unable to confirm this since we did not have any clinical data regarding etiology of the cardiac arrest. Other segments with high epCO_2 values were linked to low ventilation rates in the previous minute (between 2 and 4 vpm).

Our study has allowed us to model the ETCO_2 variation with ventilation rate during CPR. In a swine model of cardiac arrest, Gazmuri et al. used mechanical ventilation controlling tidal volume and respiratory rate [25]. Authors adjusted a curve to their experimental data which provided the variation of ETCO_2 level as a function of the ventilation exchanged volume in time (measured in liters per minute). Considering an average swine weight of 33 kg and a constant tidal volume of 6 ml/kg per ventilation, the ETCO_2 level at a constant ventilation rate of 5 vpm was 1.75 times the ETCO_2 level at 10 vpm. The ETCO_2 at 15 vpm was 0.75 times the level at 10 vpm. Their curve was similar to the one we have depicted in Fig 6, and reported values by Gazmuri et al. were comparable to those obtained applying our hypothesis.

One of the potential clinical applications of our study is to facilitate the analysis of the relationship between ETCO_2 and CPR quality. Resuscitation guidelines encourage the use of waveform capnography to monitor CPR quality. However, the variation of ETCO_2 with ventilation rate and chest compression quality parameters is not yet well understood, and current guidelines do not establish any specific ETCO_2 target to provide guidance on CPR quality.

Two recent studies have investigated these relationships [14, 15]. Sheak et al. conducted a multicenter cohort study of 583 in-hospital and out-of-hospital cardiac arrests. After averaging ETCO_2 values, compression depth, compression rate and ventilation rate over 15-s epochs, they used a multiple linear regression model to predict ETCO_2 variation based on the other three variables [14]. In their study, for every 10 mm increase in depth, ETCO_2 rose 1.4 mmHg ($p < 0.001$); for every 10 vpm increase in ventilation rate, ETCO_2 dropped 3.0 mmHg ($p < 0.001$); and compression rate was not a predictor of ETCO_2 variation. Murphy et al. conducted an observational prospective study with similar objectives including 230 patients [15]. In this case, ETCO_2 level, chest compression data and ventilation rate were averaged over 1-min epochs. The association between log-transformed ETCO_2 and CPR variables was assessed through linear mixed effect models. The authors concluded that a 10 mm increase in compression depth was associated with a 4.0% increase in ETCO_2 ($p < 0.0001$); a 10 vpm increase in ventilation rate with a 17.4% decrease in ETCO_2 ($p < 0.0001$); and a 10 cpm increase in compression rate with a 1.7% increase in ETCO_2 ($p = 0.02$) [15].

Comparison of the studies is challenging because Sheak et al. reported absolute differences, while Murphy et al. reported relative differences. In any case, their results are quite distinct. Estimated variations with compression depth in both studies would only match for an average ETCO_2 level of 35 mmHg, and variations with ventilation rate only for an average ETCO_2 level of 17.2 mmHg. Additionally, the conclusions of both studies significantly diverge from what would be expected during resuscitation episodes. According to their results, increasing compression depth from 30 to 50 mm (from suboptimal to the minimum recommended depth) would only raise ETCO_2 by 2.8 mmHg (or 8%). The main factor compromising the applicability of their models is that the nature of dependence of ETCO_2 variations with compression variables and with ventilation rate may differ, i.e., it may not be linear or logarithmic for all the studied variables. Including all of them in the same model may have an additional confounding effect. According to the novel approach presented in our study, the change in ETCO_2 in a given interval which is attributable to chest compressions could be estimated by removing the influence of concurrent ventilations, which we can now model.

Another clinical application of our findings is related to the interpretation of ETCO_2 as an indicator of ROSC and prognostication during CPR. Resuscitation guidelines highlight that an increase of ETCO_2 during CPR may indicate ROSC, and that low ETCO_2 values may reflect a poor patient prognosis. However, studies in this field have not yet achieved high sensitivity and specificity in ROSC detection, nor reported a strong correlation between the ETCO_2 level and resuscitation outcome [16–20, 24]. We suggest that, since the ETCO_2 level varies significantly with ventilation rate, this parameter may act as an important confounding factor in the

cited studies. Our results provide a way of compensating for the effect of ventilation rate when analyzing ETCO_2 values.

Limitations

There are several limitations in our study that could be grouped in two categories. The first category refers to the proper definition of the model during pauses in chest compressions, and the other one to the extrapolation of the model to the scenario of ventilations during ongoing chest compressions.

The mathematical model for the epCO_2 decay with each ventilation has been obtained under the assumption of equal tidal volume per ventilation. Although ventilations are consecutive within each segment, there is no evidence that consecutive ventilations are administered with a similar tidal volume. The value of ETCO_2 depends on the ventilation rate and tidal volume provided with each ventilation [25]. Absence of volume data, a common situation in pre-hospital settings is an important limiting factor of the model.

Considerably different duration of plateau phases found in our capnograms compelled us to rely on a modified measure of ETCO_2 for a systematic comparison of consecutive ventilations. This does not correspond to how ETCO_2 is formally measured (at the end of the plateau phase), so we defined a new metric: epCO_2 . This metric attempts to estimate the value of ETCO_2 that would have been measured if all ventilations in the compression pause would have had the same duration. This approximation may introduce an error in the model.

Approximately 75% of the ventilation rates measured in our segments were above the recommended 10 vpm. Our data are consistent with previous works reporting that excessive ventilation rates are common in resuscitation [33, 34]. Hyperventilation may result in significantly increased intrathoracic pressure and decreased coronary perfusion pressures and survival rates.

We applied a 3-s guard to annotate the beginning of each segment, considering that a sustained low flow state is reached after that delay from the interruption of chest compressions. This time may not be generalized for every patient.

When the model is extrapolated to the ongoing chest compressions scenario we only took into account the influence of ventilation rate on the variation of ETCO_2 . We did not considered factors associated to chest compressions that have a role in ETCO_2 variation, such as the following:

Chest compressions with a depth compliant with current guidelines produce measurable and substantial ventilation volumes [35], with 81% of the passive tidal volumes recorded during chest compressions being lower than 20 ml. Chest compressions alone do not provide physiologically significant tidal volumes but may produce alterations in the capnogram.

During compressions, intrathoracic pressure increases and the lung volume decreases [36]. Lung volume becomes lower than the functional residual capacity, which is recovered only when CPR is interrupted. Lung volume reduction during chest compressions can promote progressive atelectasis and pulmonary congestion. These interactions caused by chest compressions may involve alterations of the ETCO_2 level, not contemplated in our model.

Intrathoracic airway closure is a phenomenon associated with lung volume reduction limiting the delivered ventilation [36]. The negative pressure produced by chest compressions in the alveoli cannot be transmitted at airway opening and no inspiratory flow is generated. No respiratory tidal volume can be produced during decompression affecting the exhaled CO_2 .

Studies related to ventilation during CPR are scarce. The complex relations between compressions and ventilations during CPR, although still not well understood, could somehow modulate the exhaled CO_2 concentration [33, 36].

We are aware of the simplicity of the proposed model and of the role of the confounding factors that affect $ETCO_2$ values during resuscitation besides ventilation rate, such as the etiology of the cardiac arrest or the administration of drugs [22], which were unavailable in our retrospective data. These other considerations may be unknown during treatment as well, necessitating reliance on the limited data available in real time. Our method may overcome one of the many confounders of $ETCO_2$ interpretation during chest compressions. The formulae proposed in the present study are promising hypotheses, but need to be confirmed with further analysis of resuscitation recordings.

Conclusion

We have modeled the decrease in exhaled CO_2 concentration with ventilations during chest compression pauses in CPR. On average, each ventilation produced a decrease of 10% in the measured exhaled CO_2 value. This finding allowed us to hypothesize a mathematical model for explaining the effect of chest compressions on $ETCO_2$ compensating for the influence of ventilation rate during CPR. However, further work is required to confirm the validity of this model during ongoing chest compressions.

Supporting information

S1 File. Annotations and curve fitting results for all segments included in the study. (XLSX)

Acknowledgments

Thanks to the EMS providers and staff of Tualatin Valley Fire & Rescue for their dedication and efforts to support research on CPR quality.

Author Contributions

Conceptualization: Jose Julio Gutiérrez, Jesus María Ruiz, Sofia Ruiz de Gauna.

Data curation: Jose Julio Gutiérrez, Jesus María Ruiz, Digna María González-Otero, Mikel Leturiondo.

Formal analysis: Jose Julio Gutiérrez, Jesus María Ruiz, Sofia Ruiz de Gauna.

Funding acquisition: Jesus María Ruiz, Sofia Ruiz de Gauna.

Investigation: Jose Julio Gutiérrez, Jesus María Ruiz, Sofia Ruiz de Gauna.

Methodology: Jose Julio Gutiérrez, Jesus María Ruiz.

Project administration: Jesus María Ruiz, Sofia Ruiz de Gauna.

Resources: Jesus María Ruiz, Sofia Ruiz de Gauna, Mikel Leturiondo, James Knox Russell, Carlos Corcuera, Juan Francisco Urtusagasti, Mohamud Ramzan Daya.

Software: Jose Julio Gutiérrez, Digna María González-Otero, Mikel Leturiondo, James Knox Russell.

Supervision: Jose Julio Gutiérrez, Jesus María Ruiz, Sofia Ruiz de Gauna, James Knox Russell, Mohamud Ramzan Daya.

Validation: Jose Julio Gutiérrez, Jesus María Ruiz, Digna María González-Otero, Mikel Leturiondo.

Visualization: Jose Julio Gutiérrez, Jesus María Ruiz, Digna María González-Otero, Mikel Leturiondo.

Writing – original draft: Jose Julio Gutiérrez, Jesus María Ruiz, Sofía Ruiz de Gauna, Mikel Leturiondo.

Writing – review & editing: Jesus María Ruiz, Sofía Ruiz de Gauna, Digna María González-Otero, James Knox Russell, Carlos Corcuera, Juan Francisco Urtusagasti, Mohamud Ramzan Daya.

References

- Perkins GD, Handley AJ, Koster RW, Castrén M, Smyth MA, Olasveengen T, et al. European Resuscitation Council Guidelines for Resuscitation 2015: Section 2. Adult basic life support and automated external defibrillation. *Resuscitation*. 2015; 95:81–99. <https://doi.org/10.1016/j.resuscitation.2015.07.015> PMID: 26477420
- Stiell IG, Brown SP, Nichol G, Cheskes S, Vaillancourt C, Callaway CW, et al. What is the optimal chest compression depth during out-of-hospital cardiac arrest resuscitation of adult patients? *Circulation*. 2014; 130:1962–1970. <https://doi.org/10.1161/CIRCULATIONAHA.114.008671> PMID: 25252721
- Vadeboncoeur T, Stolz U, Panchal A, Silver A, Venuti M, Tobin J, et al. Chest compression depth and survival in out-of-hospital cardiac arrest. *Resuscitation*. 2014; 85(2):182–188. <https://doi.org/10.1016/j.resuscitation.2013.10.002> PMID: 24125742
- Idris AH, Guffey D, Pepe PE, Brown SP, Brooks SC, Callaway CW, et al. Chest compression rates and survival following out-of-hospital cardiac arrest. *Critical care medicine*. 2015; 43(4):840–848. <https://doi.org/10.1097/CCM.0000000000000824> PMID: 25565457
- Sutton RM, Friess SH, Maltese MR, Naim MY, Bratinov G, Weiland TR, et al. Hemodynamic-directed cardiopulmonary resuscitation during in-hospital cardiac arrest. *Resuscitation*. 2014; 85(8):983–986. <https://doi.org/10.1016/j.resuscitation.2014.04.015> PMID: 24783998
- Babbs CF. We still need a real-time hemodynamic monitor for CPR. *Resuscitation*. 2013; 84(10):1297–1298. <https://doi.org/10.1016/j.resuscitation.2013.06.005> PMID: 23791810
- Friess SH, Sutton RM, French B, Bhalala U, Maltese MR, Naim MY, et al. Hemodynamic directed CPR improves cerebral perfusion pressure and brain tissue oxygenation. *Resuscitation*. 2014; 85(9):1298–1303. <https://doi.org/10.1016/j.resuscitation.2014.05.040> PMID: 24945902
- Weil MH, Bisera J, Trevino RP, Rackow EC. Cardiac output and end-tidal carbon dioxide. *Critical care medicine*. 1985; 13(11):907–909. <https://doi.org/10.1097/00003246-198511000-00011> PMID: 3931979
- Sanders AB, Atlas M, Ewy GA, Kern KB, Bragg S. Expired PCO₂ as an index of coronary perfusion pressure. *The American journal of emergency medicine*. 1985; 3(2):147–149. [https://doi.org/10.1016/0735-6757\(85\)90039-7](https://doi.org/10.1016/0735-6757(85)90039-7) PMID: 3918548
- Gudipati CV, Weil MH, Bisera J, Deshmukh HG, Rackow EC. Expired carbon dioxide: a noninvasive monitor of cardiopulmonary resuscitation. *Circulation*. 1988; 77(1):234–239. <https://doi.org/10.1161/01.cir.77.1.234> PMID: 3121209
- Meaney PA, Bobrow BJ, Mancini ME, Christenson J, De Caen AR, Bhanji F, et al. Cardiopulmonary resuscitation quality: improving cardiac resuscitation outcomes both inside and outside the hospital: a consensus statement from the American Heart Association. *Circulation*. 2013; 128(4):417–435. <https://doi.org/10.1161/CIR.0b013e31829d8654> PMID: 23801105
- Soar J, Nolan JP, Böttiger BW, Perkins GD, Lott C, Carli P, et al. European Resuscitation Council Guidelines for Resuscitation 2015: Section 3. Adult advanced life support. *Resuscitation*. 2015; 95:100–147. <https://doi.org/10.1016/j.resuscitation.2015.07.016> PMID: 26477701
- Link MS, Berkow LC, Kudenchuk PJ, Halperin HR, Hess EP, Moitra VK, et al. Part 7: adult advanced cardiovascular life support: 2015 American Heart Association guidelines update for cardiopulmonary resuscitation and emergency cardiovascular care. *Circulation*. 2015; 132(18 suppl 2):S444–S464. <https://doi.org/10.1161/CIR.0000000000000261> PMID: 26472995
- Sheak KR, Wiebe DJ, Leary M, Babaeizadeh S, Yuen TC, Zive D, et al. Quantitative relationship between end-tidal carbon dioxide and CPR quality during both in-hospital and out-of-hospital cardiac arrest. *Resuscitation*. 2015; 89:149–154. <https://doi.org/10.1016/j.resuscitation.2015.01.026> PMID: 25643651
- Murphy RA, Bobrow BJ, Spaite DW, Hu C, McDannold R, Vadeboncoeur TF. Association between pre-hospital CPR quality and end-tidal carbon dioxide levels in out-of-hospital cardiac arrest. *Prehospital*

- Emergency Care. 2016; 20(3):369–377. <https://doi.org/10.3109/10903127.2015.1115929> PMID: 26830353
16. Pokorná M, Nečas E, Kratochvíl J, Skřípský R, Andriák M, Franěk O. A sudden increase in partial pressure end-tidal carbon dioxide (PETCO₂) at the moment of return of spontaneous circulation. *The Journal of emergency medicine*. 2010; 38(5):614–621. <https://doi.org/10.1016/j.jemermed.2009.04.064> PMID: 19570645
 17. Lui CT, Poon KM, Tsui KL. Abrupt rise of end tidal carbon dioxide level was a specific but non-sensitive marker of return of spontaneous circulation in patient with out-of-hospital cardiac arrest. *Resuscitation*. 2016; 104:53–58. <https://doi.org/10.1016/j.resuscitation.2016.04.018> PMID: 27157439
 18. Rognås L, Hansen TM, Kirkegaard H, Tønnesen E. Predicting the lack of ROSC during pre-hospital CPR: Should an end-tidal CO₂ of 1.3 kPa be used as a cut-off value? *Resuscitation*. 2014; 85(3):332–335. <https://doi.org/10.1016/j.resuscitation.2013.12.009> PMID: 24361671
 19. Poon KM, Lui CT, Tsui KL. Prognostication of out-of-hospital cardiac arrest patients by 3-min end-tidal capnometry level in emergency department. *Resuscitation*. 2016; 102:80–84. <https://doi.org/10.1016/j.resuscitation.2016.02.021> PMID: 26948821
 20. Wang AY, Huang CH, Chang WT, Tsai MS, Wang CH, Chen WJ. Initial end-tidal CO₂ partial pressure predicts outcomes of in-hospital cardiac arrest. *The American journal of emergency medicine*. 2016; 34(12):2367–2371. <https://doi.org/10.1016/j.ajem.2016.08.052> PMID: 27638460
 21. Pantazopoulos C, Xanthos T, Pantazopoulos I, Papalois A, Kouskouni E, Iacovidou N. A review of carbon dioxide monitoring during adult cardiopulmonary resuscitation. *Heart, Lung and Circulation*. 2015; 24(11):1053–1061. <https://doi.org/10.1016/j.hlc.2015.05.013> PMID: 26150002
 22. Sandroni C, De Santis P, D'Arrigo S. Capnography during cardiac arrest. *Resuscitation*. 2018; 132:73–77. <https://doi.org/10.1016/j.resuscitation.2018.08.018> PMID: 30142399
 23. Cone DC, Cahill JC, Wayne MA. *Cardiopulmonary Resuscitation*. In: Gravenstein JS, Jaffe MB, Gravenstein N, Paulus DA, editors. *Capnography*. 2nd ed. Cambridge; 2011. p. 185–194.
 24. Paiva EF, Paxton JH, O'Neil BJ. The use of end-tidal carbon dioxide (ETCO₂) measurement to guide management of cardiac arrest: a systematic review. *Resuscitation*. 2018; 123:1–7. <https://doi.org/10.1016/j.resuscitation.2017.12.003> PMID: 29217394
 25. Gazmuri RJ, Ayoub IM, Radhakrishnan J, Motl J, Upadhyaya MP. Clinically plausible hyperventilation does not exert adverse hemodynamic effects during CPR but markedly reduces end-tidal PCO₂. *Resuscitation*. 2012; 83(2):259–264. <https://doi.org/10.1016/j.resuscitation.2011.07.034> PMID: 21854734
 26. Ruiz JM, Ruiz de Gauna S, González-Otero DM, Saiz P, Gutiérrez JJ, Veintemillas JF, et al. Circulation assessment by automated external defibrillators during cardiopulmonary resuscitation. *Resuscitation*. 2018; 128:158–163. <https://doi.org/10.1016/j.resuscitation.2018.04.036> PMID: 29733921
 27. Berg RA, Sanders AB, Kern KB, Hilwig RW, Heidenreich JW, Porter ME, et al. Adverse hemodynamic effects of interrupting chest compressions for rescue breathing during cardiopulmonary resuscitation for ventricular fibrillation cardiac arrest. *Circulation*. 2001; 104(20):2465–2470. <https://doi.org/10.1161/hc4501.098926> PMID: 11705826
 28. Steen S, Liao Q, Pierre L, Paskevicius A, Sjöberg T. The critical importance of minimal delay between chest compressions and subsequent defibrillation: a haemodynamic explanation. *Resuscitation*. 2003; 58(3):249–258. [https://doi.org/10.1016/s0300-9572\(03\)00265-x](https://doi.org/10.1016/s0300-9572(03)00265-x) PMID: 12969599
 29. Schipke J, Heusch G, Sani A, Gams E, Winter J. Static filling pressure in patients during induced ventricular fibrillation. *American Journal of Physiology-Heart and Circulatory Physiology*. 2003; 285(6):H2510–H2515. <https://doi.org/10.1152/ajpheart.00604.2003> PMID: 12907428
 30. Leturiondo M, Ruiz de Gauna S, Ruiz JM, Gutiérrez JJ, Leturiondo LA, González-Otero DM, et al. Influence of chest compression artefact on capnogram-based ventilation detection during out-of-hospital cardiopulmonary resuscitation. *Resuscitation*. 2018; 124:63–68. <https://doi.org/10.1016/j.resuscitation.2017.12.013> PMID: 29246741
 31. Gutiérrez JJ, Leturiondo M, Ruiz de Gauna S, Ruiz JM, Leturiondo LA, Gonzalez-Otero DM, et al. Enhancing Ventilation Detection During Cardiopulmonary Resuscitation by Filtering Chest Compression Artifact from the Capnography Waveform. *PLOS ONE*. 2018; 13(8):e0201565. <https://doi.org/10.1371/journal.pone.0201565> PMID: 30071008
 32. Grmec Š, Lah K, Tušek-Bunc K. Difference in end-tidal CO₂ between asphyxia cardiac arrest and ventricular fibrillation/pulseless ventricular tachycardia cardiac arrest in the prehospital setting. *Critical Care*. 2003; 7(6):R139–R144. <https://doi.org/10.1186/cc2369> PMID: 14624688
 33. Auferheide TP, Sigurdsson G, Pirralo RG, Yannopoulos D, McKnite S, Von Briesen C, Sparks CW, Conrad CJ, Provo TA, Lurie KG. Hyperventilation-induced hypotension during cardiopulmonary resuscitation. *Circulation*. 2004; 109(16):1960–1965. <https://doi.org/10.1161/01.CIR.0000126594.79136.61> PMID: 15066941

34. Aufderheide TP, Lurie KG. Death by hyperventilation: a common and life-threatening problem during cardiopulmonary resuscitation. *Critical care medicine*. 2004; 32(9):S345–S351. <https://doi.org/10.1097/01.ccm.0000134335.46859.09> PMID: 15508657
35. McDannold R, Bobrow BJ, Chikani V, Silver A, Spaitte DW, Vadeboncoeur T. Quantification of ventilation volumes produced by compressions during emergency department cardiopulmonary resuscitation. *The American journal of emergency medicine*. 2018; 36(9):1640–1644. <https://doi.org/10.1016/j.ajem.2018.06.057> PMID: 30017691
36. Cordioli RL, Grieco DL, Charbonney E, Richard JC, Savary D. New physiological insights in ventilation during cardiopulmonary resuscitation. *Current opinion in critical care*. 2019; 25(1):37–44. <https://doi.org/10.1097/MCC.0000000000000573> PMID: 30531537

AP014

Shock success and its determinants in refractory ventricular fibrillation during out-of-hospital cardiac arrest

Joris Nas^{1,*}, Judith Bonnes¹, Jos Thannhauser¹, Eliene Starreveld¹, Pierre van Grunsven¹, Gjerrit Meinsma², Niels van Royen¹, Joep Smeets¹, Menko Jan de Boer¹, Marc Brouwer¹

¹ Radboudumc, Nijmegen, Netherlands

² University of Twente, Enschede, Netherlands

Purpose of the study: Optimising timing of shocks using predictors of shock success may contribute to a more personalised resuscitation strategy, and is currently under investigation for initial ventricular fibrillation (VF). However, the majority of patients requires additional shocks during the course of the resuscitation. More information is needed on shock success and its determinants in this particular subset of patients with refractory VF.

Methods and materials: Per-shock analysis on cardiac arrest patients (Nijmegen, the Netherlands, 2008–2011) receiving >1 shock on VF (107 patients; 342 shocks). Following current guidelines, shocks were divided into shocks on recurrent (previous shock terminated VF) or on persisting VF (previous shock did not terminate VF), Fig. 1. Initial shocks were excluded. Predictors included defibrillator-derived parameters: amplitude spectrum area (AMSA, a VF-waveform measure), VF time intervals (e.g. pre-shock VF duration) and the number of preceding successful shocks. Shock success was defined as return of organized rhythm.

Results: Shock success was markedly higher for shocks on recurrent VF ($n=214$) vs. persisting VF ($n=128$): 65% vs. 32%, $p<0.001$. For recurrent VF, higher AMSA and increasing numbers of preceding successful shocks were independently associated with shock success (adjusted odds ratio [aOR] 1.15 per mVHz increase, $p=0.001$; aOR=1.43 per additional preceding shock, $p=0.03$). C-statistic for AMSA=0.63. For persisting VF, we found that longer pre-shock VF duration was significantly associated with reduced shock success (OR=0.96 per 30 s increase, $p=0.04$, C-statistic=0.72).

Conclusions: This study underscores the importance of distinguishing different types of refractory VF, given the considerable differences in shock success and its determinants. Defibrillation failure for a shock on persisting VF is twice as likely as on recurrent VF. For persisting VF, shocks following longer periods of pre-shock VF duration had lower defibrillation success, which warrants future studies on the impact of a strategy with earlier and/or repetitive defibrillation attempts.

<https://doi.org/10.1016/j.resuscitation.2018.07.056>

AP015

A model for quantifying the influence of ventilations on end-tidal carbon dioxide variation during out-of-hospital cardiac arrest

Jose Julio Gutiérrez¹, Sofía Ruiz de Gauna^{1,*}, Jesus María Ruiz¹, Mikel Leturiondo¹, James Knox Russell², Mohamud Daya²

¹ University of the Basque Country, UPV/EHU, Bilbao, Spain

² Oregon Health&Science University, OHSU, Portland (OR), USA

Introduction: End-tidal carbon dioxide (ETCO₂) depends on pulmonary blood flow therefore provides a surrogate indicator of cardiac output generated by cardiopulmonary resuscitation (CPR). Advanced life support resuscitation guidelines recommend using capnography for CPR quality assessment. Chest compressions and ventilations have opposing effects on ETCO₂ during CPR: compressions generate blood flow causing a rise in pulmonary CO₂ concentration while ventilations exchange high CO₂ concentrated volumes with air or oxygen, decreasing CO₂ concentration in the lungs.

Purpose of the study: To quantify ETCO₂ decrease per each administered ventilation during out-of-hospital CPR.

Materials and methods: Fifty out-of-hospital cardiac arrest episodes containing the continuous capnogram, the compression depth and transthoracic impedance signals, and the ECG acquired from defibrillation pads were randomly selected from a larger database [1]. To isolate the effect of ventilations on ETCO₂ we located chest compression pauses between consecutive compression series, where more than three ventilations were provided, and with a non-pulsatile rhythm. In each selected pause, we annotated the ETCO₂ values corresponding to each ventilation (Fig. 1, red dots). We analysed the relationship $x_{n+1} = K \cdot x_n$, where x_n and x_{n+1} were the ETCO₂ levels of two consecutive ventilations. Factor K was calculated using least-square curve fitting (Fig. 1, dashed line). Adjusted R^2 was used to examine the goodness of fit.

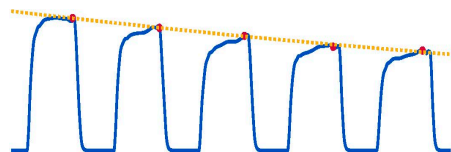


Fig. 1. Annotated capnogram and curve fitting.

Results: Twenty-two (22) pauses were included in the study. Median (IQR) adjusted K factor was 0.91 (0.89–0.93). Adjusted R^2 was 0.98 (0.95–0.99). This means that each ventilation produces an ETCO₂ decrease of about 9%.

Conclusions: Knowledge of ETCO₂ variation with each assisted ventilation could be used to help better assess the influence of chest compression metrics such as depth and rate on ETCO₂ measurements during CPR.

Reference

[1] Leturiondo, et al. Resuscitation 2018;124:63–8.

<https://doi.org/10.1016/j.resuscitation.2018.07.057>

OBJECTIVE 4: TO DEVELOP NOVEL STRATEGIES TO IDENTIFY ROSC USING THE CAPNOGRAM AS THE REFERENCE

Indexed journals

A6 "Assessment of the evolution of end-tidal carbon dioxide within chest compression pauses to detect restoration of spontaneous circulation"

Authors: J.J. Gutiérrez, M. Leturiondo, S. Ruiz de Gauna, J. Ruiz, I. Azcarate, D.M. González-Otero, J.F. Urtusagasti, J.K. Russell, M.R. Daya

Published in: PLoS One 2020, *acceptance pending*

Type of publication: Journal paper indexed in JCR

Quality indices: Ranking: 27/71 (Q2). JCR impact factor: 2.740

Assessment of the evolution of end-tidal carbon dioxide within chest compression pauses to detect restoration of spontaneous circulation

Jose Julio Gutiérrez¹ Mikel Leturiondo¹ Sofia Ruiz de Gauna^{1*} Jesus María Ruiz¹ Izaskun Azcarate¹ Digna María González-Otero^{1,2} Juan Francisco Urtusagasti³ James Knox Russell⁴ Mohamud Ramzan Daya⁴

1 Department of Communications Engineering, University of the Basque Country, UPV/EHU, Bilbao, Spain

2 Bexen Cardio, Ermua, Spain

3 Emergentziak-Osakidetza, Basque Country Health System, Basque Country, Spain

4 Oregon Health & Science University (OHSU), Portland, USA

* sofia.ruizdegauna@ehu.eus

Abstract

Background: Measurement of end-tidal CO₂ (ETCO₂) can help to monitor circulation during cardiopulmonary resuscitation (CPR). However, early detection of restoration of spontaneous circulation (ROSC) during CPR using waveform capnography remains a challenge. Several factors may affect ETCO₂ level during CPR, especially the quality of chest compressions and ventilations. If ventilation volume and rate remain stable, ETCO₂ gradually decreases in the absence of circulation when chest compressions are discontinued. If ETCO₂ remains constant or tends to increase, spontaneous circulation may be present. The aim of this study was to demonstrate that the assessment of the ETCO₂ variation during chest compression pauses could be a valuable adjunct to detect ROSC.

Methods: We conducted a retrospective analysis of adult out-of-hospital cardiac arrest (OHCA) episodes treated by the advanced life support (ALS). Continuous chest compressions and ventilations were provided manually. Segments of capnography signal during pauses in chest compressions were selected, including at least three ventilations and with durations less than 20 s. Segments were classified as ROSC or non-ROSC according to case chart annotation and examination of the ECG and transthoracic impedance signals. The percentage variation of ETCO₂ between consecutive ventilations was computed and its average value, ΔET_{avg} , was used as a single feature to discriminate between ROSC and non-ROSC segments.

Results: A total of 481 OHCA episodes (one per patient) were included in the study. After segment selection, 384 segments (130 ROSC, 254 non-ROSC) from 205 episodes (30.7% female, median age 66) were included in the study. Median (IQR) ΔET_{avg} was 0.0 (-0.7, 0.9)% for ROSC segments and -11.0 (-14.1, -8.0)% for non-ROSC segments ($p < 0.0001$). Best performance for ROSC detection yielded a sensitivity of 95.4% (95% CI: 90.1%, 98.1%), a specificity of 94.9% (91.4%, 97.1%), and a positive predictive value of 90.5% (84.3%, 94.5%). Our method allowed for ROSC detection during the first compression pause in 95.4% of the patients.

Conclusion: Assessment of ETCO₂ variation during pauses in chest compressions is a valuable metric for detecting ROSC. This metric could help confirm ROSC during pauses for rhythm assessment in ALS settings.

Introduction

Waveform capnography provides a continuous non-invasive measure of the concentration of partial pressure of carbon dioxide (PCO_2) during the breathing cycle. The value of PCO_2 at the end of expiration is known as end-tidal carbon dioxide (ETCO_2), and can be used to indirectly monitor cardiac output and pulmonary blood flow [1–3]. During resuscitation chest compressions generate low cardiac output, resulting in low ETCO_2 values [4].

According to current advanced life support (ALS) guidelines [5,6], monitoring ETCO_2 level during resuscitation is beneficial for several reasons including: supervision of cardiopulmonary resuscitation (CPR) quality [7–10], prediction of patient's outcome [11–15], and early recognition of return of spontaneous circulation (ROSC) [16–19]. ROSC may be identified through an increase in ETCO_2 during CPR. Early recognition of ROSC prevents unnecessary administration of chest compressions and adrenaline [20,21]. However, inappropriate interruptions of chest compressions can reduce the chance of survival [22–24]. In order to provide optimal therapy, interruptions in CPR for assessing the presence of ROSC should be minimized [5,6].

Accurate detection of ROSC using waveform capnography in pre-hospital ALS settings remains a challenge. Existing methods are based on the detection of sudden increases in the level of ETCO_2 [16–19]. However, the obtained results lack sensitivity and specificity. The level of ETCO_2 during CPR depends, among other factors, on patient's tissue metabolic activity, on the blood flow generated by chest compressions, on the volume of each breath, and on the rate of ventilation [20,21]. High quality chest compressions can raise ETCO_2 , while an increase in ventilation volume or rate reduces ETCO_2 levels [25]. If ventilation volume and rate remain constant and chest compressions are discontinued, ETCO_2 levels decrease in the absence of a perfusing rhythm (PR).

The aim of this study was to investigate if the assessment of the evolution of ETCO_2 during chest compression pauses could allow for ROSC detection. If an organized rhythm is observed in the electrocardiogram (ECG) during the compression pause for rhythm assessment, the analysis of the ETCO_2 trend could help confirm ROSC. A decay in ETCO_2 would indicate pulseless electrical activity (PEA), and therefore no ROSC. Conversely, if the ETCO_2 level remained constant or increased, the presence of a PR and, therefore, ROSC could be presumed.

Methods

Data collection

This is a retrospective study of adult out-of-hospital cardiac arrest (OHCA) cases attended by Tualatin Valley Fire & Rescue (TVF&R), an ALS emergency medical service agency (Tigard, Oregon, USA) from 2006 through 2017. The database is part of the Portland Resuscitation Outcomes Consortium Epidemiological Cardiac Arrest Registry approved by the Oregon Health&Science University (OHSU) Institutional Review Board (IRB00001736). The database does not include patient identifying information.

Episodes were recorded using Heartstart MRx monitor-defibrillators (Philips, USA), equipped with capnography monitoring using sidestream technology (Microstream™, Oridion Systems Ltd., Israel) and CPR quality monitoring (Q-CPR™). Airway management techniques included Bag-valve-mask (BMV) ventilation, supraglottic airway (SGA) devices and endotracheal tube (ETT). In the early years, CPR followed the 30:2 approach moving to continuous chest compressions (without pauses for ventilations) in 2012.

Segment selection

Our working hypothesis was that the variation of $ETCO_2$ between consecutive ventilations during chest compression pauses would allow for reliable ROSC detection. Two biomedical engineers (JJG and JMR) visually inspected four signals extracted from the OHCA defibrillator recordings: capnogram, compression depth signal, ECG and transthoracic impedance (TTI). A capnogram with minimal artefact was required to reliably annotate $ETCO_2$ values. Segments of capnography signal during pauses in chest compressions were identified. Only segments shorter than 20 s, with at least three ventilations, and with $ETCO_2$ values equal or higher than 10 mmHg were included in the analysis. $ETCO_2$ values lower than 10 mmHg were assumed to indicate absence of ROSC [5].

The selected segments were then classified as ROSC or non-ROSC. We reviewed the ROSC annotations by the ALS providers and confirmed the presence of an organized rhythm in the ECG. Then, in case of doubt between an organized non-perfusing (PEA) or PR, we examined the TTI signal to locate its circulation component [26]. We selected a single ROSC segment per patient, the first segment without chest compressions after the first clinical annotation of ROSC. Conversely, several non-ROSC segments per single patient were included. Fig. 1 shows two segments corresponding to ROSC (panel A) and non-ROSC (panel B). Capnogram, compression depth, ECG and TTI signals are depicted for each segment. In both segments, the compression depth signal is a flat line, reflecting the absence of chest compressions. The ECG in panel A shows a PR confirmed by the presence of low amplitude ripples between the large fluctuations caused by ventilation in the TTI [26]. Conversely, the ECG in panel B corresponds to a non-perfusing rhythm, confirmed by the absence of ripples in the TTI.

Segments characterization

For each included segment, the following values were annotated in the capnogram (Fig. 1): the start and end of each segment in seconds (t_s , t_e), depicted in the figure with vertical red lines; the number of ventilations within each segment (nv); and the $ETCO_2$ value per ventilation (ET_n), for $n = 1 \dots nv$. ET_n were calculated as the maximum concentration of CO_2 reached in the capnogram plateau, and are depicted in the figure with red dots. Once a segment met the inclusion criteria, it was characterized by four features:

- Mean ventilation rate (ventilations per minute, vpm): $v_r = \frac{nv}{t_e - t_s} \cdot 60$.
- ET_0 (mmHg): the $ETCO_2$ value for the first ventilation.
- ΔET_n (%): percentage variation of ET_n between consecutive ventilations calculated as $\Delta ET_n = \frac{ET_n - ET_{n-1}}{ET_{n-1}} \cdot 100$ for $n = 1 \dots nv - 1$. Positive ΔET_n means a positive trend in $ETCO_2$ between consecutive ventilations while negative ΔET_n means a negative trend. A zero value indicates a stable $ETCO_2$.
- ΔET_{avg} (%): the average variation calculated as the mean of percentage variation ΔET_n .

Method for ROSC detection

Discrimination between ROSC and non-ROSC segments was conducted using the ΔET_{avg} feature, as a metric of the positive or negative trend in $ETCO_2$ variation. We compared the ΔET_{avg} values with a detection threshold, Th : segments presenting ΔET_{avg} greater than the threshold were classified as ROSC. Values equal to or less than Th were classified as non-ROSC.

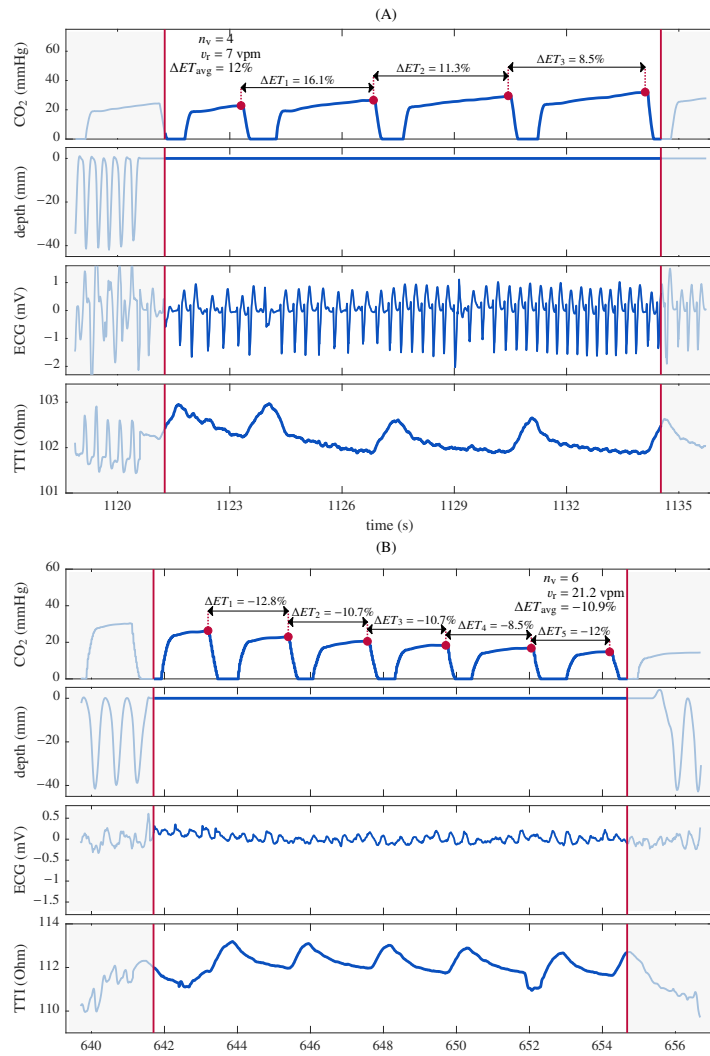


Fig 1. Examples of segment annotation. (A) ROSC segment and (B) non-ROSC segment. Capnogram, compression depth, ECG and transthoracic impedance (TTI) are depicted for each segment.

Statistical analysis

Different threshold values Th were used to test the accuracy of ROSC detection using the feature ΔET_{avg} . Ten-fold cross-validation (multiple train/test split) was used to assess the predictive ability of the discrimination method. Sensitivity (Se) was defined as the proportion of ROSC segments that had a positive result. Specificity (Sp) was defined as the proportion of non-ROSC segments that had a negative result. Positive predictive values (PPV) and negative predictive values (NPV) were also calculated. Their corresponding 95% confidence intervals (CI) were also reported.

Results were reported as median (IQR) since distributions did not pass the Lilliefors normality test. Comparison between groups was performed using the Wilcoxon rank sum test. P -values lower than 0.05 were considered significant. The distribution of ET_0 , v_r and ΔET_{avg} per segment were depicted using box plots.

We also analysed the results with respect to the airway management technique, ETT or SGA.

Results

Concurrent signals of interest (capnogram, compression depth, ECG and TTI signals) were available in 980 adult OHCA cases (one per patient), as illustrated in Fig. 2, of which 390 included information regarding clinical ROSC annotation. Cases with poor ECG, TTI or chest compression signal quality were discarded (173 ROSC; 61 non-ROSC). We also excluded episodes with high proportion of non-legible capnogram signals (40 ROSC; 225 non-ROSC). A total of 481 (177 ROSC; 304 non-ROSC) OHCA cases were eligible for analysis and segment selection.

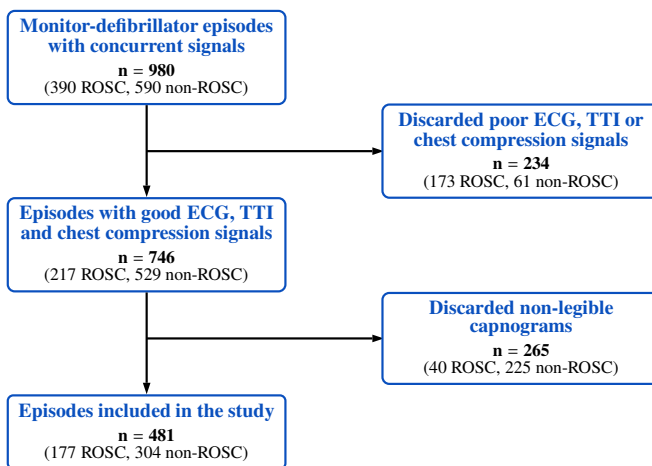


Fig 2. Flowchart of episode selection.

Table 1. Segments characterization as a function of the airway type and ROSC condition. Values are reported as median (IQR).

	SGA		ETT		TOTAL	
	ROSC	non-ROSC	ROSC	non-ROSC	ROSC	non-ROSC
Episodes	48	39	80	35	130	75
Segments	48	115	80	132	130	254
Duration (s)	17.0 (16.0,18.6)	15.3 (12.4,18.2)	17.7 (16.2,19)	16.2 (13.0,18)	17.5 (16.1,18.7)	15.9 (12.6,18.0)
nv	4 (3,5)	3 (3,4)	4 (3,5)	3 (3,5)	4 (3,5)	3 (3,4)
v_r (vpm)	12.8 (11.0,17.2)	14.5 (12.3,17.8)	13.6 (9.8,17.8)	14.6 (10.6,19.1)	13.3 (10.4,17.5)	14.5 (11.1,18.6)
ET_0 (mmHg)	50.9 (40.3,60.8)	30.3 (22.2,39.9)	41.8 (32.0,55.8)	24.9 (15.1,37.7)	45.8 (34.7,58.4)	29.4 (19.1,39.6)
ΔET_{avg} (%)	0.0 (-0.7,1.1)	-10.2 (-12.8,-7.3)	0.3 (-0.5,1.3)	-11.4 (-14.5,-7.9)	0.0 (-0.7,0.9)	-11.0 (-14.1,-8.0)

nv: ventilations per segment; v_r : ventilation rate in ventilations per minute (vpm); ET_0 : initial $ETCO_2$; ΔET_{avg} : average $ETCO_2$ variation.

The inclusion criteria were met by 384 (130 ROSC; 254 non-ROSC) segments from 205 patients. The median age of the patients was 66 years (55-79), and 63 of them (30.7%) were female. Eighty seven (87) patients had their airway managed with SGA (42.4%), and 115 with ETT (56.1%). Airway type was not known for the remaining 3 episodes (1.5%).

Fig. 3 shows some examples of the calculation of the parameter ΔET_{avg} for ROSC and non-ROSC segments.

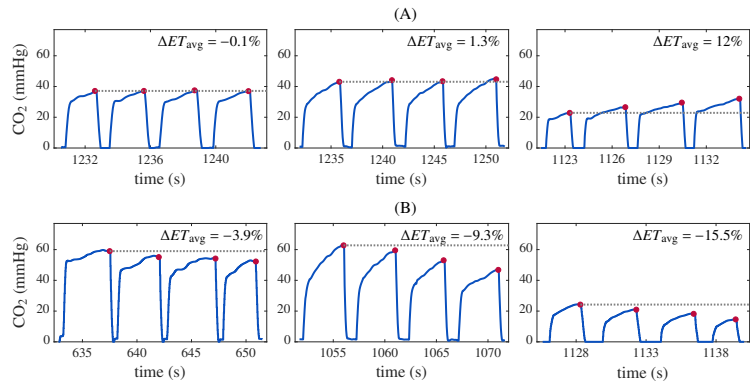


Fig 3. Illustration of the behavior of ΔET_{avg} . ROSC (A) and non-ROSC (B) capnogram segments with different ΔET_{avg} values.

Table 1 shows the distributions (median, IQR) of the analysed parameters. The median (IQR) v_r was 13.3 (10.4, 17.5) vpm for ROSC segments, and 14.5 (11.1, 18.6) vpm for non-ROSC segments ($p < 0.0002$). The obtained results of ET_0 values were 45.8 (34.7, 58.4) mmHg for ROSC segments, and 29.4 (19.1, 39.6) mmHg for non-ROSC segments ($p < 0.0001$). ΔET_{avg} presented values of 0.0 (-0.7, 0.9)% for ROSC segments, and -11.0 (-14.1, -8.0)% for non-ROSC segments ($p < 0.0001$).

Fig. 4 shows the distributions of ET_0 , v_r and ΔET_{avg} , for ROSC and non-ROSC segments. Distributions of ET_0 and v_r presented wide overlapping ranges for ROSC and non-ROSC populations, while for ΔET_{avg} a small overlap was observed.

Table 2 shows the ROSC/non-ROSC classification performance of our proposed classifier. Results are provided considering all ventilations in the segment, only the first

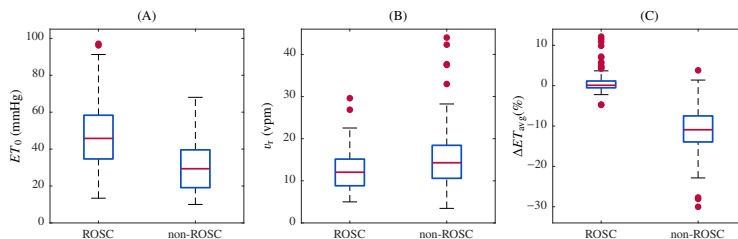


Fig 4. Statistical distributions for ROSC and non-ROSC segments. Initial ET_{CO_2} (ET_0), ventilation rate (v_r), and average variation (ΔET_{avg}) for all ROSC and non-ROSC segments included in the study.

Table 2. ROSC detection results, as a function of the number of considered ventilations per segment. Durations are reported as median (IQR). The 95% confidence intervals are in parenthesis.

	All ventilations	First 3 ventilations	First 2 ventilations
Duration (s)	16.3 (12.9, 18.1)	11.9 (9.3, 14.8)	7.7 (6.0, 10.2)
Se (%)	95.4 (90.1, 98.1)	93.8 (88.1, 97.0)	90.0 (83.5, 94.2)
Sp (%)	94.9 (91.4, 97.1)	95.3 (91.8, 97.4)	89.4 (84.9, 92.6)
PPV (%)	90.5 (84.3, 94.5)	91.0 (84.9, 94.9)	81.3 (74.0, 86.8)
NPV (%)	97.6 (94.7, 99.0)	96.8 (93.7, 98.5)	94.6 (90.9, 96.9)

Se: sensitivity; Sp: specificity; PPV: positive predictive value; NPV: negative predictive value.

three ventilations, and only the first two ventilations. When all the ventilations of each segment were considered, the median (IQR) of the duration was 16.3 (12.9, 18.1) s, and the obtained results were Se = 95.4% (95% CI: 90.1%, 98.1%) and Sp = 94.9% (91.4%, 97.1%). Considering the first 3 ventilations of each segment the duration was 11.9 (9.3, 14.8) s, with Se = 93.8% (88.1%, 97.0%) and Sp = 95.3% (91.8%, 97.4%). Considering the first 2 ventilations of each segment the duration was 7.7 (6.0, 10.2) s, with Se = 90.0% (83.5%, 94.2%) and Sp = 89.4% (84.9%, 92.6%). This method confirmed the clinical decision of ROSC during the first chest compression pause in 95.4% of the episodes.

There were statistically significant differences between airway types for ET_0 with the ROSC and non-ROSC populations ($p = 0.01$ in both cases). However, no significant differences were found for v_r ($p = 0.87$ and $p = 0.97$ for ROSC and non-ROSC, respectively) and for ΔET_{avg} ($p = 0.2$ and $p = 0.1$, respectively). Se and Sp values tended to be higher for ETT segments than for SGA segments. For ETT, Se and Sp were 98.8% (92.3%, 99.9%) and 99.2% (95.2%, 99.9%), respectively; whereas for SGA, Se was = 95.8% (84.6%, 99.3%) and Sp was = 95.7% (89.7%, 98.4%).

Discussion

High quality CPR requires minimizing interruptions in chest compressions, and needed pauses should be kept as short as possible to maximize perfusion [27]. For a prompt detection of ROSC, current ALS guidelines recommend pulse assessment if, after two minutes of CPR, the ECG shows a rhythm compatible with pulse, or when the patient shows movement or spontaneous breathing [5]. The reliable and automated detection of

ROSC based on the signals and data provided by the monitor-defibrillator would be valuable, on the one hand, to prevent prolonged detrimental interruptions of CPR with PEA, and, on the other hand, to avoid potentially harmful chest compressions and unnecessary drug administration to patients with PR.

Several methods for the automated detection of circulation based on the ECG and the TTI signals can be found in the literature [26,28–33]. In general, they rely on the analysis of the signals during chest compression pauses, looking for an organized rhythm in the ECG and the circulation component of the TTI. Since ECG and TTI signals are typically the only available signals in automated external defibrillators, these methods were intended primarily for basic life support (BLS) settings.

During ALS, the capnogram can be useful for ROSC detection, as it is an indirect indicator of perfusion. Pokorná et al. studied the significance of a sudden increase in ETCO_2 during ALS OHCA episodes [18]. ETCO_2 values were higher when ROSC was achieved ($p < 0.0001$). Analyzing an increase of 10 mmHg in the measured ETCO_2 during two min periods, they obtained a sensitivity of 80% with a specificity of 59%. Davis et al. analysed the prediction of ROSC based on the heart rate and ETCO_2 [34]. For a heart rate greater than 40 bpm and a ETCO_2 level above 20 mmHg, ROSC was detected with PPV = 95% and NPV = 99%. Lui et al. evaluated the diagnostic accuracy of an abrupt and sustained increase in ETCO_2 to indicate ROSC in OHCA patients [19]. For an ETCO_2 rise greater than 10 mmHg, ROSC was detected with a sensitivity of 33% and a specificity of 97%. Brinkrolf et al. assessed the detection of ROSC by identifying ETCO_2 trends in real time [16]. The study showed that ROSC time series presented larger percentages of positive trends than non-ROSC time series ($p = 0.003$). ROSC was detected with a sensitivity of 73.9% and a specificity of 58.4%. Finally, Elola et al. used the ECG and the TTI for ROSC assessment during chest compression pauses. When they included the mean ETCO_2 value of the minute before the beginning of the chest compression pause in the classifier, they obtained high sensitivity and specificity values [35].

In spite of the efforts made, to the best of our knowledge there is no monitor-defibrillator providing an automated assessment for the detection of ROSC [22]. In general, the proposed methods present either low sensitivity and specificity values or are based in parameters which can not be automatically obtained by the equipment.

In this work we demonstrated that the decay or increment of the level of ETCO_2 during chest compression pauses allows differentiation between non-ROSC and ROSC segments. In non-ROSC scenarios when chest compressions are interrupted there is no blood flow and therefore, the level of ETCO_2 decreases with each ventilation; whereas when ROSC is achieved, blood flow exists and the level of ETCO_2 should increase or at least remain constant. The ETCO_2 value measured in the first ventilation within the chest compression pause is influenced by several factors, such as the quality of chest compressions and ventilations. Therefore, this value is not a reliable indicator of ROSC. Our method does not rely on absolute measurements, but on the ETCO_2 variation. This approach yielded a sensitivity of 95.4% and specificity of 94.9% for predicting the presence of ROSC.

ALS guidelines recommend not interrupting chest compressions for more than 10 s [5]. With our criterium of pauses no longer than 20 s we obtained good performance results, above 90% for all metrics. To test the algorithm with pauses closer to the recommended 10 s, we applied the method to the first three and two ventilations of the included segments. In case of three ventilations, the median duration of the segments was 11 s and the performance was similar to the global results. In case of two ventilations, the median duration was 7.7 s and the performance slightly decreased, with values close to 90%, except for PPV (81.3%).

Our study has a direct clinical application. During chest compression pauses for

pulse check, the ECG signal is not affected by the artefact caused by compressions and it can be directly analysed to establish whether the electrical activity of the heart is compatible with a pulse-generating rhythm. ECGs compatible with pulse-generating rhythms can be PEA (non-ROSC) or PR (ROSC). Direct observation of the evolution of ETCO_2 in the capnogram would allow us to determine whether there is ROSC or not. ROSC is more likely if the level of ETCO_2 is maintained or increased, whereas if the level clearly decreases non-ROSC should be suspected. Fig. 3 illustrates this idea. In the top panel, three ROSC segments with four ventilations each are depicted, in which the level of ETCO_2 remains constant (left), slightly rises (middle), or significantly increases (right). In the bottom panel, three non-ROSC segments with four ventilations are represented. The level of ETCO_2 slightly decreases (left), sharply decays (middle), and significantly decreases (right).

Limitations

Our study did not consider the variability in ventilation volumes (unavailable in our database and generally in the field). We hypothesize that our method would be a reliable tool in clinical practice when ventilations are administered with stable volumes.

In our study, ROSC was confirmed by clinicians' annotations and by the analysis of the ECG and of the circulation component in the TTI. This methodology has been widely used in the literature as a surrogate for circulation assessment, and constitutes the best possible approach in the absence of invasive indicators. Still, we recognize the challenge of a real determination of ROSC in pre-hospital settings.

The database was completed over a long period of time. Guidelines changed and the EMS systems moved from 30:2 compression-ventilation ratio to continuous compressions. Recommended depth and rate of chest compressions also changed (2010 and 2015 guidelines). However, the results of this study should not be affected as the analysis was performed during chest compression pauses.

All the recordings of the database were obtained using the capnograph Microstream™, Oridion Systems Ltd., Israel. ETCO_2 levels could be slightly influenced by the equipment, so it would be helpful to validate our findings using different capnographs. Also, a large number of recordings were discarded due to poor signal quality. This work would deserve validation with more data to ensure that our results are generalizable.

Conclusion

Assessment of ETCO_2 variation during pauses in chest compressions is a valuable metric to detect ROSC. Decrease suggests a non-ROSC state while constant or positive variation reflects ROSC. The metric we propose in our study could help confirm the presence or absence of circulation during pauses for pulse check, for ALS agencies that have ETCO_2 monitoring capability.

Supporting information

S1 File. Segment Characterization. Detailed results per recording, segment and individual ventilation within each segment (see Table 1 for reference).

Acknowledgments

Thanks to the EMS providers and staff of Tualatin Valley Fire & Rescue (TVF&R) for their dedication and efforts to support research on CPR quality.

References

1. Weil MH, Bisera J, Trevino RP, Rackow EC. Cardiac output and end-tidal carbon dioxide. *Crit Care Med.* 1985;13(11):907–909.
2. Stock MC. Capnography for adults. *Crit Care Clin.* 1995;11(1):219–232.
3. Sanders AB, Atlas M, Ewy GA, Kern KB, Bragg S. Expired PCO₂ as an index of coronary perfusion pressure. *Am J Emerg Med.* 1985;3(2):147–149.
4. Gudipati CV, Weil MH, Bisera J, Deshmukh HG, Rackow EC. Expired carbon dioxide: a noninvasive monitor of cardiopulmonary resuscitation. *Circulation.* 1988;77(1):234–239.
5. Soar J, Nolan JP, Böttiger BW, Perkins GD, Lott C, Carli P, et al. European Resuscitation Council Guidelines for Resuscitation 2015: Section 3. Adult advanced life support. *Resuscitation.* 2015;95:100–147.
6. Link MS, Berkow LC, Kudenchuk PJ, Halperin HR, Hess EP, Moitra VK, et al. Part 7: adult advanced cardiovascular life support: 2015 American Heart Association guidelines update for cardiopulmonary resuscitation and emergency cardiovascular care. *Circulation.* 2015;132(18 suppl 2):S444–S464.
7. Sheak KR, Wiebe DJ, Leary M, Babaeizadeh S, Yuen TC, Zive D, et al. Quantitative relationship between end-tidal carbon dioxide and CPR quality during both in-hospital and out-of-hospital cardiac arrest. *Resuscitation.* 2015;89:149–154.
8. Murphy RA, Bobrow BJ, Spaite DW, Hu C, McDannold R, Vadeboncoeur TF. Association between prehospital CPR quality and end-tidal carbon dioxide levels in out-of-hospital cardiac arrest. *Prehosp Emerg Care.* 2016;20(3):369–377.
9. Hamrick JL, Hamrick JT, Lee JK, Lee BH, Koehler RC, Shaffner DH. Efficacy of chest compressions directed by end-tidal CO₂ feedback in a pediatric resuscitation model of basic life support. *J Am Heart Assoc.* 2014;3(2):e000450.
10. Paiva EF, Paxton JH, O’Neil BJ. The use of end-tidal carbon dioxide (ETCO₂) measurement to guide management of cardiac arrest: a systematic review. *Resuscitation.* 2018;123:1–7.
11. Levine RL, Wayne MA, Miller CC. End-tidal carbon dioxide and outcome of out-of-hospital cardiac arrest. *N Engl J Med.* 1997;337(5):301–306.
12. Kolar M, Križmarić M, Klemen P, Grmec Š. Partial pressure of end-tidal carbon dioxide successful predicts cardiopulmonary resuscitation in the field: a prospective observational study. *Crit Care.* 2008;12(5):R115.
13. Rognås L, Hansen TM, Kirkegaard H, Tønnesen E. Predicting the lack of ROSC during pre-hospital CPR: Should an end-tidal CO₂ of 1.3 kPa be used as a cut-off value? *Resuscitation.* 2014;85(3):332–335.
14. Poon KM, Lui CT, Tsui KL. Prognostication of out-of-hospital cardiac arrest patients by 3-min end-tidal capnometry level in emergency department. *Resuscitation.* 2016;102:80–84.
15. Wang AY, Huang CH, Chang WT, Tsai MS, Wang CH, Chen WJ. Initial end-tidal CO₂ partial pressure predicts outcomes of in-hospital cardiac arrest. *Am J Emerg Med.* 2016;34(12):2367–2371.

16. Brinkrolf P, Borowski M, Metelmann C, Lukas RP, Pidde-Küllenber L, Bohn A. Predicting ROSC in out-of-hospital cardiac arrest using expiratory carbon dioxide concentration: Is trend-detection instead of absolute threshold values the key? *Resuscitation*. 2018;122:19–24.
17. Sehra R, Underwood K, Checchia P. End tidal CO₂ is a quantitative measure of cardiac arrest. *Pacing Clin Electrophysiol*. 2003;26(1p2):515–517.
18. Pokorná M, Nečas E, Kratochvíl J, Skřípský R, Andrlík M, Franěk O. A sudden increase in partial pressure end-tidal carbon dioxide (PETCO₂) at the moment of return of spontaneous circulation. *J Emerg Med*. 2010;38(5):614–621.
19. Lui CT, Poon KM, Tsui KL. Abrupt rise of end tidal carbon dioxide level was a specific but non-sensitive marker of return of spontaneous circulation in patient with out-of-hospital cardiac arrest. *Resuscitation*. 2016;104:53–58.
20. Pantazopoulos C, Xanthos T, Pantazopoulos I, Papalois A, Kouskoumi E, Iacovidou N. A review of carbon dioxide monitoring during adult cardiopulmonary resuscitation. *Heart Lung Circ*. 2015;24(11):1053–1061.
21. Sandroni C, De Santis P, D'Arrigo S. Capnography during cardiac arrest. *Resuscitation*. 2018;132:73–77.
22. Sandroni C, Ristagno G. End-tidal CO₂ to detect recovery of spontaneous circulation during cardiopulmonary resuscitation: We are not ready yet. *Resuscitation*. 2016;104:A5 – A6.
doi:<https://doi.org/10.1016/j.resuscitation.2016.05.018>.
23. Edelson D, Abella B, Kramer-Johansen J, Wik L, Myklebust H, Barry A, et al. Effects of compression depth and pre-shock pauses predict defibrillation failure during cardiac arrest. *Resuscitation*. 2006;71:137–45.
doi:[10.1016/j.resuscitation.2006.04.008](https://doi.org/10.1016/j.resuscitation.2006.04.008).
24. Vaillancourt C, Brown S, Christenson J, Andrusiek D, Powell J, Nichol G, et al. The Impact of Increased Chest Compression Fraction on Return of Spontaneous Circulation for Out-of-Hospital Cardiac Arrest Patients not in Ventricular Fibrillation. *Resuscitation*. 2011;82:1501–7.
doi:[10.1016/j.resuscitation.2011.07.011](https://doi.org/10.1016/j.resuscitation.2011.07.011).
25. Gutiérrez JJ, Ruiz JM, Ruiz de Gauna S, González-Otero DM, Leturiondo M, Russell JK, et al. Modeling the impact of ventilations on the capnogram in out-of-hospital cardiac arrest. *PLOS ONE*. 2020;15(2):e0228395.
26. Circulation assessment by automated external defibrillators during cardiopulmonary resuscitation. *Resuscitation*;128.
27. Meaney PA, Bobrow BJ, Mancini ME, Christenson J, De Caen BF A R, Abella BS, et al. Cardiopulmonary resuscitation quality: Improving cardiac resuscitation outcomes both inside and outside the hospital. *Circulation*. 2013;128:417–435.
28. Pellis T, Bisera J, Tang W, Weil MH. Expanding automatic external defibrillators to include automated detection of cardiac, respiratory, and cardiorespiratory arrest. *Crit Care Med*. 2002;30(4 Suppl):S176–8.
doi:[10.1097/00003246-200204001-00012](https://doi.org/10.1097/00003246-200204001-00012).

29. Losert H, Risdal M, Sterz F, Nysæther J, Köhler K, Eftestøl T, et al. Thoracic-impedance changes measured via defibrillator pads can monitor signs of circulation. *Resuscitation*. 2007;73(2):221–228. doi:<https://doi.org/10.1016/j.resuscitation.2006.10.001>.
30. Risdal M, Aase SO, Kramer-Johansen J, Eftesol T. Automatic Identification of Return of Spontaneous Circulation During Cardiopulmonary Resuscitation. *IEEE Trans Biomed Eng*. 2008;55(1):60–68. doi:10.1109/TBME.2007.910644.
31. Cromie N, Allen J, Turner C, Anderson J, Adgey A. The impedance cardiogram recorded through two electrocardiogram/ defibrillator pads as a determinant of cardiac arrest during experimental studies. *Crit Care Med*. 2008;36:1578–1584. doi:10.1097/CCM.0b013e318170a03b.
32. Cromie N, Allen J, Navarro C, Turner C, Anderson J, Adgey A. Assessment of the impedance cardiogram recorded by an automated external defibrillator during clinical cardiac arrest. *Crit Care Med*. 2009;38:510–517. doi:10.1097/CCM.0b013e3181c02ca1.
33. Alonso E, Aramendi E, Daya M, Irusta U, Chicote B, Russell J, et al. Circulation detection using the electrocardiogram and the thoracic impedance acquired by defibrillation pads. *Resuscitation*. 2016;99:56–62. doi:10.1016/j.resuscitation.2015.11.014.
34. Davis DP, Sell RE, Wilkes N, Sarno R, Husa RD, Castillo EM, et al. Electrical and mechanical recovery of cardiac function following out-of-hospital cardiac arrest. *Resuscitation*. 2013;84(1):25–30. doi:<https://doi.org/10.1016/j.resuscitation.2012.07.040>.
35. Elola A, Aramendi E, Irusta U, Alonso E, Lu Y, Chang M, et al. Capnography: A support tool for the Detection of Return of Spontaneous Circulation in Out-of-Hospital Cardiac Arrest. *Resuscitation*. 2019;142. doi:10.1016/j.resuscitation.2019.03.048.